Multidisciplinary approach to conceptual modelling of Topusko hydrothermal system

Pavić, Mirja

Sveučilište u Zagrebu

Faculty of Mining, Geology and Petroleum Engineering

Mirja Pavić

MULTIDISCIPLINARY APPROACH TO CONCEPTUAL MODELLING OF TOPUSKO HYDROTHERMAL SYSTEM

DOCTORAL DISSERTATION

Zagreb, 2024

University of Zagreb

Faculty of Mining, Geology and Petroleum Engineering

Mirja Pavić

MULTIDISCIPLINARY APPROACH TO CONCEPTUAL MODELLING OF TOPUSKO HYDROTHERMAL SYSTEM

DOCTORAL DISSERTATION

Supervisors:
Senior Research Assoc. Staša Borović, Ph. D.
Prof. Željko Duić, Ph. D.

Zagreb, 2024

Rudarsko-geološko-naftni fakultet

Mirja Pavić

MULTIDISCIPLINARNI PRISTUP IZRADI KONCEPTUALNOGA MODELA HIDROTERMALNOGA SUSTAVA TOPUSKO

DOKTORSKI RAD

Mentori:
dr. sc. Staša Borović, viša znanstvena suradnica
dr. sc. Željko Duić, redoviti profesor

Zagreb, 2024.

Supervisors:

Staša Borović, Ph. D.
Senior Research Associate at the Croatian Geological Survey

Željko Duić, Ph. D.
Professor at the Faculty of Mining, Geology and Petroleum Engineering

Acknowledgements

I would like to express my gratitude to my supervisor, Staša Borović, PhD, for her invaluable guidance, constant support, and knowledge sharing, as well as the constructive advice provided and encouragement throughout this journey.

I am grateful to my supervisor, Prof. Željko Duić, PhD, for accepting the role of a supervisor and for the numerous advice and suggestions that significantly enhanced the quality of this doctoral dissertation.

I am also profoundly thankful to the members of my dissertation evaluation committee, Assoc. Prof. Bojan Matoš, PhD, Prof. Hrvoje Meaški, PhD, and Prof. Tomislav Kurevija, PhD, for their constructive feedback, challenging questions, and invaluable advice that significantly contributed to the quality of this work.

Gratitude is extended to Lječilište Topusko, Top Terme d.o.o., and Dr. Domagoj Mosler, for their generous cooperation, invaluable assistance, and the provision of existing data, which greatly contributed to the success of this research.

I sincerely thank my colleagues and friends for their moral support and for making this journey more enjoyable. Your constant encouragement helped me stay focused and motivated throughout this process.

I want to express my appreciation to the co-authors of the scientific papers for their valuable contributions, dedication, and successful collaboration.

I would also like to acknowledge the financial support from the Croatian Science Foundation (HRZZ), grant number UIP-2019-04-1218, which made schooling and this research possible.

Finally, I am truly grateful to my family, especially my parents, brother, and Matko, for their endless love, patience, and constant support. Your belief in me made this achievement possible.

Thank you all.

ABSTRACT

Geothermal waters of the Republic of Croatia hold significant energy potential for heating, electricity production, and direct cascading water use in various locations. Due to relatively low usage levels and growing awareness of using renewable energy sources, interest in this resource is expected to increase. Hydrothermal systems, transferring the Earth's internal heat to the surface, vary considerably worldwide due to their different formation mechanisms. They are differentiated based on geological, hydrogeological, and thermal characteristics, necessitating distinct methodological approaches for research. Hydrothermal systems in the Pannonian part of Croatia, where the naturally circulating water transfers heat to the surface, experience higher than average terrestrial heat flow from the asthenosphere due to a regionally thinned lithosphere in the Pannonian Basin System (PBS). Pannonian part of Croatia, known for its elevated geothermal gradient, is located at the SW margin of PBS, which is a back-arc basin developed as a result of the Miocene extensional disintegration of orogenic terrains and subsequent events of basin evolution.

The Topusko hydrothermal system (THS), where natural thermal springs with temperatures up to 53 °C emerge, is located at the tectonic boundary of two major tectonic units: the Dinarides in the SW and the southwestern margin of the PBS to the NE. Therefore, the Topusko THS is characterised by favourable geothermal characteristics (average geothermal gradient approximately 40 °C/km). In the past fifty years, thermal water has served as a basis for developing tourism and health care centres, and since the 1980s, it has been utilised for district heating. Despite the great natural potential of the Topusko geothermal resource, geological research is scarce, and unpublished reports on well construction and revitalisation make up most of the available data. Here, multidisciplinary research, including hydrogeological, geothermal, hydrogeochemical, structural, and geophysical investigations, was conducted with the objective of refining the available conceptual model, which was finally physically validated by constructing a numerical model of THS. Good conceptual and numerical models of groundwater flow and heat transport enable the delineation and protection of recharge areas, the determination of sustainable extraction rates, and ensuring the sustainable use of natural thermal springs.

The primary objectives of the presented work within the scope of the doctoral dissertation were to characterise naturally emerging thermal waters, reconstruct the geological setting, and refine the existing conceptual model through hydrogeochemical, geophysical, and hydrogeological analyses. The research included detailed hydrogeochemical characterisation,

which revealed Ca-HCO_3 facies of Topusko thermal waters heated in a Mesozoic carbonate aquifer with an estimated equilibrium temperature of 78-90 °C, based on historical and new data, respectively. The thermal water emerges through an identified fault damage zone in Topusko, which provides the permeability necessary for the upwelling of thermal water. Aquifer transmissivity values from step-drawdown tests were found to range between 1.8×10^{-2} and 2.3×10^{-2} m^2/s.

Further, a two-year hydrogeochemical and isotopic monitoring program identified that the thermal waters are of meteoric origin, recharged during colder climatic conditions around the late Pleistocene to Early Holocene, with the last atmospheric contact approximately nine thousand years ago. Stable and radioactive isotopes, alongside chemical geothermometers, were used to understand the origin and interactions of these waters with the system. Monitoring of hydrogeochemical parameters in Topusko thermal waters provided further insights into system changes from baseline levels, aiding in the identification of potential anthropogenic impacts and natural changes on the system.

Integrating structural, geochemical, and hydrogeological data led to a novel conceptual model of the Topusko hydrothermal system. The stratigraphic sequence and regional structural setting were defined based on geological maps and extensive field investigations, showing that the thermal waters circulate within a carbonate aquifer, receiving diffuse recharge from Triassic carbonates about 13 km south of Topusko. The regional thrusts and the Topusko anticline structure facilitate the gravity-driven flow of groundwater in a northward direction and its subsequent upwelling at the Topusko discharge area. Numerical fluid flow and heat transport simulations corroborate the proposed conceptual model, showing a thermal anomaly approaching the field temperature observations. In particular, a thermal anomaly was modelled in the Topusko subsurface with temperature values of 31.3 °C and 59.5 °C at the surface and the base of the thermal aquifer, respectively.

Presented research enhanced the understanding of the THS, highlighting the influence of regional and local geological structures on fluid dynamics. These insights are crucial for the sustainable utilisation and environmental protection of the thermal resources in the area, paving the path for future multidisciplinary research to further refine the conceptual model of THS.

Keywords: hydrothermal system, thermal spring, conceptual modelling, multidisciplinary approach, fractured carbonates, Topusko

Prošireni sažetak

Geotermalne vode Republike Hrvatske imaju značajan energetski potencijal za grijanje, proizvodnju električne energije i neposredno kaskadno korištenje vode na brojnim lokacijama. S obzirom na niski stupanj korištenja geotermalnog potencijala u Hrvatskoj i porast svijesti o potrebi korištenja obnovljivih izvora energije, očekuje se povećanje interesa za ovaj resurs u bliskoj budućnosti (Roscini i dr., 2020; Directive EU/2023/2413). Kako bi se on koristio na održiv način, potrebno je poznavanje procesa koji ga pokreću i utječu na njega.

Hidrotermalni sustavi, koji prenose unutarnju toplinu Zemlje na površinu, značajno se razlikuju u svijetu zbog različitih mehanizama formiranja. Razlikuju se na temelju geoloških, hidrogeoloških i toplinskih karakteristika, što zahtijeva različite metodološke pristupe istraživanju. Hidrotermalne sustave u panonskom dijelu Hrvatske, gdje prirodna cirkuliracija vode prenosi toplinu na površinu, karakterizira povišeni toplinski tok iz astenosfere (76 mW/m^2), zbog regionalno stanjene litosfere u Panonskom bazenskom sustavu (PBS). Panonski dio Hrvatske poznat je po povišenom geotermalnom gradijentu (49 °C/km) (Bošnjak i dr., 1998). Nalazi se na JZ rubu PBS-a, zalučnog bazena nastalog kao rezultat miocenske ekstenzije te dezintegracije orogenih terena i naknadnih događaja tijekom evolucije bazena (Tomljenović & Csontos, 2001; Schmid i dr., 2008; Horváth i dr., 2015).

U proučavanju hidrotermalnih sustava potrebno je odrediti porijeklo fluida i područje prihranjivanja, prostorno rasprostiranje vodonosnika, smjer toka fluida i dubinu do koje se spušta te uzroke i načine zagrijavanja i izviranja. Potencijalno područje prihranjivanja u ranim fazama istraživanja se određuje geološkom prospekcijom, odnosno definiranjem izdanaka dobro propusnih stijena na topografski istaknutim područjima. Što se tiče mogućnosti zagrijavanje vode, važno je utvrditi postoji li na istraživanom području dostatni toplinski tok iz unutrašnjosti Zemlje te omogućuju li stijene prijenos topline prema površini. Isto je tako nužno utvrditi postoje li strukture kojima se oborinska voda može spuštati na veću dubinu, zagrijati i, naposljetku, izvirati.

Šire područje istraživanja (300 km^2) nalazi se otprilike 60 km južno od Zagreba u Sisačko-moslavačkoj županiji, na SI rubu Dinarida i JZ rubu PBS-a te pripada tektonskoj jedinici Unutarnjih Dinarida (Schmid i dr., 2004; Vlahović i dr., 2005; Horváth i dr., 2015; Pavelić i Kovačić, 2018). Termalni izvori u Topuskom, temperatura do 53 °C, nalaze se u Glinskoj depresiji uz istočne padine Petrove gore. Multidisciplinarna istraživanja koja uključuju hidrogeološka, geotermijska, hidrogeokemijska, strukturna i geofizička istraživanja, provedena su sa svrhom izrade i utočnjivanja postojećeg konceptualnog modela hidrotermalnog sustava

Topusko (THS), koji je i fizički validiran izradom numeričkog modela toka podzemne vode i prijenosa topline. Dobar konceptualni te pouzdan numerički model toka podzemne vode i prijenosa topline omogućuje ocrtavanje i zaštitu područja prihranjivanja, određivanje održivih količina crpljenja i osiguravanje dugotrajno održivog korištenja termalnog izvorišta.

Ciljevi i hipoteze

Glavni ciljevi ovog rada uključuju cjelovitu geokemijsku karakterizaciju termalne vode i određivanje ravnotežne temperature geotermalnog rezervoara, rekonstrukciju strukturnog sklopa izvorišnog područja pomoću metode električne tomografije, kako bi se identificirale pretpostavljene rasjedne strukture u podzemlju, utvrđivanje hidrogeoloških parametara geotermalnog vodonosnika u području izviranja hidrotermalnog sustava Topuskog iz novih hidrodinamičkih mjerenja, rekonstrukciju strukturnog sklopa šireg područja prihranivanja i geotermalnog vodonosnika na temelju interpretacije prikupljenih strukturno-geoloških podataka, geološko modeliranje THS-a na temelju novih prikupljenih podataka te numeričko modeliranje toka fluida i prijenosa topline u THS-u na temelju novih podataka. Ciljevi su bazirani na četirima hipotezama: (i) geotermalni vodonosnik u Topuskom je hidrotermalnog postanka, (ii) područje prihranjivanja geotermalnog vodonosnika THS-a je zapadno od navlake Petrove gore, (iii) prirodni termalni izvori u Topuskom nalaze se u oštećenoj zoni rasjeda koja ima dovoljno visoku propusnost da omogući izviranje termalne vode i (iv) temperature u geotermalnom vodonosniku su više nego na prirodnim izvorima.

Znanstveni doprinos

Određivanje hidrogeoloških, hidrogeokemijskih i geotermijskih značajki hidrotermalnog sustava Topusko pomaže u osiguravanju njegovog budućeg održivog korištenja. Definiranje područja prihranjivanja provedeno je sa ciljem zaštite od antropogenih utjecaja koji bi pogoršali količinsko i kemijsko stanje geotermalnog vodonosnika. Provedena multidisciplinarna istraživanja poslužit će za definiranje metodologije za proučavanje karbonatnih geotermalnih vodonosnika hidrotermalnog postanka, koji prihranjuju najveći broj prirodnih termalnih izvorišta u Hrvatskoj.

Metode i postupci

Metodologija se sastoji od četiri različite vrste istraživanja, koje su svojstvene primijenjenim geološkim istraživanjima: (i) bibliografsko istraživanje, (ii) terenski rad, (iii) laboratorijsko istraživanje i (iv) kabinetsko istraživanje.

(i) Prikupljena je i pregledana postojeća literatura i podatci kako bi se identificirale praznine u dosadašnjim saznanjima o području istraživanja te kako bi se predložena istraživanja pozicionirala unutar postojeće baze podataka te oblikovale hipoteze doktorske disertacije.
(ii) Terenski rad uključuje prikupljanje terenskih podataka za hidrokemijska, geofizička, hidrodinamička i strukurno geološka istraživanja na području THS-a.

Monitoring termalne vode u Topuskom proveden je u trajanju dvije godine (2021. - 2023.). Temperatura se kontinuirano pratila korištenjem automatskih uređaja za bilježenje podataka (Onset HOBO U12-015 Stainless Steel Temperature Data Logger). *In situ* mjerenja (na licu mjesta) (pomoću multiparametarske sonde WTW Multi 3630 IDS), preuzimanje podataka iz automatskih mjerača te uzorkovanja termalne vode i oborine za hidrogeokemijske analize provodila su se svaki mjesec. Uzorci vode prikupljani su u polietilenskim bočicama od 100 i 200 ml koje sprječavaju isparavanje te su čuvane u hladnjaku. Koncentracija bikarbonatnog aniona određivana je *in situ* volumetrijskom titracijom pomoću digitalnog titratora (HACH 16900). U izvorišnom području THS-a provedeno je geofizičko profiliranje metodom električne tomografije (ERT), okomito i paralelno s identificiranim i pretpostavljenim podzemnim strukturama. ERT mjerenja su izvedena korištenjem POLARES 2.0 sustava za električno snimanje (P.A.S.I. srl) kako bi se istražila hipoteza o rasjedima potpomognutom prirodnom izviranju termalne vode. Za procjenu hidrogeoloških parametara vodonosnika provedeno je ispitivanje postojećih bušotina metodom testiranja u koracima pomoću digitalnog manometra (Keller LEX1) budući da je termalni vodonosnik u Topuskom arteškog tipa. Geološko i strukturno modeliranje područja istraživanja temeljeno je na postojećim literaturnim i novo prikupljenim terenskim podatcima izdanaka, što je rezultiralo novom interpretacijom regionalnih struktura i njihove evolucije.
(iii) Nakon svake kampanje uzorkovanja, provedena je analiza glavnih aniona i kationa (ionska kromatografija na DIONEX ICS-6000 DP uređaju; Thermo Fischer Scientific Inc., Waltham, Massachusetts, SAD) i analiza izotopa ^{2}H i ^{18}O (spektrofotometrijska metoda, Picarro L2130-I izotopski i plinski analizator). Hach DR3900 spektrofotometar korišten je za određivanje sadržaja SiO_2 u uzorcima termalne vode. Glavni anionski i kationski sastav, koncentracije SiO_2 i stabilni izotopi vode analizirani su u Hidrokemijskom laboratoriju Zavoda za hidrogeologiju i inženjersku geologiju Hrvatskoga geološkog instituta. Glavni ionski sastav uzoraka pružio je uvid u mineraloški sastav vodonosnika, kao i moguće miješanje s vodom iz plićih hladnih vodonosnika u području izviranja (Blake i dr., 2016). Također, korišten je za geotermometriju, zajedno sa sadržajem silicijevog dioksida (SiO_2), za izračunavanje ravnotežnih temperatura ležišta korištenjem različitih empirijskih formula (Blasco i dr., 2017; Ármannsson &

Fridriksson, 2009). Pomoću omjera stabilnih izotopa ^{2}H i ^{18}O u termalnoj vodi i oborini ispitano je meteorsko podrijetlo termalne vode. Osim toga, uzorkovanje vode provedeno je tijekom razdoblja minimalnog i maksimalnog zahvaćanja vode iz bušotina za analize radioaktivnih izotopa (^{3}H i ^{14}C) i analize stabilnih izotopa sulfatnog aniona (^{34}S i ^{18}O). Uzorci su analizirani u vanjskim laboratorijima: ^{3}H i ^{14}C u Laboratoriju za mjerenje niskih radioaktivnosti pri Institutu Ruđer Bošković u Zagrebu, a stabilni izotopi sulfatnog aniona u Laboratoriju za određivanje izotopa u okolišu i hidrološkom ciklusu, Hydroisotop GmbH u Njemačkoj. Na temelju aktivnosti radioaktivnih izotopa određeno je srednje vrijeme zadržavanja vode (od zadnjeg kontakta s atmosferom), kao i moguće miješanje s plitkom podzemnom vodom u izvorišnom području. Analiza ^{34}S i ^{18}O korištena je kao alat za procjenu porijekla sulfata u termalnim izvorima (Thiébaud i dr., 2010), koje ranije nije utvrđivano.

(iv) Obrada prikupljenih hidrokemijskih podataka rađena je u računalnim programima Excel, Diagrammes (Simler, 2012) i Grapher, koji su poslužili za određivanje hidrokemijskih facijesa, indeksa saturacije određenih minerala (npr. kalcit i dolomit), izračun ukupne otopljene krute tvari (eng. total dissolved solids, TDS) i grafički prikaz odnosa glavnih aniona i kationa te izotopnih odnosa u uzorcima termalne vode i oborine. Podaci prikupljeni hidrodinamičkim mjerenjima korišteni su za procjenu transmisivnosti termalnog vodonosnika kroz dobro utvrđenu eksperimentalnu vezu između transmisivnosti i specifičnog kapaciteta zdenaca. Konkretno, korištene su empirijske jednadžbe koje su predložili Fabbri (1997) i Verbovšek (2008) budući da su razvijene za karbonatne termalne, odnosno dolomitne vodonosnike. Obrada dobivenih ERT podataka izvedena je korištenjem Res2DInv računalnog programa. Za potrebe geoloških i strukturnih istraživanja izrađena je kompozitna geološka karta područja istraživanja korištenjem listova osnovnih geoloških karata bivše Jugoslavije u mjerilu 1:100.000, kao i geološka karta bivše Jugoslavije u mjerilu 1:500.000. Izrađen je opis geološke građe šireg područja istraživanja, uključujući kompozitni geološki stup koji ocrtava litostratigrafski i kronostratigrafski slijed naslaga na tom području. Sinteza postojećih podataka napravljena je pomoću GIS računalnog programa i alata za grafičko uređivanje. Na temelju obrađenih prikupljenih podataka interpretirani su regionalni geološki odnosi i strukture, utvrđeni su glavni regionalni rasjedni sustavi na istraživanom području kako bi se rekonstruirao strukturni sklop šireg istraživanog područja te geometrija geotermalnog vodonosnika na regionalnoj razini. Fizička validacija konceptualnog modela numeričkim simulacijama, koja se često koristi za testiranje hipoteza o regionalnim i lokalnim tokovima fluida (Havril i dr., 2016; Montanari i dr. 2017), izvedena je korištenjem komercijalnog programa FEFLOW (Diersch, 2014). Navedene faze rada su se vremenski i sadržajno preklapale i nadopunjavale.

Rezultati i zaključci

Primarni ciljevi doktorske disertacije bili su načiniti potpunu karakterizaciju voda prirodnog termalnog izvorišta, rekonstruirati geološku građu i regionalni strukturni sklop šireg istraživanog područja te u konačnici poboljšati postojeći konceptualni model kroz hidrogeokemijska, geofizička i hidrogeološka istražvanja i pripadajuće analize. Istraživanje je uključivalo detaljnu hidrogeokemijsku karakterizaciju, koja je otkrila Ca-HCO_3 facijes termalnih voda THS-a koje potječu iz mezozojskog karbonatnog vodonosnika u kojem se zagrijavaju do procijenjene ravnotežne temperature od 78 – 90 °C. Termalna voda istječe kroz identificiranu rasjednu zonu u Topuskom, koja osigurava potrebnu propusnost za izviranje termalne vode. Utvrđeno je da se vrijednosti transmisivnosti vodonosnika, izračunate iz rezultata pokusnog crpljenja u koracima, kreću između $1{,}8\times10^{-2}$ i $2{,}3\times10^{-2}$ m^2/s.

Dvogodišnji program hidrogeokemijskog i izotopnog praćenja pokazao je da su termalne vode meteorskog porijekla, da se prihranjivanje odvijalo tijekom hladnijih klimatskih uvjeta oko kasnog pleistocena do ranog holocena, s posljednjim atmosferskim kontaktom prije približno devet tisuća godina. Stabilni i radioaktivni izotopi, uz kemijske geotermometre, korišteni su za definiranje porijekla i interakcija ovih voda sa sustavom. Praćenje vrijednosti hidrogeokemijskih parametara u termalnim vodama THS-a daje uvid u promjene sustava u odnosu na početne razine, što pomaže u identifikaciji potencijalnih antropogenih utjecaja i prirodnih promjena na sustav.

Integracija postojećih i novoprikupljenih strukturnih, geokemijskih i hidrogeoloških podataka dovela je do izrade novog konceptualnog modela THS-a. Stratigrafski slijed i regionalna strukturna građa definirani su temeljem geoloških karata i opsežnih terenskih istraživanja. Rezultati ukazuju da termalne vode cirkuliraju unutar karbonatnog vodonosnika, koji se prihranjuje iz trijaskih karbonata oko 13 km južno od Topuskog. Regionalne navlake i struktura antiklinale Topusko omogućuju gravitacijski tok podzemne vode u smjeru sjevera i njezino izdizanje u području istjecanja u Topuskom. Numeričke simulacije toka fluida i prijenosa topline potvrđuju predloženi konceptualni model, pokazujući toplinsku anomaliju koja se približava temperaturama opažanim u stvarnosti. Modelirana je toplinska anomalija u podzemlju Topuskog s temperaturnim vrijednostima od 31,3 °C na površini odnosno 59,5 °C na dnu termalnog vodonosnika.

Provedeno istraživanje u okviru izrade doktorske disertacije značajno je unaprijedilo razumijevanje THS-a te naglasilo utjecaj regionalnih i lokalnih geoloških struktura na dinamiku fluida. Ovi su uvidi vrlo značajni za održivo korištenje i zaštitu hidrotermalnog sustava u cjelini

te će usmjeriti buduća multidisciplinarnim istraživanjima za daljnje usavršavanje konceptualnog modela THS-a.

Ključne riječi: hidrotermalni sustav, termalni izvor, konceptualni model, multidisciplinarni pristup, razlomljeni karbonati, Topusko

Table of contents

List of Figures

1. INTRODUCTION

1.1. General background on hydrothermal systems in the Pannonian part of Croatia

Geothermal energy, derived from thermal energy stored within the Earth's interior, has a significant role in the European Union's clean energy transition, as outlined in the European Green Deal (European Commission, 2019). As a renewable energy source, it provides a clean alternative to conventional energy generation methods by eliminating combustion, thus facilitating compliance with environmental standards and regulations (Aliyu & Garba, 2019; Roscini et al., 2020; Directive EU/2023/2413). The characteristics, classification and utilisation of geothermal resources are linked to the geological and hydrogeological settings, as well as the thermal aspects of the associated geothermal systems. Geothermal systems, transferring the Earth's internal heat to the surface, vary considerably globally due to their different formation processes (Mocek, 2014). In geothermal systems, heat transfer can occur through various mechanisms, but when it involves naturally circulating water in either a liquid or vapour state, it is classified as a hydrothermal system (Ojha et al., 2021; Khodayar & Björnsson, 2024). These systems are usually categorised based on their temperature. A hydrothermal system is considered low-temperature if the fluid in the aquifer has a temperature below 90 °C, making it insufficient for electrical energy production (Bowen, 1989; Williams et al., 2011).

A review study by Goldscheider et al. (2010) emphasises the significance of deep carbonate rock aquifers, particularly those exhibiting some degree of karstification, as a source of thermal water outside volcanic regions. While a comprehensive global evaluation of these resources remains elusive, numerous documented examples highlight their vital role in supplying thermal baths and geothermal facilities. The authors point to Europe's largest naturally flowing thermal water system, originating from Triassic carbonate rocks and feeding the renowned baths of Budapest, Hungary, as a prime example (Dublansky, 1995; Balderer et al., 2014). Similarly, this trend extends globally amongst other countries, such as Switzerland (Volpi, 2018), France (Widhen et al., 2023), Italy (Torresan et al., 2022), the UK (Farr & Bottrell, 2013), Turkey (Dilsiz, 2004), Poland (Kaminskaite-Baranauskiene et al., 2023), Jordan (Schäffer & Sass, 2014), Tunisia (Dhia, 1987), Canada (Grasby et al., 2000), and China (Lei et al., 2022), with Stuttgart, Germany, boasting Europe's second-highest concentration of mineral and thermal springs, again associated with a karst aquifer (Goldscheider et al., 2003;

Ufrecht, 2006, 2015). These widespread occurrences underscore the important role that karst aquifers play in providing thermal water resources across the globe.

Karst landscapes are characterised by the occurrence of prominent springs (Ford & Williams, 2007), where the ones with elevated temperatures are termed as thermal springs. They are often distinguished based on the temperature, although the definitions for related terms such as cold, lukewarm, warm and hot are absent. Therefore, two common thresholds are frequently utilised, including the average local air temperature and the temperature of the human body, making the springs whose temperature is more than 5 °C above the mean annual air temperature thermal (Goldschier et al., 2010; Pentecost, 2003). This definition has a clear limitation: a spring with a temperature of 5 °C qualifies as thermal in colder regions, whereas a spring in the tropics must reach 20 °C to meet the criterion. Considering the climatic conditions of the area where springs occur is essential. According to Borović & Marković (2015) and Kovačić (1998), thermal spring localities in the Pannonian part of Croatia are traditionally categorised using a modified balneological scale from subthermal (13 – 20 °C), hypothermal (20 – 34 °C), homeothermal (34 – 38 °C) to hyperthermal (>38 °C). It is visible that the balneological scale is formed in relation to the human body temperatures (lower than, similar to, and above that temperature). The modification is made in the lower part of the spectrum (subthermal) and refers to temperatures above-average air temperatures in the Pannonian part of Croatia, where the majority of natural thermal springs are situated.

In such non-volcanic areas, various heat sources and transport mechanisms contribute to the formation and functioning of hydrothermal systems (Drogue, 1985; Bowen, 1989). Earth's residual internal heat and radioactive decay act as primary sources. The average continental thermal gradient (30 °C/km) translates to a heat flow of 65 mW/m², though volcanic zones can exhibit much higher gradients (100 – 200 °C/km or more) (Economides & Ungemach, 1987). Heat transfer occurs by mechanisms of conduction, convection, and radiation , with fluid convection being the most efficient (Sass, 2007). Upwelling thermal groundwater in discharge zones further elevates near-surface geothermal gradients and heat flow (Bredehoeft & Papadopulos, 1965; Goldscheider, 2010).

The Pannonian Basin System (PBS), including the Croatian part at the SW edge, is a significant area of interest for geothermal research due to its geological and tectonic characteristics. Natural thermal springs fed by fractured and karsified carbonate aquifers are found in approximately two dozen localities in the Croatian part of the PBS, with temperatures reaching up to 62 °C (Borović et al., 2016). These springs are the discharge features of hydrothermal systems, often characterised by recharge in the mountainous hinterlands and

water circulation through carbonate geothermal aquifers. The elevated heat flow in this region is attributed to a higher-than-average geothermal gradient (49 °C/km), resulting from the thinned lithosphere due to Miocene back-arc extension, which allows substantial heat flow (76 mW/m^2) from the asthenosphere to the surface (Bošnjak et al., 1998; Horváth et al., 2015; Leneky et al., 2002).

In the PBS, three levels of the regional flow of thermal water have been identified: i) gravity flows in the Neogene-Quaternary clastic rocks and sediments of the basin fill (the shallowest), ii) gravity flows in pre-Neogene confined carbonate aquifers below them, and iii) flow caused by overpressure in the deepest Mesozoic aquifers (Figure 1, Horváth et al., 2015; Vass et al., 2018). As the main geothermal aquifers in Croatia, the Mesozoic carbonate rocks often crop out as inselbergs or along the basin margins, which implies greater recharge in these marginal parts where the aquifer is shallower and is covered by thinner Neogene deposits (Stevanović et al., 2015; Havril et al., 2016). In a study by Deming (2002), subsurface waters were sorted into oceanic, meteoric, and evolved water. In such hydrothermal systems, where the natural discharge of thermal water is present, the water is dominantly of meteoric origin (Ármannsson, 2012; IAEA, 2013). Still, sometimes connate and magmatic waters are involved. Thermal water is considered a form of evolved water, which can originate from the ocean or the atmosphere, where the initial composition undergoes changes through physical and chemical processes. The groundwater flow in such systems is primarily gravity-driven, influenced by topographic gradients between the recharge and discharge areas (Horváth et al., 2015).

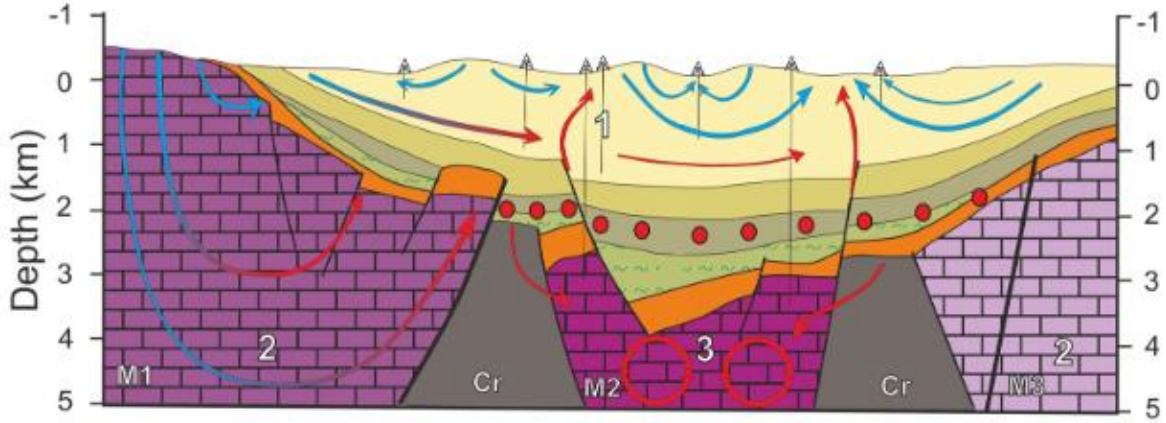

Figure 1. From Horvath et al. (2015). A N-S cross-section depicts the main grounwater flow systems and associated geothermal resources in the Pannonian Basin System. The color gradient of arrows (blue to red) signifies increasing water temperature. Two gravity-driven flow systems are identified: (1) within the porous sedimentary basin fill and (2) in Mesozoic carbonates (including Eocene and/or Miocene formations in some areas). Additionally, a high-pressure system (3) exists beneath a sealing layer (red ellipses) and encompasses lower Pannonian and Early to Middle Miocene basin fill along with fractured basement rocks. The abbreviations M1, M2, and M3 represent Mesozoic carbonate rocks. Cr stands for the crystalline basement.

In specific hydrogeological settings, groundwater recharge occurs through various mechanisms. These include mountain front or hillslope runoff, seepage from sinkholes, and contributions from surface water bodies such as lakes, rivers, and canals (Anderson et al., 2015). Comprehending the evolution of thermal water within the geological context and structure of the karst system, along with the flow patterns and boundary conditions in terms of hydraulics and geochemistry, is crucial in the development of a conceptual model of the hydrothermal system. Understanding the factors governing hydrothermal resources at a system level is essential for their sustainable utilisation. This involves identifying recharge areas to refine existing conceptual models, assessing groundwater balance, and enhancing the comprehension of regional and local flow patterns.

Although the water circulation in such karst hydrothermal systems is primarily gravity-driven, resulting from topographic gradients (Tóth, 2009), temperature-induced density gradients promote the upward flow of heated water towards springs, with reduced water viscosity further accelerating circulation. Groundwater flow is significantly influenced by fractures and faults, which can act as conduits or barriers depending on various factors, making their hydraulic function challenging to predict (Caine et al. 1996; Underschultz et al. 2005). High-permeability faults are essential for the development of thermal systems (Forster & Smith 1988a, b; Keegan-Treloar et al., 2022). The dip of faults affects the depth of circulation and, consequently, the temperature of the water, which is why thermal springs are often aligned along the fault lines (Grasby & Hutcheon, 2001; Li et al., 2007; Faulkner et al., 2010; Worthington et al., 2019; Pouraskarparast et al., 2024).

In hydrothermal system research, methods applicable to various tectonic settings and system segments are typically employed. These include field investigations and geophysical data acquisition to reconstruct the geological framework and tectonic evolution. Field investigations reveal surface geological relations, fracture network systems, and fault patterns, providing invaluable insights into subsurface geological reconstruction processes (Muffler & Cataldi, 1978; Flóvenz et al., 2012; Kosović et al., 2023, 2024). Integrating these datasets allows the construction of robust 2D or 3D geological models, essential for understanding hydrothermal aquifer architecture and principal faults. Hydrothermal systems require detailed studies of fluid origin, recharge areas, aquifer geometry, heat transfer mechanisms, fluid flow direction, and conditions under which hydrothermal features manifest at the surface. Identifying and monitoring these parameters is crucial for sustainable geothermal resource management, ensuring constant recharge and protecting the system from adverse impacts (Fetter, 2001; Marini, 2004; Heasler, 2009). All of the mentioned investigations aid in updating and

improving conceptual models of hydrothermal systems. A conceptual model is a simplified representation of a hydrothermal system, integrating geological, hydrological, and geothermal information, helping us visualise the flow paths of heated water, recharge and discharge areas, and the overall structure of the system. This research focused on developing and refining a robust conceptual model for the specific case of the Topusko hydrothermal system situated in the Pannonian part of Croatia.

1.2. Overview of the study area

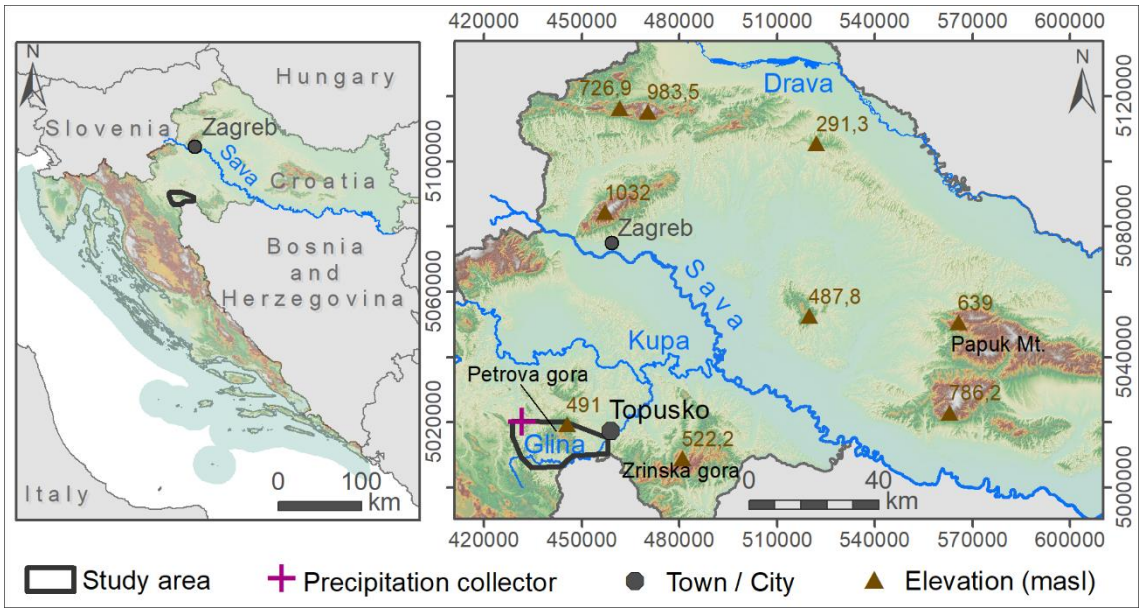

Figure 2. Generalised geographical setting of the study area, i.e., the Topusko hydrothermal system, which is situated between the Petrova gora Mt. to the west and Zrinska gora Mt. to the east. Coordinate system: EPSG 3765.

The town of Topusko, located about 60 km south of Zagreb, is positioned at an altitude of 122 masl between Petrova gora Mt. to the west and Zrinska gora Mt. to the east (Figure 2). Geomorphologically, the city area is a part of the floodplain along the middle course of the Glina river. As of the 2011 census (DZS, 2022), Topusko had 2310 inhabitants and has been inhabited since ancient times due to its rich thermal water springs and ore deposits, with traces dating back to the Neolithic or Copper Age (Šimunić, 2008). The area is renowned for its clay and peat 'mud baths' and thermal water used in balneotherapy (Pavleković, 1986; Čepelak & Mandić, 1989; Čepelak, 2007). During the Croatian War of Independence (1991-1995), Topusko suffered extensive destruction, and much of the damage remains unrepaired to this day. Despite the significant natural potential of the Topusko geothermal resource, geological

investigations remained scarce, with most available data consisting of unpublished reports on well construction and revitalisation.

Topusko experiences a moderate continental climate, slightly influenced by the Mediterranean climate of the northern Adriatic (Zaninović, 2008). Annual precipitation averages around 900 mm, peaking at 1400 mm, mainly in early summer and late autumn. Temperatures range from an average of -1.1 °C in January to 20.8 °C in July, with an annual average of 10.0 °C (DHMZ, 2021).

In the area of Topusko, there are three natural thermal springs with a total yield of approximately 25 l/s (Bać & Herak, 1962; Bahun & Raljević, 1969), and temperatures ranging from 46 °C (Blatne kupelji) to 53 °C (Livadski izvor) (Figure 3) (Pavić et al., 2024a). The artesian thermal springs in Topusko have been renowned since Roman times, ranking as the second warmest in Croatia (Šimunić, 2008; Borović et al., 2016). Previous hydrochemical analyses of thermal water show CaMg-HCO_3 facies indicating water accumulation in carbonate rocks (i.e., dolomite or limestone; Čubranić, 1984). Three production wells were drilled up to the depth of 250 m in the immediate vicinity of the natural springs during the 1980s (Figure 3). They are currently used for heating, recreational and medicinal purposes, with a total capacity of 200 l/s and pressure of around 1.4 bar (Pavić et al., 2023). The decrease in pressure from 2.18 bar (1978) to 1.5 bar (1982) was observed and attributed to overexploitation (Šegotić & Šmit, 2007).

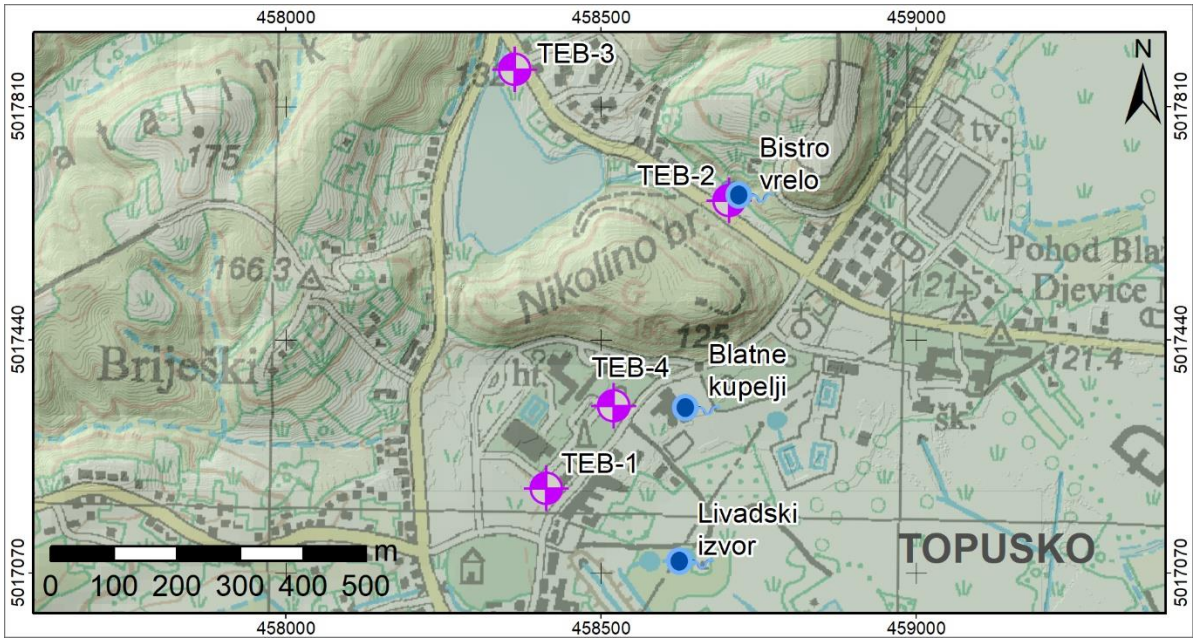

Figure 3. Topusko city area with the location of thermal springs (Livadski izvor, Blatne kupelji and Bistro vrelo) and production wells (TEB–1–4). Coordinate system: EPSG 3765.

Thermal water with temperatures up to 65 °C has been utilised since the 1980s for health and recreational purposes and district heating (Čubranić, 1984; Šegotić & Šmit, 2007). However, the geological features driving the development of the Topusko hydrothermal system (THS) and regulating regional groundwater flow direction remained unclear. In the initial stages of THS research, the potential recharge area was identified by locating outcrops of permeable rocks in topographically elevated regions around Topusko. However, the absence of systematic and detailed structural-geological and hydrogeological studies has impeded the reconstruction of the regional geological relations and understanding of the THS functioning. Although available publications and unpublished reports propose conflicting hypotheses, the most commonly referenced conceptual model dates back to the early 2000s (Šimunić, 2008).

Šimunić (2008) proposed that the THS recharge area is located west of the Petrova gora Mt., where Triassic carbonates crop out. According to the proposed model, the water circulates from W to E below the Petrova gora Mt. nappe, heats up due to geothermal gradient, and discharges in highly permeable fault damage zones in Topusko. Besides the mentioned publication, detailed bibliographic research determined that there were no published scientific papers or doctoral dissertations on the topic of the mentioned investigations in the THS area before this research. Only one professional article, one book chapter, four unpublished reports from the Archive of the Croatian Geological Survey (HGI-CGS), and two graduate theses were identified. In this study, as a result, unpublished reports collected from users of thermal springs made up the majority of the initial dataset for the study area (20 reports dating from 1978 to 2013).

1.3. Multidisciplinary approach to conceptual modelling

In the study of hydrothermal systems, it is necessary to determine the origin of the fluid and the area of recharge, the spatial aquifer distribution, the direction of the fluid flow and the depth to which it descends, as well as the causes and the means of heating and upwelling to the surface. Multidisciplinary research, which includes hydrogeological, geothermal, hydrogeochemical, structural, and geophysical investigations, was used to construct a conceptual model of the THS based on the synthesis of acquired results from different research methods. The applied methodology consisted of four different types of research, which are inherent to applied geological research: (i) bibliographic research, (ii) fieldwork, (iii) laboratory research, and (iv) desk research.

(i) Collection and review of existing literature and data was done to identify gaps in the field of research and area of interest, position our research within the existing knowledge base, and formulate the doctoral dissertation's hypotheses.

(ii) Fieldwork was done for the acquisition of new data and included re-ambulation of geological maps and detailed hydrogeological and structural mapping; performing hydrodynamic measurements at existing abstraction wells was done to determine hydrogeological parameters of geothermal aquifers; continuous monitoring of groundwater temperatures at thermal springs was established, as well as periodic monthly hydrogeological monitoring and sampling at thermal springs for major anion and cation and stable isotopes ^{2}H and ^{18}O analyses (a); water sampling during minimum and maximum production for radioactive isotope analyses (^{3}H and ^{14}C) and stable ^{34}S and ^{18}O isotope analyses from sulphate anion (b), and ERT geophysical profiling in the area of thermal water discharge. Figure 4 shows field sampling locations for hydrogeological monitoring, including the precipitation collector positioned in the assumed recharge area (Figure 4A), sampling locations TEB-4 well in Topusko (Figure 4B), and *in situ* measurements and sampling at Livadski izvor spring (Figure 4C, D).

(iii) Laboratory research included hydrogeochemical analyses of thermal water samples done in the Hydrochemical laboratory of the HGI-CGS (a), and those listed under (b) subcontracted from other laboratories (Hydroisotop GmbH in Germany and Ruđer Bošković Institute in Croatia).

(iv) Desk research included analysing and interpreting acquired structural-geological, hydrogeochemical, hydrogeological, thermal, and geophysical data. After data interpretation, 2D geological modelling based on existing and newly acquired data followed, along with the conceptualisation of THS and its functioning, attributing hydraulic and thermal parameters to modelled geological units, creation of 2D numerical fluid flow and heat transport models, and final renewed conceptualisation of THS and its functioning.

Figure 4. The precipitation collector is positioned in the assumed recharge area (A), TEB-4 well in Topusko (B), and *in situ* measurements and sampling at Livadski izvor spring (C, D).

1.4. Objectives and hypotheses of research

The main objectives of the research:

1. Establish a complete geochemical characterisation of the thermal water and determine the geothermal reservoir equilibrium temperature;
2. Reconstruct the structural setting of the discharge area using electrical resistivity tomography to identify the supposed fault structures in the subsurface;
3. Determine hydrogeological parameters of the geothermal aquifer in the discharge area of the Topusko hydrothermal system from new hydrodynamic measurements;
4. Reconstruct the structural setting of the proposed recharge area and geothermal aquifer based on the interpretation of collected structural-geological data;
5. Perform geological modelling of the Topusko hydrothermal system based on newly acquired data;

6. Perform numerical modelling of fluid flow and heat transport in the Topusko hydrothermal system based on newly acquired data.

In accordance with the purpose of the research and the defined objectives, the research hypotheses were formulated as follows:

1. Topusko geothermal aquifer is of hydrothermal origin.
2. Recharge area of the Topusko geothermal aquifer is west of the Petrova gora nappe.
3. The natural thermal springs in Topusko occur in a fault damage zone of intersecting faults, which has high enough permeability to enable the upwelling of thermal water.
4. Temperatures in the geothermal aquifer are higher than at the natural springs.

1.5. Scientific contribution

This research makes significant scientific contributions to the understanding of THS functioning by determining its hydrogeological, hydrogeochemical, and geothermal characteristics. It aims to ensure the sustainable future use of this geothermal resource. By defining the recharge area of THS, this research will help in the future protection of the geothermal aquifer from adverse impacts, preserving its good quantitative and chemical status. Additionally, the applied multidisciplinary methodology serves as a foundation for the development of a methodology for studying carbonate geothermal aquifers of hydrothermal origin, which supply water to the largest number of natural thermal springs in Croatia. The proposed novel and updated conceptual model of THS will promote its sustainable utilisation and benefit its future research.

2. ORIGINAL SCIENTIFIC PAPERS

2.1. Multidisciplinary Research of Thermal Springs Area in Topusko (Croatia)

By

Mirja Pavić, Ivan Kosović, Marco Pola, Kosta Urumović, Maja Briški and Staša Borović

sustainability

MDPI

Article

Multidisciplinary Research of Thermal Springs Area in Topusko (Croatia)

Mirja Pavić, Ivan Kosović *, Marco Pola, Kosta Urumović, Maja Briški and Staša Borović

Croatian Geological Survey, Ulica Milana Sachsa 2, HR-10000 Zagreb, Croatia; mpavic@hgi-cgs.hr (M.P.); mpola@hgi-cgs.hr (M.P.); kurumovic@hgi-cgs.hr (K.U.); mbriski@hgi-cgs.hr (M.B.); sborovic@hgi-cgs.hr (S.B.)
* Correspondence: ikosovic@hgi-cgs.hr; Tel.: +385-1-6160-831

Abstract: Topusko is the second warmest natural thermal water spring area in Croatia, located at the southwest edge of the Pannonian Basin System. Due to favourable geothermal properties, these waters have been used for heating and health and recreational tourism since the 1980s. Thermal springs with temperatures up to 50 °C are the final part of an intermediate-scale hydrothermal system. However, systematic research on the Topusko spring area has not been conducted to lay the foundation for sustainable resource utilisation. Multidisciplinary research including the hydrogeochemical characterisation of naturally emerging thermal water, an electrical resistivity tomography (ERT) investigation conducted to reconstruct the subsurface geology, and hydrogeological parametrisation of the geothermal aquifer was carried out to refine the existing local conceptual model. The results show Ca-HCO_3 facies of Topusko thermal waters, which get heated in a Mesozoic carbonate aquifer. The water equilibrium temperature in the geothermal aquifer is estimated to be 78 °C based on the *SiO_2-quartz* geothermometer. The fault damage zone, which enables the upwelling of thermal water, was identified by ERT investigations. The transmissivity values of the aquifer derived from the results of step-drawdown tests range from 1.8×10^{-2} to 2.3×10^{-2} m^2/s. Further multidisciplinary research is necessary to improve the existing conceptual model of the Topusko hydrothermal system.

Keywords: thermal spring; hydrogeochemical characteristics; electrical resistivity tomography; hydrogeological parameters; hydrothermal system; Croatia

Citation: Pavić, M.; Kosović, I.; Pola, M.; Urumović, K.; Briški, M.; Borović, S. Multidisciplinary Research of Thermal Springs Area in Topusko (Croatia). *Sustainability* **2023**, *15*, 5498. https://doi.org/10.3390/su15065498

Academic Editor: Ozgur Kisi

Received: 28 February 2023
Revised: 15 March 2023
Accepted: 16 March 2023
Published: 21 March 2023

1. Introduction

Geothermal energy is a renewable energy source that encompasses the thermal energy generated and/or stored in the subsurface, representing a strong driver of the EU's clean energy transition as envisioned by the European Green Deal [1–5]. It is considered an inherently clean form of energy without combustion that facilitates meeting environmental standards and regulations. When it can be economically extracted from an aquifer and used for generating electric power or any domestic, agricultural, or industrial application, it forms a geothermal resource [6]. The availability of a geothermal resource can contribute to domestic economic health, decrease the annual energy trade deficit, and reduce dependence on imported energy. Its characteristics and possible modalities of utilisation are closely related to the geological and hydrogeological setting of the connected geothermal system. To classify a geological system as geothermal, three main elements must be present: a source of heat and fluid, an aquifer that accumulates them, and a barrier that retains them [7].

There are several classifications for geothermal resources based on their geological or engineering characteristics [8–10]. According to [10], there are three main types of geothermal resources based on their geological characteristics and the heat transfer mechanism: (i) hydrothermal convection resources, (ii) hot igneous resources, and (iii) conduction-dominated resources. When the underlying mechanism of heat transfer involves the convection of water in a liquid or vapour state, it is considered a hydrothermal system. Hydrothermal systems include a recharge area where meteoric water infiltrates into the

subsurface, a geothermal aquifer where water gets heated by terrestrial heat flow, and a discharge area where the heated water flows out in the form of natural thermal springs [7,11]. The outflow of thermal waters is generally driven by favourable structural conditions that increase the local permeability [10–12].

Determining the geological and hydrogeological settings driving a hydrothermal system is crucial in order to understand its development and renewability. The renewability of a hydrothermal system depends on continuous and sufficient recharge by meteoric water and heat inflow, while sustainable utilisation depends on both the local hydrogeological characteristics and the exploitation scheme. As many European and Croatian strategic documents regulating energy, tourism, and environmental protection envisage the use of thermal water in order to transit towards climate neutrality, a detailed characterisation of the resource is needed to assess its renewability and propose a long-term sustainable utilisation scenario.

The characterisation of resources through hydrogeochemical, geophysical, hydrodynamic, and geological investigations is commonly used for the exploration of hydrothermal resources and to assess their renewability and the sustainability of utilisation practices [7,11,13–15]. Hydrogeochemical methods are an effective tool to determine the origin of the geothermal fluid, the interaction with the aquifer, aquifer equilibrium temperature, water mean residence time, and possible mixing processes [16–18]. Geophysical methods can be used to reconstruct the geological and structural settings in the subsurface assessing the volume of the aquifer and the geometry of the fault network that drives the fluid flow [19–21]. In addition, the management of the geothermal aquifer requires an assessment of the hydrogeological parameters of an aquifer, such as hydraulic conductivity, transmissivity, and porosity.

Geothermal waters in the Republic of Croatia have significant potential for large-scale heat generation, cascading water uses, and local power generation [22]. They generally occur in areas of high surface heat flow and are predominantly hosted in Mesozoic carbonate rock [23,24]. One of the most relevant thermal manifestations in Croatia is represented by the thermal springs in Topusko, being the second warmest natural spring area in Croatia. Springs with temperatures of up to 50 °C attracted people's attention already in Roman times [25]. Four exploitation wells were drilled in the 1980s with depths of 80–250 m, enabling the outflow of artesian waters of up to 66 °C. Thermal waters have been directly used for heating and balneology. During the Croatian War of Independence (1991–1995), the area of Topusko suffered enormous destruction, and the damage has not been fully repaired to this day. Before that, the consumption of thermal water for therapy, recreation, and heating of residential and commercial buildings was higher.

Despite the great natural potential of the Topusko geothermal resource, research is scarce, and unpublished reports on well construction and revitalisation make up most of the available data. Multidisciplinary research of the discharge area is one of the steps leading to the development of an improved conceptual model of the Topusko hydrothermal system (THS). The main objectives of this work are (i) the hydrogeochemical characterisation of the naturally emerging thermal water and the estimation of the aquifer equilibrium temperature, (ii) the reconstruction of the subsurface geological setting and the identification of preferential flow paths allowing the thermal water outflow in the spring area, and (iii) the hydrogeological parameterisation of the geothermal aquifer.

2. Materials and Methods

2.1. Study Area

The town of Topusko is located approximately 60 km south of Zagreb in the lowlands along the eastern slopes of Petrova gora hill (Figure 1). Geomorphologically, the Topusko area belongs to the floodplain along the middle course of the Glina river. According to the 2021 census, the town of Topusko had 2310 inhabitants [26]. This area has been inhabited since ancient times due to the rich thermal water springs and ore deposits. A moderate continental climate prevails in the study area, slightly influenced by the Mediterranean

climate of the northern Adriatic [27]. The annual average precipitation is 900 mm and up to 1400 mm in the period of 1961–1990 (Sisak meteorological station), with peaks at the beginning of summer and the end of autumn. Average monthly air temperatures range from −1.1 °C in January to 20.8 °C in July, while the annual average is 10 °C [28].

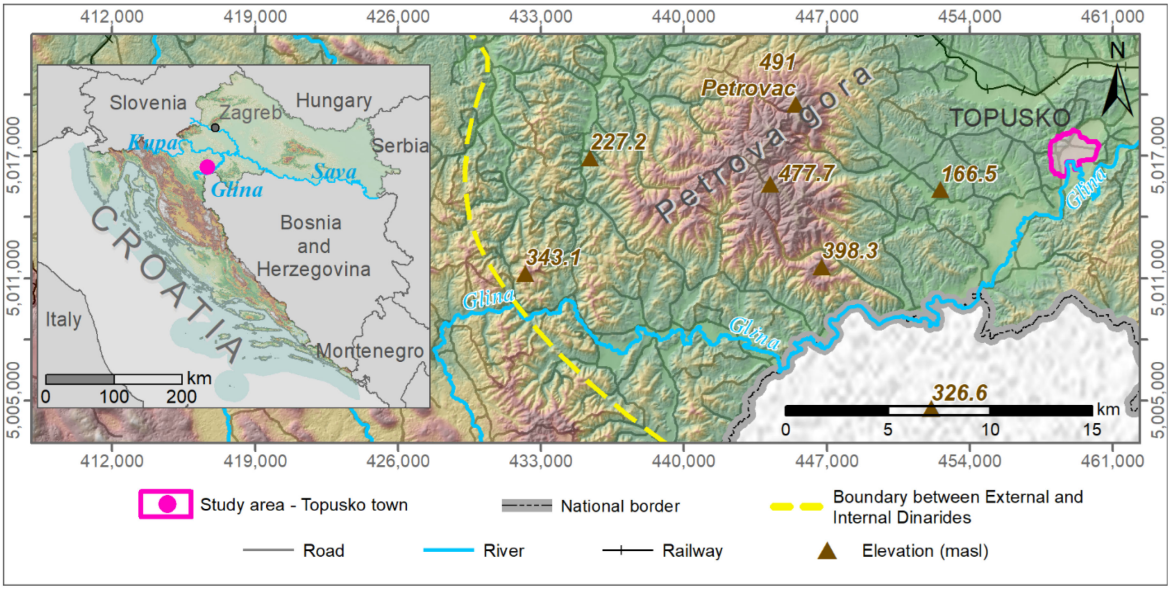

Figure 1. Geographical setting of the study area. The division between the major tectonic units of the External and Internal Dinarides (W and E, respectively) is simplified from [29–31]. Coordinate system: EPSG 3765.

Geological and Hydrogeological Setting

The study area is located at the NE margin of the Dinarides, belonging to the tectonic unit of the Internal Dinarides [23,29]. Figure 1 shows the tectonic contact dividing External and Internal Dinarides. External Dinarides are characterised by a thick sequence of Mesozoic carbonates (up to 8 km), being part of the Adriatic microplate [29,32]. The Internal Dinarides consist of a set of complex nappe sheets comprising continental-derived deposits sedimented at the distal edge of the Adriatic microplate, formed mainly during the last orogeny from the Cretaceous to the Cenozoic [30]. Furthermore, the Topusko area is located at the southwest margin of the Pannonian Basin System, sharing its favourable geothermal characteristics connected to back-arc crustal thinning. In the Croatian part of the Pannonian basin, natural thermal water springs emerge at two dozen localities, with temperatures up to 58 °C [24,33].

The surface geology in the area of Topusko is mostly characterised by Pliocene to Holocene sedimentary deposits (hereafter referred to as Plio–Quaternary deposits) up to 90 m thick. They consist of clays, sands, and gravels laying discordantly over older lithological units (Figure 2). Locally, older deposits consisting of loose Badenian arenites (M_4) crop out. Below these units, the occurrence of Miocene marls and sandstones and Mesozoic dolomites interlayered with sandstones and marls was determined by drilling. The spring area is presumed to be bounded by three faults that form a block in the form of a three-sided prism (Figure 2), enabling the uplifting of Triassic carbonates, which were determined to be the aquifer [34].

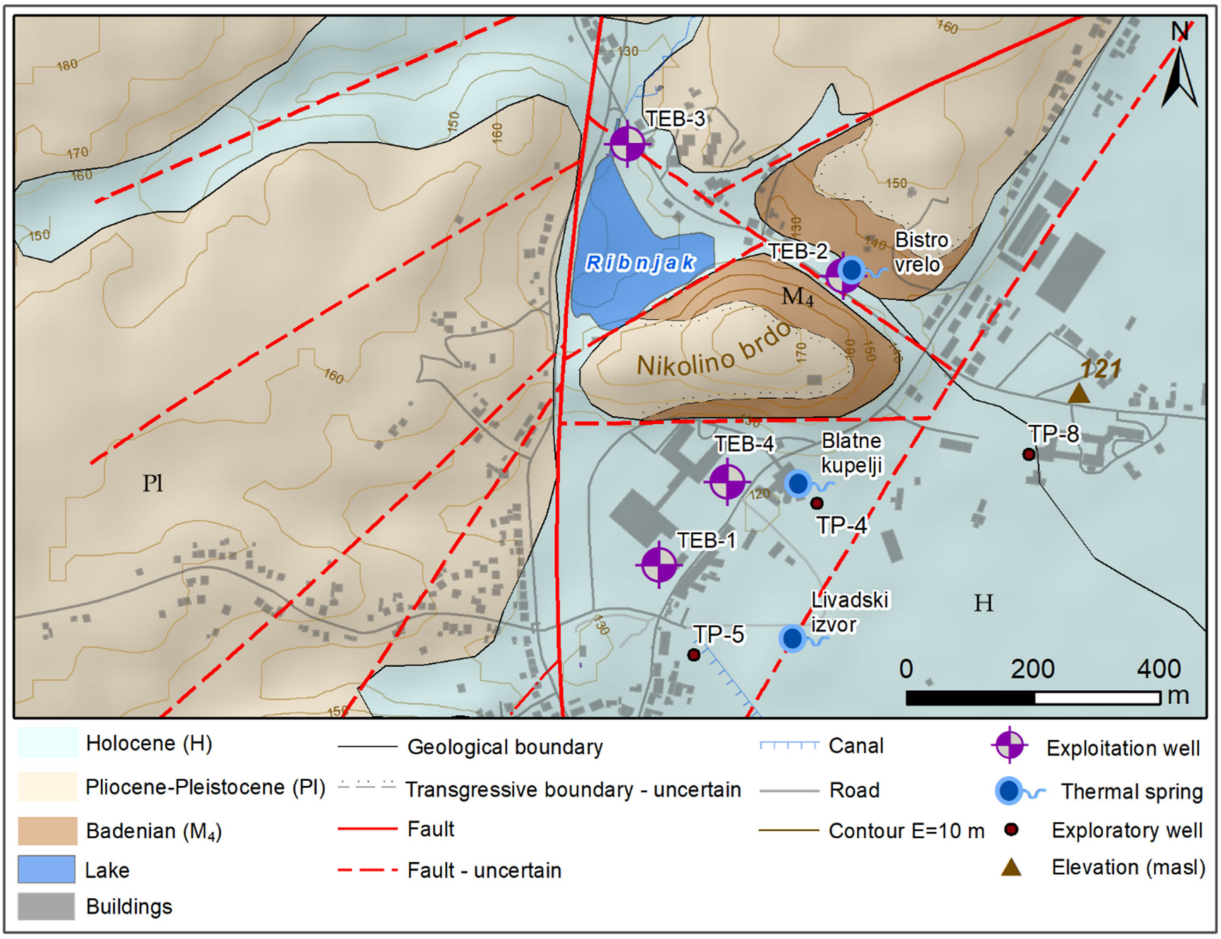

Figure 2. Geological map of the study area modified from [34,35] with the positions of natural thermal springs and exploitation and exploratory wells in Topusko town.

There are three natural artesian thermal springs (Figure 2; Livadski izvor, Blatne kupelji, and Bistro vrelo springs) with temperatures up to 50 °C and an estimated total capacity of approximately 20 L/s [36,37]. In particular, the Livadski izvor spring is the second warmest thermal spring in Croatia. Four exploitation wells (TEB-1 to 4) were drilled during the 1980s based on the results of eight exploratory wells (i.e., TP 1 to 7 with depths up to 50 m and temperatures between 28 and 62 °C, and TP 8 with a depth of 170 m and temperature of 62 °C). TEB-1, 3, and 4 have constantly been operating, being the source for heating, balneology, and health tourism in Topusko. TEB-2 was damaged, and it is no longer in operation. The wells are artesian with a pressure of 0.5 to 2.3 bar, a temperature of 64 to 68 °C, and an estimated total capacity of 200 L/s [38,39]. A water permit was issued in 1998, allowing exploitation with a maximum flow rate of 151 L/s. However, annual consumption data (2009–2013) show that the actual average flow rate is approximately 30 L/s, pointing to very low utilisation.

From a hydrogeological perspective, Mesozoic carbonates represent the geothermal aquifer of the THS, while younger Neogene sediments characterised by generally lower permeability represent the aquitard at the top of the aquifer [35,40].

Šimunić [34] proposed a conceptual model of THS. The recharge area is to the west of the Petrova gora hills, where Triassic carbonates crop out. Infiltrated waters flow in the Mesozoic carbonates below the Paleozoic metamorphic units of the Petrova gora nappe, reaching a depth of 3 km. In Topusko, a set of faults forming a block in the shape of a three-sided prism enabled the uplifting of the aquifer. However, the geological relations that enable the emergence of thermal water on the surface are still not fully understood.

2.2. Geochemical Investigations

2.2.1. Chemical Composition of Groundwater

The chemical composition of groundwater is determined by the original composition of the infiltrated water and the chemical reactions occurring in the aquifer during its flow. Its final composition is influenced by many factors including altitude, vegetation, climate, and the mineralogical composition of the aquifer. The principal anion and cation composition gives insight into the mineralogical composition of the aquifer, as well as possible mixing with water from shallower cold aquifers in the spring areas [17,41]. In addition, selected chemical compounds can be used to calculate the aquifer equilibrium temperature by using different empirical formulae [42–44].

Hydrochemical analyses conducted during several sampling campaigns in the 1980s were collected for this work [36,45–47]. The hydrogeochemical parameters of thermal water samples included groundwater temperature (T), pH, major ions (Ca^{2+}, Mg^{2+}, Na^{+}, K^{+}, $HCO_3{}^{-}$, $SO_4{}^{2-}$, and Cl^{-}), and silica (SiO_2). The quality of the analysis was tested by evaluating the charge balance and its error through the equation:

$$\text{Charge balance error } (\%) = \frac{\sum_{\text{cations}} - \sum_{\text{anions}}}{\sum_{\text{ions}}} \times 100, \quad (1)$$

where the ionic concentrations are in meq/L. Samples with a charge balance error of more than ±2% were excluded from further analysis [17,48,49].

Processing of acquired data was carried out in Excel and DIAGRAMMES computer software, which was used to make the Piper diagram and to calculate total dissolved solids (TDS) [50]. A trilinear Piper diagram was used to graphically determine groundwater hydrochemical facies based on the chemical composition of thermal water samples and their dominant ions [51,52]. In addition, the equivalent ratio of Ca^{2+}/Mg^{2+}, $(Ca^{2+} + Mg^{2+})/(HCO_3{}^{-})$, $(Ca^{2+} + Mg^{2+})/(HCO_3{}^{-} + SO_4{}^{2-})$, and the molar ratio of $Ca^{2+}/(Mg^{2+} + Ca^{2+})$ vs. $SO_4{}^{2-}/(SO_4{}^{2-} + HCO_3{}^{-})$ in groundwater were graphically analysed, detailing the water–rock interactions in the system.

2.2.2. Geothermometers

The maximum temperature reached by the thermal waters in the aquifer is an important parameter determining the potential of using an individual geothermal resource [18]. This parameter can be determined using chemical geothermometers. Chemical geothermometry is based on the temperature dependence of mineral–fluid equilibrium. The main assumptions of geothermometry are that (i) fluids are in chemical equilibrium, (ii) the mineral assemblage is thermodynamically stable, and (iii) thermal water retains its chemical properties during its upwelling to the surface [53].

Classical chemical geothermometers, which include the dissolved silica geothermometer *SiO_2-quartz* and *SiO_2-chalcedony*, were used to predict the aquifer temperature of the THS. They consist of experimentally calibrated equations ([54] (2), [55] (3), and [56] (4) for the *SiO_2-quartz* geothermometer; [55] (5) and [57] (6) for the *SiO_2-chalcedony* geothermometer) that enable the determination of the water temperature in the aquifer using the SiO_2 concentrations. The equations used for the *SiO_2-quartz* geothermometers are:

$$T = \frac{1315}{5.205 - \log(SiO_2)} - 273.15\ (^{\circ}C), \quad (2)$$

$$T = \frac{1309}{5.19 - \log(SiO_2)} - 273.15\ (^{\circ}C), \quad (3)$$

$$T = \frac{1315}{0.435 - \log(SiO_2)} - 273.15\ (^{\circ}C). \quad (4)$$

The equation used for the *SiO_2-chalcedony* geothermometers are:

$$T = \frac{1032}{0.435 - \log(SiO_2)} - 273.15\ (^{\circ}C), \quad (5)$$

$$T = \frac{1112}{4.91 - \log(SiO_2)} - 273.15\ (^{\circ}C). \quad (6)$$

Concentration units are in mg/L, except for (4), which is in mol/L. The application of a quartz geothermometer is recommended for aquifer temperatures above 150 °C. Below that, chalcedony usually controls the dissolved silica content [11,18].

2.3. Hydrogeological Investigations

Well tests on TEB-1 and 3 were conducted in September 2021 and 2022 to assess the hydrogeological characteristics of the aquifer. Due to the construction of the wells, step-drawdown tests with variable pumping rates (Q) were carried out by estimating the wells' efficiencies and the transmissivity of the aquifer. The water pressure was measured at a time interval of 1 s using a digital manometer (Keller LEX1) with a resolution of 0.1 mbar, while the water temperature was measured once for every pumping rate step. The water density was determined from its temperature, and the pressure drop was converted in drawdown (Δ in m).

The drawdown results were determined from both aquifer and well losses [58]. The aquifer losses (B) are head losses occurring in the aquifer that vary linearly with the well discharge. Well losses can be linear (B′) and non-linear (C) and are caused respectively by (i) the damage to the aquifer during the drilling and the completion of the well and (ii) the turbulent flow in the well and its surroundings. Linear and non-linear losses can be determined using the equation [59]:

$$\Delta = (B + B')Q + CQ^n, \quad (7)$$

with n varying from 1.5 and 3.5. The generally accepted value of n = 2 was used in the interpretation of the step-drawdown test results [60].

The B + B′ and C parameters were calculated through a linear regression from the experimental Δ and Q values [61]:

$$\frac{\Delta}{Q} = (B + B') + CQ \quad (8)$$

Different statistical indicators were used to assess the reliability of the linear regression. The B + B′ and C coefficients were used to calculate the theoretical Δ at the measured Q. The well efficiency was calculated as the ratio between the linear losses and the total Δ.

The collected data were also used to assess the transmissivity of the thermal aquifer through the well-established experimental relation between the transmissivity of the aquifer and the specific capacity of the well (SC = Q/Δ). Both experimental and theoretical Δ were used to calculate SC. The aquifer transmissivity (T) was estimated following the equations:

$$T\ (m^2/day) = 0.85 \times SC^{1.07}, \quad (9)$$

$$T\ (m^2/s) = 2.39 \times SC^{1.07}. \quad (10)$$

These equations [62,63] were considered since they were developed, respectively, for a carbonate thermal aquifer in Italy and dolomite aquifers in Slovenia. SC was calculated for steps showing well efficiency higher than 50%, and an average value of SC was used to determine T.

2.4. Geophysical Investigations

Geophysical investigations can be used to reconstruct the geological and structural settings of the subsurface based on the physical properties of the different geological elements. These methods are fruitful where the geological setting is concealed below the alluvial cover and boreholes could provide only partial reconstruction due to lateral variations in the geological setting. Electrical resistivity tomography (ERT) is a non-invasive and fast geophysical method, usually applied to obtain high-resolution 2D images of the subsurface resistivity. This method can be used to define the geometry of an aquifer, delineate the structural and lithological setting of the subsurface, and determine the geometry of faults and the width of the connected, water-saturated fault zones [64–66].

Three ERT profiles (TOP-1, TOP-2, and TOP-3) were recorded in 2021. The ERT surveys were performed using the POLARES 2.0 electrical imaging system by P.A.S.I. srl, which uses a sinusoidal alternating current of variable frequency. A multi-electrode resistivity system consisting of stainless-steel electrodes with constant spacing, connected by a multi-core cable, was used [67,68]. Surveys were performed using a Wenner–Schlumberger array at a frequency of 1.79 Hz and a maximum phase of 20° (delay of the voltage signal with respect to the current signal). This configuration resolves horizontal and vertical structures, maintaining a good investigation depth (i.e., approximately one-fifth of the section length in the central part of the profile [69–72]). The TOP-1 profile was measured using 64 electrodes spaced 5 m apart, resulting in a total length of 315 m. TOP-2 and 3 profiles were conducted using 32 and 48 electrodes, respectively, and an electrode spacing of 10 m, resulting in a total profile length of 310 m and 470 m, respectively.

RES2DINV resistivity inversion software was used to invert the apparent resistivity data measured in the field into a 2D resistivity model of the subsurface [73]. The smoothness-constrained least-squares method [74,75] based on an L2 norm [76,77] was used for the data inversion. This method minimises the square of the differences between the measured and calculated apparent resistivity values and typically produces smoothly varying resistivity distributions.

The stratigraphic logs of the wells provided hard data to corroborate the interpretation of the resistivity models. In particular, the TOP-1 profile crosses the TEB-2 well, while TOP-2 and TOP-3 profiles are located in the close vicinity of the TEB-4 well.

3. Results

3.1. Geochemical Characterisation of Thermal Groundwater

3.1.1. Major Ions Chemistry

A total of 39 chemical analyses of major ion content from thermal waters in Topusko were collected from unpublished reports. Nine samples with a reaction error over ±2% were excluded from further analysis. Table 1 shows the concentrations of major ions of sampled thermal water, along with temperature, pH, and SiO_2 measurements. The data are organised based on the sampling location.

The monitored thermal spring Livadski izvor showed a temperature of 50 °C, while the exploitation and exploration wells showed average temperatures of 65 and 51 °C, respectively. Thermal water pH was neutral to slightly basic, averaging 7.0 and 7.5 for Livadski izvor spring and exploitation wells, respectively (Table 1). TDS ranged from 505 to 592 mg/L, being within the range for thermal springs in carbonate aquifers of the Inner Dinarides, which generally show TDS lower than 1 g/L [78]. Nonetheless, the generally low concentrations of the cations and anions resulting in low mineralisation of the groundwater in the study area indicate a precipitation recharge-dominated groundwater system.

Table 1. Physical and chemical parameters of sampled thermal waters.

Name	Depth	Date	T	pH	Ca^{2+}	Mg^{2+}	Na^{+}	K^{+}	HCO_3^{-}	SO_4^{2-}	Cl^{-}	TDS*	SiO_2
	m		°C	-	mg/L								
Livadski izvor	0	1904	49.5	-	89.39	19.74	18.27	12.69	270.4	108.10	19.40	586	29.96
		12/1988	50	7.0	85.20	17.50	15.20	7.20	244.4	89.20	21.30	521	25.6
TEB-1	243	5/1983	66	7.2	87.10	18.20	23.30	9.30	268.5	103.30	22.00	581	31.0
		7/1983	64.5	7.65	88.00	18.20	17.20	6.00	240.0	107.00	21.20	550	30.0
		9/1983	65	7.6	88.00	18.20	24.00	4.00	238.0	110.00	22.70	554	30.5
		11/1983	66	7.4	86.20	19.40	16.80	9.80	262.2	100.00	20.00	566	32.0
		2/1984	65	7.3	95.90	11.28	18.10	11.30	268.4	95.63	21.94	564	25.8
		10/1985	65	7.7	84.20	17.40	15.30	10.60	238.0	104.2	22.50	542	29.5
TEB-2	150	5/1983	67	7.1	90.20	17.60	18.40	11.10	259.3	96.00	22.30	553	24.0
		7/1983	66	7.1	90.20	18.20	22.00	10.10	265.4	104.00	21.50	579	30.0
		9/1983	67	7.4	86.00	17.60	22.00	6.00	231.0	105.70	22.50	540	30.5
		11/1983	67	7.2	86.00	18.20	18.70	11.10	250.2	102.80	23.00	560	31.0
		10/1985	68	7.9	85.10	17.40	15.80	9.20	244.1	104.5	23.30	547	28.9
TEB-3	163	5/1983	66	7	88.20	18.80	18.30	7.80	262.4	100.40	21.90	556	24.0
		7/1983	62	7.65	86.20	18.20	17.00	6.00	244.0	100.80	20.90	539	29.0
		9/1983	63	7.6	96.00	18.80	18.00	3.90	286.8	96.50	22.70	588	28.5
		11/1983	66	7.3	88.20	17.60	18.40	10.00	250.2	108.60	22.00	566	32.0
		2/1984	66	7.25	85.88	16.49	24.50	13.20	268.4	94.41	21.85	567	26.3
		12/1988	-	7.2	88.20	19.60	12.80	11.40	228.8	98.76	39.00	563	30.80
TEB-4	80.8	11/1985	64	7.1	84.20	16.30	15.42	15.60	247.10	100.40	22.10	544	23.5
TP-5	50	1978	36	7.65	84.16	15.80	14.00	20.80	268.0	83.10	19.70	543	23.4
TP-4	50	5/1983	52	7.2	87.10	18.20	23.10	8.26	280.6	101.00	21.60	578	23.6
		7/1983	52	7.65	84.20	15.80	16.90	8.20	232.0	88.50	21.00	505	21.0
		9/1983	54	7.1	92.00	17.00	19.00	4.00	259.3	90.00	22.90	549	28.0
		11/1983	52	7.3	86.20	16.80	18.80	11.60	268.5	89.00	22.60	556	26.5
TP-8	170	5/1983	58	7.15	90.20	18.20	16.10	11.40	265.0	107.80	22.30	576	28.0
		7/1983	53	7.8	87.20	17.00	17.80	9.00	238.0	100.00	20.90	528	24.0
		9/1983	53	7	90.20	18.20	18.00	10.70	259.0	102.70	22.10	566	28.0
		11/1983	54	7.4	94.20	18.20	15.70	12.70	268.5	102.80	23.00	581	29.0
		2/1984	48	7.3	87.31	19.96	24.60	11.30	268.4	116.40	20.71	592	26.9

Charge balance errors are ±2%. TDS* was calculated in Diagrammes software, V6.5 [50].

The major anion and cation composition of thermal water is graphically presented in the Piper diagram (Figure 3) [51]. All samples show Ca-HCO_3 hydrochemical facies [79], with a dominance of Ca^{2+} cation followed by Mg^{2+}, which is a characteristic of groundwater in carbonate aquifers [80–82]. The ion composition is almost constant over time, which indicates a large and stable hydrothermal system.

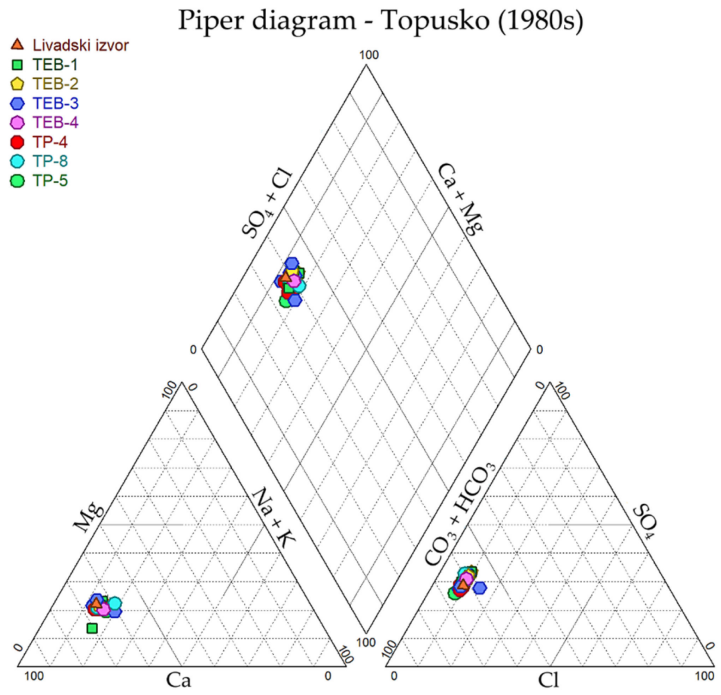

Figure 3. Piper diagram of the examined samples.

The diagram in Figure 4a shows the $Ca^{2+}/(Ca^{2+} + Mg^{2+})$ mole ratio in Topusko thermal waters compared with freshwater samples from the carbonate–evaporite formation aquifer [83]. A mole ratio of 1 corresponds to the dissolution of pure calcite, while 0.5 corresponds to the dissolution of stoichiometric dolomite. All samples from Topusko are characterised by values from 0.81 to 0.89 (average 0.83), indicating that groundwater reacts with both dolomite and calcite. In Figure 4b, the Ca^{2+}/Mg^{2+} ratio diagram shows the dominance of Ca^{2+} in all sampled thermal waters, which should be 1 in a system dominated by pure dolomite. This ratio suggests the interaction of Topusko thermal water with limestones [84,85], pointing to their occurrence in the aquifer together with the dolomites found in the thermal wells. Figure 4c shows the ratio of $Ca^{2+} + Mg^{2+}$ and HCO_3^-. According to the stoichiometry of the reaction of carbonate rock dissolution, the milligram equivalent ratio of $(Ca^{2+} + Mg^{2+})/(HCO_3^-)$ should be 1 when HCO_3^- is derived from the dissolution of carbonate minerals (calcite and dolomite) and only carbonic acid is involved in the reaction. Collected thermal groundwater samples have an average equivalent ratio of 1.4, suggesting that the dissolved inorganic carbon is mainly composed of bicarbonate and related to carbonate dissolution. This ratio positions the samples slightly above the 1:1 line, indicating an excess of $Ca^{2+} + Mg^{2+}$ ions over HCO_3^- and reflecting an additional source of Ca^{2+} and Mg^{2+}. The milligram equivalent ratio of $(Ca^{2+} + Mg^{2+})/(HCO_3^- + SO_4^{2-})$ for the thermal water samples is 0.9, almost on the 1:1 line (Figure 4d), indicating that in addition to HCO_3^-, the $SO4_2^-$ ion is also involved in balancing Ca^{2+} and Mg^{2+}. The dissolution of carbonate rocks with carbonic acid is accompanied by sulphuric acid. If the gypsum dissolution was the main natural process, Ca^{2+}/SO_4^{2-} would have had an equivalent ratio of 1. Instead, the samples showed an equivalent ratio of 2.1, suggesting that the excess of Ca^{2+} comes from carbonate dissolution, and the origin of the sulphate anion remains undetermined. The dissolution resulting from silicate weathering may have contributed to the groundwater chemistry, providing the additional source of Ca^{2+} and Mg^{2+} balanced by sulphate anions [80,86,87].

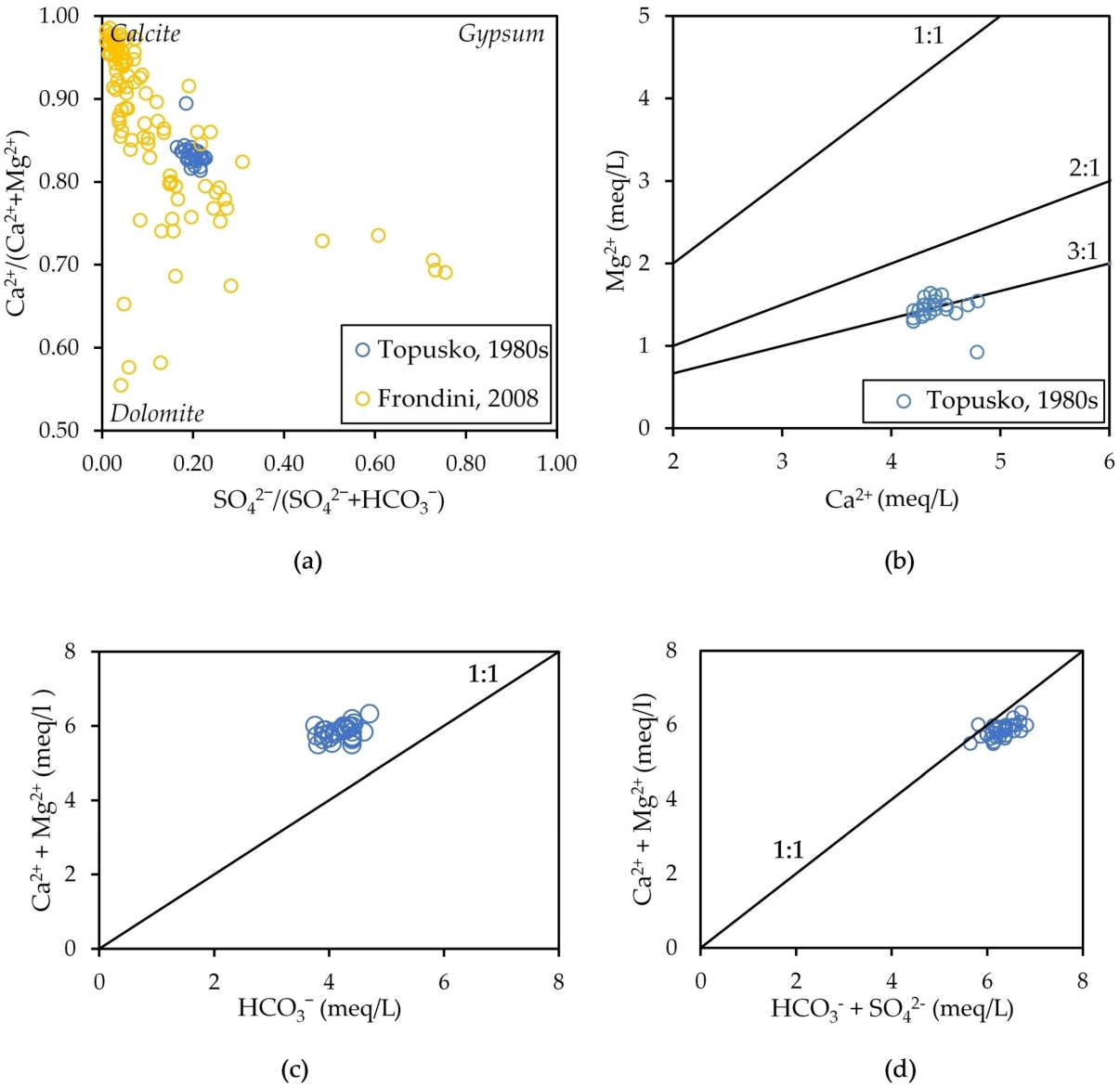

Figure 4. Scatter plots of major ions. (**a**) $Ca^{2+}/(Ca^{2+} + Mg^{2+})$ vs. $SO_4^{2-}/(SO_4^{2-} + HCO_3^-)$ diagram; (**b**) Ca^{2+}/Mg^{2+} diagram with different Ca^{2+}/Mg^{2+} ratios; (**c**) $(Ca^{2+} + Mg^{2+})/(HCO_3^-)$ diagram; (**d**) $(Ca^{2+} + Mg^{2+})/(HCO_3^- + SO_4^{2-})$.

Figures 3 and 4 point to (i) carbonate dissolution as the primary process driving the solute content in the thermal waters of Topusko, (ii) the interaction of the waters with Mesozoic carbonates that represent the main aquifer of THS, and (iii) the presence of limestone and dolomite rock in the system.

3.1.2. Geothermometrical Results

Table 2 shows the results obtained by the application of *SiO_2-quartz* and *SiO_2-chalcedony* geothermometers for assessing the aquifer equilibrium temperature of the THS. The average mass concentration of SiO_2 (Table 1) is 27.8 mg/L for the Livadski izvor spring and ranges from 23.5 to 29.8 mg/L for wells TEB-1 to 4. These silica concentrations provide an aquifer equilibration temperature of 76 °C applying the *SiO_2-quartz* and 46 °C applying *SiO_2-chalcedony* geothermometers. The medians of the calculated temperatures are 78 °C and 47 °C, respectively.

Table 2. Temperatures (°C) calculated by applying experimentally calibrated *SiO_2-quartz* and *SiO_2-chalcedony* geothermometers for the Topusko thermal water samples.

Name	Truesdell (1976) [54]	Fournier (1977) [55]	Michard (1979) [56]	Fournier (1977) [55]	Arnòrsson et al. (1983) [57]
	SiO_2-Quartz			*SiO_2-Chalcedony*	
Livadski izvor	76	76	78	45	48
TEB-1	79	79	78	48	51
TEB-2	78	78	80	46	49
TEB-3	77	77	78	46	49
TEB-4	70	70	71	38	41

The temperatures calculated using the chalcedony geothermometers are slightly lower than the measured temperature in the natural thermal spring and significantly lower than temperatures measured in wells. Consequently, these results are unreliable since the water temperature would have decreased during its ascent to the surface due to the cooling effect.

Therefore, quartz is the phase most likely to control the dissolved silica content in thermal waters [88]. Dissolved silica is most likely released into the water due to chert dissolution or clay mineral alteration [46,47]. The average aquifer temperature of THS is predicted to be approximately 78 °C, as several studies showed realistic results for the temperatures obtained with experimentally calibrated *SiO_2-quartz* geothermometers [88,89].

3.2. Hydrogeological Parametrisation Results

3.2.1. TEB-1 Step-Drawdown Test

Six pumping rates (Q) ranging from 2.7 to 24.1 L/s were used, resulting in a progressive decline in water pressure from 1.4 to 1.05 bar. The density of water was calculated using its temperature, and the pressure drop was converted to drawdown (in m), yielding a maximum reduction of 3.62 m with a flow rate of 23.41 L/s. A representative pressure value for every pumping rate was calculated using the last 100 measurements in the step (P_{fin} in Table SA1 of Figure S1).

The linear regression between Δ/Q and Q (Table SA2 of Figure S1) resulted in an intercept of 62.78, corresponding to B + B′, and a slope of 3686.34, corresponding to C. The high coefficient of determination and the low standard errors (r^2 and se, respectively, in Table SA2 of Figure S1) suggest a good fit between the regression and the data. The B + B′ and C values were inserted into (7), obtaining the theoretical drawdown vs. flow rate curve (Table SA3 in Figure S1) for the TEB-1 well:

$$\Delta = 62.78Q + 3686.3Q^2 \quad (11)$$

The obtained parameters were used to determine the well efficiency. The well efficiency is good (70–80%) at low flow rates, and it drastically drops to approximately 40% at higher flow rates, suggesting significant head losses in the well. Poor well efficiency is also suggested by the C value, indicating severe clogging in the well [58].

An average specific capacity was calculated from the flow rates and the drawdowns of the first to fourth testing steps since the fifth and sixth steps showed the highest well losses reflecting the lowest efficiency. The resulting transmissivity from Equations (9) and (10) was approximately 2×10^{-2} m^2/s, which corresponds to a hydraulic conductivity of approximately 2×10^{-4} m/s considering that the thickness of the aquifer in TEB-1 is 106 m [47].

3.2.2. TEB-3 Step-Drawdown Test

Four pumping rates (Q) ranging from 2.8 to 12.8 L/s were used, resulting in a progressive decline in water pressure from 0.7 to 0.66 bar. The density of water was calculated using its temperature, and the pressure drop was converted to drawdown (in m), yielding a maximum reduction of 0.35 m with a flow rate of 12.8 L/s. A representative pressure

value for every pumping rate was calculated using the last 100 measurements in the step (P_{fin} in Table SB1 of Figure S2).

The linear regression between Δ/Q and Q (Table SB2 of Figure S2) resulted in an intercept of 9.81, corresponding to B + B′, and a slope of 1316.4, corresponding to C. The Pearson coefficient $r > 0$ ($r = 0.84$) shows a positive correlation, indicating an increase in pressure drop (Δ/Q) with an increase in the pumping rate (Q). Compared to TEB-1 results, the linear correlation between the variables is weaker. However, medium to low standard errors (se in Table SB2 of Figure S2) suggest a relatively good fit between the regression and the data. Therefore, a linear relationship between these two variables is considered. The B + B′ and C values were inserted in (7), obtaining the theoretical drawdown vs. flow rate curve (Table SB3 in Figure S2) for the TEB-3 well:

$$\Delta = 9.81Q + 1316.4Q^2 \quad (12)$$

The obtained parameters were used to calculate the well efficiency. The well efficiency is good (60–70%) at low flow rates, and it drops to approximately 37% at higher flow rates, suggesting significant head losses in the well.

An average specific capacity was calculated from the flow rates and the drawdowns of the first and second testing steps. The resulting transmissivity for both Equations (9) and (10) in Section 2.3 was 1.1×10^{-2} m^2/s and 1.4×10^{-2} m^2/s, respectively. However, since the stratigraphic log of the well is not available, the corresponding hydraulic conductivity was not calculated.

3.3. Interpretation of ERT Results

Figure 5 shows three cross-sections (TOP-1, 2, and 3) of continuous 2D resistivity models of the subsurface.

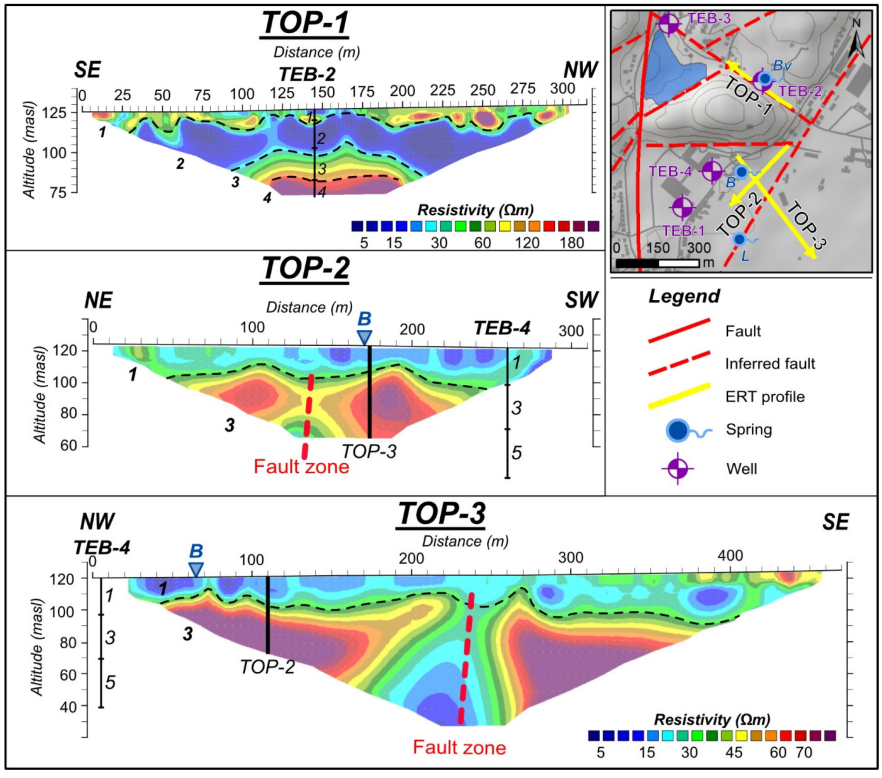

Figure 5. Inverted resistivity profiles TOP-1, 2 and 3 and the locations of ERT profiles within the study area. TOP-2 and 3 share the same resistivity values displayed in the legend. Locations of natural thermal springs are also presented: B is Blatne kupelji spring, Bv is Bistro vrelo spring, and L is Livadski izvor spring.

The TOP-1 profile reached an investigation depth of approximately 50 m. The data inversion resulted in an RMS error of 12.5% with resistivity values between 2 and 650 Ωm. Four layers could be distinguished based on resistivity distribution (Figure 5). The upper layer (1) has a variable thickness of 5–10 m and is characterised by resistivity values ranging from 35 to 100 Ωm. This zone contains local anomalies with both low (5–30 Ωm) and high (generally 100–150 Ωm, and up to 650 Ωm at 250 m distance) resistivity values. Considering the stratigraphic log of the TEB-2 well, this layer can be interpreted as Plio–Quaternary alluvial and proluvial deposits comprising unconsolidated sediments with variable grain sizes. The observed resistivity variations are consistent with the typical lateral heterogeneity of such deposits, with clays characterised by low and sands by high resistivities. The second layer (2) has a relatively constant thickness of approximately 20 m and shows lower resistivity values ranging from 5 to 25 Ωm. According to the stratigraphic log of TEB-2, this layer can be interpreted as Miocene marls, which is consistent with the observed resistivity range. The third layer (3) has a constant thickness of 35 m and resistivities ranging from 80 to 140 Ωm, which are consistent with the values expected for Miocene sandstones saturated with thermal water as detected in the TEB-2. Below layer 3 follows a layer characterised by resistivity values of 150 to 300 Ωm (4). According to the stratigraphic log of the TEB-2, this layer corresponds to Miocene interbedded sandstones and marls.

The profiles TOP-2 and TOP-3 reached an investigation depth of approximately 60 and 80 m, respectively, and the data inversion resulted in an RMS error of 6.2% and 7.6%, respectively. Their interpretations are comparable because they show similar resistivity distributions (Figure 5). Resistivity inversion values range from 5 to 110 Ωm, and two layers could be distinguished. The upper layer (1) shows a variable thickness from 10 to 25 m and is characterised by resistivity values generally from 5 to 45 Ωm. This layer was interpreted as Plio–Quaternary deposits based on the stratigraphic log of the TEB-4 well. The resistivities of these deposits generally correspond to the values observed in the TOP-1 profile. The lower layer (3) shows higher resistivities ranging from 60 to 110 Ωm. Based on the stratigraphic log of TEB-4, the resistivities of this layer can be linked to Miocene sandstone deposits. Similarly, the values of this layer can be correlated with the resistivity values of layer 3 in the TOP-1 profile. Furthermore, the TOP-2 and TOP-3 profiles show a sudden decrease in the resistivity within layer 3. The low resistivity anomaly is located at approximately 140 m in TOP-2 with values from 30 to 50 Ωm and at approximately 240 m in TOP-3 with values from 5 to 30 Ωm. These anomalies can be interpreted as highly permeable fault damage zones, which enable the upwelling of thermal waters. Due to its high secondary porosity, the fault zone could store a higher volume of thermal water, resulting in lower resistivity values than in the unfractured surrounding sandstones.

4. Discussion and Conclusions

In Topusko town, thermal waters have been used for heating, medicinal, and recreational purposes since the 1980s. However, detailed research on the processes driving this hydrothermal system has never been conducted. Multidisciplinary research (i.e., hydrogeochemistry, hydrogeology, and geophysics) was conducted in Topusko to improve the existing local conceptual model.

According to [18], the first step in geothermal exploration is a geochemical characterisation of thermal water. Thermal springs in Topusko show a discharge temperature of 50 °C (Livadski izvor), while nearby exploitation wells produce water of an average temperature of 65 °C and a near-neutral pH. Thermal water major ions content shows Ca-HCO_3 hydrochemical facies and indicates the origin of all samples from the same aquifer. According to [90], thermal waters have medium to low mineralisation [52,91], corroborating the precipitation recharge-dominated groundwater system. The major anion and cation composition does not show significant changes over time, which suggests a large and stable hydrothermal system. Carbonate dissolution is the primary process driving the solute content in the thermal water, which suggests the interaction of the water with

Mesozoic carbonates and supports the assumption that they represent the main geothermal aquifer of THS. The Ca^{2+}/Mg^{2+} ratio shows the dominance of Ca^{2+} in all samples, which would be 1 in a system with a predominance of dolomite formations, as proposed by [34]. The results of this research (Figure 4) indicate a water–rock interaction with both limestones and dolomites, suggesting that both lithologies are present in the system. The premise by [34] was probably based on the observed dolomite outcrops W of Petrova gora nappe.

Hydrochemical data were used to assess the aquifer equilibrium temperature. A minimum groundwater circulation depth [17] can be calculated using the surface temperature of the water as the ratio between (i) the temperature difference of measured spring or well temperature and the local average annual surface temperature (°C) and (ii) the local geothermal heat gradient (°C/km). This calculation is based on the assumption that cooling is negligible, as occurring in artesian aquifers or springs/wells with high flow rates. The minimum groundwater circulation depth for Topusko water was calculated as approximately 1.1 km. Furthermore, the aquifer temperature was estimated using a classical chemical *SiO_2-quartz* geothermometer. The results pointed to an aquifer equilibrium temperature of 78 °C, suggesting a circulation depth of 2 km and considering a geothermal gradient of 35–40 °C/km [92]. The main limitation of hydrochemical investigations was that recent data are lacking and it was necessary to rely on older existing data. Since the 1980s, analytical techniques have been improved in general, and many other parameters are now routinely measured, which was not the case in those times.

Electrical resistivity tomography (ERT) survey was conducted, identifying fault damage zones in the spring area, which provide a preferential pathway for groundwater upwelling to the surface from a confined geothermal aquifer [12] since no significant flow is expected through confining units. In addition, the geographical location of the springs themselves may indicate the fault occurrence below the surface. The correlation between the observed resistivity and lithology, together with nearby stratigraphic well logs, helped to refine the conceptual model of the local geological setting.

Step-drawdown tests on wells TEB-1 and 3 were performed in order to estimate a substantial hydrogeological parameter—transmissivity (T). It is approximately 2×10^{-2} m^2/s, which corresponds to a hydraulic conductivity (K) of approximately 2×10^{-4} m/s, considering that the thickness of the carbonate aquifer in TEB-1 is 106 m. The calculated hydraulic conductivity value is within the range of hydraulic conductivities for fractured carbonates commonly found in the literature [81,93].

The presented research improved the local conceptual model of THS. The main findings point to (i) faults-driven thermal springs, (ii) the geothermal aquifer hosted in Mesozoic carbonates, comprising limestones and dolomites, (iii) the equilibrium aquifer temperature estimated at 78 °C, and (iv) the hydraulic conductivity of the geothermal aquifer in the spring area up to 2×10^{-4} m/s.

A further step would include detailing the regional conceptual model since the existence of a hydrothermal system is generally the result of a delicate balance between the flow rate, dissolution/precipitation processes, and local/regional scale structural setting. In order to use the existing thermal water resource sustainably, the functioning of the whole system, from recharge to discharge area, needs to be subjected to multidisciplinary study. Hydrothermal systems can change due to local or distant events (i.e., climate changes, earthquakes, and thermal water abstraction) that could alter the water source, the preferential flow paths, the subsurface thermal characteristics, or the permeability field in the fractured geothermal aquifer [94]. Hydrogeochemical monitoring helps to detect such changes, and it is considered one of the most effective tools to assess the response of the aquifer to production stress, including recharge and pressure drop [18]. The choice of method suitable for the disposal of utilised thermal water also depends on the quality of the thermal fluids and local hydrogeological and environmental conditions. Future research should involve monitoring the thermal waters in Topusko and the application of both chemical and isotopic analyses [11,18,89].

In addition to hydrochemical surveys, in the search and determination of the recharge area, the second step would be scanning for carbonates on the surface and conducting structural–geological research to understand the regional geological setting and possible flow directions. This will provide more evidence for the hypotheses on the recharge area of the Topusko geothermal aquifer.

Multidisciplinary research is an indispensable tool for the development and improvement of the existing conceptual model of THS. The integration of local and regional models will serve as a base for the sustainable utilisation of THS, as increasing interest in this resource is expected in the near future.

Supplementary Materials: The following supporting information can be downloaded at: https://www.mdpi.com/article/10.3390/su15065498/s1, Figure S1: Interpretation of the step-drawdown test results conducted in the TEB-1 well; Figure S2: Interpretation of the step-drawdown test results conducted in the TEB-3 well.

Author Contributions: Conceptualisation and methodology, M.P. (Marco Pola), S.B. and M.P. (Mirja Pavić); data collection by all authors; data curation, M.P. (Mirja Pavić), M.P. (Marco Pola), M.B. and I.K.; software and formal analysis, I.K., M.P. (Marco Pola), M.P. (Mirja Pavić), K.U. and M.B.; writing—original draft preparation, M.P. (Mirja Pavić); writing—review and editing, M.P. (Marco Pola), M.P. (Mirja Pavić) and S.B.; visualisation, M.P. (Marco Pola), M.P. (Mirja Pavić) and I.K.; supervision, S.B.; research design and funding acquisition, S.B.; project administration, M.P. (Mirja Pavić) and S.B. All authors have read and agreed to the published version of the manuscript.

Funding: This research was funded by Croatian Science Foundation (HRZZ), grant number UIP-2019-04-1218.

Institutional Review Board Statement: Not applicable.

Informed Consent Statement: Not applicable.

Data Availability Statement: Data available on request from the authors.

Acknowledgments: The authors would like to thank Lječilište Topusko and Top-Terme d.o.o. for cordial cooperation, logistic help on-site, and sharing of existing materials (unpublished reports from their archives).

Conflicts of Interest: The authors declare no conflict of interest.

References

1. A European Green Deal—European Commission. Available online: europhttps://commission.europa.eu/strategy-and-policy/priorities-2019-2024/european-green-deal_ena.eu (accessed on 16 January 2022).
2. CORDIS-EU Research Results—Supporting the Development of Europe's Geothermal Energy Sector. Available online: https://cordis.europa.eu/article/id/442048-supporting-the-development-of-europe-s-geothermal-energy-sector (accessed on 16 January 2022).
3. Aliyu, S.; Garba, M.M. Review on current global geothermal energy potentials and the future prospects. *Int. J. Adv. Sci. Eng.* **2019**, *5*, 10-31695. [CrossRef]
4. Roscini, A.V.; Rapf, O.; Kockat, J.; Milne, C.; Jeffries, B.; D'angiolella, R. *On the Way to a Climate-Neutral Europe Contributions from the Building Sector to A Strengthened 2030 Climate Target*; Buildings Performance Institute Europe (BPIE): Brussels, Belgium, 2020; Available online: www.bpie.eu (accessed on 14 November 2022).
5. Avci, A.C.; Kaygusuz, O.; Kaygusuz, K. Geothermal energy for sustainable development. *J. Eng. Appl. Sci.* **2020**, *9*, 1414–1426.
6. Gupta, H.; Sukanta, R. Geothermal systems and resources. In *Geothermal Energy*; Gupta, H., Sukanta, R., Eds.; Elsevier: Amsterdam, The Netherlands, 2007; pp. 49–59. [CrossRef]
7. Muffler, L.P.J.; Cataldi, R. Methods for regional assessment of geothermal resources. *Geothermics* **1978**, *7*, 53–89. [CrossRef]
8. Moeck, I.S. Catalog of geothermal play types based on geologic controls. *Renew. Sustain. Energy Rev.* **2014**, *37*, 867–882. [CrossRef]
9. Zarrouk, S.J.; McLean, K. Chapter 2—Geothermal systems. In *Geothermal Well Test Analysis*; Zarrouk, S.J., McLean, K., Eds.; Academic Press: Cambridge, MA, USA, 2019; pp. 13–38. [CrossRef]
10. Blair, P.D. Geothermal Resources and Technology: Introduction. In *Mechanical Engineers' Handbook*, 4th ed.; Kutz, M., Ed.; Energy and Power; John Wiley & Sons, Inc.: Hoboken, NJ, USA, 2014; Volume 4, pp. 1–17. [CrossRef]
11. Hochstein, M.P. Classification and assessment of geothermal resources. In *Small Geothermal Resources—A Guide to Development and Utilization*; Dickson, M.H., Fanelli, M., Eds.; UNITAR/UNDP Centre for Small Energy Resources: Rome, Italy, 1990; pp. 31–59.

12. Keegan-Treloar, R.; Irvine, D.J.; Solórzano-Rivas, S.C.; Werner, A.D.; Banks, E.W.; Currell, M.J. Fault-controlled springs: A review. *Earth-Sci. Rev.* **2022**, *230*, 104058. [CrossRef]
13. Bowen, R. Geothermal Exploration. In *Geothermal Resources*, 2nd ed.; Springer: Dordrecht, The Netherlands, 1989; pp. 117–158. [CrossRef]
14. Torresan, F.; Piccinini, L.; Cacace, M.; Pola, M.; Zampieri, D.; Fabbri, P. Numerical modeling as a tool for evaluating the renewability of geothermal resources: The case study of the Euganean Geothermal System (NE Italy). *Env. Geochem. Health* **2022**, *44*, 2135–2162. [CrossRef]
15. Pola, M.; Cacace, M.; Fabbri, P.; Piccinini, L.; Zampieri, D.; Torresan, F. Fault control on a thermal anomaly: Conceptual and numerical modeling of a low-temperature geothermal system in the Southern Alps foreland basin (NE Italy). *J. Geophys. Res. Solid Earth* **2020**, *125*, e2019JB017394. [CrossRef]
16. Pastorelli, S.; Marini, L.; Hunziker, J.C. Water chemistry and isotope composition of the Acquarossa thermal system, Ticino, Switzerland. *Geothermics* **1999**, *28*, 75–93. [CrossRef]
17. Mazor, E. *Chemical and Isotopic Groundwater Hydrology*, 3rd ed.; Marcel Dekker: New York, NY, USA, 2004; pp. 13–179.
18. D'Amore, F.; Arnórsson, S. Geothermometry. In *Isotopic and Chemical Techniques in Geothermal Exploration, Development and Use*; Arnórsson, S., Ed.; International Atomic Energy Agency: Vienna, Austria, 2000.
19. Bruhn, D.; Manzella, A.; Vuataz, F.; Faulds, J.; Moeck, I.; Erbas, K. Exploration Methods. In *Geothermal Energy Systems*; Wiley-VCH Verlag GmbH & Co. KGaA: Weinheim, Germany, 2010; pp. 37–112, ISBN 9783527408313.
20. Hasan, M.; Shang, Y.; Meng, H.; Shao, P.; Yi, X. Application of electrical resistivity tomography (ERT) for rock mass quality evaluation. *Sci. Rep.* **2021**, *11*, 23683. [CrossRef]
21. Nabi, A.; Liu, X.; Gong, Z.; Ali, A. Electrical resistivity imaging of active faults in palaeoseismology: Case studies from Karachi Arc, southern Kirthar Fold Belt, Pakistan. *NRIAG J. Astron. Geophys.* **2020**, *9*, 116–128. [CrossRef]
22. Borović, S.; Marković, I. Utilization and tourism valorisation of geothermal waters in Croatia. *Renew. Sustain. Energy Rev.* **2015**, *44*, 52–63. [CrossRef]
23. Horváth, F.; Musitz, B.; Balázs, A.; Végh, A.; Uhrin, A.; Nádor, A.; Koroknai, B.; Pap, N.; Tóth, T.; Wórum, G. Evolution of the Pannonian basin and its geothermal resources. *Geothermics* **2015**, *53*, 328–352. [CrossRef]
24. Borović, S.; Marković, T.; Larva, O.; Brkić, Ž.; Mraz, V. Mineral and Thermal Waters in the Croatian Part of the Pannonian Basin. In *Mineral and Thermal Waters of Southeastern Europe*; Papić, P., Ed.; Springer: Cham, Switzerland, 2016; pp. 31–45. [CrossRef]
25. Čučković, L.; Ožanić, M.; Abramović, M. *Topusko: Monografija*; Aura: Sisak, Croatia, 2009. (In Croatian)
26. Državni Zavod za Statistiku—Popis '21. Available online: https://popis2021.hr (accessed on 22 November 2022). (In Croatian)
27. Zaninović, K.; Gajić-Čapka, M.; Perčec Tadić, M.; Vučetić, M.; Milković, J.; Bajić, A.; Cindrić, K.; Cvitan, L.; Katušin, Z.; Kaučić, D. *Klimatski atlas Hrvatske/Climate atlas of Croatia 1961–1990, 1971–2000*; Državni Hidrometeorološki Zavod: Zagreb, Croatia, 2008. (In Croatian and English)
28. DHMZ—Državni Hidrometeorološki Zavod. Available online: https://meteo.hr/klima.php?section=klima_podaci&param=k2_1 (accessed on 18 January 2021).
29. Schmid, S.M.; Fügenschuh, B.; Kissling, E.; Schuster, R. Tectonic map and overall architecture of the Alpine orogen. *Eclogae Geol. Helvetiae.* **2004**, *7*, 93–117. [CrossRef]
30. Schmid, S.M.; Bernoulli, D.; Fügenschuh, B.; Matenco, L.; Schefer, S.; Schuster, R.; Tischler, M.; Ustaszewski, K. The Alpine-Carpathian-Dinaridic orogenic system: Correlation and evolution of tectonic units. *Swiss J. Geosci.* **2008**, *101*, 139–183. [CrossRef]
31. Handy, M.R.M.; Schmid, S.; Bousquet, R.; Kissling, E.; Bernoulli, D. Reconciling plate-tectonic reconstructions of Alpine Tethys with the geological–geophysical record of spreading and subduction in the Alps. *Earth-Sci. Rev.* **2010**, *102*, 121–158. [CrossRef]
32. Vlahović, I.; Tišljar, J.; Velić, I.; Matičec, D. Evolution of the Adriatic Carbonate Platform: Palaeogeography, main events and depositional dynamics. *Palaeogeogr. Palaeoclimatol. Palaeoecol.* **2005**, *220*, 333–360. [CrossRef]
33. Marković, T.; Borović, S.; Larva, O. Geochemical characteristics of thermal waters of Hrvatsko zagorje. *Geol. Croat.* **2015**, *68*, 67–77. [CrossRef]
34. Šimunić, A. Topusko. In *Mineral and Thermal Waters of the Republic of Croatia*; Šimunić, A., Hećimović, I., Eds.; Croatian Geological Survey: Zagreb, Croatia, 2008; pp. 185–195. (In Croatian)
35. Korolija, B.; Živaljević, T.; Šimunić, A. *Osnovna geološka Karta SFRJ 1:100 000, List Slunj. L 33-104 [Basic Geological Map of SFRY 1:100000, Geology of the Slunj sheet L33-104]*; Institut za geološka istraživanja: Zagreb, Croatia; Geološki zavod: Sarajevo, Bosnia and Herzegovina; Savezni Geološki Zavod: Beograd, Yugoslavia, 1980. (In Croatian)
36. Bahun, S.; Raljević, B. *Mineralna, Termalna i Ljekovita Vrela [Mineral and Thermal Springs]*; unpublished report; Institute for Geological Research: Zagreb, Yugoslavia, 1969; p. 4769/5. (In Croatian)
37. INA-Projekt Zagreb. *Elaborat o Rezervama i Bilanci Termalnih Voda u Topuskom [Report on the Reserves and Mass Balance of Thermal Water in Topusko]*; unpublished report; INA-Projekt, OOUR Kompleksna geološka istraživanja: Zagreb, Yugoslavia, 1984. (In Croatian)
38. Čubranić, A. *Osmatranje Termalnih Voda u Topuskom [Monitoring of Thermal Waters in Topusko]*; unpublished report; INA-Projekt, OOUR Kompleksna Geološka Istraživanja: Zagreb, Croatia, 1984. (In Croatian)
39. Šegotić, B.; Šmit, I. *Studija Optimirane Energetske Učinkovitosti Korištenja Geotermalnih Voda [Study of Optimized Energy Efficiency of Geothermal Water Use]*; unpublished report; Termoinženjering-projektiranje: Zagreb, Croatia, 2007. (In Croatian)

40. Korolija, B.; Živaljević, T.; Šimunić, A. *Osnovna geološka Karta SFRJ. Tumač za list Slunj [Basic Geological Map of SFRY 1:100000, Guide for the Slunj Sheet L33-104]*; Institut za geološka istraživanja: Zagreb, Croatia; Geološki zavod: Sarajevo, Bosnia and Herzegovina; Savezni Geološki Zavod: Beograd, Yugoslavia, 1980. (In Croatian)
41. Blake, S.; Henry, T.; Murray, J.; Flood, R.; Muller, M.R.; Jones, A.G.; Rath, V. Compositional multivariate statistical analysis of thermal groundwater provenance: A hydrogeochemical case study from Ireland. *Appl. Geochem.* **2016**, *75*, 171–188. [CrossRef]
42. Verma, S.P.; Pandarinath, K.; Santoyo, E. SolGeo: A new computer program for solute geothermometers and its application to Mexican geothermal fields. *Geothermics* **2008**, *37*, 597–621. [CrossRef]
43. Pola, M.; Fabbri, P.; Piccinini, L.; Zampieri, D. Conceptual and numerical models of a tectonically-controlled geothermal system: A case study of the Euganean Geothermal System, Northern Italy. *Cent. Eur. Geol.* **2015**, *58*, 129–151. [CrossRef]
44. Powell, T.; Cumming, W. Spreadsheets for Geothermal Water and Gas Geochemistry. In Proceedings of the Thirty-Fifth Workshop on Geothermal Reservoir Engineering, Stanford University, California, CA, USA, 1–3 February 2010.
45. Dumančić, E.; Čubranić, A. *Prijedlog Projekta Sanacije Livadskih Izvora [Project Proposal—Revitalisation of Livadski Izvori Spring]*; unpublished report; INA-Projekt Zagreb: Zagreb, Yugoslavia, 1989; p. 5517. (In Croatian)
46. Blinja, T. *Izvedba Eksploatacione Bušotine TEB-4 u Topuskom [Construction of the Exploitation Well TEB-4 in Topusko]*; unpublished report; INA-Projekt: Zagreb, Yugoslavia, 1986. (In Croatian)
47. Blinja, T. *Sanacioni Radovi Eksploatacionih Bušotina TEB-1 i TEB-2 u Topuskom [Revitalisation of Exploitation Wells TEB-1 and 2 in Topusko]*; unpublished report; INA-Projekt, OOUR Kompleksna geološka istraživanja: Zagreb, Croatia, 1986. (In Croatian)
48. Nevada Division of Environmental Protection (NDEP). Evaluation of Inorganic Chemical Analysis. Available online: https://ndep.nv.gov/uploads/documents/sept-2009-cation-anion-balance-guide.pdf (accessed on 22 August 2022).
49. Appelo, C.A.J.; Postma, D. *Geochemistry, Groundwater and Pollution*, 2nd ed.; A.A. Balkema Publishers: Leiden, The Netherlands, 2005; pp. 17–18.
50. Simler, R. *Software Diagrammes, V6.5, Laboratoire d'Hydrologie d'Avignon*; Université d'Avignon et pays du Vaucluse: Avignon, France, 2012.
51. Piper, A.M. A Graphic Procedure in the Geochemical Interpretation of Water-Analyses. *Am. Geophys. Union Trans.* **1944**, *25*, 914–923. [CrossRef]
52. Fetter, C.W. *Applied Hydrogeology*, 4th ed.; Lynch, P., Ed.; Prentice Hall: Upper Saddle River, NJ, USA, 2001.
53. Romano, P.; Liotta, M. Using and abusing Giggenbach ternary Na-K-Mg diagram. *Chem. Geol.* **2020**, *541*, 119577. [CrossRef]
54. Truesdell, A.H. Geochemical techniques in exploration, summary of section III. In Proceedings of the Second United Nations Symposium on the Development, Use of Geothermal Resources, San Francisco, CA, USA, 20 May 1975; pp. 3–29.
55. Fournier, R.O. Chemical geothermometers and mixing models for geothermal systems. *Geothermics* **1977**, *5*, 41–50. [CrossRef]
56. Michard, G. Gothermométres Chimiques. *Bull. BRGM* **1979**, *2*, 183–189.
57. Arnòrsson, S.; Gunnlaugsson, E.; Svavarsson, H. The chemistry of geothermal waters in Iceland. III. Chemical geothermometry in geothermal investigations. *Geochim.Cosmochim. Acta* **1983**, *47*, 567–577. [CrossRef]
58. Kruseman, G.P.; De Ridder, N.A.; Verweij, J.M. *Analysis and Evaluation of Pumping Test Data*, 2nd ed.; International institute for land reclamation and improvement: Wageningen, The Netherlands, 1994.
59. Rorabaugh, M.J. Graphical and theoretical analysis of step-drawdown test of artesian well. *Trans. Am. Soc. Civ. Eng.* **1953**, *79*, 1–23.
60. Jacob, C.E. Drawdown test to determine effective radius of artesian well. *Trans. Am. Soc. Civ. Eng.* **1947**, *112*, 1047–1064. [CrossRef]
61. Bruin, J.; Hudson, H.E. Selected Methods for Pumping Test Analysis. In *Illinois State Water Survey*; State Ilinois University: Springfield, IL, USA, 1955.
62. Fabbri, P. Transmissivity in the Geothermal Euganean Basin: A Geostatistical Analysis. *Ground Water* **1997**, *35*, 881–887. [CrossRef]
63. Verbovšek, T. Estimation of transmissivity and hydraulic conductivity from specific capacity and specific capacity index in dolomite aquifers. *J. Hydrol. Eng.* **2008**, *13*, 817–823. [CrossRef]
64. Diaferia, I.; Barchi, M.; Loddo, M.; Schiavone, D.; Siniscalchi, A. Detailed imaging of tectonic structures by multiscale earth resistivity tomographies: The Colfiorito normal faults (Central Italy). *Geophys. Res. Lett.* **2006**, *33*, L09305. [CrossRef]
65. Pérez-Estay, N.; Molina-Piernas, E.; Roquer, T.; Aravena, D.; Araya Vargas, J.; Morata, D.; Arancibia, G.; Valdenegro, P.; García, K.; Elizalde, D. Shallow anatomy of hydrothermal systems controlled by the Liquiñe-Ofqui Fault System and the Andean Transverse Faults: Geophysical imaging of fluid pathways and practical implications for geothermal exploration. *Geothermics* **2022**, *104*, 102435. [CrossRef]
66. Siniscalchi, A.; Tripaldi, S.; Neri, M.; Giammanco, S.; Piscitelli, S.; Balasco, M.; Behncke, B.; Magrì, C.; Naudet, V.; Rizzo, E. Insights into fluid circulation across the Pernicana Fault (Mt. Etna, Italy) and implications for flank instability. *J. Volcanol. Geotherm. Res.* **2010**, *193*, 137–142. [CrossRef]
67. Briški, M.; Stroj, A.; Kosović, I.; Borović, S. Characterization of Aquifers in Metamorphic Rocks by Combined Use of Electrical Resistivity Tomography and Monitoring of Spring Hydrodynamics. *Geosciences* **2020**, *10*, 137. [CrossRef]
68. Giustini, F.; Brilli, M.; Carlucci, G.; Ciotoli, G.; Gaudiosi, L.; Mancini, M.; Simionato, M. Geophysical and geochemical multi-method investigations for reconstructing subsurfaces, alluvial sedimentology, and structural geology (Tiber valley, Rome). *Int. J. Earth. Sci. (Geol. Rundsch.)* **2022**, *112*, 197–216. [CrossRef]

69. Ward, S.H. Resistivity and induced polarization methods. In *Geotechnical and Environmental Geophysics*; Ward, S.H., Ed.; Society of Exploration Geophysicists: Tulsa, Ok, USA, 1990; Volume I, pp. 147–190.
70. Sharma, P.V. *Environmental and Engineering Geophysics*; Cambridge University Press: Cambridge, UK, 1997.
71. Reynolds, J.M. *An Introduction to Applied and Environmental Geophysics*, 2nd ed.; Wiley: New York, NY, USA, 2011.
72. Loke, M.H. *Tutorial: 2-D and 3-D Electrical Imaging Surveys*; Geotomo Software: Penang, Malaysia, 2020; Available online: https://www.geotomosoft.com/downloads.php (accessed on 27 February 2020).
73. Loke, M.H.; Barker, R.D. Rapid least-squares inversion of apparent resistivity pseudosections using a quasi-Newton method. *Geophys. Prospect.* **1996**, *44*, 131–152. [CrossRef]
74. DeGroot-Hedlin, C.; Constable, S. Occam's inversion to generate smooth, two-dimensional models from magnetotelluric data. *Geophysics* **1990**, *55*, 1613–1624. [CrossRef]
75. Sasaki, Y. Resolution of resistivity tomography inferred from numerical simulation. *Geophys.Prospect.* **1992**, *40*, 453–464. [CrossRef]
76. Ellis, R.G.; Oldenburg, D.W. Applied geophysical inversion. *Geophys. J. Int.* **1994**, *116*, 5–11. [CrossRef]
77. Ellis, R.G.; Farquharson, C.G.; Oldenburg, D.W. Approximate inverse mapping inversion of the COPROD2 data. *J. Geomagn. Geoelectr.* **1993**, *45*, 1001–1012. [CrossRef]
78. Milenić, D.; Krunić, O.Ž.; Milankovic, D. Thermomineral waters of inner Dinarides Karst. *Acta Carsologica* **2012**, *41*, 235–252. [CrossRef]
79. Freeze, R.A.; Cherry, J.A. *Groundwater*; Prentice Hall Inc.: Englewood Cliffs, NJ, USA, 1979; Volume 7632, p. 604.
80. Li, Z.; Huang, T.; Ma, B.; Long, Y.; Zhang, F.; Tian, J.; Li, Y.; Pang, Z. Baseline groundwater quality before shale gas development in Xishui, Southwest China: Analyses of hydrochemistry and multiple environmental isotopes (2H, 18O, 13C, 87Sr/86Sr, 11B, and Noble Gas Isotopes). *Water* **2020**, *12*, 1741. [CrossRef]
81. Wang, Z.; Torres, M.; Paudel, P.; Hu, L.; Yang, G.; Chu, X. Assessing the karst groundwater quality and hydrogeochemical characteristics of a prominent dolomite aquifer in Guizhou, China. *Water* **2020**, *12*, 2584. [CrossRef]
82. Patekar, M.; Bašić, M.; Pola, M.; Kosović, I.; Terzić, J.; Lucca, A.; Mittempergher, S.; Berio, L.; Borović, S. Multidisciplinary investigations of a karst aquifer for managed aquifer recharge applications on the island of Vis (Croatia). *Acque Sotter. Ital. J. Groundw.* **2022**, *11*, 37–48. [CrossRef]
83. Frondini, F. Geochemistry of regional aquifer systems hosted by carbonate-evaporite formations in Umbria and southern Tuscany (central Italy). *Appl. Geochem.* **2008**, *23*, 2091–2104. [CrossRef]
84. Hilberg, S.; Schneider, J.F. The Aquifer Characteristics of the Dolomite Formation a New Approach for Providing Drinking Water in the Northern Calcareous Alps Region in Germany and Austria. *Water Resour. Manag.* **2011**, *25*, 2705–2729. [CrossRef]
85. Fellehner, M. Der Hauptdolomit als Grundwasserspeicher in den Nördlichen Kalkalpen. Ph.D. Thesis, Philipps-Universität, Marburg, Deutschland, 30 June 2004.
86. Li, X.; Wu, P.; Han, Z.; Zha, X.; Ye, H.; Qin, Y. Effects of mining activities on evolution of water quality of karst waters in Midwestern Guizhou, China: Evidences from hydrochemistry and isotopic composition. *Environ. Sci. Pollut. Res.* **2018**, *25*, 1220–1230. [CrossRef]
87. Sun, C.; Wang, S.; Chen, W. Hydrochemical Characteristics and the Relationship between Surface and Groundwater in a Typical 'Mountain–Oasis' Ecosystem in Central Asia. *Sustainability* **2022**, *14*, 7453. [CrossRef]
88. Blasco, M.; Auqué, L.F.; Gimeno, M.J. Geochemical evolution of thermal waters in Carbonate—Evaporitic systems: The triggering effect of halite dissolution in the dedolomitisation and albitisation processes. *J. Hydrol.* **2019**, *570*, 623–636. [CrossRef]
89. Blasco, M.; Gimeno, M.J.; Auqué, L.F. Low temperature geothermal systems in carbonate-evaporitic rocks: Mineral equilibria assumptions and geothermometrical calculations. Insights from the Arnedillo thermal waters (Spain). *Sci. Total Environ.* **2018**, *615*, 526–539. [CrossRef]
90. Hiscock, K.M.; Bense, V.F. *Hydrogeology: Principles and Practice*, 2nd ed.; John Wiley & Sons Ltd: Hoboken, NY, USA, 2014.
91. Halle, R. *Kemizam i Obradba Vode [Water Chemistry and Treatment]*; Faculty of Mining, Geology and Petroleum Engineering, University of Zagreb: Zagreb, Croatia, 2004. (In Croatian)
92. Macenić, M.; Kurevija, T.; Medved, I. Novel geothermal gradient map of the Croatian part of the Pannonian Basin System based on data interpretation from 154 deep exploration wells. *Renew. Sustain. Energy Rev.* **2020**, *132*, 110069. [CrossRef]
93. Domenico, P.A.; Schwartz, F.W. *Physical and Chemical Hydrogeology*; John Wiley & Sons: New York, NY, USA, 1990.
94. Heasler, H.; Jaworowski, C.; Foley, D. Geothermal systems and monitoring hydrothermal features. In *Geological Monitoring*; Young, R., Norby, L., Eds.; Geological Society of America: Boulder, CO, USA, 2009; pp. 105–140. [CrossRef]

Step-drawdown test

Well: TEB-1 **Municipality: Topusko** **Date: *16-Sep-21***

Table A1

Step	Q (l/s)	Q (m^3/s)	P_{in} (bar)	P_{fin} (bar)	Density (kg/m^3)	Δ (m)	Δ/Q (s/m^2)
0	0.00	***0.0000***	***1.3992***	1.3992	981.46	0.00	
1	2.69	***0.0027***	***1.3992***	1.3819	981.46	0.18	66.87
2	3.12	***0.0031***	***1.3819***	1.3735	981.46	0.27	85.57
3	3.90	***0.0039***	***1.3735***	1.3718	981.46	0.29	73.09
4	6.95	***0.0070***	***1.3718***	1.3414	981.46	0.60	86.43
5	24.08	***0.0241***	***1.3414***	1.0598	981.46	3.52	146.38
6	23.41	***0.0234***	***1.3910***	1.0502	981.46	3.62	154.82
REC	0.00	***0.0000***	***1.0598***	1.3910	981.46	0.09	

Table A2

LINEAR REGRESSION Δ/Q = b + mQ			
m	b	**3686.34**	**62.78**
se_m	se_b	340.06	4.83
r^2	se_y	**0.97**	7.77
F	d_f	117.51	4.00
ss_{reg}	ss_{res}	7100.12	241.68

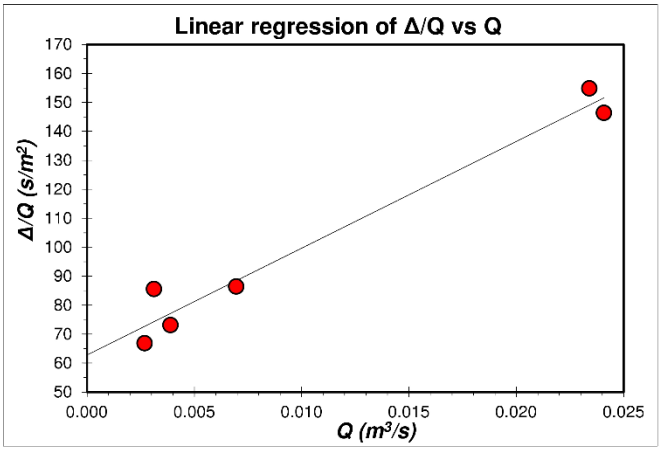

Table A3

$\Delta = (B+B')Q + CQ^2$

B= aquifer loss; B' = linear well loss; C = well loss

Δ = 62.8 Q + 3686.3 Q^2

Field data		Linear regression			Well efficiency
Q (m^3/s)	Δ (m)	(B+B')Q (m)	CQ^2 (m)	Δ (m)	(%)
0.000	0.000	0.000	0.000	0.000	
0.003	0.180	0.169	0.027	0.196	86.36
0.003	0.267	0.196	0.036	0.232	84.52
0.004	0.285	0.245	0.056	0.301	81.37
0.007	0.601	0.436	0.178	0.614	71.02
0.024	3.525	1.512	2.138	3.649	41.43
0.023	3.624	1.470	2.020	3.490	42.11
0.000	0.085	0.000	0.000	0.000	

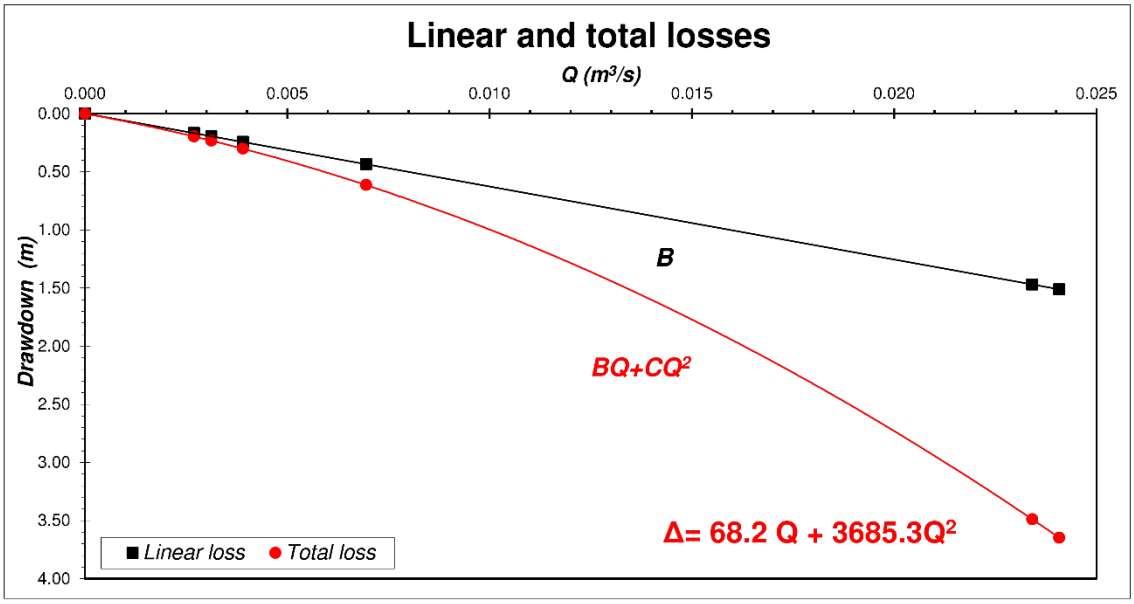

Figure S1: Interpretation of the step-drawdown test results conducted in the TEB-1 well.

Step-drawdown test

Well: TEB-3 **Municipality: Topusko** **Date: *30-Sep-22***

Table B1

Step	Q (l/s)	Q (m^3/s)	P_{in} (bar)	P_{fin} (bar)	Density (kg/m^3)	Δ (m)	Δ/Q (s/m^2)
0	0.00	***0.0000***	***0.6940***	0.6940	987.65	0.00	
1	2.88	***0.0029***	***0.6940***	0.6891	987.65	0.05	17.76
2	4.67	***0.0047***	***0.6891***	0.6891	985.86	0.05	10.92
3	12.81	***0.0128***	***0.6891***	0.6599	984.03	0.35	27.61
4	8.67	***0.0087***	***0.6599***	0.6763	983.11	0.18	21.18
REC	0.00	***0.0000***	***0.6763***	0.6891	983.11	0.05	

Table B2

LINEAR REGRESSION Δ/Q = b + mQ			
m	b	**1316.43**	**9.81**
se_m	se_b	609.35	5.00
r^2	se_y	**0.70**	4.67
F	d_f	4.67	2.00
ss_{reg}	ss_{res}	101.70	43.58

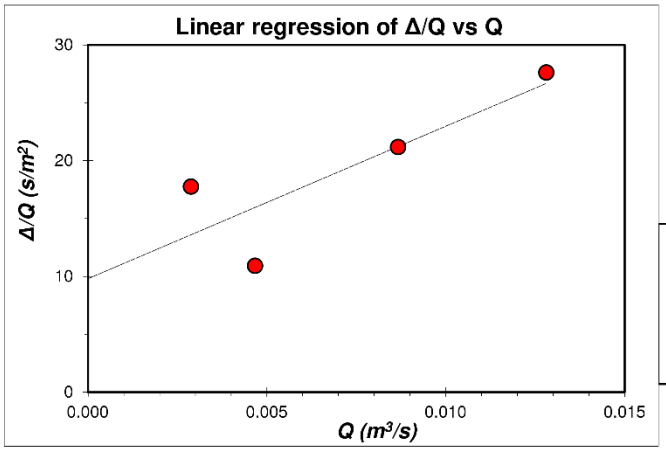

Table B3

Δ = (B+B')Q + CQ^2 *B= aquifer loss; B' = linear well loss; C = well loss*					
Δ = 9.8 Q + 1316.4 Q^2					
Field data		**Linear regression**			**Well efficiency**
Q (m^3/s)	Δ (m)	(B+B')Q (m)	CQ^2 (m)	Δ (m)	(%)
0.000	0.000	0.000	0.000	0.000	
0.003	0.051	0.028	0.011	0.039	72.13
0.005	0.051	0.046	0.029	0.075	61.48
0.013	0.354	0.126	0.216	0.342	36.78
0.009	0.184	0.085	0.099	0.184	46.23
0.000	0.051	0.000	0.000	0.000	

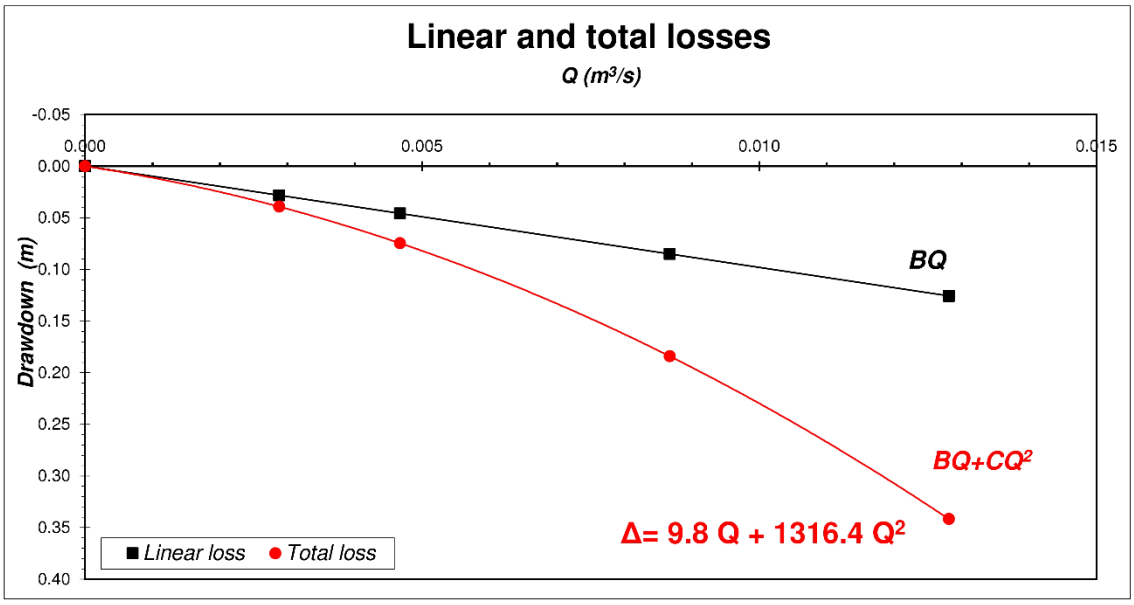

Figure S2: Interpretation of the step-drawdown test results conducted in the TEB-3 well.

2.2. Hydrogeochemical and environmental isotope study of Topusko thermal waters, Croatia

By

Mirja Pavić, Maja Briški, Marco Pola and Staša Borović

Environ Geochem Health (2024) 46:133
https://doi.org/10.1007/s10653-024-01904-9

ORIGINAL PAPER

Hydrogeochemical and environmental isotope study of Topusko thermal waters, Croatia

Mirja Pavić · Maja Briški · Marco Pola · Staša Borović

Received: 3 November 2023 / Accepted: 6 February 2024 / Published online: 14 March 2024

Abstract Thermal waters in Topusko (Croatia), with temperatures of up to 65 °C, have been used for heating, health, and recreational tourism for the past fifty years. Hydrogeochemical monitoring can provide insights into deeper geological processes and indicate system changes from baseline levels. It helps to identify potential anthropogenic impacts, as well as natural changes. Hydrogeochemical, geothermometrical, and environmental isotope studies of thermal waters in Topusko were conducted to improve the existing conceptual model of the Topusko hydrothermal system (THS), providing a baseline for continuous monitoring of the thermal resource. 2-year thermal springs and precipitation monitoring took place from March 2021 until March 2023. Major anions and cations, stable and radioactive isotopes (i.e. ^{18}O, ^{2}H, SO_4^{2-}, ^{3}H and ^{14}C) and geothermometers were used to assess the origin of thermal waters in Topusko and their interaction with thermal aquifer. The results indicate the meteoric origin of thermal water, which was recharged in colder climatic conditions around the late Pleistocene–Early Holocene. Thermal water was last in contact with the atmosphere before approximately 9.5 kyr. Ca-HCO_3 hydrochemical facies suggests carbonate dissolution as the dominant process driving the solute content. Geothermometrical results indicate an equilibrium temperature in the reservoir of 90 °C.

Keywords Thermal water · Hydrochemical analyses · Stable water isotopes · Groundwater mean residence time · Topusko

M. Pavić · M. Briški · M. Pola · S. Borović (✉)
Croatian Geological Survey, Sachsova 2, 10000 Zagreb, Croatia
e-mail: sborovic@hgi-cgs.hr

Introduction

Thermal waters, characterised by elevated temperature values and unique chemical compositions, are valuable natural resources with applications in energetics, recreation, and therapy. Studying hydrogeochemical properties and environmental isotopes in thermal waters provides insights into their origin, hydrological processes, and water–rock interactions. These waters, ranging from 20 °C to above 225 °C globally, exhibit distinct geochemical characteristics influenced by geological, hydrogeological, and thermal characteristics. Comprehending their hydrogeochemical behaviour is essential for sustainable resource management, geothermal exploration, and environmental monitoring (Ármannsson & Fridriksson, 2009).

Examination of aqueous geochemistry is important in all phases of geothermal aquifer exploration, evaluation, and utilisation (Haizlip, 2016; Marini, 2004). Hydrogeochemical monitoring helps evaluate hydrothermal systems by determination of the geochemical baseline levels, tracking changes, and

assessing the impact of water abstraction on the system. It involves analysing water chemistry, subsurface temperatures, and thermal and non-thermal groundwater interactions. Continuous geochemical surveys enable comparisons of existing and new data, aiding in the detection of anthropogenic impacts (i.e. the response of the aquifer to production stress) and natural variations (i.e. climate change and modifications of flow pathways due to earthquakes). Monitoring is essential for resource protection, legislative compliance, documentation of disturbances or natural changes, and scientific research (Heasler et al., 2009; Pryer, 2021). Continuous datasets are required to ensure adequate quantities of fluids with the necessary temperatures and pressures in the geothermal aquifer.

The chemical composition of groundwater is usually determined by the original composition of the infiltrated water and factors like altitude, vegetation, climate, aquifer mineralogy, and chemical reactions during its flow (Mazor, 2004). The analysis of the major ion and isotopic content, *in situ* parameters, spatial distribution, water composition evolution, and hydrochemical identification of water type are all useful tools for evaluating water chemistry and comprehensive characterisation of hydrothermal systems (Hounslow, 1995; Young, 1985). These analyses serve multiple purposes, including the differentiation of water types by observing the major ions content and determining parameters such as the temperatures attained at different depths (Verma et al., 2008) or the water mean residence time (MRT) (Plummer & Glynn, 2013). Moreover, they offer insights into the mineralogical composition of the aquifer and potential mixing with water from shallower cold aquifers in the spring areas (Blake et al., 2016). Various chemical geothermometers are used to estimate the aquifer equilibrium temperatures (Blasco et al., 2019; Karingithi, 1984). Tritium concentrations are used to assess the potential mixing of thermal waters with shallow groundwater (Janik et al., 1985; Lewis et al., 1989). Comparing stable water isotopes $\delta^{18}O$ and $\delta^{2}H$ in thermal water with the local meteoric water lines helps confirm/identify thermal water origin (Rman, 2016; Szocs et al., 2013). Analysis of ^{14}C and $\delta^{13}C$ of thermal water dissolved inorganic content is often used to estimate the time of thermal water infiltration into the subsurface in the assumed recharge area. Finally, analyses of $\delta^{34}S$ and $\delta^{18}O$ serve as a tool for assessing the origin of sulphates in the thermal water (Miljević et al., 2013; Porowski, 2014; Thiébaud et al., 2010).

The thermal springs in Topusko, situated in Central Croatia, reach temperatures of up to 53 °C. These springs are located in an area characterised by elevated heat flow at the southwest edge of the Pannonian Basin System (Horváth et al., 2015), representing a component of an intermediate-scale hydrothermal system. Geothermal systems exhibit distinct chemical compositions that influence their potential applications, and based on Moeck's (2014) classification, Topusko is a non-magmatic conduction-dominated hydrothermal system (CD2d type). Despite limited prior investigations, thermal water in Topusko has been extensively utilised for district heating, health and spa purposes since the 1980s. Pavić et al. (2023) examined the historical geochemical data of thermal water, identified a possible fault zone responsible for thermal water outflow, and conducted a step-drawdown test to assess the transmissivity of the aquifer. Understanding the hydrogeochemical behaviour, thermal characteristics, and isotopic signatures of these waters is crucial for sustainable resource management, geothermal energy utilisation, and therapeutic applications.

Despite the prominence of Topusko as a thermal water site, comprehensive scientific investigations encompassing hydrogeochemical, geothermometric, and environmental isotopic aspects are limited. Therefore, this study aims to bridge this research gap by conducting an integrated analysis of the hydrogeochemical properties and environmental isotopes in Topusko thermal waters.

During the two-year research, the primary objective was to thoroughly monitor thermal springs and thermal water while establishing a geochemical baseline. Additionally, the study examined water–rock interactions, provided a detailed characterisation of thermal water geochemistry, determined aquifer equilibrium temperatures, investigated the sulphate origin in thermal water, and estimated the water MRT within the system.

Investigation of Topusko thermal springs adds to the growing body of knowledge about this particular location and offers information on the broader subject of geothermal research and utilisation. It emphasises the essential role that hydrogeochemical monitoring has in unravelling the complexities of hydrothermal

systems, protecting these resources, and fulfilling the needs of scientific research and energy production.

Materials and methods

Study area: geological and hydrogeological setting

The thermal springs in Topusko are located in Central Croatia, within the southwest edge of the Pannonian Basin System (PBS). Pannonian part of Croatia is characterised by a higher than average geothermal gradient (49 ℃/km) and heat flux (76 mW/m^2) due to back-arc crustal thinning in the PBS (Bošnjak, 1998; Horváth et al., 2015). These thermal waters have been used for centuries and have played a fundamental role in the development of tourism and healthcare facilities over the past five decades (Borović & Marković, 2015). The climate in the study area is moderate continental, slightly influenced by the Mediterranean climate of the northern Adriatic (Zaninović et al., 2008). The average annual precipitation is approximately 900 mm, and the annual average air temperature is 10.0 °C (DHMZ, 2021).

Thermal springs are generally part of intermediate-scale hydrothermal systems, including recharge areas in the mountainous hinterlands and geothermal aquifers, which are mainly hosted in Mesozoic carbonate rocks in Croatia (Borović et al., 2016). According to Šimunić (2008), the aquifer receives recharge from dolomite deposits outcropping west of Petrova Gora nappe. As a result, both the local and regional contexts must be considered.

The wider study area (W from Topusko) belongs to the Internal Dinarides tectonic unit and is situated at the NE margin of the Dinarides and SW margin of the PBS (Horváth et al., 2015; Pavelić & Kovačić, 2018; Schmid et al., 2004). In the west, the study area is bounded by a tectonic contact dividing Internal from External Dinarides (Fig. 1). The Internal Dinarides consist of a set of complex nappe sheets comprised of continental-derived material sedimented at the distal edge of the Adriatic microplate (Schmid et al., 2008). The External Dinarides are characterised by very thick sequences of Mesozoic carbonates, up to 8 km, deposited at the Adriatic Carbonate Platform (Schmid et al., 2004; Vlahović et al., 2005). Figure 1 shows that the majority of the THS study area is comprised of Late Paleozoic and Triassic deposits (P, T_1, T_2), while in the vicinity of the thermal water discharge area, the Holocene, Quaternary and Plio-Quaternary deposits (H; Q; Pl, Q) cover up older rocks, structures, and faults, which makes subsurface geological relations quite challenging to reconstruct.

According to the Basic geological map sheet Slunj (Korolija et al., 1980b), the oldest deposits in the research area belong to the clastic development of the younger Paleozoic found on Petrova Gora (P), schists, quartz-greywacke sandstones, shales, and fine-grained conglomerates of questionable total thickness. The Lower Triassic deposits (T_1) continuously follow clastic development, composed of red-violet mica-schist, light reddish mica-schist sandstones, and grey-greenish schist marls. The Middle and Upper Triassic deposits ($T_{2,3}$) consist predominantly of carbonate limestone and dolomite rocks, which are intensively karstified south of the Topusko. SW from the thermal spring area, Jurassic sedimentary, metamorphic and orthometamorphic rocks ($J_{2,3}$; J_2) outcrop to small extents, belonging to the ophiolitic-sedimentary thrust complex. They are represented by quartz-greywacke sandstones, shales and cherts, metamorphosed sediments (pelites and psammites), cherts, limestones and pyroclastic rocks, and amphibolites and amphibolite schist, respectively (Šikić et al., 2009). Deposits belonging to External Dinarides are dominantly represented by intensively karstified Mesozoic limestones and dolomites (J, K). Palaeocene (Pc, E) clastic deposits are also characterised by flysch development (conglomerates, sandstones, silt, marls, clays).

Neogene deposits (Figs. 1 and 2; M; M_4; Pl,Q; Q (Pl. H)) are primarily transgressive to all older rocks. These sediments are represented by the surface occurrence of clastites, fine-grained and coarse-grained conglomerates, sandstones, silts, marls, clays, lithothamnium limestone, fine- to coarse-grained gravels, sands, and conglomeratic sands (Hrvatski geološki institut, 2009; Korolija et al., 1980b).

From a hydrogeological point of view, Triassic carbonates represent artesian geothermal aquifers in the area of the Topusko HTS. The complex of Paleozoic deposits, out of which Petrova Gora is mainly built, forms an impermeable core complex, together with individual lower Triassic elements of the structural setting (Bahun & Raljević, 1969; Šimunić et al., 2008). Low permeability younger Neogene deposits cover the geothermal aquifer in the discharge area.

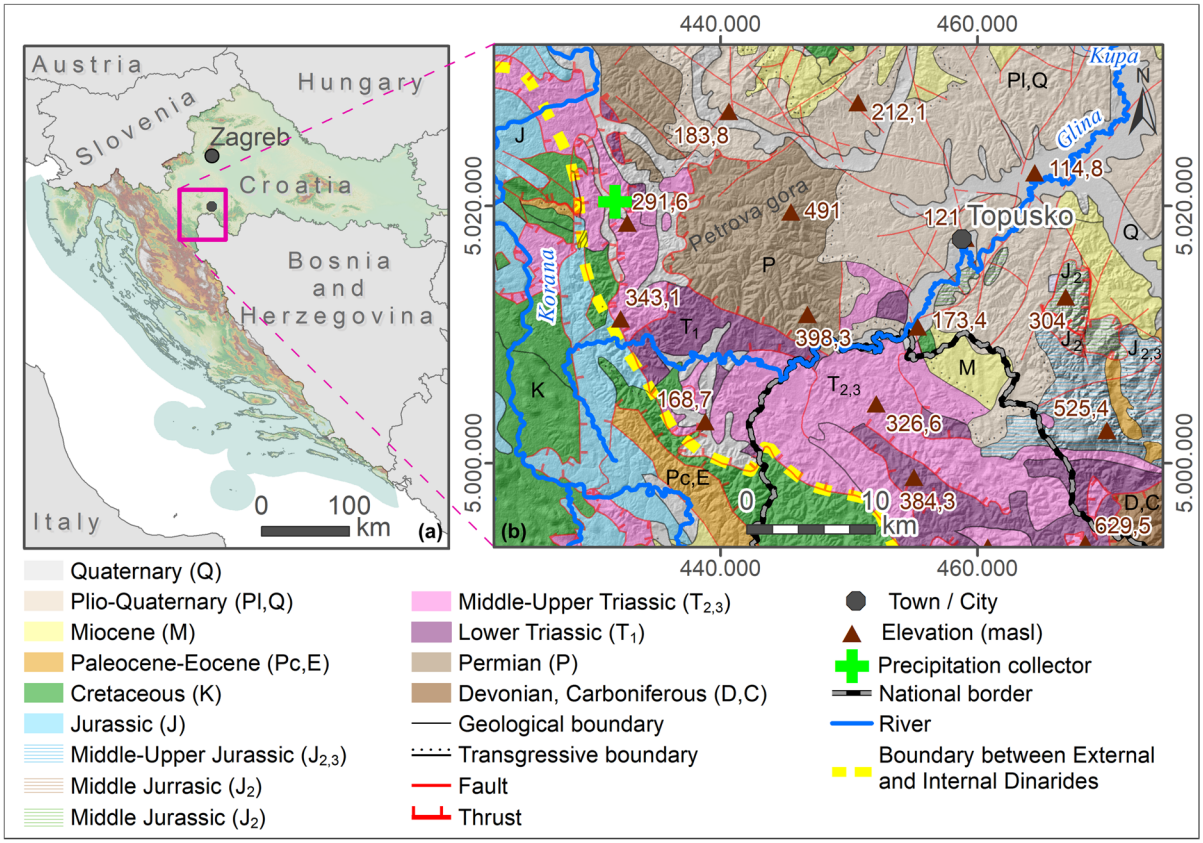

Fig. 1 Geographical position (**a**) and geological map of a wider study area of THS (**b**) (HGI-CGS, 2009; Korolija et al., 1980a; Savezni geološki zavod, 1970)

In the area of Topusko, there are three natural thermal springs with a total capacity of approximately 25 L/s and temperatures ranging from 46 °C (Blatne kupelji) to 53 °C (Livadski izvor). There are four exploitation wells near the natural thermal springs. Exploitation wells TEB-1, TEB-2, TEB-3, and TEB-4 were drilled in the period 1982–1989. TEB-1 (243 m), TEB-3 (163 m), and TEB-4 (80.8 m) are used for spa and heating purposes, while TEB-2 is damaged and no longer in operation. Total well capacity is estimated at 200 L/s with water temperature of up to 65 °C. The wells are artesian with a pressure of 0.5 to 2.3 bar (Čubranić, 1984; Šegotić & Šmit, 2007). According to Šimunić et al. (2008), the spring area is bounded by three faults that form a block in the form of a three-sided prism, enabling the uplifting of Triassic carbonates, which was determined by drilling (Fig. 2). Pavić et al. (2023) identified fault damage zones in the spring area that provide a preferential pathway for groundwater upwelling to the surface from a confined geothermal aquifer.

Water sampling and analyses

The monitoring of thermal waters and cumulative precipitation collection in the Topusko study area was conducted for two years, from March 2021 to February 2023 and April 2021 to March 2023, respectively. Sampling and monitoring points include two natural thermal springs, Livadski izvor and Blatne kupelji, and well TEB-4. The temperature was continuously monitored at the thermal springs using automatic data loggers (Onset HOBO Water level loggers 30, which were replaced by the Onset HOBO U12-015 Stainless Steel Temperature Data Logger in July 2021 due to repeated malfunctions caused probably by its exposure to higher water temperatures). Periodic monitoring included monthly *in situ* measurements, data

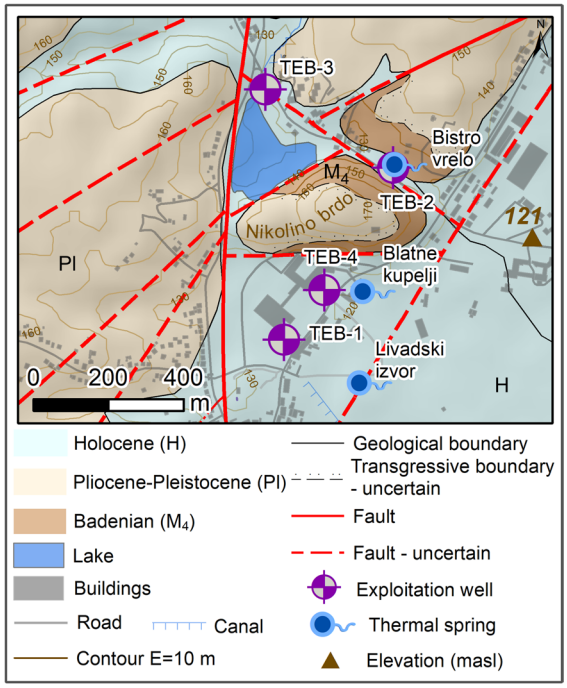

Fig. 2 Geological map of the thermal spring area in Topusko. Locations of exploitation wells and natural thermal springs are presented: Blatne kupelji spring, Bistro vrelo spring, and Livadski izvor spring (modified after Pavić et al., 2023)

retrievals from automatic loggers, and thermal water and cumulative precipitation sampling for subsequent hydrogeochemical analyses. After each sampling campaign, principal anions and cations, silica (SiO_2) concentration, and stable water isotope content (^2H and ^{18}O) were analysed. In addition, water sampling was conducted during minimum and maximum water abstraction periods for radioactive isotope analyses (^3H and ^{14}C) and stable isotope analyses from sulphate anion (^{34}S and ^{18}O).

The monthly thermal water samples were collected in polyethylene bottles (Ármannsson, 2012) of 100- and 200-mL volume and stored at 4 °C until the upcoming analyses. Cumulative precipitation samples were acquired by Palmex RAIN SAMPLER RS1B, specially designed for collecting and storing samples without evaporation. *In situ* measurements of key physico-chemical parameters (temperature (T), pH and electrical conductivity (EC)) were conducted using the WTW Multi 3320 multiparameter probe. Additionally, alkalinity (bicarbonate concentration) was determined in the field using a digital titrator (HACH 16900), by volumetric, titrimetric method with 1.6 N H_2SO_4, and bromocresol green indicator.

Thermal water samples have been analysed at the Croatian Geological Institute laboratory for the major ions content using ion chromatography (Thermo Scientific Dionex ICS-6000 HPIC System). The analysis of stable oxygen and hydrogen isotopes in water was done using a Picarro analyser (Picarro L2130-i Isotope and Gas Concentration Analyser). During sample measurements, international standards produced by the USGS (isotope reference material USGS 46, USGS47, and USGS48) were also measured, allowing subsequent result calibration for each measurement. Measurement precision was ± 0.2 ‰ for $\delta^{18}O$ and ± 1 ‰ for δ^2H. Results are presented in delta notation (‰), normalised to the international measurement standard VSMOW (Vienna Standard Mean Ocean Water) (Craig, 1961; Mazor, 2004). Hach DR3900 Spectrophotometer was used to determine SiO_2 content in the thermal water samples. Laboratory for low-level radioactivity of Ruđer Bošković Institute determined tritium activity concentration in two thermal water samples from well TEB-4 with the method of electrolytic enrichment (*LNA-PS 7.2/3 Determination of ^3H activity concentration)* using the liquid scintillation counter Quantulus 1220. The same laboratory determined relative specific ^{14}C activity in the same samples by accelerator mass spectrometry (AMS) technique (AMS-14C) (Krajcar Bronić et al., 2010; Sironić et al., 2013). In addition, three thermal water samples were analysed in the Hydrosiotop laboratory in Germany to determine $\delta^{34}S$ and $\delta^{18}O$ values of sulphate anion. The isotopic compositions are given in traditional delta notations (‰) with respect to the VSMOW standard for oxygen and CDT (Canyon Diablo Troilite) for sulphur.

Data processing methods

The acquired major ions data were processed in Excel and "Diagrammes V6.72" software (Simler, 2012). They were used to calculate total dissolved solids (TDS) content and saturation indexes of calcite and dolomite (SI) to evaluate chemical equilibrium in thermal water samples. The quality of the major ions analyses was tested by assessing the charge balance and its error through the equation:

$$\text{Charge balance error}\,(\%) = \frac{\sum_{\text{cations}} - \sum_{\text{anions}}}{\sum_{\text{ions}}} \times 100(\%) \quad (1)$$

where the ionic concentrations are in meq/L. Samples with a charge balance error of more than 5% were excluded from further analyses (Appelo & Postma, 2005; Mazor, 2004). The remaining dataset, together with measured in situ parameters, is presented graphically by box plot diagram and by descriptive statistic: arithmetic mean (Average), minimum (Min) and maximum (Max), and the standard deviation (St. dev).

Piper diagram (Piper, 1944) and molar and equivalent ratios of major ions ($Ca^{2+} + Mg^{2+}$ vs $HCO_3^- + SO_4^{2-}$, Ca^{2+} vs SO_4^{2-}, Na^+ vs Cl^-, etc.) were used to identify the hydrochemical facies of thermal water, the water–rock interaction processes, and the dominant lithology in the recharge area (Komatsu et al., 2021; Serianz et al., 2020; Xu et al., 2019).

The saturation indexes (SI) of the main minerals in the aquifer were calculated to assess whether these minerals are close to or far from equilibrium with their solubility products (Clark, 2015; López-Chicano et al., 2001). The index gives the saturation degree of the groundwater sample with respect to minerals based on the equation (Appelo & Postma, 2005):

$$\text{SI} = \log\left(\frac{\text{IAP}}{K}\right), \quad (2)$$

where IAP is the ion activity product, and K represents the solubility product. The equilibrium conditions between the mineral and the solution are represented by a straight line on a logarithmic plot, where SI takes the zero value. If greater than zero, the mineral is supersaturated and can precipitate (SI > 0), and less than zero reflects undersaturation and possible dissolution if the specific mineral is present. According to many authors (Chelnokov et al., 2022; López-Chicano et al., 2001; Plummer et al., 1990; Serianz et al., 2020), the assumed range of SI uncertainty for calcite is ± 0.1 and ± 0.5 for dolomite. The accepted equilibrium range is indicated as a grey rectangle area in the results section. The study of the saturation index (SI) is crucial in assessing the potential for precipitation or dissolution of minerals in thermal waters. It also provides information on the water's capacity to corrode materials or deposit mineral scales, which is critical to understanding the impacts on subsurface infrastructure and environmental systems (Appelo & Postma, 2005; Taghavi et al., 2019).

Comparing the stable water isotopic composition (δ^2H and $\delta^{18}O$) of precipitation and thermal spring water provides insight into the origin, residence time, and features of water transport through the system (Edwards et al., 2007; IAEA, 1970; Tijani et al., 2022). Excel and online statistic calculator Statistic Kingdom (2017) were used for stable water isotope data preparation, observation of the relationship between δ^2H and $\delta^{18}O$, statistical analyses, determination of outliers and testing isotope content distribution for normality before construction of local meteoric water line (LMWL). The δ^2H excess (d-excess; Dansgaard, 1964) was calculated for each sample following the equation:

$$d - \text{excess}\,(‰) = \delta^2H - 8\delta^{18}O \quad (3)$$

It can be interpreted as an index of deviation from the global meteoric water line GMWL (Craig, 1961), which has a *d*-excess value of 10‰. This excess, caused by kinetic evaporation (non-equilibrium) during the formation of the primary vapour mass, can be a valuable tool to determine the origin of water and conditions during the vapour formation (Clark, 2015). Linear regression model of precipitation stable water isotope data and Chauvenet's Criterion test (Taylor, 1997) on d-excess values were used to identify outliers before LMWL calculation, following the method described by Benjamin et al. (2005). A Quantile–Quantile plot (Q-Q plot) was used as a graphical tool, together with the Shapiro–Wilk W-test, to identify deviations from the normality of the data. LMWL was calculated using the ordinary least square regression (OLSR), excluding outlier data. This simple linear regression model is one of the three types of linear regression analyses recommended by the IAEA (Hughes & Crawford, 2012; IAEA, 1992). Finally, $\delta^{18}O$ and δ^2H values of thermal water samples were compared to OLSR LMWL to study the relationship between precipitation and groundwater.

Tritium can be used to determine the mean groundwater residence time or mixing processes in the aquifer since the concentration in groundwater reflects the atmospheric concentration when the water was last in contact with the atmosphere. The half-life of tritium is 12.32 years, and its concentrations are measured in

tritium units (TU) (1 TU = 0.118 Bq l^{-1}, which represents one ^{3}H atom in 10^{18} atoms of hydrogen) (Fetter, 2001; IAEA, 2005, 2013; Rozanski et al., 1991). The classification after Motzer (2007) was used in this study: tritium content < 0.8 TU indicates the recharge at least before 1950, tritium activity concentrations of 0.8 − 4 TU suggest a mix of sub-modern and modern water, while 5 − 15 TU concentrations indicate modern recharge (< 5 to 10 years). Detection of tritium in thermal water could imply mixing with the groundwater of modern recharge, which can further be a sign of thermal water overexploitation.

NetpathXL software (Parkhurst & Charlton, 2008; Plummer et al., 1994) was used to correct the initial ^{14}C activity ($^{14}C_0$) and to estimate radiocarbon ages of dissolved inorganic carbon (DIC) in a single thermal water sample, in which the initial and final water are defined as the same sample (Plummer & Glynn, 2013). This approach to radiocarbon dating is done without consideration of the geochemical mass balance reactions. Han and Plummer's graphical method (2012) was used to evaluate dominant geochemical processes occurring in geothermal aquifers, which affected the DIC carbon isotope content before ^{14}C radioactive decay, and to qualitatively estimate the radiocarbon age of thermal water samples. The radiocarbon DIC groundwater age (t) in years BP can be estimated by applying the ^{14}C decay equation, assuming advective piston-flow conditions:

$$t = -\frac{t_{1/2}}{\ln 2} \ln\left(\frac{^{14}C}{^{14}C_0}\right), \quad (4)$$

where $t_{1/2}$ is the ^{14}C half-life (Libby—5570 yr or physical 5730 yr), ^{14}C content of DIC measured from the collected groundwater sample, and the initial $^{14}C_0$ DIC value without considering impacts of geochemical processes on water chemistry (Geyh, 2000, 2005; IAEA, 1970). Radiocarbon dating of groundwater is undoubtedly one of the most challenging and frequently disputed applications of radiocarbon dating introduced by Münnich (1957) and Münnich and Roether (1967). Considerable challenges in the interpretation of presented results arise due to the potential influence of geochemical reactions ("reservoir effect"), such as carbonate dissolution, ion exchange, and isotopic exchanges, which can complicate the accurate ^{14}C ages by altering the initial ^{14}C content independently of radioactive decay. Geochemical processes often reduce the ^{14}C content beyond radioactive decay, leading to apparently older than expected groundwater ages. In this work, for the application of traditional adjustment models, we use the lowercase 'pmc' for the ^{14}C content of DIC (^{14}C DIC), which represents the ^{14}C content without normalisation (IAEA, 2013).

Different chemical geothermometers (silica and cation) were used to estimate the equilibrium temperature of thermal water in the aquifer. Chemical geothermometry represents the classical approach for estimating thermal water temperature within a deep aquifer. It relies on various empirical or experimentally derived calibrations based on temperature-dependent heterogeneous chemical reactions (Flóvenz et al., 2012). Classical chemical geothermometers use elemental content controlled by these reactions to infer the reservoir temperature (e.g. as seen in studies by Truesdell, 1976; Marini, 2004; Blasco et al., 2018). This approach assumes that these elemental contents remain unaltered during the water's ascent to the surface without significant modifications due to interactions with the surrounding rocks, attaining the equilibrium state.

Stable isotopes ($\delta^{18}O$ and $\delta^{34}S$) of sulphate anion (SO_4^{2-}) in thermal water were compared with the graphical classification provided by Porowski (2014, 2019) to determine the origin of sulphates in thermal water, as successfully applied by many authors (Bouaicha et al., 2019; Eastoe et al., 2022; Fórizs et al., 2019; Miljević et al., 2013).

Results and discussion

Major ions chemistry

A total of 72 thermal water samples were analysed. Based on the calculated charge balance error, two samples collected from Livadski izvor and Blatne kupelji thermal springs were excluded from the analysis. Table 1 shows the mean values and ranges of the groundwater physico-chemical parameters measured in situ, the major ions, and the silica concentration.

The graphical representation of the data summarised in Table 1 is shown in Fig. 3 in the form of a box-plot diagram, which indicates that analysed thermal water samples originate from the same thermal

Table 1 Descriptive statistics of in situ physico-chemical parameters, major ions, and silica content of Topusko thermal water

Sampling site	Statistics	T °C	pH –	EC µS/cm	TDS*	Ca^{2+} mg/L	Mg^{2+}	Na^{+}	K^{+}	HCO_3^-	SO_4^{2-}	Cl^-	NO_3^-	SiO_2
Livadski izvor spring	Mean	52.4	6.50	620	546	80.8	16.3	17.7	11.0	244.7	98.3	17.5	0.6	38.1
	Min	51.4	6.38	582	497	78.2	14.6	17.3	10.7	231.8	78.6	14.5	0.3	35.3
	Max	53.2	6.76	635	562	82.4	16.9	17.9	11.3	257.4	106.8	19.4	2.9	40.5
	St. dev	0.5	0.09	10	14	0.8	0.5	0.2	0.2	6.8	7.3	1.3	0.8	1.4
Blatne kupelji spring	Mean	48.0	6.85	636	556	83.4	16.7	17.9	11.1	249.6	100.7	17.87	0.5	37.8
	Min	44.1	6.51	593	503	78.7	14.8	17.6	10.9	233.0	81.6	14.64	0.3	28.6
	Max	51.9	7.40	650	574	86.0	17.3	18.2	11.5	258.6	108.7	19.68	0.6	41.0
	St. dev	2.3	0.31	13	15	1.8	0.5	0.2	0.2	6.0	7.4	1.3	0.1	2.3
Well TEB-4	Mean	64.1	6.56	626	555	82.0	16.7	17.9	11.2	248.9	100.0	17.63	–	39.1
	Min	61.1	6.35	607	502	79.6	15.0	17.5	10.9	234.2	75.4	12.81	–	36.3
	Max	65.2	6.71	670	577	82.8	17.2	18.2	11.5	268.4	109.2	19.60	–	41.4
	St. dev	1.0	0.09	14	17	0.7	0.4	0.2	0.2	7.7	8.7	1.7	–	1.5

Charge balance errors are ± 5%. *TDS was calculated using Diagrammes V6.72 software (Simler, 2012)

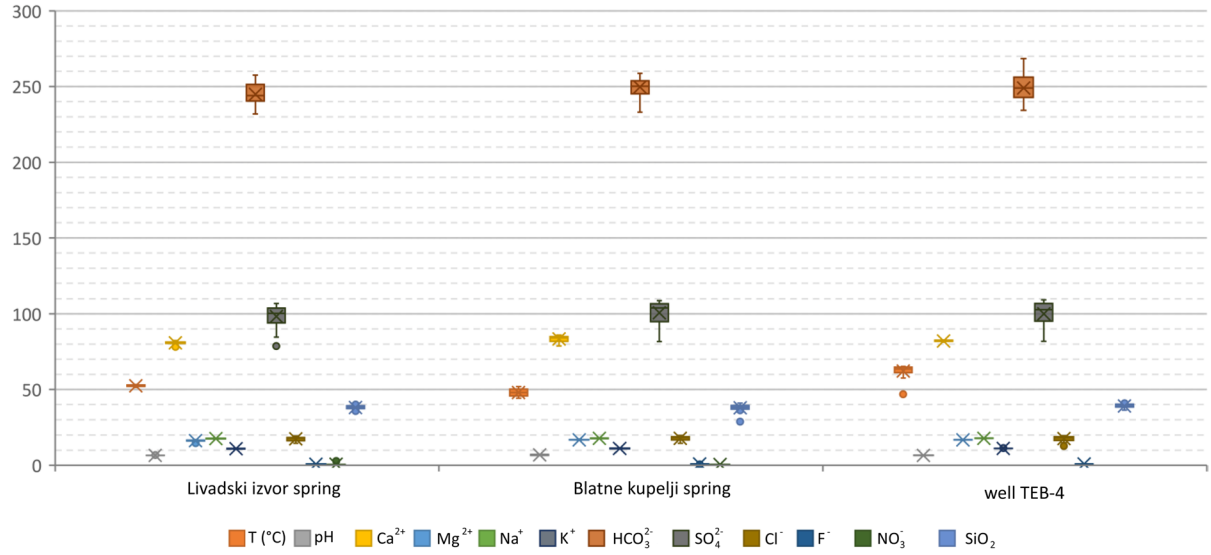

Fig. 3 Box-plot of Topusko thermal water major ions (mg/L), temperature T (°C), and pH

aquifer and display constant properties over the monitored period.

Thermal water pH is slightly acidic, with average values in the monitored objects from 6.5 to 6.8. The electrical conductivity (EC) ranges from 582 µS/cm to 680 µS/cm, being increased by the temperature effect, where the parameter values are proportionally increased with respect to temperature and not due to high mineralisation or high concentrations of HCO_3^- and SO_4^{2-} (Hermans et al., 2014). Total dissolved solids (TDS) in thermal water range from 497 to 577 mg/L and serve as a good indicator of water mineralisation (Hiscock & Bense, 2014), which can be characterised as medium to low. The TDS values are within the range for thermal waters of Internal Dinarides, which generally show TDS lower than 1 g/L (Milenić et al., 2012). The generally low mineralisation of the thermal water indicates a precipitation

recharge-dominated groundwater system, and water with a TDS < 1000 mg/L is considered fresh (Halle, 2004).

Continuous temperature measurements in thermal springs are presented in Fig. 4. The average recorded temperatures for thermal spring Livadski izvor are 52.68 °C and 48.04 °C for Blatne kupelji. Maximal measured temperatures are 53.66 °C and 52.42 °C, respectively. The temperature of thermal waters varies from 42.68 °C to 53.66 °C in the springs, while the temperature of water in TEB-4 well is 65 °C. Annual changes in temperature follow the seasonal changes in the air temperature, with more amplified amplitudes recorded at Blatne kupelji spring (up to 10 °C).

In samples from Topusko thermal water, major cations concentrations follow the order $Ca^{2+} > Na^{+} > Mg^{2+} > K^{+}$, with the dominance of Ca^{2+} (~80 mg/L) and comparable Na^{+} and Mg^{2+} concentrations (17 mg/L). The dominant anion in thermal water samples is HCO_3^{-}, ranging from 232 to 268 mg/L for all three sampling locations, followed by relatively high concentrations of SO_4^{2-} anion, ranging from 75 to 109 mg/L. The composition of the major ions of thermal water is shown graphically using Piper's diagram (Fig. 5) (Piper, 1944). According to the composition of the major anions and cations, the samples show Ca-HCO_3 hydrochemical facies (Freeze & Cherry, 1979), as indicated by the dominant presence of Ca^{2+} and HCO_3^{-} in the Piper diagram. This composition suggests that the limestone is the dominant source of dissolved solutes in the aquifer and prevailing in the catchment area, together with dolomites, as the dominance of Ca^{2+} cation followed by Mg^{2+}, with lower content of alkali metals, is characteristic of groundwater in worldwide carbonate aquifers (Goldscheider et al., 2010; Lei et al., 2022; Li et al., 2020; Patekar et al., 2022; Wang et al., 2020). Plotting of sample composition in the Piper diagram in almost the same spot indicates

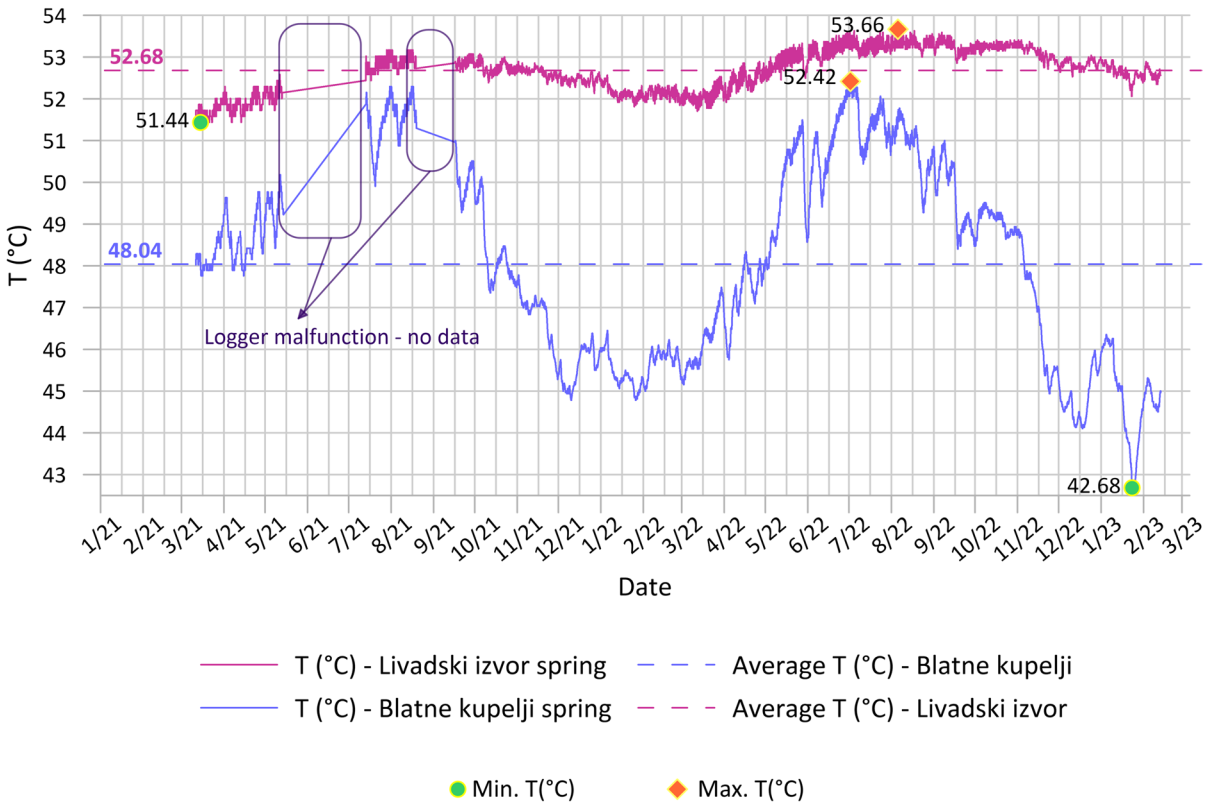

Fig. 4 Continuous temperature data measured at thermal springs Livadski izvor and Blatne kupelji from March 2021 to February 2023

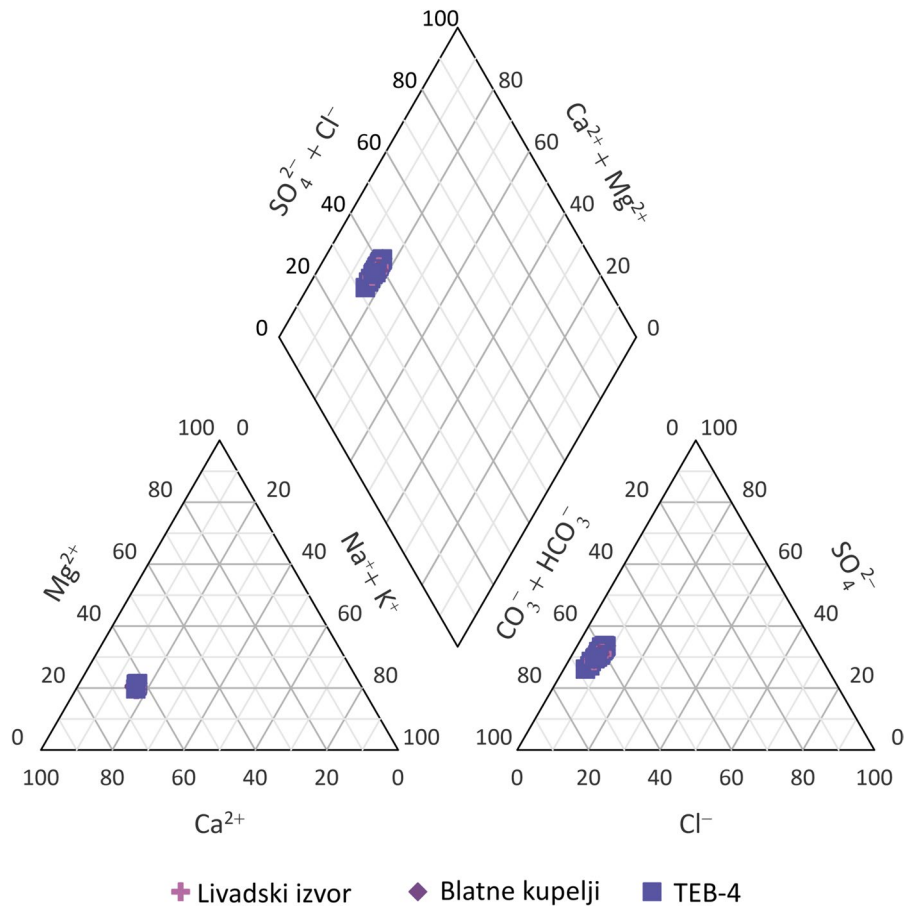

Fig. 5 Piper diagram of thermal water samples from the discharge area of Topusko HTS (March 2021–February 2023)

a large and stable system where the ion composition is more or less constant with no significant changes over time.

Assuming that the initial composition of Topusko thermal waters originates from precipitation, which is usually the primary recharge source for most groundwaters (Ármannsson, 2012), during the water cycle, the initial composition of water is altered mainly through rock-weathering, evaporation and other geochemical processes that occur in the aquifer (i.e. dissolution, ion exchange, sulphate reduction, etc.) (Appelo & Postma, 2005; Fetter, 2001; Halle, 2004; Mazor, 2004). In order to get a better understanding of water–rock interaction and geochemical processes governing the solute content in thermal water, biplot diagrams of molar or equivalent ratios of major anions and cations were studied (Clark, 2015; Garrels, 1976; Hounslow, 1995; Rman, 2016; Xu et al., 2019; Zhang et al., 2016). Due to the plausible flow of Topusko water in a carbonate aquifer, the Ca^{2+}/Mg^{2+} molar ratio was investigated (Fig. 6a). The stoichiometry ratio of dominant dolomite dissolution would be 1 and mixed limestone with dolomite 2 (Fellehner, 2004; Gao et al., 2017; Hilberg & Schneider, 2011). Topusko water shows the equivalent ratio of 3, pointing to a surplus of Ca^{2+} over Mg^{2+}. Such ratio suggests a prevailing interaction of thermal water with limestone, followed by dolomite, as well as possible additional sources of Ca^{2+}.

Additionally, the relationship between ($Ca^{2+} + Mg^{2+}$) and HCO_3^- in Fig. 6b shows the surplus of cations over HCO_3^-, suggesting an additional source of Ca^{2+} besides carbonate dissolution. Possible sources could be ion exchange, gypsum dissolution, silicate weathering, or incongruent dissolutions of dolomite. The following bivariate plots were examined to narrow the occurrence of one or more of these processes. The scatter plot ($Ca^{2+} + Mg^{2+}$) versus ($HCO_3^- + SO_4^{2-}$) is commonly used to identify ion exchange processes (Fisher & Mullican, 1997;

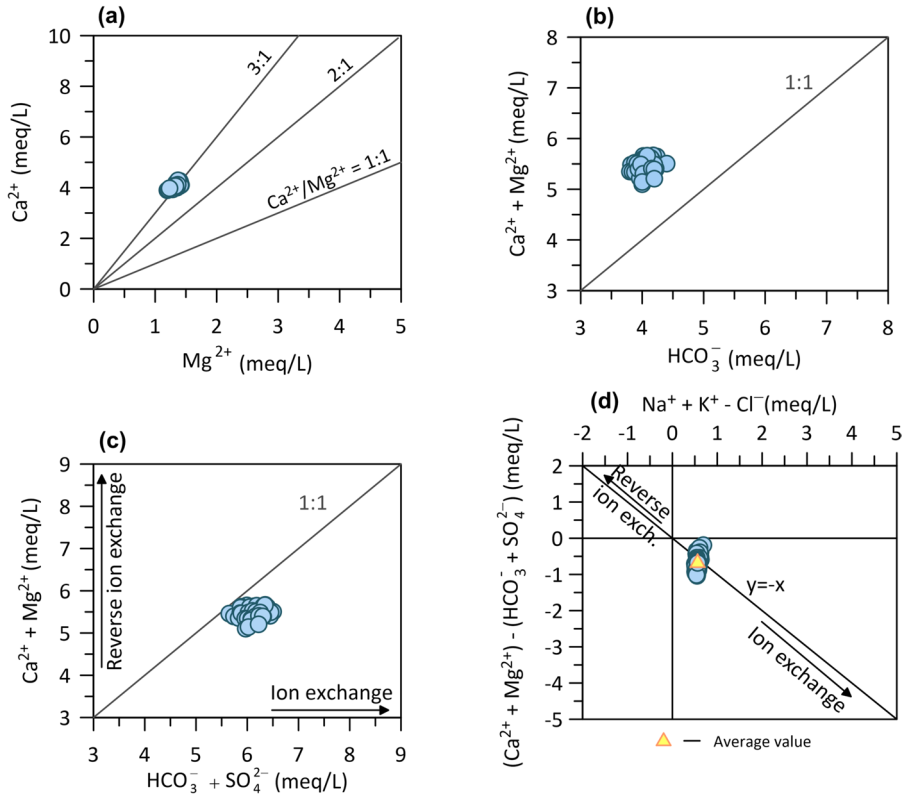

Fig. 6 Biplots of **a** Ca^{2+} vs Mg^{2+}, **b** $(Ca^{2+}+Mg^{2+})$ versus HCO_3^-, **c** $(Ca^{2+}+Mg^{2+})$ versus $(HCO_3^-+SO_4^{2-})$ and **d** $(Ca^{2+}+Mg^{2+})-(HCO_3^-+SO_4^{2-})$ versus Na^++K^+-Cl^-

Nematollahi et al., 2016; Tay et al., 2015; Tziritis et al., 2016). As depicted in Fig. 6c, SO_4^{2-} participates in balancing the solution in addition to HCO_3^-. The equiline represents the stoichiometry correlation between these ions, which assumes carbonate and gypsum (and anhydrite) dissolution as the dominant and equally represented process controlling solution composition. Samples show a ratio of 0.9 resulting from a $(Ca^{2+}+Mg^{2+})$ depletion with respect to $HCO_3^- + SO_4^{2-}$, suggesting the cation exchange process occurs in the aquifer along with carbonate minerals dissolution. As a result, Na^+ and K^+ must balance the excess in the solution's negative charges.

For further evaluation of the previously assumed ion exchange process, a bivariate plot $(Ca^{2+}+Mg^{2+})-(HCO_3^- + SO_4^{2-})$ versus $(Na^+ + K^+ - Cl^-)$ was examined (Fig. 6d) (García et al., 2001; Xiao et al., 2017). Samples plotting at the centre of the plot would indicate the absence of ion exchange or reverse or ion exchange processes. In the case of ion exchange as a significant controlling process, the samples would plot on the line with slope − 1 (y = − x). Results indicate that Na^+, K^+, Ca^{2+}, and Mg^{2+} in Topusko thermal aquifer participate in ion exchange reactions. The graph in Fig. 6d shows the decrease in Ca^{2+} and Mg^{2+} content versus the increase in Na^+ and K^+. Such phenomena can be explained by an ion exchange process where Na^+ is removed from clay minerals and replaced by Ca^{2+} from the solution:

$$Ca^{2+} + 2Na - Clay \rightarrow 2Na^+ + Ca - Clay,$$

The ion exchange process reduces the concentrations of Ca^{2+} and Mg^{2+} and increases the Na^+ concentration in groundwater. Furthermore, the weathering of albite could also contribute to Na^+. According to Zhang et al. (2016), such a process might reflect longer groundwater residence times and longer flow paths, facilitating cation exchange reactions between the thermal water and aquifer matrix. Marković et al. (2015) showed an additional process of ion exchange

occurring along carbonate dissolution and controlling the major ion chemistry in the thermal waters of Hrvatsko Zagorje.

The occurrence of evaporite mineral gypsum dissolution in the thermal aquifer was investigated through the Ca^{2+}/SO_4^{2-} (Fig. 7a). Usually, the primary assumption regarding sources of sulphates in the groundwater is the dissolution of gypsum and/or anhydrite, which results in the Ca^{2+}/SO_4^{2-} stoichiometry equivalent ratio of 1. Topusko water has an average value of the Ca^{2+}/SO_4^{2-} ratio 2, which distributes all samples above the gypsum dissolution line. An excess of Ca^{2+} relative to sulphate anion indicates other sources of cation in addition to gypsum, such as calcite, dolomite or silicates (i.e. minerals like feldspar). Pavić et al. (2023) investigated historical chemical analyses of Topusko water and argued that gypsum dissolution is a minor process together with the dominant carbonate dissolution.

Dissolution of halite was additionally investigated to evaluate the source of Na^+ (Fig. 7b). Na^+ vs Cl^- biplot shows most samples plot above 1:1 equiline, with the ratio value of 1.5, suggesting that halite dissolution is not a primary source of Na^+. Excess of Na^+ over Cl^- indicates other sources of Na^+, such as albite (plagioclase) weathering or ion exchange (i.e. natural softening). Ion exchange occurs when the equivalent ratio of Na^+ versus $(Na^+ + Cl^-)$ is greater than 0.5 (Hounslow, 1995). The calculated ratio for thermal water samples shows a value of 0.6, corroborating the results obtained by the $(Ca^{2+} + Mg^{2+}) - (HCO_3^- + SO_4^{2-})$ versus $(Na^+ + K^+ - Cl^-)$ ratio (Fig. 6d).

Ca^{2+}/Na^+ and HCO_3^-/Na^+ ion ratios can be used to distinguish between silicate and carbonate weathering (Fig. 8a).

Research by Drever and Hurcomb in (1986) (cited in Hounslow, 1995) has shown that the process of silicate weathering leads to a water Na/Ca ratio resembling that of the plagioclase mineral it originated from. The molar ratios of Ca^{2+}/Na^+ greater than 10 imply solely carbonate weathering in the catchment area. Contrarily, the weathering of feldspar produces more alkali cations, and as a result, the Ca^{2+}/Na^+ ratio is typically smaller than 1 (Clark, 2015; Gaillardet et al., 1999). The Ca^{2+}/Na^+ molar ratio of 3

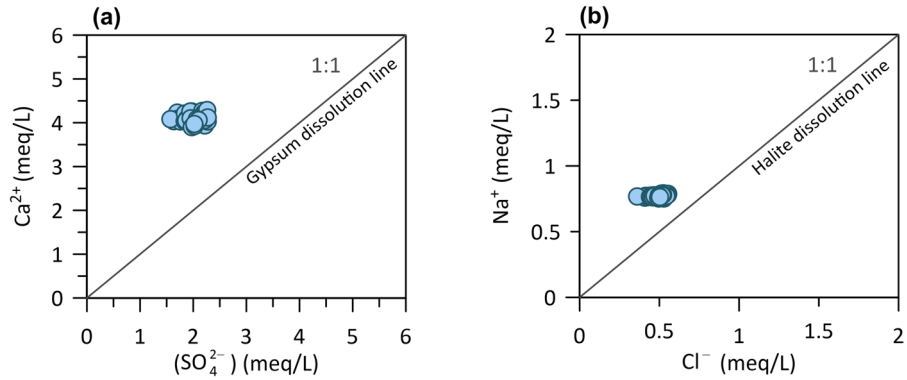

Fig. 7 Biplot scatter diagrams of **a** Ca^{2+} versus SO_4^{2-} and **b** Na^+ vs Cl^-

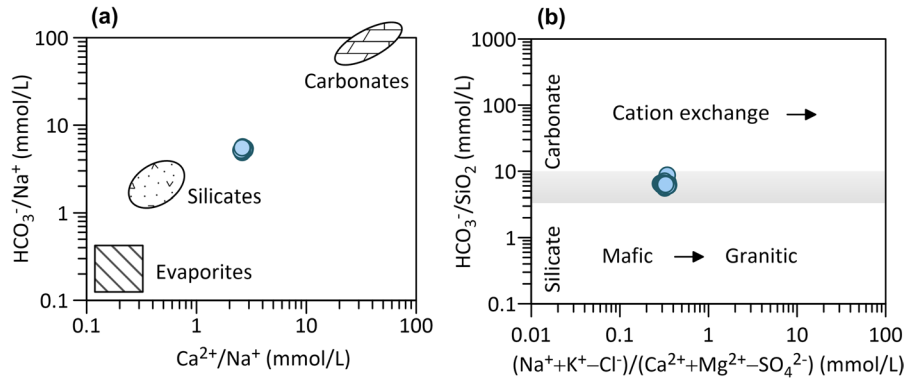

Fig. 8 Molar ratios in thermal water samples as indicators of silicate versus carbonate weathering (**a**, modified after I. Clark, 2015; Gaillardet et al., 1999). Chloride and sulphate corrections are made to account for evaporite contributions in the right-hand chart (**b**)

in Topusko thermal water samples is a manifestation of approximately 25–30% of silicate weathering and around 75% of carbonate weathering. Figure 8b corroborates previous indications of dominant carbonate dissolution and cation exchange processes in the thermal aquifer.

Considerable silica is released into solution by weathering albite and orthoclase (alkali feldspar) compared to other silicates (Clark, 2015; Hounslow, 1995). An arbitrary division of dominant silicate or carbonate weathering can be performed using the HCO_3^-/SiO_2 molar ratio being less than five or greater than ten for predominant silicate or carbonate dissolution, respectively. Figure 9a displays the bicarbonate/silica ratio of around 6 in the investigated thermal water. In addition, the ratio of $Mg^{2+}/(Mg^{2+} + Ca^{2+})$ greater than 0.5 would indicate silicate weathering, whereas in Topusko thermal water samples is 0.25, implying limestone-dolomite weathering process occurring during water chemical evolution (Fig. 9b). Thermal water samples fall between categories where the interpretation of results is ambiguous. The ratio of SiO_2/(Na + K-Cl) between values of 1 and two is indicative of albite weathering and less than 1 of cation exchange. Thermal water samples take on the value around 1.2, again corroborating the previously deducted impression on albite weathering in the aquifer or along the flow path.

If some uncertainties are still present, it is advisable to look at TDS values, which are usually lower for dominantly silicate weathering in the system (100–200 mg/L) than dominantly carbonate (500 mg/L or higher). In addition, considering the regional geological map, the surface outcrops of silicate lithologies (Jurassic siliciclastic deposits) are present at the surface SW from Topusko and can be expected in the subsurface.

The studied ratios point to carbonate dissolution as the main source of major ions and the ion exchange process in the thermal aquifer as the dominant source of Na^+ occurrence. The ion exchange process might occur in the final part of thermal water rise to the surface due to contact with Miocene sediments and Cretaceous flysch (Mišić, 2022).

Since the main thermal aquifer is composed of calcite and dolomite, their SIs were further investigated (Fig. 10). The results show that most samples from TEB-4 have saturation index values close to zero, falling within the uncertainty range (grey rectangle) and indicating that calcite and dolomite are in equilibrium in these waters. On the other hand, most of the samples from Livadski izvor spring had saturation index values below zero, indicating undersaturation. These results underline the dynamic nature of the interactions between minerals and thermal water, with most samples of TEB-4 showing a state of equilibrium in terms of calcite and dolomite saturation. Such results suggest that equilibrium water–rock interaction had been attained in the aquifer (Appelo & Postma, 2005).

Stable water isotopes

The $\delta^{18}O$ and δ^2H values for the thermal waters in the study area ranged from − 11.03‰ to − 10.73‰ and from − 76.02‰ to − 74.28‰, respectively. A total of 24 precipitation samples were analysed, with values

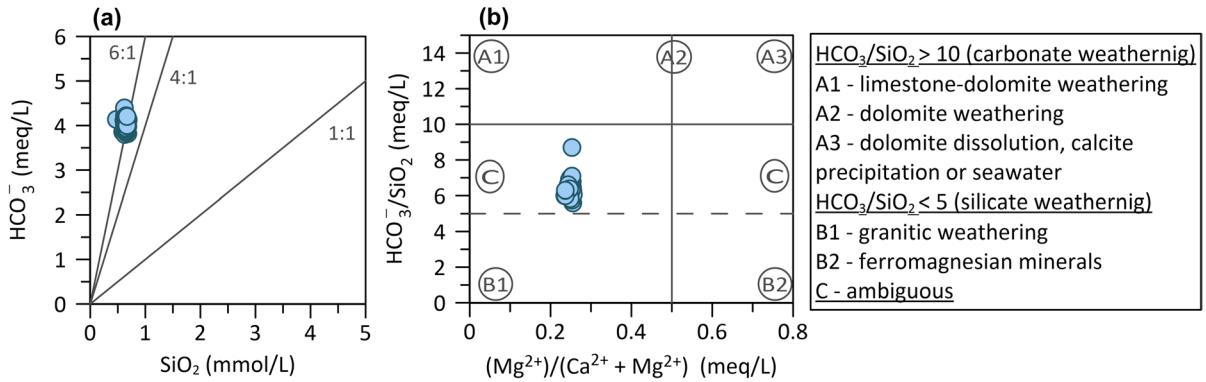

Fig. 9 Biplot of HCO_3^- vs SiO_2 ratio and HCO_3^-/SiO_2 vs $Mg2^+/(Ca2^+ + Mg2^+)$ equivalent ratio. Modified from Hounslow (1995) and (de Carvalho Filho et al., 2022)

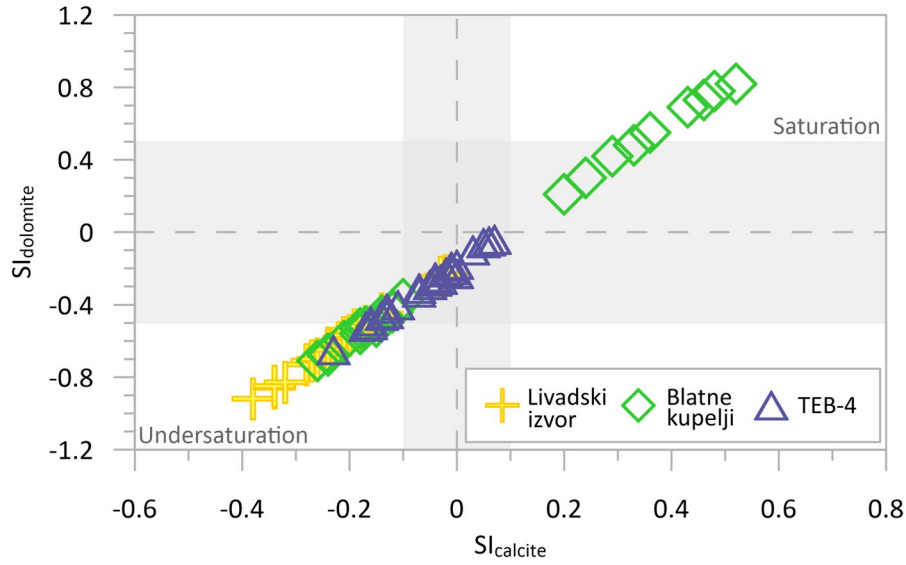

Fig. 10 Calculated saturation indexes (SI) with respect to calcite and dolomite for three sampling objects

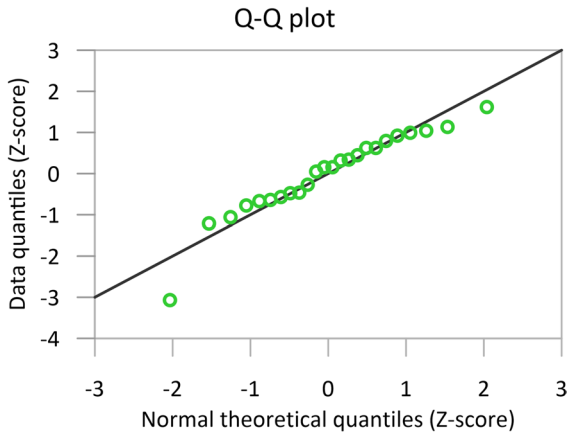

Fig. 11 Q–Q plot of δ^2H and $\delta^{18}O$ (d-excess) precipitation data

of $\delta^{18}O$ and δ^2H ranging from − 13.80‰ to − 3.96‰ and from − 100.21‰ to − 20.73‰, respectively (Briški et al., 2023).

Construction of LMWL and comparison with thermal water composition

A Q-Q plot was used to assess the normality of precipitation stable water isotope data before statistical analysis. Figure 11 indicates that most d-excess normalised values closely adhere to a theoretical normal distribution. However, one data point deviates significantly from the dataset. Despite this outlier, the W-test suggests that the remaining values do not deviate substantially from normal distribution, with an asymmetrical skewness. Using Chauvenet's Criterion, the outlier identified was removed (precipitation sampled in August 2022), and subsequent analysis showed that the dataset now exhibited a normal distribution with potentially symmetrical skewness.

Based on the simple linear regression model, the local meteoric water line (OLSR LMWL) is:

$$\delta^2H = 7.98\delta^{18}O + 12.48$$

The diagram in Fig. 12 shows the isotopic composition (δ^2H and $\delta^{18}O$) of all collected samples of thermal waters and precipitation in the area of the Topusko hydrothermal system together with calculated OLSR LMWL. The thermal water samples are distributed on the LMWL, confirming the meteoric origin of discharged thermal water in the spring area and showing that the secondary processes, such as evaporation of precipitation before infiltration, are negligible (Mazor, 2004). The weighted arithmetic mean value, calculated following Mance (2014), of the collected precipitation samples is $\delta^{18}O = -9.40$ ‰ (Fig. 12). Typically, the weighted mean annual value of $\delta^{18}O$ and δ^2H in precipitation represents the isotopic signature of groundwater (Clark, 2015). The mean value of the thermal water samples is approximately − 10.92‰ with minor

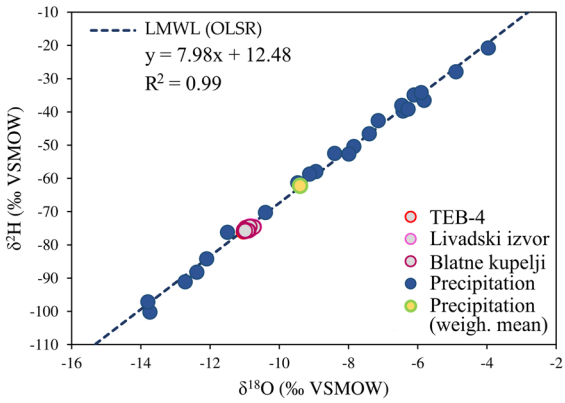

Fig. 12 Isotopic composition δ^2H and $\delta^{18}O$ of all collected thermal water and precipitation samples in the area of the Topusko hydrothermal system together with calculated OLSR LMWL

variations among the sampled objects. Lower mean values of stable isotopes of thermal waters in relation to weighted mean precipitation values (-1.51 ‰) may indicate a different area of recharge (i.e. a higher altitude) or that the recharge took place in colder climatic conditions in comparison with present (Bayari et al., 2009; Mazor, 2004; Porowski, 2014). Since there are no substantial changes in altitude in the investigated area (Fig. 2), the observed shift could be justified by different climatic conditions, suggesting that the Topusko thermal waters are relatively old.

Paleogroundwater

Paleogroundwaters, recharged during past glaciation events, exhibit distinct isotopic characteristics, being isotopically depleted relative to modern meteoric groundwaters and shifted along GMWL towards negative values (Clark et al., 2000; Grasby & Chen, 2005; Porowski, 2014). The "paleoclimatic effect" was exemplified by Porowski (2014) in the Great Hungarian Plain, where Pleistocene recharge had $\delta^{18}O$ values below −10 ‰ and the values of ^{14}C activity less than 10 pMC (i.e. 20 ka BP). To account for potential altitude effects, δ^2H and $\delta^{18}O$ values from nearby measurements in Zagreb and Mt. Medvednica (10 km north of Zagreb station) were considered, revealing a consistent vertical isotopic gradient of −0.28‰ per 100 m (Krajcar-Bronić et al., 1998; Vreča et al., 2006). Kern et al. (2020) recommend the use of values of −1.2‰/km for $\delta^{18}O$ and −7.9‰/km for δ^2H as an 'altitude' effect in the Adriatic Pannonian region for modern precipitation. This information allowed for the estimation of precipitation recharge elevation from ≈700 to ≈1200 m above sea level of THS. Notably, the absence of high mountains in the region supports the idea of geothermal aquifer recharge during different climate conditions, indicating paleogroundwater in Topusko.

In the assumed recharge area, d-excess values for precipitation ranged from 9.73‰ to 15.81‰, with thermal water values falling within this range, averaging 12.1‰. These observed d-excess values reflect the climate conditions at the time of recharge, which may have been notably different from the present. While the study area is close to the Mediterranean coast, it appears that continental precipitation is the primary source of recharge, as suggested by mixing of vapour sources in thermal water d-excess values (Kostrova et al., 2020; Chizhova et al., 2022).

Tritium content

Table 2 shows tritium concentrations of analysed thermal water samples. The tritium activity concentrations for samples collected during the minimum abstraction rates are below the detection limit. The absence of detectable tritium suggests that geothermal waters are sub-modern (Motzer, 2007) and have infiltrated the subsurface before 1950.

The tritium concentration of the sample collected after the heating season, when the abstraction rates are maximal, was determined to be 0.89 ± 0.82 TU,

Table 2 Results of tritium activity concentrations of thermal water samples

Well, sampling date	Depth (m)	Conditions	Bq/L	TU (tritium unit)
TEB-4; 12.5.2022	80.8	Maximal use of thermal water*	0.10 ± 0.10	0.89 ± 0.82
TEB-4; 13.9.2022	80.8	Minimal use of thermal water	0.02 ± 0.03**	0.14 ± 0.28**

* The end of the district heating season, which lasts around 205 days. ** Below detection limit

indicating the mixing of sub-modern and modern water (Motzer, 2007). However, this interpretation should be carefully considered since the measured value is at the limit between the two categories. This result could suggest a mixing of the thermal water with modern water from shallow aquifers connected to a local pressure drop in the thermal aquifer due to thermal water abstraction for heating and health purposes. Although the thermal aquifer is confined and artesian, its upper confining layer is probably leaky, providing a connection with the shallow colder aquifer hosted in the Quaternary cover. Such results are not representative of tritium content in the thermal aquifer. Similar tritium concentration activity results in thermal springs and interpretations were reported by Young (1985).

Carbon isotopes of dissolved inorganic carbon (DIC)

Topusko thermal water samples have ^{14}C activity of 11.6–13.1 pMC and ^{14}C DIC apparent age between 16,330 and 16,790 ± 40 years BP (Table 3). Conventional radiocarbon age results suggest that the groundwater was recharged during the Late Pleistocene, close to the last glacial maximum (LGM), around 18,000 years BP (Clark et al., 2009; Hughes et al., 2013, 2022a; Prell et al., 1980), by paleo-precipitation. High values for the $\delta^{13}C$ measured with respect to VPDB in water samples are consistent and range from − 4.1 to − 4.3 ‰, indicating possible dilution with "dead carbon", mixing or isotopic exchange (Gallagher et al., 2000).

Single-sample-based correction models

Traditional adjustment models (Eichinger, 1983; Fontes & Garnier, 1979; Ingerson & Pearson, 1964; Mook et al., 1974; Plummer & Sprinkle, 2001; Tamers, 1975) were used to calculate initial ^{14}C content and adjusted ^{14}C ages based on DIC content from a single well TEB-4 and major ions composition data. The parameters used in traditional models' calculations via NetpathXL are assumed to be 100 pMC for the initial ^{14}C value of the soil CO_2, solid carbonate minerals are assumed to have $\delta^{13}C$ of 0 ‰ and ^{14}C of 0 ‰ and the $\delta^{13}C$ of soil gas CO_2 was calculated by assuming that the dissolved CO_2 is in isotopic equilibrium with the soil gas (Han & Plummer, 2016). However, in reality, these values exhibit spatial and temporal variations, impacting the certainty of ^{14}C age estimations, which depend on both model choice and estimated ^{14}C and ^{13}C values of soil CO_2 and carbonate minerals (Han & Plummer, 2016; Wood et al., 2014). Concentrations of total dissolved inorganic carbon (TDIC) were assumed to be equal to bicarbonate (alkalinity), considering the pH-dependent distribution of dissolved carbonate species (Mook, 2000). In most systems closed to soil CO_2, HCO_3^- is the predominant species, and TDIC is mainly in the form of alkalinity (HCO_3^-) (Bottrell et al., 2019; Han & Plummer, 2016).

Han graphical method

The Han et al. (2012) graphical method was used to identify geochemical processes that affect the chemical composition of thermal water and for qualitative estimation of the radiocarbon age of thermal groundwater samples. The graphs in Fig. 13 show the relationship between $\delta^{13}C$ (‰) and the reciprocal of DIC concentration ([DIC]) (I), the relationship between measured ^{14}C activity (pMC) and 1/[DIC] (II), and the relationship between measured ^{14}C activity (pMC) and $\delta^{13}C$ (‰) (III). It is assumed that DIC and HCO_3^- concentrations are almost equal regarding Topusko water chemical evolution following recharge, which is determined by plotting data points left of line X in graphs I and II. Since the value of $\delta^{13}C$ soil gas CO_2 at the time of recharge is unknown, it is assumed to be − 26 ‰, which is today's measured

Table 3 Carbon isotope data of DIC and ^{14}C apparent age of Topusko thermal water

Well, sampling date	Conditions	^{14}C (pMC)	^{14}C (pmc)	$\delta^{13}C$ (‰ VPDB)	Apparent DIC ^{14}C age (BP)
TEB-4; 12.5.2022	Maximal use of thermal water*	13.1 ± 0.1	26.8	-4.3	16 330 ± 40
TEB-4; 13.9.2022	Minimal use of thermal water	12.4 ± 0.1	25.3	-4.3	16 790 ± 40

*The end of the district heating season, which lasts around 205 days

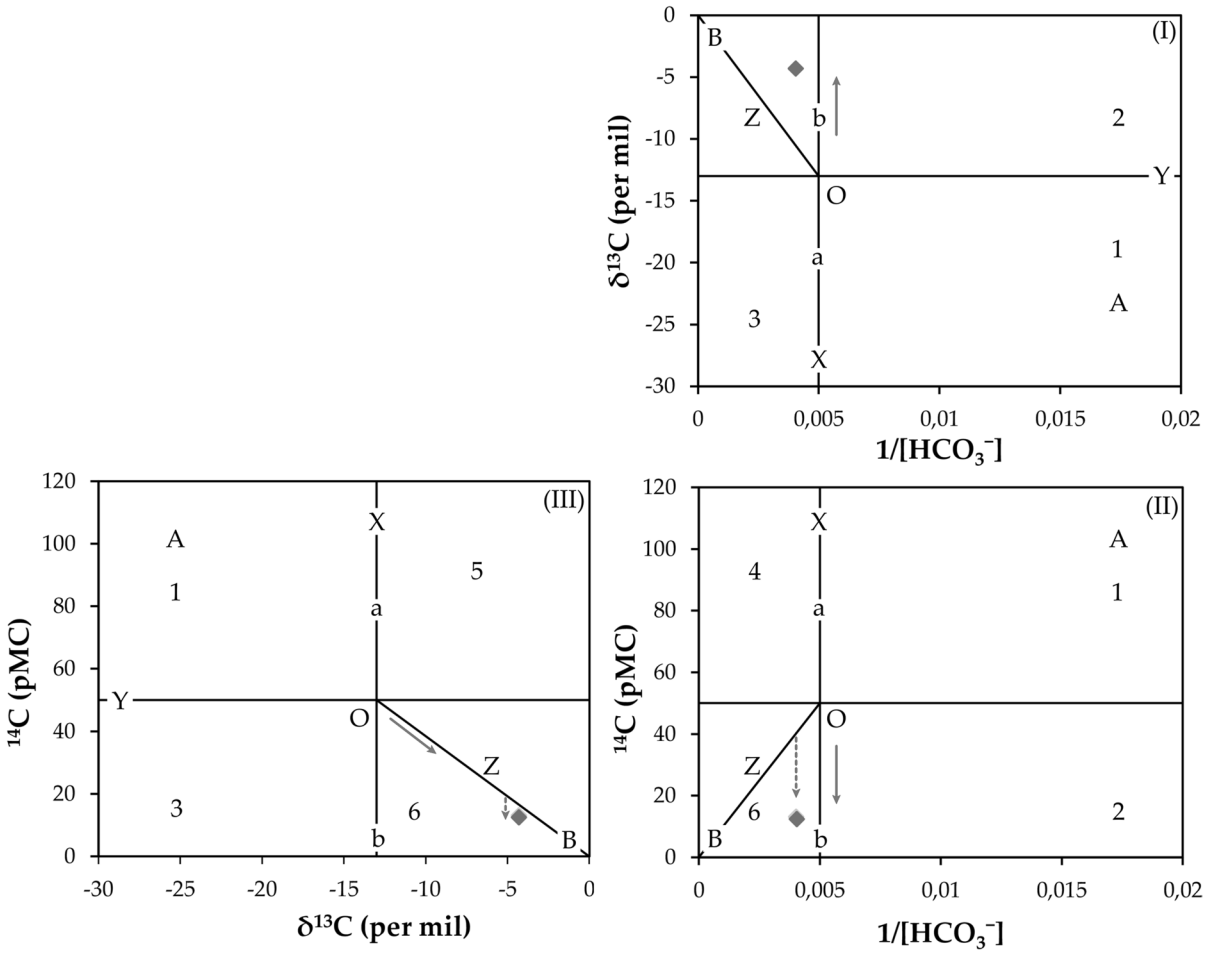

Fig. 13 Graphical representation modified after Han et al. (2012) shows chemical and isotopic evolution of DIC in Topusko thermal water. The full-line arrows represent the isotopic exchange between water and solid carbonate, and the dashed-line arrows represent the decay of ^{14}C

average concentration of C_3 type of plants (Cerling et al., 1993; Han & Wassenaar, 2021; Mook, 2000). The initial ^{14}C value of soil CO_2 is assumed to be 100 pMC. The assigned ^{14}C and $\delta^{13}C$ values for carbonate minerals are 0 pMC and 0 ‰, respectively (Han & Plummer, 2016). In our study, Tamer's point, the 'primary' carbon isotopic composition of DIC (*mainly* $CO_{2(aq)}+HCO_3^-$) is located at − 13 ‰ for $\delta^{13}C$ and 50 pMC. A more detailed explanation of diagram construction and application is provided by Han et al. (2012).

The samples are plotted in region 6 of the Han graph (Fig. 13; (II) and (III)), typical for "old waters". Samples plotting in this region are expected to have undergone ^{14}C decay. It is observed that the data plot very close to the carbonate dissolution line, which is indicative of a strong dilution of carbon isotopic content and a downward shift point to ^{14}C decay. The Han graph indicates two possible major processes influencing DIC and carbon isotope composition (^{13}C and ^{14}C) in thermal water: (i) isotopic exchange between water and carbonate and (ii) incongruent dissolution of carbonates. The effect of "dead carbon" introduced by the dissolution of limestones and dolomites changes the isotopic composition by increasing $\delta^{13}C$ and diluting ^{14}C concentrations from crossing point O, as carbonates are assumed to have ^{14}C-free DIC (~0 pMC). It is to reiterate that if groundwaters are old, water–rock interaction might cause the loss of the initial isotopic signature (Han & Plummer, 2016).

Based on the graphs in Fig. 13, the age of thermal water could be estimated to be around 9,250 years BP, from an initial ^{14}C content of ca. 40 pMC (vertical intersection with zero-age line Z, on graph II).

Radiocarbon age of Topusko thermal water

The radiocarbon age calculated by application of traditional models (Plummer & Glynn, 2013) and Han et al. (2012) graphical method is presented in Table 4.

The relationship between ^{3}H and ^{14}C content in groundwater and ^{13}C and ^{14}C in nature, schematically presented by Mook (2000), indicates the presence of old groundwater in the Topusko aquifer, which has a carbon isotopic footprint more similar to fossil carbonates than aged groundwater. The identified geochemical processes, which account for the reservoir effect and result in $\delta^{13}C$ enrichment and ^{14}C depletion, are strong and backing up the use of denormalised ^{14}C DIC values ('pmc') for calculation of radiocarbon age by application of traditional adjustment models to a single water analysis in the system. The various models generated corrected values of initial ^{14}C (A_0) content ranging from 59 to 100 pmc, which gave thermal water residence times of 6,668 to 10,687 years BP, based on the ^{14}C activity measured in thermal water samples. The average residence time obtained from traditional models is 8,448 years BP and 9,250 years BP for qualitative estimation using the Han–Plummer plot (A_0 ca. 40 pMC). Horvatinčić et al. (2012) reported groundwater age for a similar ^{14}C activity value from the Zagreb dolomite geothermal aquifer at $11{,}650 \pm 620$ years BP but without correction for the reservoir effect.

Along with numerous empirical methods that have been used to estimate A_0, Geyh (2000) calculated a set of A_0 values that would be better suited for characterising the initial ^{14}C activity of DIC in water discharging from distinct aquifer geological settings, which were proven to exhibit strong agreement with A_0 values frequently derived more rigorously through independent modelling. In the case of THS, where the catchment area is dominantly built of carbonates, thermal water age corrections of $-3{,}500$ to $-5{,}000$ can be expected, with the estimated initial ^{14}C activities ranging from 55 to 65 (pMC). Such calculations can roughly be considered in accordance with the results obtained for THS with the traditional model of the Mook and Han graphical method (Table 4).

Within the context of the geological time scale, the recharge of the Topusko geothermal aquifer might have occurred during the Late Pleistocene and the beginning of the Holocene, coinciding with the end of the Last Glacial Cycle—a global ice expansion period (Goñi, 2022; Palacios et al., 2022). During this period, most of western and central Europe and Eurasia was open steppe-tundra, while the Alps presented solid ice fields and montane glaciers (Li, 2022). Research by Hughes et al. (2022b) suggests that some of the lowest Pleistocene glaciers in Southern Europe formed in the coastal Dinaric Alps bordering the Adriatic Sea. During the LGM (Hughes et al., 2013), average global temperatures were around 8.3 ± 1.5 °C, with year-round ice covering about 8% of Earth's surface and 25% of the land area, while currently (as of 2012) about 3.1% of Earth's surface and 10.7%, respectively (Dubey, 2023). This suggests that climate conditions during the recharge were

Table 4 The corrected initial activities of ^{14}C DIC values and calculated radiocarbon ages using traditional adjustment models calculated via NetpathXL and Han et al. (2012) graphical method

Well	Uncorrected age	Selected adjustment models											
		Mass balance		Tamers		Ingerson and Pearson		Mook		Fontes and Garnier		Han graph	
	Age	A_0	Age	A_0	Age	A_0	Age	A_0	Age	A_0	Age	A_0	Age
	BP	pmc	BP	pmc	BP	pmc	BP	pmc	BP	pmc	BP	pmc	BP
TEB-4 12.5.2023	16,330	60.04	6,668	67.26	7,607	68.81	7,795	91.95	10,192	71.88	8,155	40.20	9,010
TEB-4 13.9.2023.*	16,790	59.56	7,078	67.69	8,136	68.26	8,205	92.16	10,687	69.51	8,355	40.40	9,491

*NetpathXL programme uses modern ^{14}C half-life (5730) and needs to be converted to Libby half-life (5570) using the equation $t_{libby} = 0.972 t_{5730}$ (L. N. Plummer & Glynn, 2013). The age differences range from 187 years to 299 for the oldest age estimation, and negligible differences can be assumed for this study and method

colder than present, corroborating the stable water isotope signature.

Stable sulphate anion isotopes $\delta^{34}S$ and $\delta^{18}O$ of SO_4^{2-}

The results of $\delta^{34}S$ and $\delta^{18}O$ of SO_4^{2-} anion in thermal water samples are presented in Table 5. The analysis found a consistent isotopic composition across sampled thermal waters, with average values of 9.3 ‰ and 8.35 ‰ for $\delta^{34}S$ and $\delta^{18}O$, respectively. This uniformity indicates a stable source or process governing the sulphate composition within this hydrothermal system.

According to the ratio of $\delta^{34}S$ and $\delta^{18}O$ of SO_4^{2-}, the sulphate in the Topusko water could be of atmospheric or evaporitic origin (Fig. 14; Porowski et al., 2019).

The atmospheric deposition (i.e. rain and snowmelt) as a source of the sulphates in the Topusko water can be excluded since the atmospheric input usually results in low concertation of sulphates. Conversely, the Topusko water has a relatively high concentration of sulphates (Table 1), which is higher than other thermal and fresh waters in Central Croatia (Borović, 2015; Marković et al., 2015; Nakić et al., 2013). Furthermore, it is unlikely that the isotopic signature of sulphates reflects the current atmospheric conditions due to the long residence time of the thermal water suggested by $\delta^{18}O$, $\delta^{2}H$, ^{3}H, and ^{14}C.

The presence of sulphate in the Topusko thermal water may be linked to the dissolution of evaporite sulphates (gypsum and/or anhydrite). The enrichment of sulphates with heavier isotopes, such as oxygen ^{18}O and sulphur ^{34}S, is a characteristic sign of evaporite sulphate dissolution. Gypsum is known to accumulate in the soil of arid regions and often occurs alongside dolomite and limestone. Given the geological composition of the Topusko geothermal aquifer, which predominantly consists of carbonates, the presence of evaporites below the aquifer is plausible. Geological mapping of the region identified gypsum outcrops NW of Cetingrad (≈ 20 km SW from Topusko), likely part of an Upper Permian evaporite

Table 5 $\delta^{34}S$ and $\delta^{18}O$ isotopic composition of SO_4^{2-} anion in thermal water samples

Well, sampling date	Conditions	$\delta^{34}S$ (‰) (CDT)	$\delta^{18}O$ (‰) (VSMOW)
TEB-4; 12.5.2022	Maximal use of thermal water*	9.2	9.3
TEB-4; 13.9.2022	Minimal use of thermal water	9.4	7.4

*The end of the district heating season, which lasts around 205 days

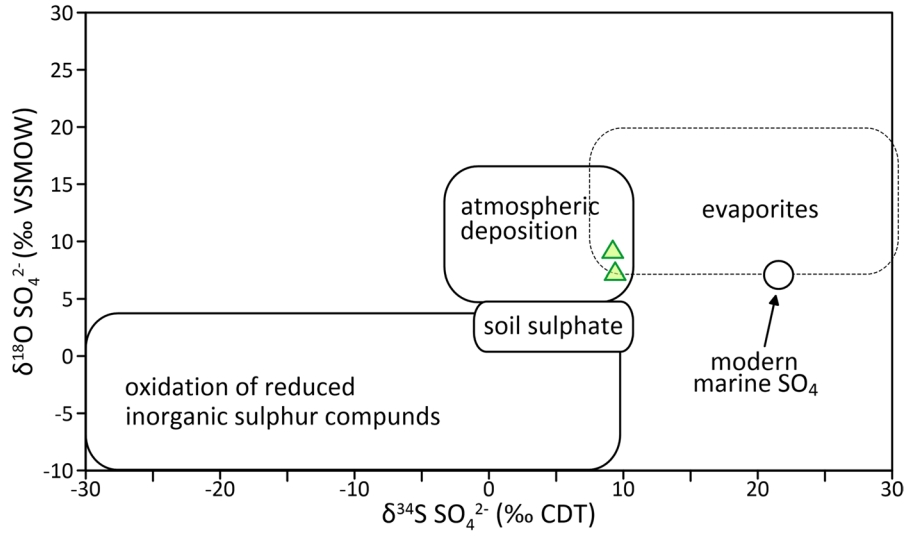

Fig. 14 The $\delta^{34}S$ versus $\delta^{18}O$ of dissolved SO_4^{2-} in thermal water of Topusko aquifer (triangles) versus the background values of typical sulphate sources (after Porowski et al., 2019)

sequence associated with fibrous gypsum and fine-grained primary dolomite (Korolija et al., 1980b).

Gypsum and anhydrite dissolve without isotope fractionation, which enables direct use of the isotopic composition of $SO4_2^-$ as a tracer for the sulphate origin (Porowski, 2014). By comparing the sulphate isotope content in Topusko thermal water to global measurements of marine evaporite deposits, notable variations in $\delta^{34}S$ values over geological time were observed. These values ranged from around + 35 ‰ during the Cambrian to less than + 10 ‰ in the Permian period. Similarly, $\delta^{18}O$ values fluctuated from approximately + 20 ‰ to around + 7 ‰ (Claypool et al., 1980). Previous studies, such as Forzis et al. (2019) in Budapest (Hungary), have used similar analyses to determine the origin of dissolved sulphates in thermal waters and concluded that the dissolved sulphate in thermal water is mainly a product of Permian evaporite dissolution. It is possible to assume that the presence of dissolved sulphate in Topusko thermal water, characterised by an average $\delta^{34}S$ value of 9.3 ‰ and an average $\delta^{18}O$ value of 8.35 ‰, can be attributed to evaporite dissolution.

Geothermometers

The equilibrium thermal water temperature in the thermal aquifer was estimated by several classical chemical geothermometers (Table 6).

The Na–K (g, h, i; Table 6) and Na–K-Ca (j, k; Table 6) geothermometers provide an average equilibrium temperature of thermal water from 263.8 °C to 526.1 °C, which is not realistic, based on the geological and hydrogeological setting in the study area, and therefore are rejected. Furthermore, these geothermometers are generally considered inadequate for low-temperature reservoirs/aquifers (Karingithi, 1984). The Ca-Mg geothermometer (l; Table 6) yields elevated temperature values, approximately 117 °C, which can potentially be influenced by uncertainties due to the disorder degree of dolomite (Blasco et al., 2017; Bruno et al., 2020). The values obtained by K-Mg geothermometers were 64 °C, similar to those obtained by SiO_2-chalcedony (approximately 60 °C), close to the wellhead and spring temperature values. These calculations are unrealistic because the temperature of the water can decrease slightly during its ascent to the surface, and there is no mechanism which would cause the water to heat up during outflow. The calculated average aquifer equilibration temperature by quartz geothermometers (a,b,c; Table 6) is 90 °C. Pavić et al. (2023) reported the predicted average aquifer temperature of THS to be approximately 78 °C using quartz geothermometers. The discrepancy could be related to the lower silica concentrations in the historical hydrochemical data. Despite the small difference, both results could be considered realistic since quartz geothermometers are generally considered the more accurate for low-temperature systems with waters with near neutral pH (Blasco et al., 2018, 2019; Borović, 2015; Rman, 2009; Witcher & Stone, 1983).

Conclusions

The paper presented and discussed the results of the first systematic monitoring of the thermal waters of the THS, and the main conclusions which can be drawn therefrom are as follows:

1. Principal ion chemistry data show that the Topusko thermal waters display Ca-HCO_3 hydrochemical facies, confirming the influence of geo-

Table 6 Temperatures (°C) calculated using experimentally calibrated chemical geothermometers (silica and cationic) for the Topusko thermal water samples

Sampling location	a (°C)	b (°C)	c (°C)	d (°C)	e (°C)	f (°C)	g (°C)	h (°C)	i (°C)	j (°C)	k (°C)	l (°C)	m (°C)
Livadski izvor spring	89.7	89.5	90.7	58.8	60.8	90.3	525.7	360.83	388.0	415.7	264.4	117.7	63.9
Blatne kupelji spring	89.3	89.2	90.4	58.4	60.5	89.9	526.1	360.99	388.2	415.8	262.5	118.0	64.0
TEB-4 well	90.8	90.6	91.8	59.9	61.9	91.4	526.5	361.21	388.6	416.1	264.4	116.9	64.0
Average	89.9	89.8	91.0	59.0	61.1	90.5	526.1	361.10	388.3	415.8	263.8	117.5	64.0

(a—Truesdell, 1976), (b—Fournier, 1977), (c—Michard, 1979), (d—Verma & Santoyo, 1997), (e—Fournier, 1977), (f—Arnórsson et al., 1983), (g—Michard, 1979), (h—Fournier, 1977), (i—Truesdell, 1976), (j—Fournier & Truesdell, 1973), (k—Benjamin et al., 1983), (l—(Chiodini et al., 1995), (m—Giggenbach, 1988))

logical formations dominated by carbonate rocks. In THS, around 75% of carbonate weathering and 25–30% of silicate weathering occur. High concentrations of Ca^{2+}, Na^{+} and Mg^{2+} were caused by mineral dissolution and cation exchange. Considering the available historical data, thermal water composition is stable. The differences were observed in the higher silica content at present, possibly due to different measurement methodologies. Ion exchange and silicate weathering cause the increase of Na^{+} from the recharge to the discharge zone.

2. Stable water isotope data, $\delta^{2}H$ and $\delta^{18}O$, suggest that the recharge of thermal water is of meteoric origin, i.e. precipitation. Lower mean values of stable isotopes (-1.51 ‰ in $\delta^{18}O$) of thermal waters in relation to weighted mean precipitation values indicate that the recharge took place in colder climatic conditions compared to the present. The $\delta^{18}O$ values of thermal water are very uniform, from − 11.3 ‰ to − 10.73 ‰, indicating deep circulation and large areal extent and thickness of the aquifer, with longer residence times in which seasonal variations of precipitation are homogenised.
3. Additionally, ^{14}C dating of DIC shows that thermal water has residence time ranging from 6,668 years BP to 10,687 years BP. The average residence time obtained from traditional models is 8,473 years BP and 9,536 years BP for qualitative estimation using the Han–Plummer plot. These ages also suggest that thermal water is representative of the colder climate in the late Pleistocene or early Holocene.
4. Tritium activity in thermal water is below the detection limit. However, after the period of extensive abstraction for district heating during winter, some tritium activity (around the detection limit) was measured in thermal water samples. Possible infiltration of modern precipitation from younger layers above is possible, as the hanging wall is not absolutely impermeable. Regular and precise measurement of tritium activity would be very useful for understanding if the abstraction rates are sustainable.
5. Chemical geothermometers were used to estimate the maximum equilibrium temperature reached by thermal waters in the aquifer. The quartz geothermometer provided the most plausible equilibrium aquifer temperature of 90 °C.
6. Data on stable sulphate anion isotopes, $\delta^{34}S$ and $\delta^{18}O$, point to gypsum and/or anhydrite dissolution at depth. Deeper boreholes or seismic profiles do not exist, so this assumption is based solely on hydrochemical data.

All of the mentioned analyses and interpretations give valuable information for the development of the conceptual model of THS by constraining the hydrogeochemical processes that drive the solute content, determining the source of recharge of the hydrothermal system, and thermal water mean residence time. Also, this research provides a quality baseline for the future monitoring and management activities of Topusko hydrothermal system, which is highly recommended due to the continuous utilisation of the resource.

Author contributions All authors were directly involved in the investigation via fieldwork and sampling. MB conducted hydrogeochemical and stable isotope laboratory analyses. M. Pavic did the analysis and interpretation of the data, the preparation of figures, and draft manuscript. M. Pola, SB and MB took part in the critical revision of the manuscript. SB was responsible for research design and funding acquisition. M. Pavić and SB are responsible for project administration. All authors have read and agreed to the submitted version of the manuscript.

Funding This research was funded by the Croatian Science Foundation (HRZZ), grant number UIP-2019-04-1218.

Declarations

Competing interests The authors declare no competing interests.

References

Appelo, C. A. J., & Postma, D. (2005). *Geochemistry, groundwater and pollution* (2nd ed.). Balkema Publishers, Lieden.

Ármannsson, H., & Fridriksson, T. (2009). *Application of geochemical methods in geothermal exploration*. https://www.researchgate.net/publication/228706025

Ármannsson, H. (2012). 7.04—Geochemical aspects of geothermal utilization. In *Comprehensive renewable energy* (pp. 97–170). Elsevier. https://doi.org/10.1016/B978-0-08-087872-0.00709-5

Arnórsson, S., Gunnlaugsson, E., & Svavarsson, H. (1983). The chemistry of geothermal waters in Iceland. III. Chemical geothermometry in geothermal investigations. *Geochimica Et Cosmochimica Acta, 47*(3), 567–577. https://doi.org/10.1016/0016-7037(83)90278-8

Bahun, S., & Raljević, B. (1969). *Mineralna, Termalna i Ljekovita Vrela* [*Mineral and Thermal Springs*]; unpublished report; Institute for Geological Research: Zagreb, Yugoslavia, 4769/5. (**In Croatian**).

Bayari, C. S., Ozyurt, N. N., & Kilani, S. (2009). Radiocarbon age distribution of groundwater in the Konya Closed Basin, central Anatolia, Turkey. *Hydrogeology Journal, 17*(2), 347–365. https://doi.org/10.1007/s10040-008-0358-2

Benjamin, L., Knobel, L. L., Hall, L. F., Cecil, L. D., & Green, J. R. (2005). Development of a local meteoric water line for southeastern Idaho, western Wyoming, and south-central Montana. *Scientific Investigations Report*. https://doi.org/10.3133/SIR20045126

Benjamin, T., Charles, R., & Vidale, R. (1983). Thermodynamic parameters and experimental data for the Na-K-Ca geothermometer. *Journal of Volcanology and Geothermal Research, 15*(1–3), 167–186. https://doi.org/10.1016/0377-0273(83)90099-9

Blake, S., Henry, T., Muller, M. R., Jones, A. G., Moore, J. P., Murray, J., Campanyà, J., Vozar, J., Walsh, J., & Rath, V. (2016). Understanding hydrothermal circulation patterns at a low-enthalpy thermal spring using audio-magnetotelluric data: A case study from Ireland. *Journal of Applied Geophysics, 132*, 1–16. https://doi.org/10.1016/j.jappgeo.2016.06.007

Blasco, M., Auqué, L. F., & Gimeno, M. J. (2017). Application of different geothermometrical techniques to a low enthalpy thermal system. *Procedia Earth and Planetary Science, 17*, 65–68. https://doi.org/10.1016/j.proeps.2016.12.034

Blasco, M., Auqué, L. F., & Gimeno, M. J. (2019). Geochemical evolution of thermal waters in carbonate–evaporitic systems: The triggering effect of halite dissolution in the dedolomitisation and albitisation processes. *Journal of Hydrology, 570*, 623–636. https://doi.org/10.1016/j.jhydrol.2019.01.013

Blasco, M., Gimeno, M. J., & Auqué, L. F. (2018). Low temperature geothermal systems in carbonate-evaporitic rocks: Mineral equilibria assumptions and geothermometrical calculations. Insights from the Arnedillo thermal waters (Spain). *Science of the Total Environment, 615*, 526–539. https://doi.org/10.1016/j.scitotenv.2017.09.269

Borović, S., & Marković, I. (2015). Utilization and tourism valorisation of geothermal waters in Croatia. In *Renewable and sustainable energy reviews* (Vol. 44, pp. 52–63). Elsevier Ltd. https://doi.org/10.1016/j.rser.2014.12.022

Borović, S. (2015). *Integrated hydrogeological-hydrogeochemical model of Daruvar geothermal aquifer* (PhD thesis). University of Zagreb, Faculty of mining, geology and petroleum engineering. pp. 148 (in Croatian).

Borović, S., Marković, T., Larva, O., Brkić, željka, & Mraz, V. (2016). Mineral and thermal waters in the Croatian Part of the Pannonian Basin. In P. Papic (Ed.), *Mineral and thermal waters of southeastern Europe* (1st ed., pp. 31–45). Springer Cham. https://doi.org/10.1007/978-3-319-25379-4

Bošnjak, R. (1998). *GEOEN: program korištenja geotermalne energije: prethodni rezultati i buduće aktivnosti* (G. Granič, Ed.). Energy Institute Hrvoje Požar.

Bottrell, S., Hipkins, E. V., Lane, J. M., Zegos, R. A., Banks, D., & Frengstad, B. S. (2019). Carbon-13 in groundwater from English and Norwegian crystalline rock aquifers: A tool for deducing the origin of alkalinity? *Sustainable Water Resources Management, 5*(1), 267–287. https://doi.org/10.1007/s40899-017-0203-7

Bouaicha, F., Dib, H., Bouteraa, O., Manchar, N., Boufaa, K., Chabour, N., & Demdoum, A. (2019). Geochemical assessment, mixing behavior and environmental impact of thermal waters in the Guelma geothermal system, Algeria. *Acta Geochimica, 38*(5), 683–702. https://doi.org/10.1007/s11631-019-00324-2

Briški, M., Pavić, M., Borović, S., & Pola, M. (2023): Stable water isotope data 2021-2023 from Hrvatsko Žarište village (near Vojnić town). PANGAEA, https://doi.org/10.1594/PANGAEA.961249, In: Briški, M et al. (2023): Stable water isotope data (δ18O and δ2H) of monthly precipitation from 2021 to 2023 (NW Croatia). PANGAEA, https://doi.org/10.1594/PANGAEA.961245

Bruno, M., Ghignone, S., Pastero, L., & Aquilano, D. (2020). The influence of Ca–Mg disorder on the growth of dolomite: A computational study. *CrystEngComm, 22*(29), 4853–4861. https://doi.org/10.1039/D0CE00663G

Cerling, T. E., Wang, Y., & Quade, J. (1993). Expansion of C4 ecosystems as an indicator of global ecological change in the late Miocene. *Nature, 361*(6410), 344–345. https://doi.org/10.1038/361344a0

Chelnokov, G., Lavrushin, V., Bragin, I., Abdullaev, A., Aidarkozhina, A., & Kharitonova, N. (2022). Geochemistry of thermal and cold mineral water and gases of the Tien Shan and the Pamir. *Water (switzerland)*. https://doi.org/10.3390/w14060838

Chiodini, G., Frondini, F., & Marini, L. (1995). Theoretical geothermometers and PCO2 indicators for aqueous solutions coming from hydrothermal systems of medium-low temperature hosted in carbonate-evaporite rocks. Application to the thermal springs of the Etruscan Swell, Italy. *Applied Geochemistry, 10*(3), 337–346. https://doi.org/10.1016/0883-2927(95)00006-6

Chizhova, J., Kireeva, M., Rets, E., Ekaykin, A., Kozachek, A., Veres, A., Zolina, O., Varentsova, N., Gorbarenko, A., Povalyaev, N., Plotnikova, V., Samsonov, T., &

Kharlamov, M. (2022). Stable isotope (δ18O, δ2H) signature of river runoff, groundwater and precipitation in three river basins in the center of East European Plain, Earth Syst. Sci. Data Discuss. [preprint], https://doi.org/10.5194/essd-2022-145

Clark, I. (2015). *Groundwater geochemistry and isotopes*. CRC Press. https://doi.org/10.1201/b18347

Clark, I. D., Douglas, M., Raven, K., & Bottomley, D. (2000). Recharge and preservation of Laurentide Glacial melt water in the Canadian Shield. *Ground Water, 38*(5), 735–742. https://doi.org/10.1111/j.1745-6584.2000.tb02709.x

Clark, P. U., Dyke, A. S., Shakun, J. D., Carlson, A. E., Clark, J., Wohlfarth, B., Mitrovica, J. X., Hostetler, S. W., & McCabe, A. M. (2009). The last glacial maximum. *Science, 325*(5941), 710–714. https://doi.org/10.1126/science.1172873

Claypool, G. E., Holser, W. T., Kaplan, I. R., Sakai, H., & Zak, I. (1980). The age curves of sulfur and oxygen isotopes in marine sulfate and their mutual interpretation. *Chemical Geology, 28*, 199–260. https://doi.org/10.1016/0009-2541(80)90047-9

Craig, H. (1961). Isotopic variations in meteoric waters. *Science, 133*(3465), 1702–1703. https://doi.org/10.1126/science.133.3465.1702

Čubranić, A. (1984). *Osmatranje Termalnih Voda u Topuskom* [*Monitoring of Thermal Waters in Topusko*]; unpublished report; INA-Projekt, OOUR Kompleksna Geološka Istraživanja: Zagreb, Croatia. (**In Croatian**).

Dansgaard, W. (1964). Stable isotopes in precipitation. *Tellus a: Dynamic Meteorology and Oceanography, 16*(4), 436–468. https://doi.org/10.3402/tellusa.v16i4.8993

de Carvalho Filho, C. A., Bomtempo, V. L., Cota, S. D. S., Minardi, P. S. P., & Passos, R. G. (2022). Use of major ions to evaluate groundwater chemistry and identify hydrochemical processes in a shallow coastal aquifer in southeast Brazil. *Environmental Earth Sciences, 81*(17), 423. https://doi.org/10.1007/s12665-022-10499-2

DHMZ—Državni Hidrometeorološki Zavod. Retrieved January 18, 2021, from https://meteo.hr/klima.php?section=klima_podaci&param=k2_1

Drever, J. I., & Hurcomb, D. R. (1986). Neutralization of atmospheric acidity by chemical weathering in an alpine drainage basin in the North Cascade Mountains. *Geology, 14*(3), 221. https://doi.org/10.1130/0091-7613(1986)14%3c221:NOAABC%3e2.0.CO;2

Dubey, A. (2023). *last glacial maximum*. *Encyclopedia Britannica*. Retrieved October 31, 2023, from https://www.britannica.com/science/Last-Glacial-Maximum

Eastoe, C., Hibbs, B., Merino, M., & Dadakis, A. (2022). Origins of Sulfate in Groundwater and Surface Water of the Rio Grande Floodplain, Texas, USA and Chihuahua, Mexico. *Hydrology*. https://doi.org/10.3390/hydrology9060095

Edwards, T. W. D., Wolfe, B. B., Gibson, J. J., & Hammarlund, D. (2007). Use of water isotope tracers in high latitude hydrology and paleohydrology. In *Long-term Environmental Change in Arctic and Antarctic Lakes* (pp. 187–207). Springer Netherlands. https://doi.org/10.1007/978-1-4020-2126-8_7

Eichinger, L. (1983). A contribution to the interpretation of ^{14}C groundwater ages considering the example of a partially confined sandstone aquifer. *Radiocarbon, 25*(2), 347–356. https://doi.org/10.1017/S0033822200005634

Fellehner, M. (2004). *Der Hauptdolomit als Grundwasserspeicher in den Nördlichen Kalkalpen* (Ph.D. thesis), Philipps-Universität, Marburg, Deutschland.

Fetter, C. W. (2001). *Applied hydrogeology* (P. Lynch, Ed.; Fourth Edition). Prentice Hall.

Fisher, R. S., & Mullican, I. W. F. (1997). Hydrochemical evolution of sodium-sulfate and sodium-chloride groundwater beneath the Northern Chihuahuan Desert, Trans-Pecos, Texas, USA. *Hydrogeology Journal, 5*(2), 4–16. https://doi.org/10.1007/s100400050102

Flóvenz, Ó. G., Hersir, G. P., Sæmundsson, K., Ármannsson, H., & Friðriksson, Þ. (2012). Geothermal energy exploration techniques. In *Comprehensive renewable energy* (pp. 51–95). Elsevier. https://doi.org/10.1016/B978-0-08-087872-0.00705-8

Fontes, J., & Garnier, J. (1979). Determination of the initial ^{14}C activity of the total dissolved carbon: A review of the existing models and a new approach. *Water Resources Research, 15*(2), 399–413. https://doi.org/10.1029/WR015i002p00399

Fórizs, I., Szabó, V. R., Deák, J., Hałas, S., Pelc, A., Trembaczowski, A., & Lorberer, Á. (2019). The origin of dissolved sulphate in the thermal waters of Budapest inferred from stable s and o isotopes. *Geosciences (switzerland)*. https://doi.org/10.3390/geosciences9100433

Fournier, R. O. (1977). Chemical geothermometers and mixing models for geothermal systems. *Geothermics, 5*(1–4), 41–50. https://doi.org/10.1016/0375-6505(77)90007-4

Fournier, R. O., & Truesdell, A. H. (1973). An empirical Na-K-Ca geothermometer for natural waters. *Geochimica Et Cosmochimica Acta, 37*(5), 1255–1275. https://doi.org/10.1016/0016-7037(73)90060-4

Freeze, R. A. & Cherry, J.A. (1979). *Groundwater*; Prentice Hall Inc.: Englewood Cliffs, NJ, USA, 1979; Volume 7632, 604.

Gaillardet, J., Dupre, B., Louvat, P., & Allegre, C. J. (1999). Global silicate weathering and CO_2 consumption rates deduced from the chemistry of large rivers. *Chemical Geology*. https://doi.org/10.1016/S0009-2541(99)00031-5

Gallagher, D., McGee, E. J., Kalin, R. M., & Mitchell, P. I. (2000). Performance of models for radiocarbon dating of groundwater: An appraisal using selected Irish aquifers. *Radiocarbon, 42*(2), 235–248. https://doi.org/10.1017/S003382220005904X

Gao, L., Zhao, J., An, Q., Wang, J., & Liu, X. (2017). A review on system performance studies of aquifer thermal energy storage. *Energy Procedia, 142*, 3537–3545. https://doi.org/10.1016/j.egypro.2017.12.242

García, M. G., Hidalgo, M. D. V., & Blesa, M. A. (2001). Geochemistry of groundwater in the alluvial plain of Tucumán province, Argentina. *Hydrogeology Journal, 9*(6), 597–610. https://doi.org/10.1007/s10040-001-0166-4

Garrels, R.M. (1976). A survey of low temperature water mineral relations. In *Interpretation of environmental isotope and hydrogeochemical data in groundwater hydrology*; International Atomic Energy Agency: Vienna, Austria, 65–84.

Geyh, M. A. (2005). Dating of old groundwater—History, potential, limits and future. In *Isotopes in the water cycle* (pp. 221–241). Springer-Verlag. https://doi.org/10.1007/1-4020-3023-1_15

Geyh, M. A. (2000). An overview of ^{14}C analysis in the study of groundwater. *Radiocarbon, 42*(1), 99–114. https://doi.org/10.1017/S0033822200053078

Giggenbach, W. F. (1988). *Geothermal solute equilibria. Derivation of Na-K-Mg-Ca geoindicators* (Vol. 52).

Goldscheider, N., Mádl-Szőnyi, J., Erőss, A., & Schill, E. (2010). Review: Thermal water resources in carbonate rock aquifers. *Hydrogeology Journal, 18*(6), 1303–1318. https://doi.org/10.1007/s10040-010-0611-3

Goñi, M. F. S. (2022). An overview of the last glacial cycle. In *European glacial landscapes* (pp. 165–169). Elsevier. https://doi.org/10.1016/B978-0-12-823498-3.00012-1

Grasby, S. E., & Chen, Z. (2005). Subglacial recharge into the Western Canada Sedimentary Basin—Impact of Pleistocene glaciation on basin hydrodynamics. *Geological Society of America Bulletin, 117*(3), 500. https://doi.org/10.1130/B25571.1

Haizlip, J. R. (2016). Application of geochemistry to resource assessment and geothermal development projects. In *Geothermal power generation: Developments and innovation* (pp. 77–106). Elsevier Inc. https://doi.org/10.1016/B978-0-08-100337-4.00004-8

Halle, R. (2004). *Kemizam i Obradba Vode [Water Chemistry and Treatment]*. Faculty of Mining, Geology and Petroleum Engineering, University of Zagreb. (In Croatian).

Han, L. F., & Plummer, L. N. (2016). A review of single-sample-based models and other approaches for radiocarbon dating of dissolved inorganic carbon in groundwater. In *Earth-science reviews* (Vol. 152, pp. 119–142). Elsevier. https://doi.org/10.1016/j.earscirev.2015.11.004

Han, L. F., Plummer, L. N., & Aggarwal, P. (2012). A graphical method to evaluate predominant geochemical processes occurring in groundwater systems for radiocarbon dating. *Chemical Geology, 318–319*, 88–112. https://doi.org/10.1016/j.chemgeo.2012.05.004

Han, L. F., & Wassenaar, L. I. (2021). Principles and uncertainties of 14C age estimations for groundwater transport and resource evaluation. *Isotopes in Environmental and Health Studies, 57*(2), 111–141. https://doi.org/10.1080/10256016.2020.1857378

Heasler, H., Jaworowski, C., & Foley, D. (2009). Geothermal systems and monitoring hydrothermal features. *Geological Monitoring*. https://doi.org/10.1130/2009.monitoring(05)

Hermans, T., Nguyen, F., Robert, T., & Revil, A. (2014). Geophysical methods for monitoring temperature changes in shallow low enthalpy geothermal systems. In *Energies* (Vol. 7, Issue 8, pp. 5083–5118). MDPI AG. https://doi.org/10.3390/en7085083

HGI-CGS (2009): Geološka karta Republike Hrvatske M1:300.000 [Geological Map of the Republic of Croatia 1:300,000—in Croatian]. Croatian Geological Survey, Department of Geology, Zagreb, https://www.hgi-cgs.hr/geoloska-karta-republike-hrvatske-1300-000/

Hilberg, S., & Schneider, J. F. (2011). The aquifer characteristics of the dolomite formation a new approach for providing drinking water in the northern Calcareous Alps Region in Germany and Austria. *Water Resources Management, 25*, 2705–2729.

Hiscock, K. M., & Bense, V. F. (2014) *Hydrogeology: Principles and practice*, 2nd ed.; John Wiley & Sons Ltd: Hoboken, NY, USA.

Horváth, F., Musitz, B., Balázs, A., Végh, A., Uhrin, A., Nádor, A., Koroknai, B., Pap, N., Tóth, T., & Wórum, G. (2015). Evolution of the Pannonian basin and its geothermal resources. In *Geothermics* (Vol. 53, pp. 328–352). Elsevier Ltd. https://doi.org/10.1016/j.geothermics.2014.07.009

Horvatinčić, N., Bronić, I. K., Obelić, B., & Barešić, J. (2012). Rudjer Bošković Institute Radiocarbon Measurements XVII. *Radiocarbon, 54*(1), 137–154. https://doi.org/10.2458/azu_js_rc.v54i1.15829

Hounslow, A. W. (1995). *Water quality data: Analysis and interpretation* (1st ed.). CRC Press. https://doi.org/10.1201/9780203734117

Hrvatski geološki institut. (2009). *Tumač Geološke karte Republike Hrvatske 1:300.000* (I. Velić & I. Vlahović, Eds.). Hrvatski geološki institut.

Hughes, P. D., Allard, J. L., & Woodward, J. C. (2022b). The Balkans: glacial landforms from the Last Glacial Maximum. In *European Glacial Landscapes* (pp. 487–495). Elsevier. https://doi.org/10.1016/B978-0-12-823498-3.00058-3

Hughes, P. D., Allard, J. L., & Woodward, J. C. (2022a). The Balkans: Glacial landforms from the Last Glacial Maximum. In *European glacial landscapes* (pp. 487–495). Elsevier. https://doi.org/10.1016/B978-0-12-823498-3.00058-3

Hughes, C. E., & Crawford, J. (2012). A new precipitation weighted method for determining the meteoric water line for hydrological applications demonstrated using Australian and global GNIP data. *Journal of Hydrology, 464–465*, 344–351. https://doi.org/10.1016/j.jhydrol.2012.07.029

Hughes, P. D., Gibbard, P. L., & Ehlers, J. (2013). Timing of glaciation during the last glacial cycle: Evaluating the concept of a global 'Last Glacial Maximum' (LGM). *Earth-Science Reviews, 125*, 171–198. https://doi.org/10.1016/j.earscirev.2013.07.003

IAEA. (1970). *Interpretation of Environmental Isotope Data in Hydrology* (Vienna, 24–28 June 1968), IAEA-TECDOC-116, IAEA, Vienna. https://www-pub.iaea.org/MTCD/Publications/PDF/te_116_web.pdf

IAEA. (1992). *Statistical treatment of data on environmental isotopes in precipitation.* Technical Report Series 331. International Atomic Energy Agency, Vienna. https://www.iaea.org/publications/1435/statistical-treatment-of-data-on-environmental-isotopes-in-precipitation

IAEA. (2005). *Isotopic Composition of Precipitation in the Mediterranean Basin in Relation to Air Circulation Patterns and Climate*, IAEA-TECDOC-1453, IAEA, Vienna. https://www-pub.iaea.org/MTCD/Publications/PDF/te_1453_web.pdf

IAEA. (2013). *Isotope Methods for Dating Old Groundwater,* Non-serial Publications, International Atomic Energy Agency, Vienna. https://www.iaea.org/publications/8880/isotope-methods-for-dating-old-groundwater

Ingerson, E. and Pearson, F.J. (1964). *Estimation of age and rate of motion of groundwater by 14C Method*. In: Miyake, Y. and Koyama, T., Eds., Recent Researches in Field of Hydrosphere, Atmosphere and Nuclear Geochemistry, Maruzen, Tokyo, 263–283.

Janik C. J., Truesdell A.H., Sammel E.A., & White A. F. (1985). Chemistry of low-temperature geothermal waters at Klamath Falls, Oregon. *1985 International symposium on geothermal energy. Geothermal Resources Council 1985 Annual Meeting.*, 325–331.

Karingithi, C. W. (1984). Chemical geothermometers for geothermal exploration. In *Fluid-Mineral equilibria in hydrothermal systems* (pp. 31–43). Society of Economic Geologists. https://doi.org/10.5382/Rev.01.03

Kern, Z., Hatvani, I. G., Czuppon, G., Fórizs, I., Erdélyi, D., Kanduč, T., Palcsu, L., & Vreča, P. (2020). Isotopic "altitude" and "continental" effects in modern precipitation across the Adriatic-Pannonian region. *Water (switzerland)*. https://doi.org/10.3390/w12061797

Komatsu, S., Okano, O., & Ueda, A. (2021). Chemical and isotopic (H, O, S, and Sr) analyses of groundwaters in a non-volcanic region, Okayama prefecture, Japan: Implications for geothermal exploration. *Geothermics, 91*, 102005. https://doi.org/10.1016/j.geothermics.2020.102005

Korolija, B., Živaljević, T., & Šimunić, A. (1980b). *Osnovna geološka Karta SFRJ. Tumač za list Slunj* [*Basic Geological Map of SFRY 1:100000, Guide for the Slunj Sheet L33–104*]; Institut za geološka istraživanja: Zagreb, Croatia; Geološki zavod: Sarajevo, Bosnia and Herzegovina; Savezni Geološki Zavod: Beograd, Yugoslavia. (In Croatian)

Korolija, B., Živaljević, T., & Šimunić, A. (1980a*) Osnovna geološka Karta SFRJ 1:100 000, List Slunj. L 33–104* [*Basic Geological Map of SFRY 1:100000, Geology of the Slunj sheet L33–104*]; Institut za geološka istraživanja: Zagreb, Croatia; Geološki zavod: Sarajevo, Bosnia and Herzegovina; Savezni Geološki Zavod: Beograd, Yugoslavia. (In Croatian)

Kostrova, S. S., Meyer, H., Fernandoy, F., Werner, M., & Tarasov, P. E. (2020). Moisture origin and stable isotope characteristics of precipitation in southeast Siberia. *Hydrological Processes, 34*(1), 51–67. https://doi.org/10.1002/hyp.13571

Krajcar Bronić, I., Horvatinčić, N., Sironić, A., Obelić, B., Barešić, J., & Felja, I. (2010). A new graphite preparation line for AMS 14C dating in the Zagreb Radiocarbon Laboratory. *Nuclear Instruments and Methods in Physics Research, Section B: Beam Interactions with Materials and Atoms, 268*(7–8), 943–946. https://doi.org/10.1016/j.nimb.2009.10.070

Krajcar-Bronić, I., Horvatinčić, N., & Obelić, B. (1998). Two decades of environmental isotope records in Croatia: Reconstruction of the past and prediction of future levels. *Radiocarbon, 40*(1), 399–416. https://doi.org/10.1017/s0033822200018282

Lei, Y., Zhao, Z., Zhang, B., Tang, X., Luo, Y., Wang, G., Gao, J., & Zhang, D. (2022). Genesis of significance of carbonated thermal water springs in Xining Basin, China. *Water (switzerland).* https://doi.org/10.3390/w14244058

Lewis, R. E., Young, H. W., & Survey, U. S. G. (1989). The hydrothermal system in central Twin Falls County, Idaho. In *Water-Resources Investigations Report*. https://doi.org/10.3133/wri884152

Li, H.(2022). *Last Glacial Period*. In Encyclopedia. Retrieved August 16, 2023, from https://encyclopedia.pub/entry/29935

Li, Z., Huang, T., Ma, B., Long, Y., Zhang, F., Tian, J., Li, Y., & Pang, Z. (2020). Baseline groundwater quality before shale gas development in Xishui, Southwest China: Analyses of hydrochemistry and multiple environmental isotopes (2H, 18O, 13C, 87Sr/86Sr, 11B, and noble gas isotopes). *Water, 12*(6), 1741. https://doi.org/10.3390/w12061741

López-Chicano, M., Bouamama, M., Vallejos, A., & Pulido-Bosch, A. (2001). Factors which determine the hydrogeochemical behaviour of karstic springs. A case study from the Betic Cordilleras, Spain. *Applied Geochemistry, 16*(9–10), 1179–1192. https://doi.org/10.1016/S0883-2927(01)00012-9

Mance, D. (2014). *Karakterizacija krškog vodonosnika temeljena na prostornim i vremenskim promjenama stabilnih izotopa vodika i kisika* (Ph.D. thesis). Zagreb: University of Zagreb, Faculty of Science. Available online: https://urn.nsk.hr/urn:nbn:hr:217:459207

Marini, L. (2004). *Geochemical techniques for the exploration and exploitation of geothermal energy*. 1–106.

Marković, T., Borović, S., & Larva, O. (2015). Geochemical characteristics of thermal waters of Hrvatsko zagorje. *Geologia Croatica, 68*(1), 67–77. https://doi.org/10.4154/gc.2015.05

Mazor, E. (2004). *Chemical and isotopic groundwater hydrology* (Third Edition). M. Dekker.

Milenić, D., Krunić, O., & Milanković, D. (2012). Thermomineral waters of inner Dinarides Karst. *Acta Carsologica*. https://doi.org/10.3986/ac.v41i2-3.560

Miljević, N., Boreli-Zdravković, D., Veličković, J., Golobočanin, D., & Mayer, B. (2013). Evaluation of the origin of sulphate at the groundwater source Ključ, Serbia. *Isotopes in Environmental and Health Studies, 49*(1), 62–72. https://doi.org/10.1080/10256016.2013.729509

Mišić, K. (2022). *Strukturna građa područja Petrove gore : diplomski rad* (Diplomski rad). [Structural analysis of Petrova gora: master's thesis]. Zagreb: University of Zagreb, Faculty of Mining, Geology and Petroleum Engineering. https://urn.nsk.hr/urn:nbn:hr:169:071799 (**in Croatian**).

Moeck, I. S. (2014). Catalog of geothermal play types based on geologic controls. In *Renewable and sustainable energy reviews* (Vol. 37, pp. 867–882). Elsevier Ltd. https://doi.org/10.1016/j.rser.2014.05.032

Mook, W. G. (2000). *Environmental isotopes in the hydrological cycle: Principles and applications*.

Mook, W. G., Bommerson, J. C., & Staverman, W. H. (1974). Carbon isotope fractionation between dissolved bicarbonate and gaseous carbon dioxide. *Earth and Planetary*

Science Letters, 22(2), 169–176. https://doi.org/10.1016/0012-821X(74)90078-8

Motzer, W. E. (2007). Age Dating Groundwater. Emeryville, CA. Retrieved June 10, 2023, from http://www.primarywaterinstitute.org/images/pdfs/Tritium_in_groundwater.pdf

Münnich, K. O., & Roether, W. (1967). *Transfer of bomb 14C and tritium from the atmosphere to the ocean Internal mixing of the ocean on the basis of tritium and 14C profiles*. IAEA. http://inis.iaea.org/search/search.aspx?orig_q=RN:38058820

Münnich, K. O. (1957). Heidelberg natural radiocarbon measurements I. *Science, 126*(3266), 194–199. https://doi.org/10.1126/science.126.3266.194

Nakić, Z., Ružičić, S., Posavec, K., Mileusnić, M., Parlov, J., Bačani, A., & Durn, G. (2013). Conceptual model for groundwater status and risk assessment—Case study of the Zagreb aquifer system. *Geologia Croatica, 66*(1), 55–76. https://doi.org/10.4154/GC.2013.05

Nematollahi, M. J., Ebrahimi, P., & Ebrahimi, M. (2016). Evaluating hydrogeochemical processes regulating groundwater quality in an unconfined aquifer. *Environmental Processes, 3*(4), 1021–1043. https://doi.org/10.1007/s40710-016-0192-9

Palacios, D., Oliva, M., & Fernández-Fernández, J. M. (2022). The impact of the quaternary ice ages on the landscape. In *Iberia, Land of Glaciers* (pp. 1–12). Elsevier. https://doi.org/10.1016/B978-0-12-821941-6.00027-X

Parkhurst, D. L., & Charlton, S. R. (2008). *NetpathXL—An excel interface to the program NETPATH*. https://doi.org/10.3133/TM6A26

Patekar, M., Bašić, M., Pola, M., Kosović, I., Terzić, J., Lucca, A., Mittempergher, S., Berio, L. R., & Borović, S. (2022). Multidisciplinary investigations of a karst reservoir for managed aquifer recharge applications on the island of Vis (Croatia). *Acque Sotterranee—Italian Journal of Groundwater*, *11*(1), 37–48. https://doi.org/10.7343/as-2022-557

Pavelić, D., & Kovačić, M. (2018). Sedimentology and stratigraphy of the Neogene rift-type North Croatian Basin (Pannonian Basin System, Croatia): A review. In *Marine and Petroleum Geology* (Vol. 91, pp. 455–469). Elsevier Ltd. https://doi.org/10.1016/j.marpetgeo.2018.01.026

Pavić, M., Kosović, I., Pola, M., Urumović, K., Briški, M., & Borović, S. (2023). Multidisciplinary research of thermal springs area in Topusko (Croatia). *Sustainability, 15*(6), 5498. https://doi.org/10.3390/su15065498

Piper, A. M. (1944). A graphic procedure in the geochemical interpretation of water-analyses. *Transactions, American Geophysical Union, 25*(6), 914. https://doi.org/10.1029/TR025i006p00914

Plummer, L.N., Prestemon, E.C., & Parkhurst, D.L. (1994). *An interactive code (NETPATH) for modeling NET geochemical reactions along a flow PATH*, version 2.0. U.S. Geological Survey Water-Resources Investigations Report 94–4169, 130 p.

Plummer, L. N., Busby, J. F., Lee, R. W., & Hanshaw, B. B. (1990). Geochemical modeling of the madison aquifer in parts of Montana, Wyoming, and South Dakota. *Water Resources Research, 26*(9), 1981–2014. https://doi.org/10.1029/WR026i009p01981

Plummer, L. N., & Glynn, P. (2013). Radiocarbon dating in groundwater systems. *Isotope methods for dating old groundwater* (pp. 33–90). International Atomic Energy Agency (IAEA).

Plummer, N., & Sprinkle, C. (2001). Radiocarbon dating of dissolved inorganic carbon in groundwater from confined parts of the Upper Floridan aquifer, Florida, USA. *Hydrogeology Journal, 9*(2), 127–150. https://doi.org/10.1007/s100400000121

Porowski, A. (2014). Isotope Hydrogeology. In B. D. and R. W. Patrick Lachassagne (Ed.), *Handbook of Engineering Hydrology* (pp. 345–375). CRC Press. https://doi.org/10.1201/b15625-18

Porowski, A., Porowska, D., & Halasn, S. (2019). Identification of sulfate sources and biogeochemical processes in an aquifer affected by Peatland: Indights from monitoring the isotopic composition of groundwater sulfate in Kampinos National Park, Poland. *Water, 11*(1388), 1–24. https://doi.org/10.3390/w11071388

Prell, W. L., Hutson, W. H., Williams, D. F., Bé, A. W. H., Geitzenauer, K., & Molfino, B. (1980). Surface circulation of the Indian Ocean during the Last Glacial Maximum, Approximately 18,000 yr B.P. *Quaternary Research, 14*(3), 309–336. https://doi.org/10.1016/0033-5894(80)90014-9

Pryer, H. (2021). *Geochemical techniques to define deep thermal spring protection zones*. https://www.gov.uk/government/publications/geochemical-techniques-to-define-deep-thermal-spring-protection-zones

Rman, N. (2009). Uporabnost ionskih geotermometrov na slovenskih termalnih vodah [Use of ion geothermometers in Slovenian thermal waters]. *Geološki zbornik*, 20, 139–142, Ljubljana. (**in Slovenian**).

Rman, N. (2016). Hydrogeochemical and isotopic tracers for identification of seasonal and long-term over-exploitation of the Pleistocene thermal waters. *Environmental Monitoring and Assessment, 188*(4), 242. https://doi.org/10.1007/s10661-016-5250-2

Rozanski, K., Gonfiantini, R., & Araguas-Araguas, L. (1991). Tritium in the global atmosphere: Distribution patterns and recent trends. *Journal of Physics G: Nuclear and Particle Physics*, *17*(S), S523–S536. https://doi.org/10.1088/0954-3899/17/S/053

Savezni geološki zavod (1970). *Geological map of SFRY 1: 500 000*. Savezni geološki zavod, Beograd, SFRY.

Schmid, S. M., Bernoulli, D., Fügenschuh, B., Matenco, L., Schefer, S., Schuster, R., Tischler, M., & Ustaszewski, K. (2008). The Alpine-Carpathian-Dinaridic orogenic system: Correlation and evolution of tectonic units. *Swiss Journal of Geosciences, 101*(1), 139–183. https://doi.org/10.1007/s00015-008-1247-3

Schmid, S. M., Fügenschuh, B., Kissling, E., & Schuster, R. (2004). Tectonic map and overall architecture of the Alpine orogen. *Eclogae Geologicae Helvetiae, 97*(1), 93–117. https://doi.org/10.1007/s00015-004-1113-x

Šegotić, B. & Šmit, I. (2007). *Studija Optimirane Energetske Učinkovitosti Korištenja Geotermalnih Voda* [Study of Optimized Energy Efficiency of Geothermal Water Use]; unpublished report; Termoinženjering-projektiranje: Zagreb, Croatia. (**in Croatian**).

Serianz, L., Rman, N., & Brenčič, M. (2020). Hydrogeochemical characterization of a warm spring system in a carbonate mountain range of the eastern Julian Alps, Slovenia. *Water (switzerland)*. https://doi.org/10.3390/w12051427

Šikić, K., Halamić, J. & Belak, M. (2009). Ofiolitno-sedimentni kompleks. In I. Velić & I. Vlahović (Eds.), *Tumač Geološke karte Republike Hrvatske 1:300.000* (pp. 54–60). Hrvatski geološki institut.

Simler, R. (2012). Software Diagrammes, V6.72, Laboratoire d'Hydrologie d'Avignon; Université d'Avignon et pays du Vaucluse: Avignon, France.

Šimunić, A. Topusko. In *Mineral and Thermal Waters of the Republic of Croatia*; Šimunić, A., Hećimović, I., Eds.; Croatian Geological Survey: Zagreb, Croatia, 2008; pp. 185–195. (**in Croatian**).

Sironić, A., Bronić, I. K., Horvatinčić, N., Barešić, J., Obelić, B., & Felja, I. (2013). Status report on the Zagreb Radiocarbon Laboratory—AMS and LSC results of VIRI intercomparison samples. *Nuclear Instruments and Methods in Physics Research, Section B: Beam Interactions with Materials and Atoms, 294*, 185–188. https://doi.org/10.1016/j.nimb.2012.01.048

Statistic Kingdom (2017). Shapiro Wilk Test Calculator (W-test). Statistics Kingdom. Accessed on 26 July, 2023, from: https://www.statskingdom.com/doc_shapiro_wilk.html

Szocs, T., Rman, N., Süveges, M., Palcsu, L., Tóth, G., & Lapanje, A. (2013). The application of isotope and chemical analyses in managing transboundary groundwater resources. *Applied Geochemistry, 32*, 95–107. https://doi.org/10.1016/j.apgeochem.2012.10.006

Taghavi, M., Mohammadi, M. H., Radfard, M., Fakhri, Y., & Javan, S. (2019). Assessment of scaling and corrosion potential of drinking water resources of Iranshahr. *MethodsX, 6*, 278–283. https://doi.org/10.1016/j.mex.2019.02.002

Tamers, M. A. (1975). Validity of radiocarbon dates on ground water. *Geophysical Surveys, 2*(2), 217–239. https://doi.org/10.1007/BF01447909

Tay, C. K., Hayford, E., Hodgson, I. O., & Kortatsi, B. K. (2015). Hydrochemical appraisal of groundwater evolution within the Lower Pra Basin, Ghana: A hierarchical cluster analysis (HCA) approach. *Environmental Earth Sciences, 73*(7), 3579–3591. https://doi.org/10.1007/s12665-014-3644-4

Taylor, J. R. (1997). *An introduction to error analysis: The study of uncertainties in physical measurements* (2nd ed.). University Science Books.

Thiébaud, E., Dzikowski, M., Gasquet, D., & Renac, C. (2010). Reconstruction of groundwater flows and chemical water evolution in an amagmatic hydrothermal system (La Léchère, French Alps). *Journal of Hydrology, 381*(3–4), 189–202. https://doi.org/10.1016/j.jhydrol.2009.11.041

Tijani, R., El Mandour, A., Chafouq, D., Elmeknassi, M., El Ghazali, F. E., & Bouchaou, L. (2022). Chemical and isotopic tracers for characterization of the groundwater in the heterogeneous system: Case from Chichaoua-Imin'tanout (Morocco). *Water (switzerland)*. https://doi.org/10.3390/w14010009

Truesdell. (1976). Summary of section III. Geochemical techniques in exploration. *Proceeding and UN Symposium on the Development and Use of Geothermal Resources*, 3–29.

Tziritis, E., Skordas, K., & Kelepertsis, A. (2016). The use of hydrogeochemical analyses and multivariate statistics for the characterization of groundwater resources in a complex aquifer system. A case study in Amyros River basin, Thessaly, central Greece. *Environmental Earth Sciences, 75*(4), 1–11. https://doi.org/10.1007/s12665-015-5204-y

Verma, S. P., Pandarinath, K., & Santoyo, E. (2008). SolGeo: A new computer program for solute geothermometers and its application to Mexican geothermal fields. *Geothermics, 37*(6), 597–621. https://doi.org/10.1016/j.geothermics.2008.07.004

Verma, S. P., & Santoyo, E. (1997). New improved equations for Nak, NaLi, and SiO_2 geothermometers by outlier detection and rejection. *Journal of Volcanology and Geothermal Research, 79*(1–2), 9–23. https://doi.org/10.1016/S0377-0273(97)00024-3

Vlahović, I., Tišljar, J., Velić, I., & Matičec, D. (2005). Evolution of the adriatic carbonate platform: Palaeogeography, main events and depositional dynamics. *Palaeogeography, Palaeoclimatology, Palaeoecology, 220*(3–4), 333–360. https://doi.org/10.1016/j.palaeo.2005.01.011

Vreča, P., Bronić, I. K., Horvatinčić, N., & Barešić, J. (2006). Isotopic characteristics of precipitation in Slovenia and Croatia: Comparison of continental and maritime stations. *Journal of Hydrology, 330*(3–4), 457–469. https://doi.org/10.1016/j.jhydrol.2006.04.005

Wang, Z., Torres, M., Paudel, P., Hu, L., Yang, G., & Chu, X. (2020). Assessing the karst groundwater quality and hydrogeochemical characteristics of a prominent dolomite aquifer in Guizhou, China. *Water (switzerland)*. https://doi.org/10.3390/W12092584

Witcher, J. C., & Stone, C. (1983). A CO2-Silica Geothermometer for Low Temperature Geothermal Resource Assessment, with Application to Resources in the Safford Basin, Arizona, report, United States. Retrieved October 27, 2023, from: https://digital.library.unt.edu/ark:/67531/metadc876560/m1/95/ University of North Texas Libraries, UNT Digital Library, https://digital.library.unt.edu; crediting UNT Libraries Government Documents Department.

Wood, C., Cook, P. G., Harrington, G. A., Meredith, K., & Kipfer, R. (2014). Factors affecting carbon-14 activity of unsaturated zone CO2 and implications for groundwater dating. *Journal of Hydrology, 519*, 465–475. https://doi.org/10.1016/j.jhydrol.2014.07.034

Xiao, Y., Shao, J., Cui, Y., Zhang, G., & Zhang, Q. (2017). Groundwater circulation and hydrogeochemical evolution in Nomhon of Qaidam Basin, northwest China. *Journal of Earth System Science*. https://doi.org/10.1007/s12040-017-0800-8

Xu, P., Zhang, Q., Qian, H., Li, M., & Hou, K. (2019). Characterization of geothermal water in the piedmont region of Qinling Mountains and Lantian-Bahe Group in Guanzhong Basin, China. *Environmental Earth Sciences*. https://doi.org/10.1007/s12665-019-8418-6

Young, H. W. (1985). *Geochemistry and hydrology of thermal springs in the Idaho Batholith and adjacent areas, central Idaho*. https://doi.org/10.3133/wri854172

Zaninović, K., Gajić-Čapka, M., Perčec Tadić, M. et al. (2008). Klimatski atlas Hrvatske/Climate atlas of Croatia 1961–1990, 1971–2000; Državni Hidrometeorološki Zavod: Zagreb, Croatia, 2008. (**in Croatian and English**).

Zhang, X., Guo, Q., Liu, M., Luo, J., Yin, Z., Zhang, C., Zhu, M., Guo, W., Li, J., & Zhou, C. (2016). Hydrogeochemical processes occurring in the hydrothermal systems of the Gonghe-Guide basin, northwestern China: critical insights from a principal components analysis (PCA). *Environmental Earth Sciences*. https://doi.org/10.1007/s12665-016-5991-9

2.3. A conceptual and numerical model of fluid flow and heat transport in the Topusko hydrothermal system

By

Mirja Pavić, Marco Pola, Bojan Matoš, Katarina Mišić, Ivan Kosović, Ivica Pavičić and Staša Borović

Geologia Croatica
Journal of the Croatian Geological Survey and the Croatian Geological Society
2024 | 77/3 | – | 9 Figs. | 1 Tab. | www.geologia-croatica.hr

A conceptual and numerical model of fluid flow and heat transport in the Topusko hydrothermal system

Mirja Pavić[1], Marco Pola[1], Bojan Matoš[2,*], Katarina Mišić[2], Ivan Kosović[1], Ivica Pavičić[2] and Staša Borović[1]

[1] Croatian Geological Survey, Sachsova 2, 10000 Zagreb, Croatia
[2] University of Zagreb, Faculty of Mining, Geology and Petroleum Engineering, Pierottijeva ulica 6, 10000 Zagreb, Croatia; (*corresponding author: bojan.matos@rgn.unizg.hr)

doi: 10.4154/gc.2024.14

Article history:
Manuscript received: May 16, 2024
Revised manuscript accepted: June 11, 2024
Available online: August 28, 2024

Abstract

A comprehensive understanding of hydrothermal systems is often obtained through the integration of conceptual and numerical modelling. This integrated approach provides a structured framework for the reconstruction and quantification of fluid dynamics in the reservoir, thereby facilitating informed decision-making for sustainable utilisation and environmental protection of the hydrothermal system. In this study, an updated conceptual model of the Topusko hydrothermal system (THS), central Croatia, is proposed based on structural, geochemical, and hydrogeological analyses. The stratigraphic sequence and the structural framework of the THS were defined based on geological maps and field investigations. As depicted by hydrochemical and isotope analyses, the thermal waters in the Topusko system (temperatures < 65 °C) are of meteoric origin and circulate in a carbonate aquifer. The THS receives diffuse recharge approximately 13 km S of Topusko, where Triassic carbonates crop out. Gravity-driven regional groundwater circulation is favoured by regional thrusts that tectonically uplifted Palaeozoic rocks of low permeability. These structures confine the fluid flow in the permeable, fractured and karstified Triassic carbonates, favouring the northward circulation of the water. A regional anticline lifts the aquifer closer to the surface in Topusko. Open fractures in the anticline hinge zone increase the fracturing and permeability field of the aquifer, promoting the rapid upwelling of thermal water resulting in the Topusko thermal springs. Numerical simulations of fluid flow and heat transport corroborate the proposed conceptual model. In particular, a thermal anomaly was modelled in the Topusko subsurface with temperature values of 31.3 °C and 59.5 °C at the surface and at the base of the thermal aquifer, respectively, approaching the field observations. These findings show that the circulation of Topusko thermal water is influenced by regional and local geological structures suggesting that the enhanced permeability field in the discharge area enables the formation of the natural thermal springs.

Keywords: thermal spring, conceptual modelling, numerical modelling, recharge area, fractured carbonates, SW Pannonian basin, central Croatia

1. INTRODUCTION

Geothermal systems, which represent a renewable resource for energy and raw material production, vary considerably worldwide due to the different mechanisms governing their formation. They are classified according to their principal properties and characteristics, including their geological, hydrogeological, geochemical, and thermal aspects (MOECK, 2014). A subset of geothermal systems is referred to as hydrothermal when the heat transfer mechanism involves circulating water, whether as liquid or vapour (OJHA et al., 2021; KHODAYAR & BJÖRNSSON, 2024). In the study of hydrothermal systems, it is necessary to determine the origin of the fluid and the area of recharge, the heat transfer mechanism, the direction of fluid flow and the depth to which it descends, the geometry of the aquifer and its hydrogeological and thermal properties, and the conditions favouring the outflow of the thermal water.

Research of hydrothermal systems usually includes the application of an integrated multidisciplinary approach. The geological framework and tectonic evolution of the area influenced by the circulation of thermal fluids are typically reconstructed by combining regional and local field investigations and geophysical data (e.g., MUFFLER & CATALDI, 1978; FLÓVENZ et al., 2012; KOSOVIĆ et al., 2023, 2024). They provide insights into the surface geometry of geological formations and fracture networks and the kinematics of fault systems that are consequently used for subsurface geological reconstructions, supported by 2D or 3D geological modelling. Hydrogeochemical research is the requisite for understanding and managing geothermal aquifers. It involves continuous monitoring of the thermal water to evaluate baseline levels, track their changes, and assess the impact of water abstraction, which is crucial for resource protection and legislative compliance (HOUNSLOW, 1995; MARINI, 2000; MAZOR, 2004; HEASLER, 2009). Analysis of groundwater chemistry and isotopic content aids in characterising hydrothermal systems, identifying water sources, estimating reservoir temperatures, and assessing potential mixing. Hydrogeological research helps in understanding the overall groundwater regime and distribution by providing data (i.e., hydraulic parameters of the aquifer and surrounding rocks, water flow velocities) on sub-

surface conditions influencing the water circulation (FETTER 2001; GOLDSCHEIDER et al.2010; SZANYI & KOVÁCS, 2010; LEI & ZHU, 2013; RMAN, 2014; FABBRI et al., 2017). Quantifying and monitoring the hydrogeological parameters of the thermal aquifer and water is necessary for predicting the exploitable water volumes with an acceptable drawdown and identifying detrimental effects on the system. Additionally, thermal parametrisation of the geological units involved in the thermal fluid flow helps define the changes in the temperature field and fluid distribution across the system (FUCHS & BALLING, 2016; XIONG et al., 2020).

The investigations mentioned above aid in the construction of a conceptual model of the studied hydrothermal system. Developing the conceptual model of a hydrothermal system consolidates the existing understanding by integrating multidisciplinary and multiscale datasets. Conceptual models describe the main processes governing both fluid flow and heat transport, which influence the volume of the hydrothermal resource and its geochemical and thermal characteristics. The aforementioned geological reconstructions serve as the foundation for a hydrogeological conceptual model of the hydrothermal system, elucidating the mechanisms governing hydrothermal resource formation (MOECK et al., 2014; CALCAGNO et al., 2014, MROCZEK et al., 2016). The physical reliability of the conceptual model can be constrained by developing variable-density fluid flow and heat transport numerical simulations of the system. Numerical models can be used for testing and quantifying the importance of different processes in the development of the geothermal resource and its physicochemical characteristics (e.g., MÁDL-SZŐNYI & TÓTH, 2015; HAVRIL et al., 2016; MONTANARI et al., 2017 BOROVIĆ et al., 2019; POLA et al., 2020; TORRESAN et al., 2022). Furthermore, they can be used to reconstruct the historical and current state of the system and to forecast future impacts (ANDERSON et al., 2015).

Thermal springs in Croatia are generally part of intermediate-scale hydrothermal systems, including recharge areas in the nearby mountainous hinterlands and geothermal aquifers mainly hosted in Mesozoic carbonate rocks (GOLDSCHEIDER et al., 2010; BOROVIĆ et al., 2016). Their occurrence is favoured by the regional thermal characteristics in central and northern Croatia that are part of the Pannonian Basin System (PBS). The tectonic setting of the PBS is characterised by the thinned lithosphere, which enables an above-average heat flow from the asthenosphere (HORVÁTH et al., 2015). In the PBS, three levels of the regional flow of thermal water have been identified: i) gravity flows in the Neogene-Quaternary clastic rocks and sediments of the basin fill (the shallowest), ii) gravity flows in pre-Neogene confined carbonate aquifers below them, and iii) flow caused by overpressure in the deepest Mesozoic aquifers (HORVÁTH et al., 2015; VASS et al., 2018). The Mesozoic carbonate rocks, representing the deepest geothermal aquifers, usually crop out either as inselbergs or along the margins of the basin. This could imply the occurrence of greater recharge in the marginal parts of the PBS, where the aquifer is shallower and covered by thinner Neogene deposits, favouring the development of local to intermediate scale hydrothermal systems (STEVANOVIĆ, 2015; HAVRIL et al., 2016).

The artesian thermal springs of Topusko have been renowned since Roman times, ranking as the second warmest in Croatia (BOROVIĆ et al., 2016; ŠIMUNIĆ, 2008). Thermal water with temperatures of up to 65°C has been used since the 1980s for health and recreational purposes and district heating. Despite this fact, the geological features driving the development of the Topusko hydrothermal system (THS) and regulating the regional groundwater flow direction remained uncertain. In the initial stages of THS research, the potential recharge area was determined by defining outcrops of permeable rocks in topographically prominent areas. The lack of previous systematic and detailed structural-geological and hydrogeological investigations hindered the reconstruction of the regional geological evolution and understanding of how the THS functions. Though available publications and unpublished reports suggest contradictory hypotheses, the most commonly used conceptual model is from the early 2000s (ŠIMUNIĆ, 2008). In this study, we propose a novel conceptual model of the THS, detailing the recharge area and main circulation paths using a collection of structural, geochemical, and hydrogeological field data. The second objective of this research involves conducting 2D numerical modelling to analyse fluid flow and heat transport within the THS. Here, the 2D numerical modelling served as a physical validation for the proposed conceptual model, supporting it with the quantification of the main processes governing the development of the Topusko geothermal resource.

2. MATERIALS AND METHODS

2.1. Tectonic setting

The THS formed in the pre-Neogene basement units of the Internal Dinarides (Fig. 1). The Internal Dinarides, as an integral part of the Adria Microplate, convey Adria's eastern passive margin that was involved in a complex tectonic collision between the Adria Microplate and European foreland during the Cretaceous-Paleogene period (SCHMID et al., 2020 with references).

This tectonic contraction (the recent convergence rate between the Adria indenter and Europe is ≤ 4.17 mm/yr according to D'AGOSTINO et al. 2008) resulted in the formation of a Dinaridic orogen system, tectonic suture zone (i.e., Sava Suture Zone), and 400 km eastward extrusion of the ALCAPA block (i.e., Eastern Alps, West Carpathians and Transdanubian ranges; TARI et al., 1999; CSONTOS & VÖRÖS, 2004). Besides the formation of an orogen-parallel thrust fault system, tectonic contraction accommodated the formation of regional dextral/sinistral faults (e.g., the Split-Karlovac fault, Periadriatic fault that extends into the Mid-Hungarian fault zone further to the E; Fig. 1), which enabled CCW/CW rotation and partial tectonic exhumation of the nearby tectonic blocks of the Adria Microplate and the Tisza-Dacia Mega-Unit (e.g. TOMLJENOVIĆ, 2002; TOMLJENOVIĆ et al., 2008; USTASZEWSKI et al., 2010; SCHMID et al., 2020).

At the same time, as the study area is positioned in the immediate vicinity of the transient zone between the Adria

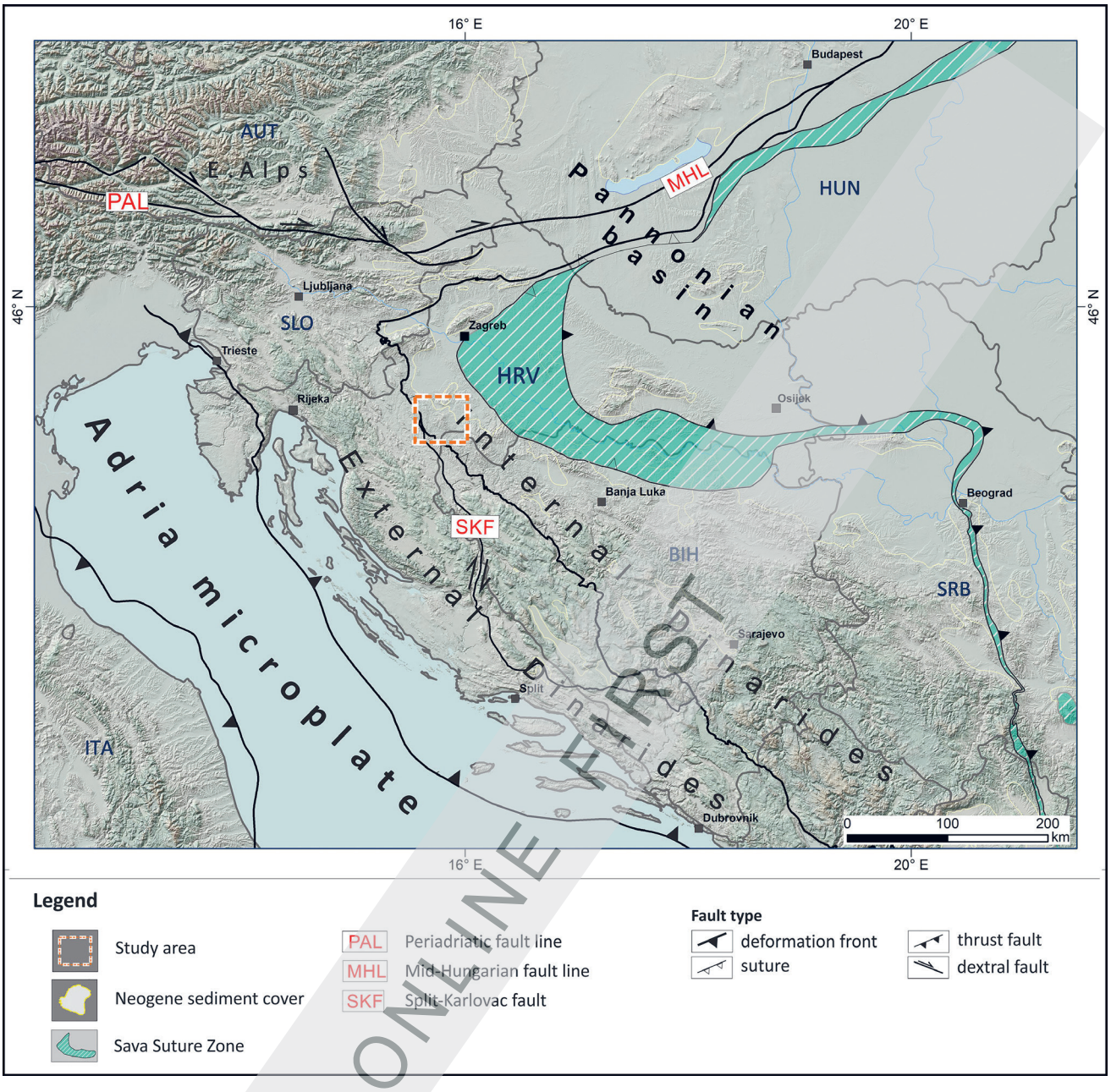

Figure 1. Regional tectonostratigraphic units that surround the study area of the THS (red dashed polygon corresponds to the extent of Fig. 3). Map shows the main regional fault systems that accommodated the tectonic collision of the Adria Microplate and European Foreland during Cretaceous-Paleogene time. The study area is located at the eastern margin of the Adria Microplate, within the Internal Dinarides, close to the Sava Suture Zone (modified after SCHMID et al., 2008; 2020).

Microplate (W) and the Tisza Mega-Unit (E), the inherited fault system is characterised by polyphase tectonic evolution and persistent structural reactivation of the faults (Fig. 2; SCHMID et al., 2008). As a result, the THS bedrock units (Fig. 3) resemble a complex lithostratigraphic mosaic of Palaeozoic-Triassic clastic and carbonate units, that are often seen in tectonic contact with younger Jurassic-Cretaceous ophiolitic mélange units (SCHMID et al., 2008), and its Paleogene-Neogene cover.

The Neogene-Quaternary tectonic evolution of the study area, on the other hand, was further affected by back-arc type formation of the PBS (ROYDEN & HORVÁTH, 1988; HORVÁTH et al., 2006; CLOETINGH at al., 2006). Formation of the PBS was characterised by repeated Early-Middle Miocene E-W oriented lithospheric extension (c. 26-11.5 Ma), along the NNW-striking normal listric faults (i.e., the Sava fault; Fig. 2), which was followed by its Late Miocene--Pliocene-Quaternary tectonic inversion due to N – S compression (e.g., PRELOGOVIĆ et al., 1998; TARI et al., 1999; TOMLJENOVIĆ & CSONTOS, 2001; CLOETINGH et al. 2006; SCHMID et al., 2008; BRÜCKL et al., 2010).

In the Croatian part of the PBS, a Neogene-Quaternary sediment succession (Fig. 3) is associated with the dominant NNW-striking Sava, Karlovac and Glina basins and subbasins, which were tectonically inverted and highly deformed during the Late Miocene-Pliocene-Quaternary periods (PAVELIĆ, 2001; PAVELIĆ et al., 2003; TOMLJENOVIĆ & CSONTOS, 2001). Tectonic deformation of the Neogene-Quaternary

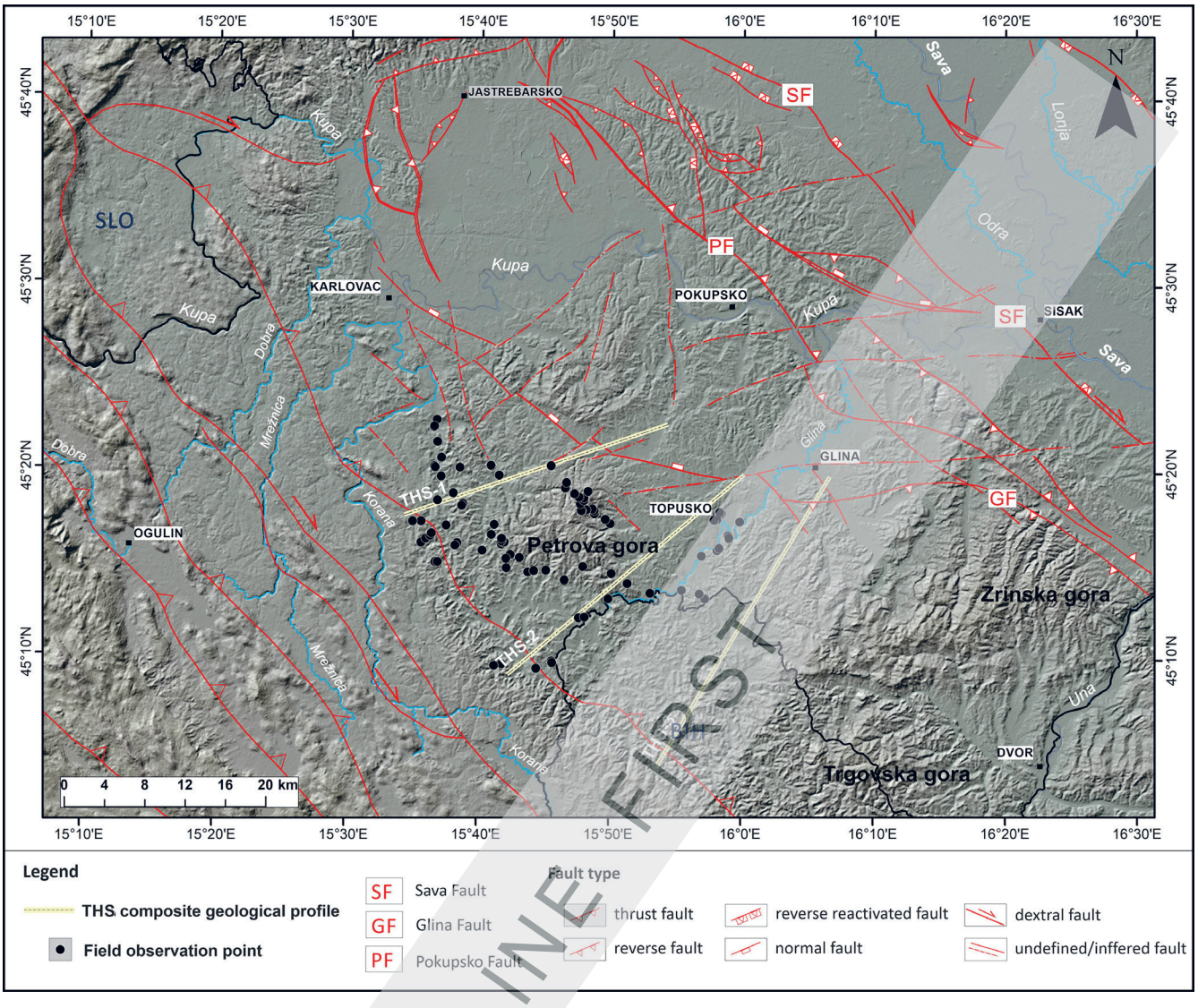

Figure 2. The structural map shows a simplified tectonic framework of the fault systems at the SW margin of the PBS. Fault abbreviations: SF – Sava fault; PF- Pokupsko fault; GF – Glina fault. Fault systems are compiled after KOROLIJA et al. (1980), VELIĆ & SOKAČ (1982), BUKOVAC et al. (1984), PIKIJA (1987), ŠIKIĆ (1990), PRELOGOVIĆ et al. (1998), TOMLJENOVIĆ & CSONTOS (2001), BENČEK et al. (2014), and HERAK & HERAK (2023).

succession in the study area is especially pronounced along the contact with the Palaeozoic-Triassic anticlinal core of the Petrova gora Mt. (HORVÁTH & TARI 1999; TOMLJENOVIĆ & CSONTOS, 2001).

Though tectonic uplift of the Petrova gora Mt. had probably already started during the Cretaceous-Paleogene contraction (similar to the other PBS pre-Neogene basement highs e.g., Trgovska gora, Slavonian Mts.), the final uplift commenced during the Late Miocene-Pliocene-Quaternary compression/transpression phase that resulted in tectonic exhumation, tectonic overprint of its Palaeozoic-Mesozoic structures, and formation of kilometre-scale folds along the reactivated and newly formed faults in the area (Fig. 2; PRELOGOVIĆ et al., 1998; TOMLJENOVIĆ & CSONTOS, 2001). Ongoing, local NNE-SSW regional compression in the study area is driven by residual Adria indentation shortening locally at the scale of 1-2 mm/yr and is accommodated along the inherited faults with slip rates below 0.1 mm/yr (GRENERCZY et al., 2005; KASTELIC & CARAFA, 2012; USTASZEWSKI et al., 2014).

2.2. Geological setting

A composite geological map covering the study area (Fig. 3) was constructed using basic geological maps of the former Yugoslavia at a scale of 1:100.000, sheets Karlovac (BENČEK et al., 2014), Sisak (PIKIJA, 1987), Slunj (KOROLIJA et al., 1980), and Bosanski Novi (ŠIKIĆ, 1990), as well as the 1:500.000 scale geological map (FEDERAL GEOLOGICAL SURVEY, 1970). A description of the subsurface geological composition was compiled, including a composite geological column that outlines the lithostratigraphic and chronostratigraphic sequence of deposits in the area. The synthesis of existing data was undertaken using GIS and graphical editing tools.

The geological setting of the study area predominantly comprises Late Palaeozoic, Triassic, and Plio-Quaternary to Quaternary deposits, which cover older Variscan bedrock and structures. In the SE part, Carboniferous deposits (C) are the oldest exposed rocks (Fig. 3). They are predominantly composed of clastic and subordinately carbonate deposits, includ-

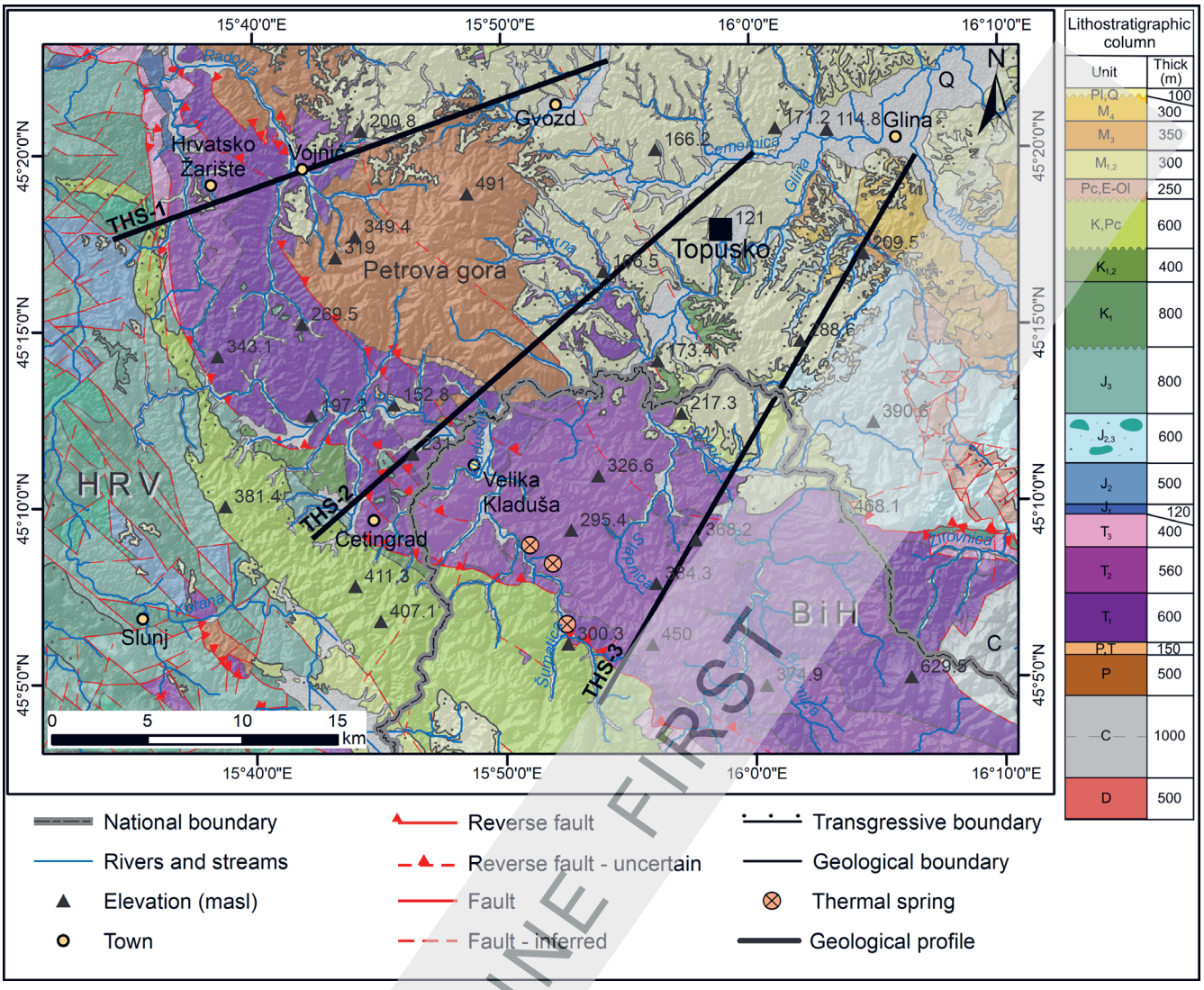

Figure 3. Geological map of the study area of the THS according to the basic geological maps of the SFRY at a scale of 1:100.000, sheets Karlovac (BENČEK et al., 2014), Sisak (PIKIJA, 1987), Slunj (KOROLIJA et al., 1980), Bosanski Novi (ŠIKIĆ, 1988) and geological maps of SFR Yugoslavia, scale 1:500.000 (FEDERAL GEOLOGICAL SURVEY, 1970). Acronyms of the lithostratigraphic units: Q – Quaternary; Pl, Pl,Q – Pliocene, Plio – Quaternary; M - Miocene; Pc,E-Ol – Paleocene and Eocene-Oligocene; K, Pc – Cretaceous-Paleogene K – Cretaceous; J - Jurassic; T - Triassic; P,T – Permian - Triassic; P – Permian; C – Carboniferous; D – Devonian. Thermal springs' locations in Bosnia and Herzegovina after HRVATOVIĆ (2005). The extent of the study area is shown in Figure 1.

ing shales, siltites, sandstones (greywacke, quartz-greywacke), and dolomitised and ankeritised limestones. Together with the Devonian deposits (D), characterised by thick lenses of clay, limonitised and schisty limestones within interbeds of shales, siltstone and sandstones form the pre-Permian low-grade metamorphic basement (ŠIKIĆ, 1990).

Continuation of the post-Carboniferous deposition sequence is characterised by a clastic sequence of younger Palaeozoic age and is found on the southern slopes of Petrova gora Mt. (Fig. 3). Permian deposits (P) are represented by schists, quartz-greywacke sandstones, shales, and fine-grained conglomerates (KOROLIJA et al., 1980). This turbidite-like complex was developed under conditions of rapid and constant infilling within the existing basement basinal structures, reaching thicknesses of 500 m. At the same time, Permo-Triassic deposits (P, T) are consistent and composed of fine-grained brick-red sandstones and sandy-clay shales (KOROLIJA et al., 1981). The quartz-rich greywackes of the Upper Permian, observed along the southern slopes of the Petrova gora Mt., are a marker that represents transitional strata from the Upper Permian to the Lower Triassic (Fig. 3), which were deposited in shallower marine environments due to orogenic uplift.

Lower Triassic (T_1) deposition of mica sandstones, siltites, and shales with a gradual transition to carbonate marls and eventually limestones and dolomites continuously followed the Upper Palaeozoic normal superposition (KOROLIJA, 1981). These deposits can be observed on the eastern slopes of Petrova gora Mt., concordantly overlapping older Permian deposits (Fig. 3). During the Middle Triassic (T_2), evidence of consistent limestone and dolomite deposition can be observed. At the local scale, within the carbonate facies, tuffs, fine-grained sandstones, and interlayers of sheet limestone with chert alongside the shales were observed. The diminishing presence of clastic and pyroclastic components within the uppermost Middle Triassic succession suggests a reduction in tectonic activity and volcanism. During the Late Triassic period (T_3), stable marine conditions enabled further massive

carbonate deposition in the area. The Upper Triassic dolomites (W of Hrvatsko Žarište, Fig. 3) are usually in tectonic contact with the Lower – Upper Cretaceous limestones.

According to SCHMID et al. (2008), Late Jurassic regional movements prompted the intraoceanic subduction of the Neotethys oceanic realm, which coexisted with the fragmentation of the Adria Microplate. This led to the Adria Microplate terrain differentiation, which resulted in variable sedimentation patterns and continuous Jurassic-Cretaceous carbonate sedimentation in the area of the Adriatic Carbonate Platform (VLAHOVIĆ et al., 2005), while clastic-carbonate-volcanic sedimentation prevailed along its passive margins. The Jurassic rock complex in the study area ($J_{2,3}$), part of this passive margin, primarily comprises a magmatic-sedimentary ophiolitic complex within the Central Dinaridic Ophiolitic Zone (SCHMID et al., 2008). This approximately 800 m thick complex consists of low-metamorphosed sedimentary rocks, (i.e., sandstones, shales, cherts, and some siltites, marly shales, and fine-grained limestones) and various magmatic rocks (i.e., basalts, gabbros, diabases; KOROLIJA et al., 1981; ŠIKIĆ, 1990).

The Cretaceous-Paleogene transgressive sequence (Fig. 3) indicates passive margin sedimentation (KOROLIJA et al., 1981). Cretaceous deposits (K_1) include limestones, greenish-gray marls, silicified sandstones, and carbonate breccias, followed by a flysch-turbidite like succession ($K_{1,2}$) (VLAHOVIĆ et al., 2005). Paleogene deposits are mainly flysch-like, with carbonate marls, marly limestones, and thin layers of shales, marls, and fine-grained sandstones (K, Pc). Palaeocene and Eocene-Oligocene flysch-like deposits (Pc, E-Ol) crop out to a small extent in the eastern part of the study area. The Neogene-Quaternary sediment succession, linked to the tectonic evolution of the Croatian part of the PBS, was deposited in half-graben structures formed during the Early-Middle Miocene (PRELOGOVIĆ et al., 1998; TOMLJENOVIĆ & CSONTOS, 2001; SAFTIĆ et al., 2003). Extensional tectonics led to basins filled with marine, lacustrine, and freshwater sediments (PAVELIĆ et al., 2003). This succession, about 1.1 km thick, includes conglomerates, sandstones, gravels, clays, marls, and limestones (M; Pl, Q; Fig. 3) (ŠIKIĆ, 1990). The youngest Pliocene and Quaternary deposits (Pl; Q), approximately 200 m thick, consist of conglomerates, sandstones, siltstones, sands, gravels, clays, and occasional interlayers of clay and coal, forming a final terrigenous/alluvial cover.

2.3. Hydrogeological setting

In the Topusko area, there are three natural artesian thermal springs with a total capacity of approx. 25 l/s (BAĆ & HERAK, 1962; BAHUN & RALJEVIĆ, 1969) and temperatures ranging from 46 °C to 53 °C. Three exploitation wells were drilled to depths of up to 250 m in the immediate vicinity of the natural springs during the 1980s. They are currently used for heating, recreational, and medicinal purposes, with a total yield of 200 l/s and pressure of around 1.4 bar (PAVIĆ et al., 2023). A decrease in pressure from 2.18 bar (1978) to 1.52 bar (1982) was observed and attributed to overexploitation (ŠEGOTIĆ & ŠMIT, 2007). The Topusko thermal water shows a slightly acidic character, with an average pH of 6.5 – 6.8. The electrical conductivity ranges from 582 µS/cm to 680 µS/cm, and the total dissolved solids are approx. 500 mg/l indicating a medium to low mineralised fresh water. Hydrochemical analyses show a Ca-HCO_3 hydrochemical facies (PAVIĆ et al., 2023, 2024) indicating water flow in carbonate rocks. Stable water isotopes δ^2H and $\delta^{18}O$ suggest a meteoric origin for thermal water and recharge during colder climatic conditions The uniform $\delta^{18}O$ values indicate deep circulation and a large, thick aquifer, which homogenises seasonal precipitation variations over longer residence times. The estimated mean residence time of approximately 8.5 – 9.5 kyr is based on ^{14}C content in DIC (PAVIĆ et al., 2024). Tritium activity in the thermal water is generally below the detection limit, but trace levels were detected after extensive abstraction for district heating during winter months, suggesting the potential infiltration of modern precipitation through the semi-permeable Neogene cover sequence of the aquifer. The most plausible equilibrium aquifer temperature was estimated at 90 °C using quartz geothermometers (PAVIĆ et al., 2023, 2024). Hydrodynamic measurements in the Topusko discharge area estimated an aquifer transmissivity of approx. 2 x 10^{-2} m^2/s (PAVIĆ et al., 2023). According to ŠIMUNIĆ (2008), a set of faults forming a block in the shape of a three-sided prism enabled the uplifting of the aquifer. The result of an electrical resistivity survey identified the damaged zones of these faults in the spring area (PAVIĆ et al., 2023).

From a hydrogeological point of view, fractured and karstified, highly permeable, Middle and Upper Triassic carbonates are the main geothermal aquifer of the THS. Lower Triassic and Permian-Triassic carbonate and clastic rocks represent the semi-confining units at the base of the reservoir, while the Palaeozoic complex is the impervious basement at the bottom of the stratigraphic sequence due to its low-grade metamorphism. Furthermore, low permeability Jurassic ophiolitic complex and Neogene-Quaternary deposits cover the geothermal aquifer. However, a limited number of deep boreholes hinders a more comprehensive understanding of local and regional scale hydrogeological conditions.

Different conceptual models of the THS have been previously proposed:

1) In the early 20th century, it was considered that the thermal water at the Topusko springs was heated by a magmatic body based on the existence of basalt outcrops in the vicinity (e.g., Lasinja GORJANOVIĆ-KRAMBERGER, 1905, 1917). To support the volcanic origin of the thermal water in Topusko, GORJANOVIĆ-KRAMBERGER (1917) postulated that mountains S of Topusko could not produce such hydrostatic pressure that would raise water from a depth of approx. 1.5 km, according to the thermal water temperature at the surface. However, these basalts are of Mesozoic age (MAJER, 1978; 1993) and Quaternary magmatic bodies behaving as a recent heat source for hydrothermal systems are absent within the PBS. Therefore, this conceptual model was abandoned.

2) BAĆ & HERAK (1962) interpreted the Palaeozoic rocks as behaving as an impermeable rock complex that regulates regional water circulation and defines the watershed of the THS together with Lower Triassic and Neogene formations. According to the same authors, permeable Middle

and Upper Triassic carbonate deposits facilitate deep groundwater circulation, especially in tectonically active areas. The thermal aquifer receives recharge in the Glina river headwaters, where Triassic carbonates crop out. The proposed primary regional flow direction is from the S to N, from the Glina area towards the Topusko depression.

3) ŠIMUNIĆ (2008) proposed that the THS recharge area is located W of the Petrova gora Mt., where Triassic carbonates crop out. According to the proposed model, the water circulates from W to E below the Petrova gora nappe, heats up by the geothermal gradient, and discharges in Topusko due to the highly permeable fault damaged zones.

2.4. Structural-geological research

Structural-geological fieldwork was conducted through field campaigns in 2021 and 2022. Field investigations involved structural and lithological data acquisition at 162 locations covering an area of approx. 2,000 km^2 (Figs. 2 and 3). During the fieldwork, observation points were archived and processed in the Avenza PDF Maps application (URL 1) and MS Excel field database, while database creation and geospatial positioning of the collected geological data were performed using the software ArcMap 10.1 (URL 2).

The structural investigations detailed the stratigraphic relationships among the main lithological units and the analysis of the tectonic and structural settings in the study area. They encompassed geometric and structural measurements of strata bedding, fractures/joint systems, and fault/shear planes. In particular, measurements of fault/shear planes included the identification of fault kinematic indicators and determination of the tectonic relationships between the observed structures. Collected structural data were used in the construction of three NE-SW striking regional structural-geological profiles (THS-1 to THS-3; Figs. 2–4). These profiles represent surface/subsurface 2D models of the distribution of geological units and structures in the area of Petrova gora Mt. (SW) and the Glina depression (NE) and they were used here for reconstruction of the geological and structural settings of the THS.

2.5. Conceptual and numerical modelling

In this study, we initially tested and compared the validity of the conceptual model proposed by ŠIMUNIĆ (2008) with the results of structural investigations and the constructed geological profiles. Furthermore, these data combined with the results of previous investigations in the Topusko area were used to update the conceptual model of the THS, which served as a base for a 2D numerical model of heat flow and fluid transport. The conceptual model was developed including: lithological field data, geological maps, hydrodynamic and electrical resistivity survey data acquired in the discharge area of Topusko, chemical and isotopic compositions of both the thermal water and the precipitation in the assumed recharge area.

The proposed conceptual model was tested by performing numerical simulations of fluid flow and heat transport accounting for the variation of the thermal water density due to the temperature distribution in the subsurface (BUNDSCHUH & CÉSAR SUÁREZ, 2010; DIERSCH, 2014). The numerical model solves the governing equations of fluid flow and heat transport, obtaining the distribution of the primary variables (i.e., hydraulic head and temperature) within the modelling domain and over time. In this research, we used the FEFLOW 7.4 software (DIERSCH, 2014), a Finite Element-based simulator specifically designed to address fluid flow and transport phenomena within porous and fractured media. The fundamental equations governing fluid flow and heat transport in these media are formulated based on conservation principles for fluid mass, momentum, and thermal energy (DIERSCH, 2014). The equations are coupled by setting a functional form behaviour for fluid density and viscosity depending on the respective primary variable of the problem. For the specific problem at hand, fluid viscosity was kept constant. In contrast, the density of the fluid varies linearly with temperature, following $\rho = \rho_0 (1 - \alpha \Delta T)$ with α being the volumetric thermal expansion coefficient of the fluid (POLA et al., 2020).

3. RESULTS

3.1. Structural-geological profiles

Structural – geological profiles THS-1 to THS-3 (Fig. 4) represent an interpretation of the surface/subsurface relationships in the study area down to an investigation depth of approx. 6 km. Constructed geological profiles include three structural domains that convey a system of thrust faults separating the External Dinaridic lithological units in the SW parts of the profiles from the Internal Dinaridic lithological units. The Internal Dinaridic units can be further subdivided into two subdomains. The SE and central part of the profiles included the Petrova gora area, while the Glina depression characterises the NE profile domains (Fig. 4).

The profiles (Figs. 2 and 4) pinpoint complex faulted and folded structures that are predominantly affected by low angle thrust faults (dip angle ≤30°; faults R1, R2, and R3 in Fig. 4) and reverse faults in their immediate hanging wall (faults R5 and R2 in Fig. 4). Besides these faults, higher angle normal and tectonically inverted normal faults are observed (dip angle ≥45°; faults R4 and R6 in Fig. 4). Constructed profiles show that the THS subsurface is composed of folded structures, with the largest Topusko anticline formed in the hanging wall of the R3 thrust fault and R5 blind fault (profile THS-3 in Fig. 4). The Petrova gora structure also resembles a larger-scale anticlinal structure that is tectonically uplifted in the hanging walls of the R1 and R2 thrust faults (profile THS-1 in Fig. 4).

The Petrova gora structure, composed of a Palaeozoic clastic sequence, is tectonically uplifted by approx. 3.5 km in relation to its R1 footwall units, which resemble an undeformed, 6 km thick, Palaeozoic-Mesozoic succession. Towards the NE, the Petrova gora structure is additionally vertically displaced by tectonically inverted normal faults (faults R3 and R4; profile THS-1 in Fig. 4). Here, vertical displacement along the R3 and R4 normal faults accommodates NE-SW oriented extension, with approx. 1.5 – 2 km vertical subsidence.

Further to the NE, the R4 fault delineates a folded system that incorporates the area of the Topusko anticline. With an approx. 4 km thick Palaeozoic-Mesozoic succession, this folded system (profile THS-3 in Fig. 4) is mainly composed of the Carboniferous-Permian clastic succession that is covered

by Triassic clastic-carbonate rocks. The Topusko anticline hinge zone is partly covered by the Jurassic ophiolitic complex and its transgressive Cretaceous clastic-carbonate succession (see Figs. 3 and 4, profile THS-3). In the area of the Topusko anticline, both the Cretaceous and Jurassic units are significantly reduced due to extensive uplift along the R5 blind

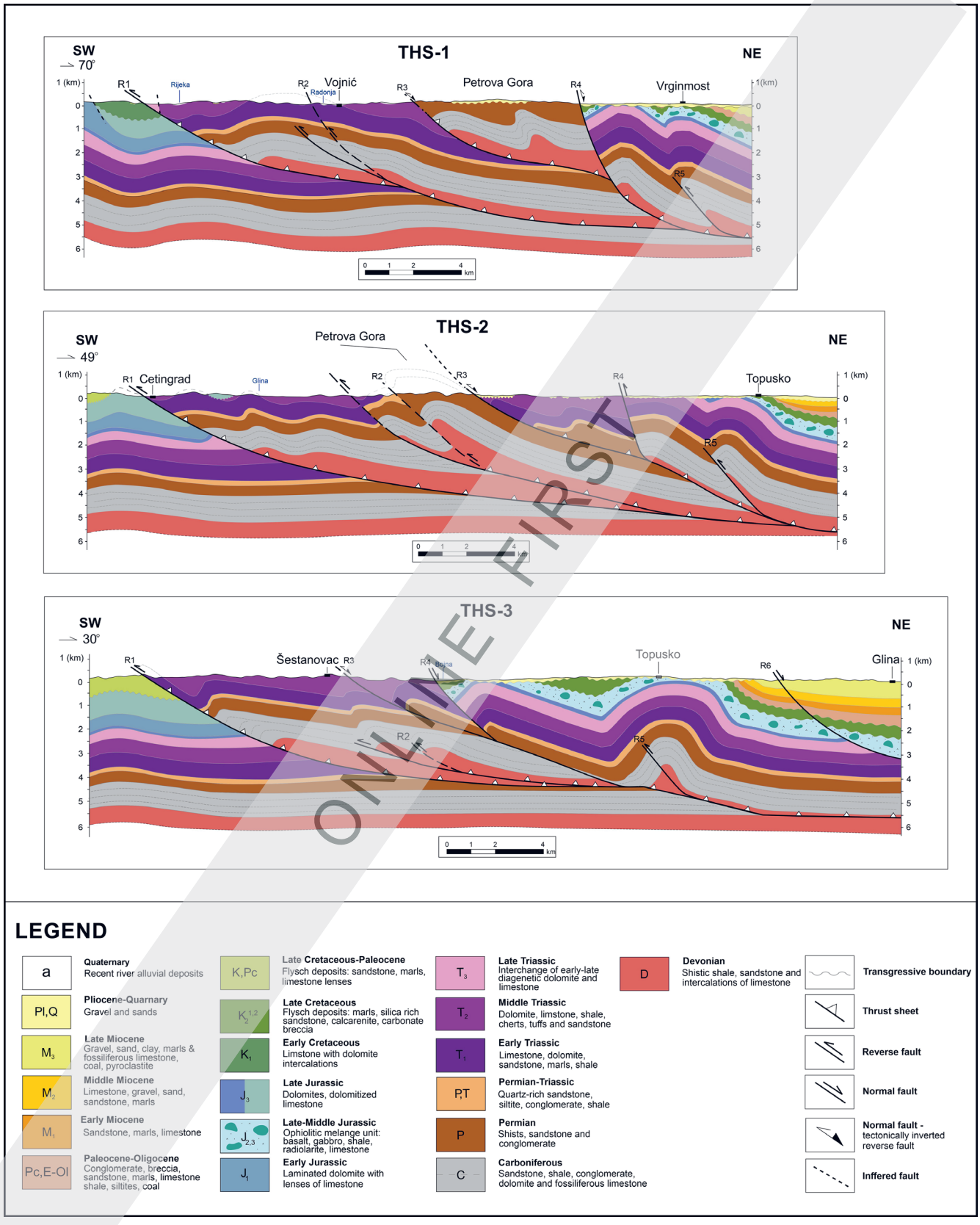

Figure 4. Structural-geological profiles in the THS area. The NE-SW striking profiles are perpendicular to the geological structures in the research area. The profiles show the Topusko anticline formed in the hanging wall of the thrust fault R3 that behaves as a low-angle detachment surface. The anticline is composed of a thick Palaeozoic-Mesozoic sequence, which is partly eroded in the immediate area of Topusko town. Towards the NE, it is covered by the thick Paleogene-Neogene sedimentary succession of the Glina depression. Horizontal and vertical scale ratio is 1:1.

fault, which resulted in hanging wall tectonic erosion. The final NE domains of the THS geological profiles incorporate the gently dipping NE limb of the Topusko anticline that is faulted by the NE dipping R6 normal fault. The R6 normal fault (vertical displacement here is approx. 500 m; profile THS-3 in Fig. 4) is part of the extensional structure of the Glina depression, which is one of the extensional basins formed during the Neogene extension of the Croatian part of the PBS. As a result, the NE segments of the THS profiles are covered by an additional approx. 2 km thick clastic-carbonate succession deposited during the Paleogene and Neogene within the Glina depression.

Reconstructed THS subsurface relationships along the profiles indicate that the observed faults and cogenetic folded structures have a history of polyphase deformation. The same asymmetric anticlinal structures (e.g., Petrova gora) in the hanging wall of the low angle detachment faults (e.g., R3 and R4 faults, Fig. 4) show indications of tectonic transport towards the SW, localised uplift and erosion (e.g., Topusko anticline), as well as NE – SW oriented extension. This implies that the interpreted faults accommodated both initial Cretaceous-Paleogene NE – SW compression and the following Neogene NE – SW extension.

3.2. Conceptual and numerical modelling of groundwater flow and heat transport in the THS

3.2.1. Novel conceptual model of the THS

The new conceptual model of the THS is established based on constructed geological profiles (Fig. 4) and previous hydrogeological and geophysical research (PAVIĆ et al., 2023, 2024). These data lead to development of an interpolated schematic geological profile, which refines the understanding of the THS (Figs. 5 & 6). Analysis of the geological profiles

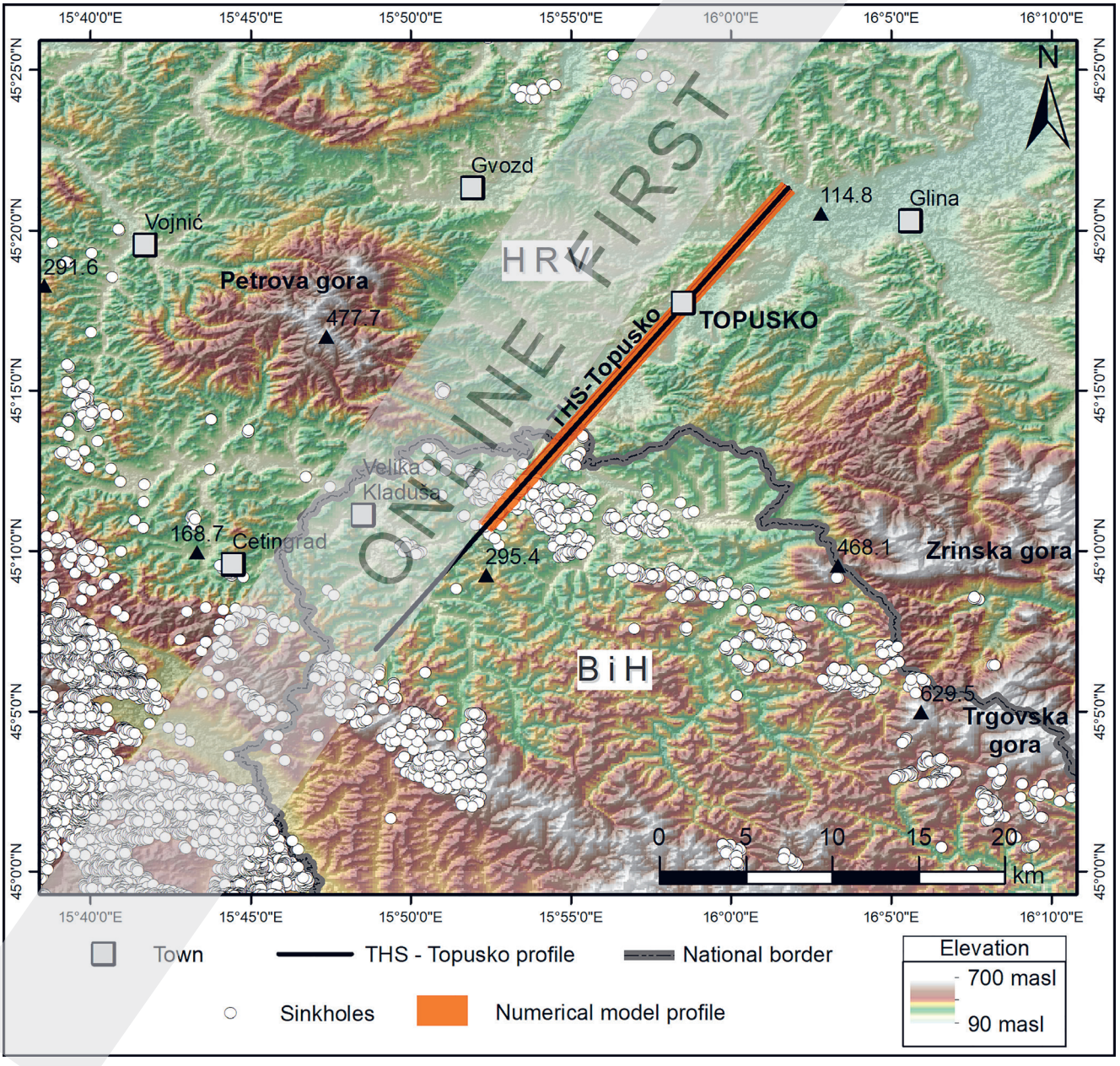

Figure. 5 Trace of the interpolated schematic geological profile of the THS (black line). Sinkholes (white circles) in the SW part of the profile indicate higher karstification of the carbonate formations, representing the potential recharge area of the THS.

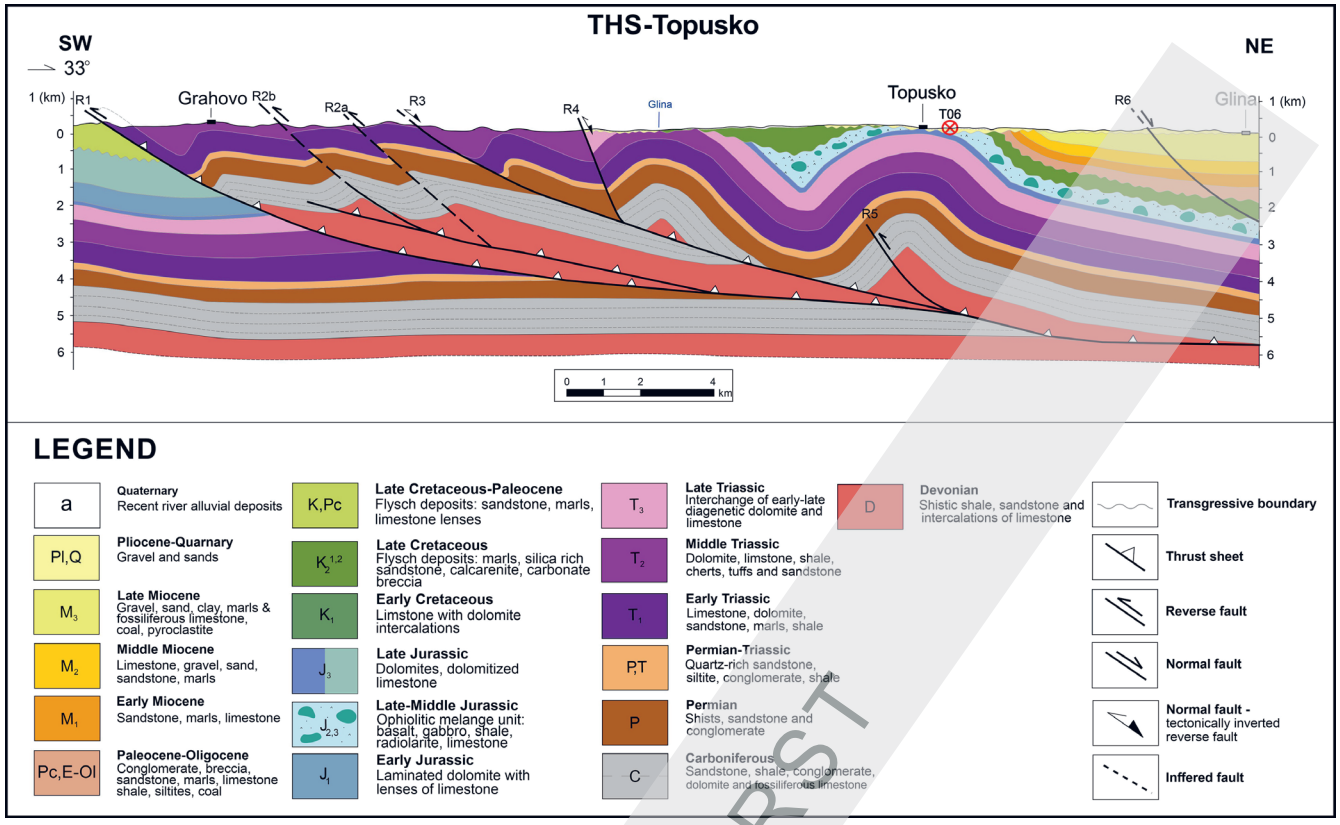

Figure 6. Interpolated geological profile of the THS. The profile is perpendicular to the Topusko anticline formed in the hanging wall of the thrust fault R3 that behaves as a low angle detachment surface. The same fault, combined with the R4 and R5 reverse faults, lifts the reservoir up to shallow depths in the immediate area of Topusko town. Horizontal and vertical scale is 1:1.

here, challenges the previously proposed hypothesis by ŠIMUNIĆ (2008) about the recharge area of the THS being W of the Petrova gora nappe. The Triassic carbonates cropping out W of the Petrova gora Mt. are hydrogeologically isolated from the discharge area in Topusko by the impermeable Petrova gora structure, which is composed of a Palaeozoic clastic sequence with low-grade metamorphism. Therefore, a regional groundwater flow from W to E becomes highly unlikely. Instead, in our conceptual model, attention is directed towards a new hypothesis: the recharge occurs S from Topusko, where Triassic carbonates are partly exposed at the surface.

The surface manifestation of thermal water in the Topusko spring area can be understood through the concept of gravity-driven groundwater flow, determined by: i) Middle-Upper Triassic carbonate complex rocks, which are the main thermal aquifer of the THS, ii) Palaeozoic-Lower Triassic and the Jurassic-Neogene formations representing the semi-confining layers at the bottom and top of the reservoir, respectively, iii) a large area characterised by intense karstification occuring approx. 13 km S of Topusko within the Triassic carbonates (Fig. 5), facilitating the infiltration and deep circulation of the meteoric water with a long residence time, and iv) the fault-thrusted regional tectonic setting and the existence of substantial hydraulic boundaries (e.g., the R3 and R4 thrust faults and near-surface fault zones), which influence the direction of the groundwater flow. The Topusko anticline within the hanging wall of the R3 thrust fault facilitates the uplift of the aquifer, bringing it closer to the surface in the thermal springs area. Cogenetic faults and fracture networks in the hinge zone of the Topusko anticline, probably affected by an extensional regime, increase the fracturing of the bedrock and the permeability field in the aquifer enabling the thermal water outflow. The occurrence of fault damage zones in the Topusko subsurface was determined by the electrical resistivity surveys (PAVIĆ et al., 2023). Hydrogeochemical research corroborates the meteoric origin of the Topusko thermal water and the interaction with the carbonate aquifer. A residence time of approx. 9 kyr is evidenced by the ^{14}C analysis of the thermal water (PAVIĆ et al., 2024). Additionally, the consistent major ion composition of the thermal water over a two-year period suggests a large and stable system. Based on all findings, it is suggested that the novel THS conceptual model favours a regional groundwater flow direction from S to N.

3.2.2. Setup of the numerical model

The physical validity of the proposed conceptual model of the THS was tested by conducting 2D numerical modelling of both the regional fluid flow and heat transport. To simulate gravity-driven groundwater flow in the THS, we adopted a shortened version of the schematic geological profile (Fig. 6), excluding the SW portion of the R3 fault. The recharge area of the THS is located NE of R3, where numerous sinkholes occur (Fig. 5). Therefore, the SW portion of the section is not strictly connected to the hydrothermal system, and was not reproduced in the numerical model to diminish the computational effort for solving the numerical simulations. The profile was digitised in GIS software and used to generate a su-

permesh in the FEFLOW software outlining the geometry of the geological units within the modelling domain. The domain was discretised through a triangular mesh employing the Triangle triangulation code (DIERSCH, 2014), which permits honouring the complex geometrical relationships of the units. The mesh was refined in the hinge zone of the Topusko anticline, in the aquifer unit, and along the main faults. Such refinement allows a better discretisation in the parts of the model where numerical instability is expected. The obtained mesh (Fig. 7) comprised 19,241 triangular elements and 9,831 nodes.

Geological units with similar hydrogeological and thermal properties were grouped, obtaining seven hydrostratigraphic units: i) Palaeozoic low-metamorphic sedimentary complex (B), ii) Permian and Permian-Triassic clastic units (P), iii) Early Triassic sedimentary rocks (T_1), iv) Middle and Late Triassic carbonates ($T_{2,3}$), v) Jurassic magmatic – sedimentary ophiolitic complex and Jurassic and Cretaceous carbonates (J), vi) Neogene siliciclastic units (N), and vii) Quaternary alluvial cover (Q). In particular, the $T_{2,3}$ hydrostratigraphic unit represents the main thermal aquifer of the THS. The equivalent porous medium approach was employed for the hydrogeological and thermal parametrisations of the hydrostratigraphic units (DIERSCH, 2014; ANDERSON et al., 2015). This approach considers the unit as a porous medium with homogeneous and isotropic properties being suitable for the numerical modelling of regional groundwater flow systems in heavily fractured and karstified carbonate rocks (TEUTSCH & SAUTER, 1991; SCANLON et al., 2003; GHASEMIZADEH et al., 2012; MÁDL-SZŐNYI & TÓTH, 2015). In a regional numerical model, the scale of these discontinuities is smaller than the representative elementary volume (i.e., the mesh size), resulting in a constant and homogeneous value of the considered parameter. For assigning the hydraulic and thermal properties (Table 1), we considered the main lithology of the hydrostratigraphic units and relied on data from the literature (CERMAK & RYBACH, 1982; DOMENICO & SCHWARTZ, 1997; FETTER, 2001; STYLIANOU et al., 2016; BOROVIĆ et al., 2018; STOBER & BUCHER, 2021; LALOUI & ROTTA LORIA, 2020), parametrisation of similar units in hydrothermal systems within the PBS (RMAN & TÓTH, 2011; MÁDL-SZŐNYI & TÓTH, 2015; HAVRIL et al., 2016), and datasets obtained from field investigations in Topusko (PAVIĆ et al., 2023). The hydraulic conductivity (K) and the porosity (φ) were assigned accounting for the role of the units in the THS. Excluding the loose sediments of the Quaternary cover (Q unit; Fig. 3), the highest K and φ values were assigned to the $T_{2,3}$ hydrostratigraphic unit representing the thermal aquifer. Conversely, the impervious basement B was reproduced using the lowest K and φ values. In the hinge zone of the Topusko anticline, K and φ were increased simulating the impact of the local scale fracturing that favours the upwelling of the thermal water. Open fractures can increase the permeability and porosity fields enhancing the fluid flow in the aquifer (i.e., FAULKNER et al., 2010; WORTHINGTON et al., 2019; POURASKARPARAST et al., 2024). The regional values of K and φ were increased by: i) two orders of magnitude and 10%, respectively, for the $T_{2,3}$, T_1, and P units, and ii) one order of magnitude and 5%, respectively, for the B unit considering the decrease of fracture apertures with depth. In particular, the K value of the $T_{2,3}$ unit in the hinge zone of the Topusko anticline was calculated from a collection of transmissivity values obtained from well tests conducted in Topusko (PAVIĆ et al., 2023). Furthermore, the thermal conductivities (λ) of the N and $T_{2,3}$ units were derived from RMAN & TÓTH (2011), MÁDL-SZŐNYI & TÓTH (2015), and HAVRIL et al. (2016), who investigated regional groundwater flow and heat transport patterns in the PBS.

Boundary conditions (BCs) for fluid flow and heat transport were applied at the border of the modelling domain following the conceptual model of the THS. The fluid flow BCs (Fig. 7A) included: i) a 2nd kind (Neumann) BC at the SW part of the top domain, and ii) a 3rd kind (Cauchy) BC at the top of the domain in the Topusko area. The Neumann BC produces an inflow in the modelling domain and was employed to simulate the recharge of the THS. The condition spanned for a length of 2 km, which corresponds to the extension of the area with a higher density of sinkholes along the modelling domain. An inflow of 90 mm/yr was imposed considering an effective infiltration of 10 % (as being used for the simulation of similar hydrothermal systems in a carbonate reservoir in Croatia; BOROVIĆ et al., 2019) and an average annual precipitation of 900 mm (DHMZ, 2021; MARTINSEN et al., 2022). The Cauchy BC simulates a fluid flux through the model boundary depending on: i) the difference between the hydraulic head imposed at the boundary and the value calculated within the domain, and ii) a transfer-rate coefficient (DIERSCH, 2014). Since it is generally used to simulate the variable outflow in springs (ANDERSON et al., 2015), it was employed in the THS numerical model to reproduce the occurrence of thermal springs in the Topusko area. The imposed hydraulic head was set as the average ground elevation (122 masl), while the transfer rate was calculated as the K of the Q unit (Table 1) divided by the thickness of the alluvial cover in Topusko obtained from the stratigraphic well logs. The heat transport BCs (Fig. 7B) included: i) a 1st kind (Dirichlet) BC at the SW and NE vertical boundaries of the modelling domain and at the top except for the Topusko area, ii) a 2nd kind (Neumann) BC at the bottom, and iii) a 3rd kind (Cauchy) BC at the top of the domain in the Topusko area. The Dirichlet BC imposes a constant value of the primary variable. In the THS model, it was used to reproduce both the ground temperature at the surface and the increasing temperature with depth due to the regional geothermal gradient at the vertical boundaries. The temperature imposed at the top was set to 10 °C, which corresponds to the mean average annual air temperature, while the values at the lateral boundary were obtained from the initial distribution of temperature. The Neumann BC was used to simulate the regional inflow of heat from the deeper parts of the crust. A value of 100 mW/m^2 was imposed being consistent with the average heat flow in the Croatian part of the PBS (LENKEY et al., 2002; HORVÁTH et al., 2015). Similarly to the fluid flow, the Cauchy BC reproduces a heat flux through the boundary depending on: i) the difference between the reference and the calculated temperature values, and ii) a transfer-rate coefficient (DIERSCH, 2014). The reference temperature was set to 10 °C following the value imposed for the Dirichlet BC, while the transfer rate was calculated as the λ of the Q unit (Table 1) divided by its thickness.

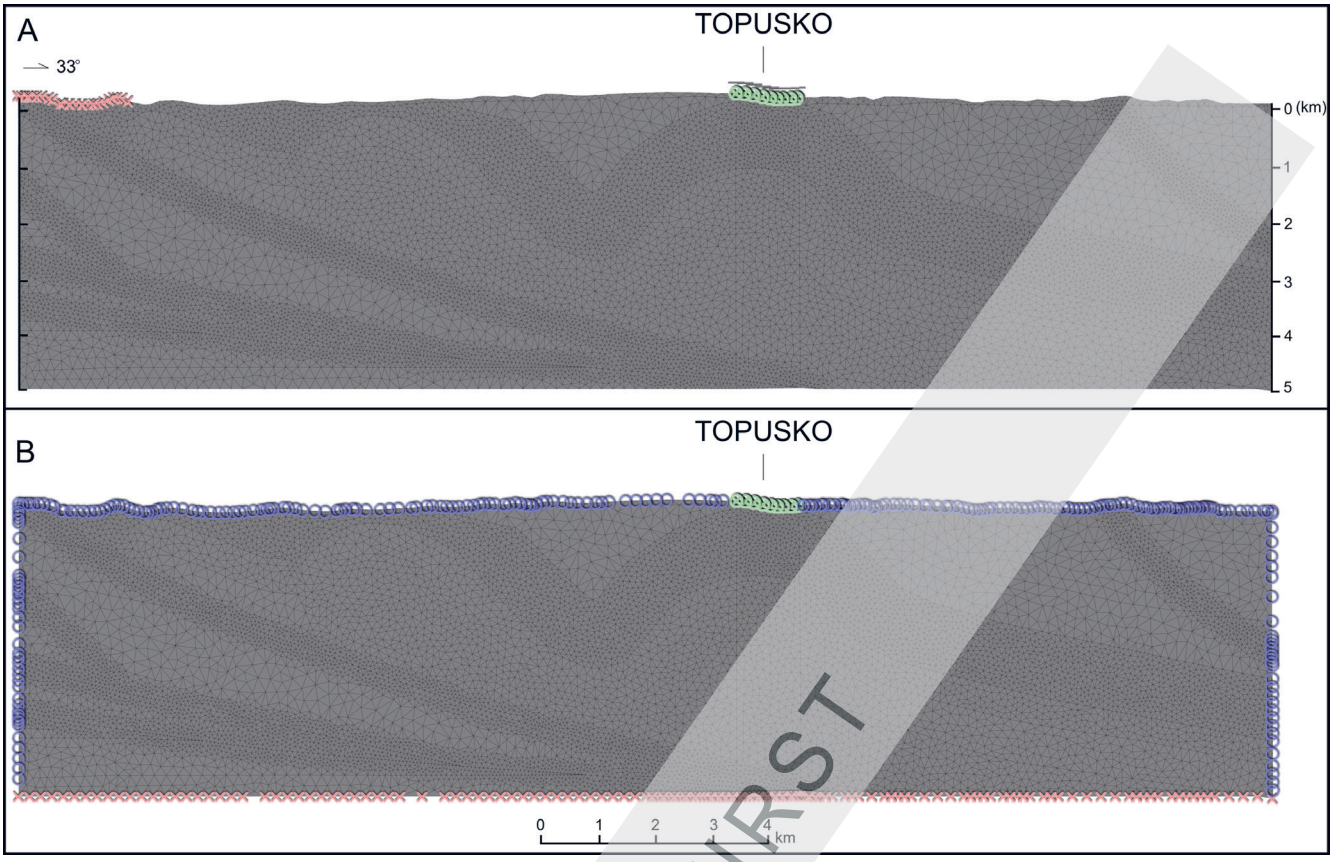

Figure 7. Fluid flow (A) and heat transport (B) boundary conditions (BCs) in the THS numerical model. Blue circles – 1st kind (Dirichlet) BC; Red crosses – 2nd kind (Neumann) BC; Green circles with crosses – 3rd kind (Cauchy) BC. Horizontal and vertical scale ratio is 1:1.

The THS numerical modelling was conducted performing transient state numerical simulations that account for the variations of the hydraulic head and temperature distributions over time. Therefore, it is important to set appropriate initial conditions for these variables achieving a better convergence of the numerical solution at the initial stages of the simulation. The initial value of the hydraulic head was set as 122 m, corresponding to the hydraulic head imposed at the fluid flow Cauchy BC. The initial distribution of the temperature was obtained through a steady-state simulation using: i) the described set of hydrogeological and thermal parameters for the hydrostratigraphic units (Table 1), ii) a 1st kind (Dirichlet) BC with a constant temperature value of 10 °C at the top of the domain, and iii) a 2nd kind (Neumann) BC at the bottom with imposed inflow of 100 mW/m^2. The resulting temperature distribution reproduces a regional geothermal gradient of 35.8 °C/km, being consistent with available regional values in the study area (30 – 40 °C/km; MACENIĆ et al., 2020).

3.2.3. Simulation results

The best simulation of the THS was conducted employing the described set of hydrogeological and thermal parameters for the hydrostratigraphic units (Table 1) and the imposed boundary and initial conditions (Fig. 7). The transient simulation was run for 100 kyr obtaining a quasi-stationary distribution of the primary variables. This condition reproduces the long-term natural state of the hydrothermal system (i.e., GARG et al., 2007; KAISER et al., 2013; HAVRIL et al., 2016;

Table 1. Hydrogeological and thermal parameters assigned to the hydrostratigraphic units in the THS numerical model.

Unit	Age	Lithology	Thick	K	Ss	φ	λ	ρc
			[m]	[m s^{-1}]	[m^{-1}]	[%]	[W m^{-1} K^{-1}]	[MJ m^{-3} K^{-1}]
Q	Quaternary	Gravel, sand, silt	90	1*10^{-4}	1*10^{-4}	20	1.6	1.3
N	Neogene	Sand, clay, silt, marls	< 2,000	2*10^{-7}	1*10^{-4}	5	1.8	1.6
J	Jurassic	Magmatic-sedimentary ophiolitic complex	750 – 1,600	2*10^{-10}	3.3*10^{-7}	5	2	2.2
$T_{2,3}$	Middle-Upper Triassic	Limestone, dolostone	400 – 1,200	2*10^{-6}	3.3*10^{-7}	10	2.5	2.52
T_1	Lower Triassic	Sandstone, marl, limestone, dolomite	600	2*10^{-9}	3.3*10^{-7}	5	2	1.6
P	Permian-Triassic	Siliciclastic rocks	650	2*10^{-11}	3.3*10^{-7}	5	3	2.1
B	Palaeozoic	Schists shales, sandstones, conglomerates with limestone and dolomite lenses	2,000 – 3,000	2*10^{-12}	3.3*10^{-7}	2	3.5	2.1

Note: K: Hydraulic conductivity (DOMENICO & SCHWARTZ, 1997; FETTER, 2001; PAVIĆ et al., 2023); φ: Porosity (DOMENICO & SCHWARTZ, 1997); λ: Thermal conductivity (CERMAK & RYBACH, 1982, RMAN & TÓTH (2011), MÁDL-SZŐNYI & TÓTH (2015), STYLIANOU et al., 2016, BOROVIĆ et al., 2018; STOBER & BUCHER, 2021); Ss: specific storativity (DOMENICO & SCHWARTZ, 1997); ρc: volumetric heat capacity (LALOUI & ROTTA LORIA, 2020)

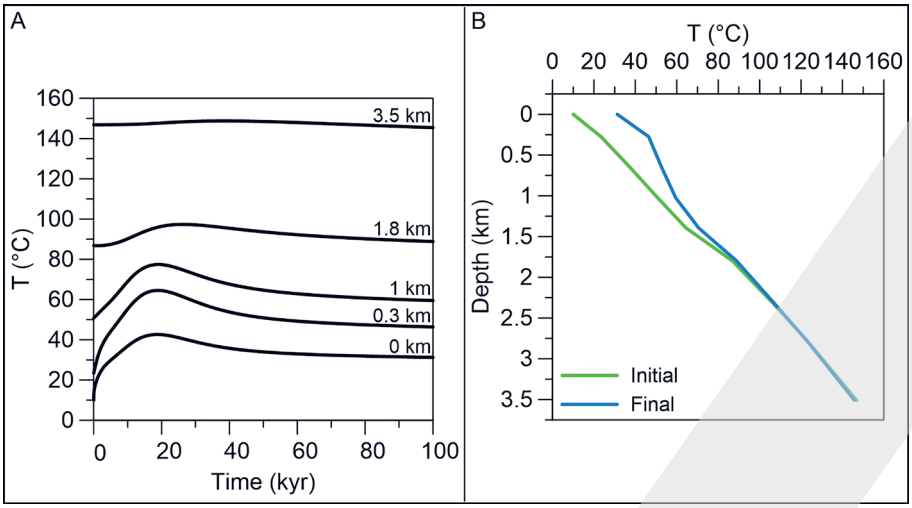

Figure 8. Modelled temperature variations over time (A) and final temperature distribution (B) in the Topusko area.

BOROVIĆ et al., 2019; POLA et al., 2020; TORRESAN et al., 2022), which is the goal of the THS numerical modelling.

The temperature variations over time at different depths in the subsurface of Topusko are represented in Fig. 8A. The simulated temperature gradually increases from the initial distribution reaching maximum values between 18 and 30 kyr depending on the considered depth. The temperature at the surface peaks to 42.6 °C at 18 kyr (initial value of 10 °C; depth = 0 km in Figs. 8A and 8B), while it reaches the maximum value of 77.4 °C at the same simulation time at base of the aquifer (initial value of 55.8 °C; depth = 1 km in Figs. 8A and 8B). The temperature differential progressively decreases with depth, being up to 2 °C in the deeper part of the modelling domain (depth = 3.5 km). After this increasing phase, the simulated temperatures progressively decrease. The final modelled temperatures at the surface and base of the aquifer are 31.3 °C and 59.5 °C (Figs. 8A and 8B), respectively, depicting a drop of 11.3 °C and 17.9 °C, respectively. The drop from the peak value decreases with the depth as well and is 3 °C in the deeper part of the modelling domain. Despite these variations, a practically constant temperature distribution is observed between 80 and 100 kyr with a maximum variation of 1.4 °C at the aquifer base. This result suggests that a quasi-stationary state of the solution was achieved.

The regional and local scale spatial distributions of temperature at the end of the simulation period (Figs. 9A and 9B, respectively) were further detailed. The temperature distribution within the aquifer at both regional and local scales exhibits significant spatial variability. In particular, a decrease from the initial values up to 14 °C is observed in the recharge area of the system where the infiltration of cold waters (10 °C as imposed by the Dirichlet BC for heat transport) occurs. Similar behaviour is observed in the recharge area of regional, topographically-driven groundwater systems (i.e., DOMENICO & PALCIAUSKAS, 1973; ANDERSON, 2005; AN et al., 2015). However, the temperature within the aquifer (pink polygon in Fig. 9) is up to 25 °C (depth of 0.7 km) as expected in shallow carbonate aquifers. The temperature in the aquifer progressively decreases eastward as depicted by the 20 °C isotherm located at a depth of approx. 1.6 km in the central part of the modelling domain. This decrease is connected to the deep circulation of the infiltrated waters in the aquifer driven by both the topographic gradient and the deepening of the strata to the SW of Topusko (Fig. 6). The temperature increases in the hinge zone of the Topusko anticline where the upwelling of the thermal water favours the rise of the isotherms toward the surface (Fig. 9B). In particular, the isotherm of 35 °C is located approx. at the top of aquifer (depth of 0.1 km), while the isotherm 50 °C approaching to the water temperature of the Topusko thermal springs is located at a depth of 0.4 km. The modelled temperature is: i) up to 44 °C in the central part of the thermal anomaly at the depth investigated by the thermal wells in Topusko (0.2 km), ii) between 56 and 74 °C at the base of the aquifer, and iii) between 80 and 100 °C at the base of the T_1 hydrostratigraphic unit, which represents the semi-confining unit at the bottom of the aquifer (depth of approx. 1.8 km; Fig. 9).

The circulation of the fluid is generally directed from the recharge area of the model to the outflow area in Topusko. The flow mostly occurs in the $T_{2,3}$ hydrostratigraphic unit where an average Darcy velocity of 0.18 m/yr (5.02×10^{-4} m/d) is modelled. It drops to 0.01 m/yr (2.9×10^{-5} m/d) in the T_1 and P hydrostratigraphic units at the bottom of the aquifer, and to 3.91×10^{-7} m/yr (1.07×10^{-9} m/d) in the impervious basement (B hydrostratigraphic unit). The direction and velocity of the flow in the aquifer show different distributions from the recharge to the outflow area depending on the K value of the hydrostratigraphic unit and the thickness of the aquifer. In the recharge area, the flow is almost horizontal with an average Darcy velocity of 0.27 m/yr (7.3×10^{-4} m/d). The velocity in the recharge area shows a high variability spanning over almost three orders of magnitude (minimum and maximum of 7.06×10^{-4} m/yr to 1.77 m/yr, respectively). In particular, the highest values are observed NE of the R3 fault (Fig. 6), where the thickness of the aquifer decreases (Fig. 9A) due to the anticline between the R3 and R4 faults. In the flow-through part of the system, the flow (average velocity of 0.17 m/yr corresponding to 4.54×10^{-4} m/d) is generally downward following the deepening of the aquifer to the SW of Topusko and resulting in the local drop of the isotherms (as depicted by

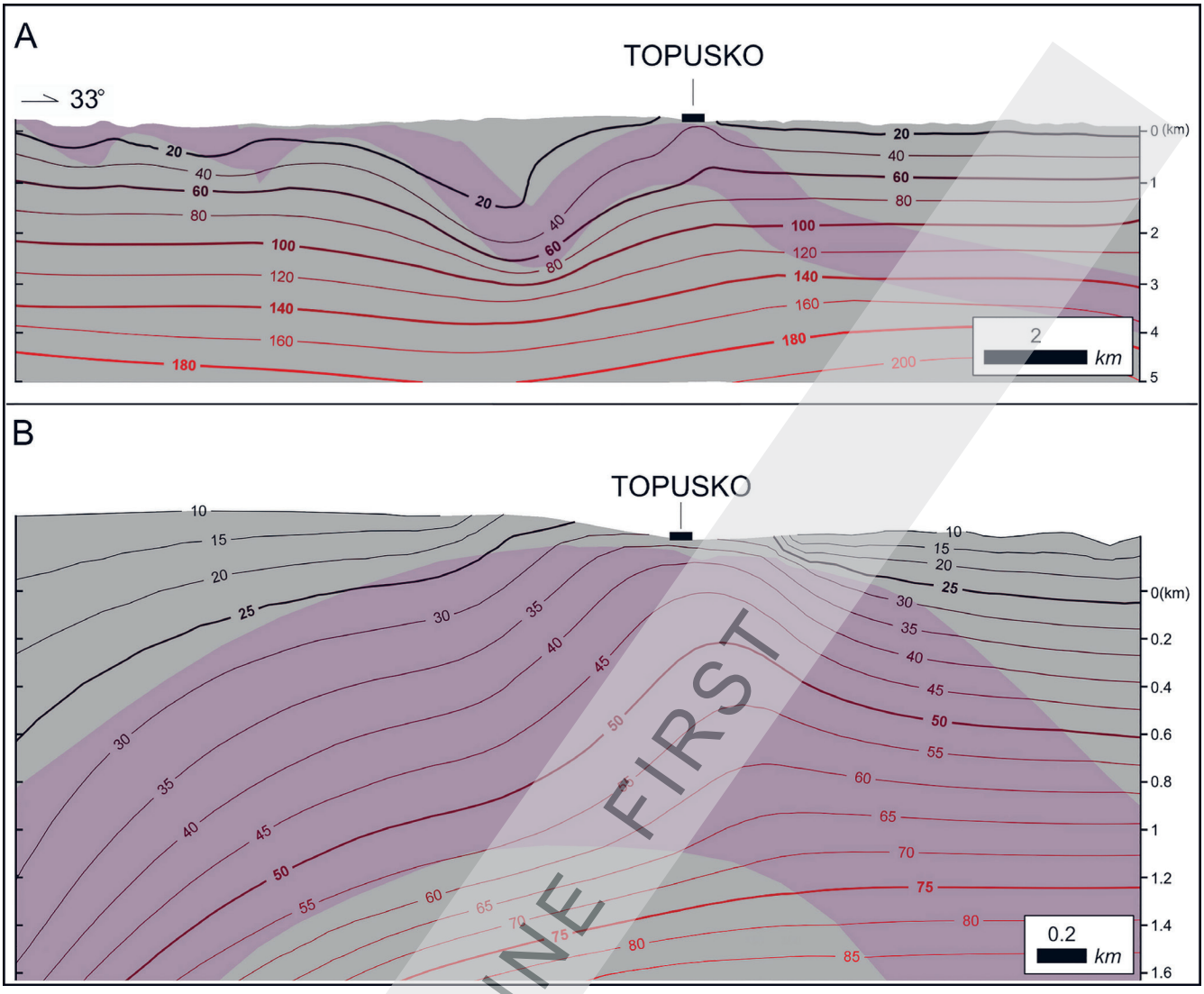

Figure 9. Regional temperature distribution in the modelling domain (A) and in the hinge zone of the Topusko anticline (B). A local temperature anomaly in the Topusko subsurface occurs reaching values of up to 74 °C at the base of the THS carbonate aquifer (pink polygon). The horizontal and vertical scale ratio is 1:1.

the 20 °C isotherm; Fig. 9A). The flow is generally upward in the southern limb of the Topusko anticline, but with similar magnitudes of the horizontal and vertical components of the Darcy velocity (average value of 0.15 m/yr corresponding to 4.16×10^{-4} m/d). In the Topusko area, the flow is upward and with a prevalent vertical component of the Darcy velocity. The average velocity value is of 0.13 m/yr (3.5×10^{-4} m/d), being slightly lower than the values observed in other parts of the aquifer, but the velocity field is more evenly distributed with minimum and maximum values of 1.21×10^{-3} and 0.28 m/yr, respectively. The Darcy velocity increases up to 0.28 m/yr in the upper part of the aquifer (i.e., the depth investigated by the thermal wells in Topusko) pointing to the quick rise of the thermal waters in the final part of the circulation path. The outflow modelled by the 3rd kind (Cauchy) BC is 0.18 m^3/yr.

4. DISCUSSION

The Topusko hydrothermal system area is located at the tectonic boundary between the External and Internal Dinarides in the vicinity of the Sava suture zone (SCHMID et al., 2020). The Palaeozoic-Mesozoic terrains in the study area experienced a complex polyphase tectonic evolution through the Cretaceous-Paleogene and the Neogene-Quaternary, which resulted in tectonic overprints of both regional shortening and extension. Observable regional shortening is associated with several NW-striking low-angle thrust faults and reverse faults (Fig. 4) that were probably formed due to the Cretaceous-Paleogene Adria Microplate and European Foreland collision (SCHMID et al., 2020). This regional NE – SW oriented shortening (TOMLJENOVIĆ & CSONTOS, 2001; SCHMID et al., 2008; USTASZEWSKI et al., 2008) resulted in the tectonic uplift of the Petrova gora Mt. and the formation of a folded system that also incorporates the Topusko anticline (Fig. 6). The polyphase tectonic history is further evidenced by structural reactivations of these faults and their tectonic inversions, which is observable in the tectonically inverted normal faults R3 and R4 (Fig. 4) indicating a NE – SW extension in the THS area. According to TOMLJENOVIĆ & CSONTOS (2001), NE – SW stretching of the inherited structures within the Croatian part of the PBS occurred during the Early-Middle Miocene due to back-arc type extension. Tectonic rejuvenation of the THS area through N – S regional contraction is observable at

the outcrop scale, with evidence of re-folding processes and mapped reverse faults within the Pliocene-Quaternary clastic sequence (e.g., USTASZEWSKI et al., 2008; HERAK et al., 2009; HERAK & HERAK, 2023).

The interpretation of the geological profiles constructed in this study suggests that the most used THS conceptual model (ŠIMUNIĆ, 2008) was based on an out-dated geological reconstruction. Furthermore, Šimunić's model was not constructed using a series of stuctural-geoloical profiles and a detailed reconstruction of subsurface relationships, but only spatial distribution of the lithological units. These shortcomings hindered the detailed understanding of complex subsurface relationships in the Topusko area. The new structural-geological interpretation was combined with geochemical and hydrogeological data (PAVIĆ et al., 2023, 2024) to propose a novel conceptual model of the THS. This model suggests that the THS is an intermediate-scale, gravity-driven, tectonically – controlled, hydrothermal system hosted in a Middle-Upper Triassic carbonate rock complex. The thermal water is of meteoric origin infiltrating approx. 13 km to the S of Topusko, where an area with intense karstification depicted by a high density of sinkholes occurs (Fig. 5). These sinkholes play a significant role in facilitating the diffuse recharge of the THS aquifer. Our interpretation in general coincides with BAĆ & HERAK's (1962) hypothesis, which identifies Middle and Upper Triassic carbonate deposits as the aquifer units facilitating deep groundwater circulation. They proposed that the thermal aquifer receives recharge from the Glina river headwaters, where Triassic carbonates are exposed, with a primary regional flow direction from S to N, aligning with our findings regarding the recharge area S of Topusko. Regional folded structures favour both the deep circulation of the infiltrated water, warming due to increased heat flow of the PBS (HORVÁTH et al., 2015), and the upwelling of the thermal water in the Topusko area. Fault and fracture systems in the hinge zone of the Topusko anticline promote the fracturing of the bedrock, the increase of the permeability field in the aquifer, and the quick rise of the thermal water from the deeper part of the reservoir. The extensional regime in the anticline hinge zone, combined with cogenetic fault and fracture systems and their permeable damage zones (PAVIĆ et al., 2023), creates a synergistic effect. This synergy enhances the overall permeability field in the discharge area, leading to the formation of abundant natural thermal springs.

The physical validity of the THS model was constrained conducting variable-density numerical simulations of fluid flow and heat transport. The numerical model was populated using a set of hydrogeological and thermal parameters from both the literature and field datasets. Boundary conditions were imposed at the borders of the modelling domain following the conceptual model of the THS. The best simulation was run for 100 kyr developing a local increase of the temperature distribution in the subsurface of Topusko (Fig. 9). In particular, the modelled temperatures were 31.3 and 44 °C at the surface and at the depth investigated by wells in Topusko, respectively. Despite these values are approx. 20 °C lower than the observed temperatures at the same depths, they can be considered as acceptable due to the simplifications imposed during the construction of the numerical model. The thermal aquifer was reproduced using an equivalent porous medium approach, which assigns homogeneous values of the hydrogeological properties, while localised highly permeable damage zones channelling the outflow of the thermal water were not considered. The implementation of such structures in the numerical model would increase the fluid flow promoting the local increase of the temperature. In addition, a temperature between 80 and 100 °C was modelled in the semi-confining unit at the bottom of the aquifer being comparable with the reservoir temperature of 90 °C calculated with geothermometers. As discussed for the surficial temperature, the effect of localised highly permeable fault zones was not included in the conducted numerical model. These areas could favour the raising of the isotherms in the deeper part of the reservoir resulting in the higher temperature values calculated with geothermometers.

The simulated temperature distribution at the local scale reproduced the field values and was almost constant during the final 20 kyr of the simulation time (Fig. 8A). This result suggested that a quasi-stationary condition reproducing the natural state of the THS was achieved for a time span that is almost twice the mean residence time of the Topusko thermal water. The simulation results indicate a predominant groundwater flow pattern towards the Topusko discharge area. They also highlight the significant influence of the hydraulic conductivity field on groundwater flow patterns within the system. The modelled Darcy velocities ranged from 0.13 m/yr (Topusko) to 0.27 m/yr (recharge area) in the aquifer and decreased within the hydrostratigraphic units below it, directly reflecting the contrasting hydraulic conductivity values of different hydrostratigraphic units. This emphasises the importance of incorporating accurate K data into groundwater flow models for reliable predictions. An outflow of 0.18 m^3/yr was modelled in the Topusko area, reproducing the thermal springs. Historical data on the flow rate of the springs before the drilling of the wells are not available and a more detailed numerical model would be needed to reproduce the effect of exploitation of the thermal water. The localised thermal anomaly in the anticline hinge zone corroborates the structural-causative processes enhancing fluid flow and heat transfer in the Topusko subsurface. Therefore, the results of the numerical modelling corroborate the validity of the conceptual model of the THS. In order to constrain the processes favouring the development of the modelled temperature distribution, the Rayleigh number (Ra) was calculated following the procedure described in TURCOTTE & SCHUBERT (1982). Ra is a dimensionless parameter indicating the threshold for the onset of free convection occurring when it exceeds the critical value of approximately 40 (TURCOTTE & SCHUBERT, 1982; NIELD & BEJAN, 1999; PESTOV, 2000; MÁDL-SZŐNYI & TÓTH, 2015). Considering the thickness of the reservoir (approx. 1 km) and its hydrogeological and thermal parametrisations, the conditions for the development of convection cells in the THS predominantly exist in the more permeable hinge zones of the Topusko anticline (Ra = 5,500 – 8,600 at temperature range simulated in the aquifer). Conduction is the predominant heat transfer mechanism in the rest of the THS aquifer (Ra < 60).

The used modelling approach proved to be a valuable initial step for understanding regional hydrogeological systems despite its simplifications. The lack of extensive boreholes or geophysical data limits the understanding of the regional geological and hydrogeological settings. Complex modelling with such limited data can lead to numerous assumptions, increasing the uncertainty of the simulations. Therefore, a simple numerical approach with a detailed hydrogeological and thermal parameterisation or robust geological reconstruction is initially preferable to reduce uncertainty. In the absence of a local dataset of hydrogeological and thermal properties, the parameterisation of hydrostratigraphic units in THS was conducted considering relevant regional studies and literature collections. Incorporating well-documented information from the literature enhanced the credibility and robustness of the model, facilitating a more comprehensive understanding of the hydrothermal system's dynamics. As fluid flow and heat transport are three-dimensional processes, the use of a 2D profile in the conducted THS representation is likely the most important simplification. This approach does not account for the proper local and regional characterisation of faults and related subsidiary structures, which are critical for fluid flow in fractured rocks. In the wider area of the THS, a dome-like anticline structure affects the geological and structural architecture in the subsurface, as illustrated in the presented profiles (Fig. 4, profiles THS-1-3). Describing this complex geological setting with the 2D model is inherently problematic, as it fails to capture the total spatial variability and structural-geological intricacies. This limitation adds to the discrepancies observed between modelled and actual temperatures and fluid flows, emphasising the need for more sophisticated modelling approaches capable of accounting for the geological complexity of the THS. The construction of a 3D model, supported by a more extensive dataset of hydrogeological, structural-geological, and thermal parameters, could improve the understanding of the thermal system dynamics. Considering the 3D geological architecture will significantly enhance the accuracy and reliability of future numerical simulations. Future investigations will focus on conducting a comprehensive 3D geological reconstruction of the subsurface based on detailed structural-geological and geophysical investigations that are necessary to characterise and justify the proposed local and regional structural-geological setting of the THS. This consequently includes the reconstruction of regional and local fault meshes for a more sophisticated numerical model.

5. CONCLUSION

The presented study utilised structural-geological field investigations and numerical modelling to develop a novel conceptual model of the THS. By constructing new geological profiles and integrating them with hydrogeological and geochemical data, we were able to provide new insights into the THS dynamics proposing a novel conceptual model. The recharge area of THS lies S of Topusko, where Triassic carbonates crop out. Regional and local scale fold and fault systems favour the deep circulation of the thermal water and the upwelling in Topusko forming a valuable geothermal resource.

Numerical modelling corroborates the proposed conceptual model of the THS. A local temperature anomaly was simulated in the Topusko subsurface reproducing the temperature field observations. The occurrence of such a localised thermal anomaly in the hinge zone of the Topusko anticline suggests an enhanced fluid flow and heat transport pointing to the impact of terrestrial heat flow and local geological structures on the system. In particular, the synergetic effect of the anticline hinge, which was determined by structural investigations, and cogenetic fault/fracture systems, which were identified by surface geophysical research, results in an enhanced permeability field in the discharge area, thereby enabling the formation of abundant natural thermal springs.

This study both advances the understanding of the THS and highlights the importance of integrating field observations with numerical modelling to physically validate and refine conceptual models. This integrated approach permits a more detailed reconstruction of the hydrogeological and thermal processes driving the development of geothermal resources. These aspects are crucial for developing site-specific exploitation plans of the resource, favouring its long-term utilisation.

ACKNOWLEDGEMENT

This research was funded by the Croatian Science Foundation (HRZZ), grant number UIP-2019-04-1218.

REFERENCES

ANDERSON, M.P. (2005): Heat as a Ground Water Tracer.– Groundwater, 43/6, 951–968. doi: 10.1111/j.1745-6584.2005.00052.x

ANDERSON, M., WOESSNER, W. & HUNT, R. (2015): Applied Ground Water Modeling: Simulation of Flow and Advective Transport.– Elsevier, London, 533 p.

AN, R., JIANG, X.-W., WANG, J.-Z., WAN, L., WANG, X.-S. & LI, H. (2015): A theoretical analysis of basin-scale groundwater temperature distribution.– Hydrogeol. J., 23/2, 397–404. doi: 10.1007/s10040-014-1197-y

BAĆ, J. & HERAK, M. (1962): Prijedlog određivanja užih i širih zaštitnih zona termomineralnih izvora u Hrvatskoj [*Recommendation for determination of wider and narrow protection zones for thermo-mineral springs in Croatia* – in Croatian].– Unpublished report, Institute for geological research, Zagreb, 147 p.

BAHUN, S. & RALJEVIĆ, B. (1969): Mineralna, termalna i ljekovita vrela [*Mineral and Thermal Springs* – in Croatian].– Unpublished report, Institute for geological research, Zagreb.

BÉKÉSI, E., LENKEY, L., LIMBERGER, J., PORKOLÁB, K., BALÁZS, A., BONTÉ, D., VRIJLANDT, M., HORVÁTH, F., CLOETINGH, S. & VAN WEES, J.D. (2018): Subsurface temperature model of the Hungarian part of the Pannonian Basin.– Global and Planetary Change, 171, 48–64. doi: 10.1016/j.gloplacha.2017.09.020

BENČEK, Đ., BUKOVAC, J., MAGAŠ, N. & ŠIMUNIĆ, A. (2014): Osnovna geološka karta Republike Hrvatske 1:100.000, List Karlovac L33-92 [*Basic Geological Map of the Republic of Croatia 1:100.000, Karlovac sheet* – in Croatian].– Croatian Geological Survey, Zagreb.

BENČEK, Đ., BUKOVAC, J., MAGAŠ, N. & ŠIMUNIĆ, A. (2014): Osnovna geološka karta Republike Hrvatske 1:100.000, Tumač za list Karlovac L33-92 [*Basic Geological Map of the Republic of Croatia 1:100.000, Explanatory notes for Karlovac sheet* – in Croatian].– Croatian Geological Survey, Zagreb, 85 p.

BOROVIĆ, S., MARKOVIĆ, T., LARVA, O., BRKIĆ, Ž. & MRAZ, V. (2016): Mineral and Thermal Waters in the Croatian Part of the Pannonian Ba-

sin.– In: PAPIĆ, P. (ed.): Mineral and Thermal Waters of Southeastern Europe. Springer, Cham.

BOROVIĆ, S., URUMOVIĆ, K., TERZIĆ, J. & PAVIČIĆ, I. (2018): Examining thermal conductivities of shallow subsurface materials for ground source heat pump utilization in the Pannonian part of Croatia.– The Mining-Geological-Petroleum Engineering Bulletin, 33/5, 27–35. doi: 10.17794/rgn.2018.5.3

BOROVIĆ, S., POLA, M., BAČANI, A. & URUMOVIĆ, K. (2019): Constraining the recharge area of a hydrothermal system in fractured carbonates by numerical modelling.– Geothermics, 82, 128–149. doi: 10.1016/j.geothermics.2019.05.017

BRÜCKL, E., BEHM, M., DECKER, K., GRAD, M., GUTERCH, A., KELLER, G.R. & THYBO, H. (2010): Crustal structure and active tectonics in the Eastern Alps.– Tectonics, 29/2. https://doi.org/10.1029/2009TC002491

BUNDSCHUH, J. & CÉSAR SUÁREZ, A.M. (2010): Introduction to the Numerical Modeling of Groundwater and Geothermal Systems.– CRC Press, London. 522 p. doi: 10.1201/b10499

BUKOVAC, J., ŠUŠNJAR, M., POLJAK, M. & ČAKALO, M. (1984): Osnovna geološka karta SFRJ 1:100.000, List Črnomelj L33–91 [*Basic Geological Map of the Republic of Croatia, 1:100.000, Črnomelj sheet* – in Croatian].– Federal Geological Survey, Belgrade.

CALCAGNO, P., BAUJARD, C., GUILLOU-FROTTIER, L., DAGALLIER, A. & GENTER, A. (2014): Estimation of the deep geothermal potential within the Tertiary Limagne basin (French Massif Central): An integrated 3D geological and thermal approach.– Geothermics, 51, 496–508. doi: 10.1016/j.geothermics.2014.02.002

CERMAK, V., & RYBACH, L. (1982): Thermal properties: Thermal conductivity and specific heat of minerals and rocks.– In: ANGENEISTER, G. (ed.): Landolt-Börnstein: Zahlenwerte and Funktionen aus Naturwissenschaften und Technik, Neue Serie, Physikalische Eigenschaften der Gesteine. Springer Verlag, Berlin, Heidelberg and New York, V/1a, 305–343.

CLOETINGH, S., CORNU, T., ZIEGLER, P.A., BEEKMAN, F. & ENTEC Working Group (2006): Neotectonics and intraplate continental topography of the northern Alpine Foreland.– Earth. Sci. Rev., 74, 127–196. doi: 10.1016/j.earscirev.2005.06.001

CRITTENDEN, J.C., TRUSSELL, R.R., HAND, D.W., HOWE, K.J. & TCHOBANOGLOUS, G. (2012): MWH's Water Treatment.– John Wiley & Sons, Inc. doi: 10.1002/9781118131473

CSONTOS, L. & VÖRÖS, A. (2004): Mesozoic plate tectonic reconstruction of the Carpathian region.– Palaeogeogr. Palaeoclimatol. Palaeoecol., 210/1, 1–56. doi: 10.1016/j.palaeo.2004.02.033

D'AGOSTINO, N., AVALLONE, A., CHELONI, D., D'ANASTASIO, E., MANTENUTO, S. & SELVAGGI, G. (2008): Active tectonics of the Adriatic region from GPS and earthquake slip vectors.– Journal of Geophysical Research: Solid Earth, 113/B12. https://doi.org/10.1029/2008JB005860

DHMZ. (2021): Monthly values and extremes.– Državni Hidrometeorološki Zavod [*Croatian Meteorological and Hydrological Service* – in Croatian]. (retrieved January 18, 2021) from https://meteo.hr/klima.php?section=klima_podaci&param=k2_1

DIERSCH, H.J.G. (2014): FEFLOW: Finite Element Modeling of Flow, Mass and Heat Transport in Porous and Fractured Media.– Springer Berlin, Heidelberg. doi: 10.1007/978-3-642-38739-5

DI NAPOLI, R., MARTORANA, R., ORSI, G., AIUPPA, A., CAMARDA, M., DE GREGORIO, S., GAGLIANO CANDELA, E., LUZIO, D., MESSINA, N., PECORAINO, G. et al. (2011): The Structure of a Hydrothermal System from an Integrated Geochemical, Geophysical, and Geological Approach: The Ischia Island Case Study.– Geochem. Geophys. Geosyst., 12/7. https://doi.org/10.1029/2010GC003476

DOMENICO, P.A. & SCHWARTZ, F.W. (1997): Physical and Chemical Hydrogeology (2nd edition).– Wiley, New York. 506 p.

DOMENICO, P. A. & PALCIAUSKAS, V. V. (1973): Theoretical Analysis of Forced Convective Heat Transfer in Regional Ground-Water Flow.– GSA Bulletin, 84/12, 3803–3814. doi: 10.1130/0016-7606(1973)84<3803:TAOFCH>2.0.CO;2

EVANS, M.A. & FISCHER, M.P. (2012): On the distribution of fluids in folds: A review of controlling factors and processes.– J. Struct. Geol., 44, 2–24. doi: 10.1016/j.jsg.2012.08.003

FABBRI, P., POLA, M., PICCININI, L., ZAMPIERI, D., ROGHEL, A. & DALLA LIBERA, N. (2017): Monitoring, utilization and sustainable development of a low-temperature geothermal resource: A case study of the Euganean Geothermal Field (NE, Italy).– Geothermics, 70, 281–294. doi: 10.1016/j.geothermics.2017.07.002.

FAULKNER, D. R., JACKSON, C. A. L., LUNN, R. J., SCHLISCHE, R. W., SHIPTON, Z. K., WIBBERLEY, C. A. J., & WITHJACK, M. O. (2010): A review of recent developments concerning the structure, mechanics and fluid flow properties of fault zones.– J. Struct. Geol., 32/11, 1557–1575. doi: 10.1016/j.jsg.2010.06.009

FEDERAL GEOLOGICAL SURVEY. (1970): Geological Map of SFRY 1:500.000.– Federal Geological Survey, Beograd.

FETTER, C.W. (2001): Applied Hydrogeology (4th edition).– Prentice Hall, Upper Saddle River, New Jersey.

FLÓVENZ, Ó.G., HERSIR, G.P., SÆMUNDSSON, K., ÁRMANNSSON, H. & FRIDRIKSSON, T. (2012): Geothermal Energy Exploration Techniques.– In: SAYIGH, A. (ed.): Comprehensive Renewable Energy, 51–95. doi: 10.1016/B978-0-08-087872-0.00705-8

FUCHS, S. & BALLING, N. (2016): Improving the temperature predictions of subsurface thermal models by using high-quality input data. Part 1: Uncertainty analysis of the thermal-conductivity parameterization.– Geothermics, 64, 42–54. doi: 10.1016/j.geothermics.2016.04.010

GARG, S.K., PRITCHETT, J.W., WANNAMAKER, P.E. & COMBS, J. (2007): Characterization of geothermal reservoirs with electrical surveys: Beowawe geothermal field.– Geothermics, 36/6, 487–517. doi: 10.1016/j.geothermics.2007.07.005

GHASEMIZADEH, R., HELLWEGER, F., BUTSCHER, C. et al. (2012): Review: Groundwater flow and transport modeling of karst aquifers, with particular reference to the North Coast Limestone aquifer system of Puerto Rico.– Hydrogeol J., 20, 1441–1461. doi: 10.1007/s10040-012-0897-4

GOLDSCHEIDER, N., MÁDL-SZŐNYI, J., ERŐSS, A. & SCHILL, E. (2010): Review: Thermal water resources in carbonate rock aquifers.– Hydrogeol. J., 18/6, 1303–1318. doi: 10.1007/s10040-010-0611-3

GORJANOVIĆ-KRAMBERGER, D. (1905): Geologijske i hidrografijske prilike oko Topuskoga s obzirom na topuske terme [*Geological and hydrographic conditions in the area of Topusko with respect to thermal spring* – in Croatian].– Works of the Yugoslav Academy of Sciences and Arts – Mathematics and Science Division, 37, 2–34.

GORJANOVIĆ-KRAMBERGER, D. (1917): Geologijske i hidrografijske prilike oko Topuskog s osobitim obzirom na Topuske terme [*Geological and hydrographic conditions in the area of Topusko with particular interest in thermal springs* – in Croatian].– Reports of discussions in Mathematics and Science Division, Yugoslav Academy of Sciences and Arts, Zagreb.

GRENERCZY, G., SELLA, G.F., STEIN, S. & KENYERES, A., (2005): Tectonic implications of the GPS velocity field in the northern Adriatic region.– Geophys. Res. Lett., 32/16. doi: 10.1029/2005GL022947

HAVRIL, T., MOLSON, J.W. & MÁDL-SZŐNYI, J. (2016): Evolution of fluid flow and heat distribution over geological time scales at the margin of unconfined and confined carbonate sequences - A numerical investigation based on the Buda Thermal Karst analogue.– Mar. and Pet. Geol., 78, 738–749. doi: 10.1016/j.marpetgeo.2016.10.001

HEASLER, H.P., JAWOROWSKI, C. & FOLEY, D. (2009): Geothermal systems and monitoring hydrothermal features.– In: YOUNG, R. & NORBY, L. (eds.): Geological Monitoring. Geological Society of America, Boulder. doi:/10.1130/2009.monitoring(05)

HERAK, D., HERAK, M. & TOMLJENOVIĆ, B. (2009): Seismicity and earthquake focal mechanisms in North-Western Croatia.– Tectonophysics, 465/1–4, 212–220. doi: 10.1016/j.tecto.2008.12.005

HERAK, M. & HERAK, D. (2023): Properties of the Petrinja (Croatia) earthquake sequence of 2020–2021 – Results of seismological research for the first six months of activity.– Tectonophysics, 858, 229885. doi: 10.1016/j.tecto.2023.229885

HORVÁTH, F. & TARI, G. (1999): The IBS Pannonian basin project: A review of the main results and their bearings on hydrocarbon exploration.– Geol. Soc. London Spec. Publ., 156, 195–213. doi: 10.1144/GSL.SP.1999.156.01.11

HORVÁTH, F., BADA, G., SZAFIÁN, P., TARI, G., ÁDÁM, A. & CLOETINGH, S. (2006): Formation and deformation of the Pannonian Basin: Constraints from observational data.– Geological Society Memoir, 32, 191–206. doi: 10.1144/GSL.MEM.2006.032.01.11

HORVÁTH, F., MUSITZ, B., BALÁZS, A., VÉGH, A., UHRIN, A., NÁDOR, A., KOROKNAI, B., PAP, N., TÓTH, T. & WÓRUM, G. (2015): Evolution of the Pannonian basin and its geothermal resources.– Geothermics, 53, 328–352. doi: 10.1016/j.geothermics.2014.07.009

HOUNSLOW, A.W. (1995): Water Quality Data: Analysis and Interpretation (1st ed.).– CRC Press. doi: 10.1201/9780203734117

HRVATOVIĆ, H. (2005): Geological Guidebook through Bosnia and Herzegovina.– Geological Survey Sarajevo-Geology Department,163 p.

KAISER, B.O., CACACE, M., & SCHECK-WENDEROTH, M. (2013): 3D coupled fluid and heat transport simulations of the Northeast German Basin and their sensitivity to the spatial discretization: different sensitivities for different mechanisms of heat transport.– Environ. Earth Sci., 70/8, 3643–3659. doi: 10.1007/s12665-013-2249-7

KASTELIC, V. & CARAFA, M.M.C. (2012): Fault slip rates for the active External Dinarides thrust-and-fold belt.– Tectonics, 31/3. doi: 10.1029/2011TC003022

KHODAYAR, M. & BJÖRNSSON, S. (2024): Conventional Geothermal Systems and Unconventional Geothermal Developments: An Overview.– Open J. Geol., 14/2, 196–246. doi: 10.4236/ojg.2024.142012

KOROLIJA, B., ŽIVALJEVIĆC, T. & ŠIMUNIĆ, A. (1980): Osnovna geološka karta SFRJ 1:100.000, List Slunj L 33–104 [*Basic Geological Map of SFRY 1:100.000, Slunj sheet* – in Croatian].– Institute for Geological Research, Zagreb, Geological Survey, Sarajevo; Federal Geological Survey, Belgrade.

KOROLIJA, B., ŽIVALJEVIĆ, T. & ŠIMUNIĆ, A. (1981): Osnovna geološka karta SFRJ 1:100.000, Tumač za list Slunj L33–104 [*Basic Geological Map of SFRY 1:100.000, Explanatory notes for Slunj sheet* – in Croatian].– Institute for geological research, Zagreb; Geological survey, Sarajevo; Federal geological survey: Belgrade.

KOSOVIĆ, I., BRIŠKI, M., PAVIĆ, M., PADOVAN, B., PAVIČIĆ, I., MATOŠ, B., POLA M. & BOROVIĆ, S. (2023): Reconstruction of Fault Architecture in the Natural Thermal Spring Area of Daruvar Hydrothermal System Using Surface Geophysical Investigations (Croatia).– Sustainability, 15/16,12134. doi: 10.3390/su151612134

KOSOVIĆ, I., MATOŠ, B., PAVIČIĆ, I., POLA, M., MILEUSNIĆ, M., PAVIĆ, M. & BOROVIĆ, S. (2024): Geological modeling of a tectonically controlled hydrothermal system in the southwestern part of the Pannonian basin (Croatia).– Front. Earth Sci., 12. doi: 10.3389/feart.2024.1401935

LALOUI, L. & ROTTA LORIA, A. F. (2020): Heat and mass transfers in the context of energy geostructures.– In: Analysis and Design of Energy Geostructures. Academic Press., 69–135. doi: 10.1016/B978-0-12-816223-1.00003-5

LEI, H. & ZHU, J. (2013): Numerical modeling of exploitation and reinjection of the Guantao geothermal reservoir in Tanggu District, Tianjin, China.– Geothermics, 48, 60–68. doi: 10.1016/j.geothermics.2013.03.008

LENKEY, L., DÖVÉNYI, P., HORVÁTH, F. & CLOETINGH, S.A.P.L. (2002): Geothermics of the Pannonian basin and its bearing on the neotectonics.– In: CLOETINGH, S.A.P.L, HORVÁTH, F., BADA, G. & LANKREIJER, A.C. (eds.): EGU Stephan Mueller Special Publication Series, 3, 29–40. doi: 10.5194/smsps-3-29-2002

MACENIĆ, M., KUREVIJA, T. & MEDVED, I. (2020): Novel geothermal gradient map of the Croatian part of the Pannonian basin system based on data interpretation from 154 deep exploration wells.– Renew. Sustain. Energy Rev., 132. doi: 10.1016/J.RSER.2020.110069

MÁDL-SZŐNYI, J. & TÓTH, Á. (2015): Basin-scale conceptual groundwater flow model for an unconfined and confined thick carbonate region.– Hydrogeol. J., 23/7, 1359–1380. doi: 10.1007/s10040-015-1274-x

MAJER, V. (1978): Stijene "dijabaz-spilit-keratofirske asocijacije" u području Abez-Lasinja u Pokuplju i Baniji (Hrvatska, Jugoslavija) [*Rocks of diabase-spilite-keratophyre association in the area of Abez-Lasinja in Pokuplje and Banije (Croatia, Yugoslavia)* – in Croatian].– Acta Geol., 9/4, 42, 137–158.

MAJER, V. (1993): Ofiolitni kompleks Banije s Pokupljem u Hrvatskoj i Pastirevo u Bosni [*Ophiolite complexes of Banija and Pokuplje in Croatia and Pastirevo in Bosnia* – in Croatian].– Acta Geol., 23/2, 39–84.

MANDAL, A., BASANTARAY, A.K., CHANDROTH, A. & MISHRA, U. (2019): Integrated Geophysical Investigation to Map Shallow Surface Alteration/Fracture Zones of Atri and Tarabalo Hot Springs, Odisha, India.– Geothermics, 77, 24–33. doi: 10.1016/j.geothermics.2018.08.007

MARINI, L. (2000): Geochemical techniques for the exploration and exploitation of geothermal energy.– Dipartamento per lo Studio del Territorio e delle sue Risorse, Universita degli Studi di Genova, Italy.

MARTINSEN, G., BESSIERE, H., CABALLERO, Y., KOCH, J., COLLADOS-LARA, A. J., MANSOUR, M., SALLASMAA, O., PULIDO-VELAZQUEZ, D., WILLIAMS, N.H., ZAADNOORDIJK, W.J. & STISEN, S. (2022). Developing a pan-European high-resolution groundwater recharge map – Combining satellite data and national survey data using machine learning.– Science of the Total Environment, 822 p. doi: 10.1016/j.scitotenv.2022.153464

MAZOR, E. (2004): Chemical and Isotopic Groundwater Hydrology, 3rd ed.– Marcel Dekker, New York, 13–179 p.

MOECK, I.S. (2014): Catalog of geothermal play types based on geologic controls.– Renewable and Sustainable Energy Reviews, 37, 867–882. doi: 10.1016/j.rser.2014.05.032

MONTANARI, D., MINISSALE, A., DOVERI, M., GOLA, G., TRUMPY, E., SANTILANO, A. & MANZELLA, A. (2017): Geothermal resources within carbonate reservoirs in western Sicily (Italy): A review.– Earth-Science Reviews, 169, 180–201. doi: 10.1016/j.earscirev.2017.04.016

MROCZEK, E.K., MILICICH, S.D., BIXLEY, P.F., SEPULVEDA, F., BERTRAND, E.A., SOENGKONO, S. et al. (2016): Ohaaki geothermal system: Refinement of a conceptual reservoir model.– Geothermics, 59, 311–324. doi: 10.1016/j.geothermics.2015.09.002

MUFFLER, P. & CATALDI, R. (1978): Methods for regional assessment of geothermal resources.– Geothermics, 7/2–4, 53–89. doi: 10.1016/0375-6505(78)90002-0

NIELD, D.A. & BEJAN, A. (1999): Convection in Porous Media (2nd Edition).– Springer, New York. doi:10.1007/978-1-4757-3033-3

OJHA, L., KARUNATILLAKE, S., KARIMI, S. & BUFFO, J. (2021): Amagmatic hydrothermal systems on Mars from radiogenic heat.– Nat. Commun., 12/1. doi: 10.1038/s41467-021-21762-8

PAVELIĆ, D. (2001): Tectonostratigraphic model for the North Croatian and North Bosnian sector of the Miocene Pannonian Basin System.– Basin Res., 13, 359–376. doi: 10.1046/j.0950-091x.2001.00155.x

PAVELIĆ, D., KOVAČIĆ, M., MIKNIĆ, M., AVANIĆ, R., VRSALJKO, D., BAKRAČ, K., TIŠLJAR, J., GALOVIĆ, I. & BORTEK, Ž. (2003): The Evolution of the Miocene Environments in the Slavonian Mts. Area (Northern Croatia).– In: VLAHOVIĆ, I. & TIŠLJAR, J. (eds.): 22nd IAS Meeting of Sedimentology – Opatija 2003, Field Trip Guidebook. Croatian Geological Survey, Zagreb.

POLA, M., CACACE, M., FABBRI, P., PICCININI, L., ZAMPIERI, D. & TORRESAN, F. (2020): Fault Control on a Thermal Anomaly: Conceptual and Numerical Modeling of a Low-Temperature Geothermal System in the Southern Alps Foreland Basin (NE Italy).– J. Geophys. Res. Solid Earth, 125/5, e2019JBO17394, doi: 10.1029/2019JB017394

PAVIĆ, M., KOSOVIĆ, I., POLA, M., URUMOVIĆ, K., BRIŠKI, M., & BOROVIĆ, S. (2023): Multidisciplinary Research of Thermal Springs Area in Topusko (Croatia).– Sustainability, 15/6, 5498. doi: 10.3390/su15065498

PAVIĆ, M., BRIŠKI, M., POLA, M., & BOROVIĆ, S. (2024): Hydrogeochemical and environmental isotope study of Topusko thermal waters, Cro-

atia.– Environ. Geochem. Health, 46/4, 133. doi: 10.1007/s10653-024-01904-9

POURASKARPARAST, Z., AGHAEI, H., COLOMBERA, L., MASOERO, E. & GHAEDI, M. (2024): Fracture aperture: A review on fundamental concepts, estimation methods, applications, and research gaps.– Mar. Pet. Geol., 164, 106818. doi: 10.1016/j.marpetgeo.2024.106818

PRELOGOVIĆ, E., SAFTIĆ, B., KUK, V., VELIĆ, J., DRAGAŠ, M. & LUČIĆ, D. (1998): Tectonic activity in the Croatian part of the Pannonian basin.– Tectonophysics, 297/1–4, 283–293. doi: 10.1016/S0040-1951(98)00173-5

RMAN, N. & TÓTH, G. (2011): Hydrogeological conceptual model.– Geological Survey of Slovenia, Ljubljana; Geological Institute of Hungary, Budapest [in Hungarian], 25 p.

RMAN, N. (2014): Analysis of long-term thermal water abstraction and its impact on low-temperature intergranular geothermal aquifers in the Mura-Zala basin, NE Slovenia.– Geothermics, 51, 214–227. doi: 10.1016/j.geothermics.2014.01.011

RMAN, N., BĂLAN, L.L., BOBOVEČKI, I., GÁL, N., JOLOVIĆ, B., LAPANJE, A. et al. (2020): Geothermal sources and utilization practice in six countries along the southern part of the Pannonian basin.– Environ. Earth Sci., 79, 1–12. doi: 10.1007/s12665-019-8746-6

ROYDEN, L.H., & HORVÁTH, F. (1988): The Pannonian Basin: A Study in Basin Evolution.– American Association of Petroleum Geologists. doi: 10.1306/M45474

SAFTIĆ, B., VELIĆ, J., SZTANO, O., JUHASZ, G. & IVKOVIĆ, Ž. (2003). Tertiary Subsurface Facies, Source Rocks and Hydrocarbon Reservoirs in the SW Part of the Pannonian Basin (Northern Croatia and South-Western Hungary). Geologia Croatica, 56/1, 101–122. doi:10.4154/232

SCANLON, B., & DUTTON, A. (2000): Groundwater Recharge in Texas.– The University of Texas at Austin, and Marios Sophocleous, Kansas Geological Survey, Lawrence, KS.

SCANLON, B.R., MACE, R.E., BARRETT, M.E. & SMITH, B. (2003): Can we simulate regional groundwater flow in a karst system using equivalent porous media models? Case study, Barton Springs Edwards aquifer, USA.– Journal of Hydrology, 2761–4, 137–158. doi: 10.1016/S0022-1694(03)00064-7

SCHMID, S.M., BERNOULLI, D., FÜGENSCHUH, B., MATENCO, L., SCHEFER, S., SCHUSTER, R., TISCHLER, M. & USTASZEWSKI, K. (2008): The Alpine-Carpathian-Dinaridic orogenic system: Correlation and evolution of tectonic units.– Swiss J. Geosci., 101, 139–183. doi: 10.1007/s00015-008-1247-3

SCHMID, S. M., FÜGENSCHUH, B., KOUNOV, A., MAŢENCO, L., NIEVERGELT, P., OBERHÄNSLI, R., PLEUGER, J., SCHEFER, S., SCHUSTER, R., TOMLJENOVIĆ, B., USTASZEWSKI, K. & VAN HINSBERGEN, D.J.J. (2020): Tectonic units of the Alpine collision zone between Eastern Alps and western Turkey.– Gondwana Research, 78, 308–374. doi: 10.1016/j.gr.2019.07.005

STEVANOVIĆ, Z., DULIĆ, I. & DUNČIĆ, M. (2015): Some experiences in tapping deep thermal waters of the Triassic karstic aquifer in the Pannonian Basin of Serbia.– Central European Geology, 581–2, 50–61. doi: 10.1556/24.58.2015.1-2.3

STYLIANOU, I., TASSOU, S., CHRISTODOULIDES, P., PANAYIDES, I. & FLORIDES, G. (2016): Measurement and analysis of thermal properties of rocks for the compilation of geothermal maps of Cyprus.– Renewable Energy, 88, 418–429. doi:10.1016/j.renene.2015.10.058"

SZANYI, J. & KOVÁCS, B. (2010): Utilization of geothermal systems in South-East Hungary.– Geothermics, 39/4, 357–364. doi: 10.1016/j.geothermics.2010.09.004

ŠEGOTIĆ, B. & ŠMIT, I. (2007): Studija optimirane energetske učinkovitosti korištenja geotermalnih voda [*Study of Optimized Energy Efficiency of Geothermal Water Use* – in Croatian].– Unpublished report, Termoinženjering-projektiranje, Zagreb.

ŠIKIĆ, K. (1990): Osnovna geološka karta Republike Hrvatske 1:100.000, list Bosanski Novi L 33–105 [*Basic Geological Map of the Republic of Croatia 1:100.000, Bosanski Novi sheet* – in Croatian].– Croatian Geological Survey, 2014.

ŠIKIĆ, K. (1990): Osnovna geološka karta Republike Hrvatske 1:100.000, Tumač za list Bosanski Novi L 33-70 [*Basic Geological Map of the Republic of Croatia 1:100.000, Explanatory notes for Bosanski Novi sheet* – in Croatian].– Croatian Geological Survey Zagreb, 2014.

ŠIMUNIĆ, A. (2008): Topusko.– In: ŠIMUNIĆ, A. & HEĆIMOVIĆ, I. (eds.): Geotermalne i mineralne vode Republike Hrvatske [*Mineral and Thermal Waters of the Republic of Croatia* – in Croatian]. Croatian Geological Survey, Zagreb.

TARI, G., DÖVÉNYI, P., DUNKL, I., HORVÁTH, F., LENKEY, L., STEFANESCU, M., SZAFIÁN, P. & TÓTH, T (1999): Lithospheric structure of the Pannonian basin derived from seismic, gravity and geothermal data.– Geol. Soc. London Spec. Publ., 156, 215–250. doi: 10.1144/GSL.SP.1999.156.01.12

TEUTSCH, G. & SAUTER, M. (1991): Groundwater modeling in karst terranes: Scale effects, data acquisition and field validation.– In: Third conference on hydrogeology, ecology, monitoring, and management of ground water in Karst Terranes.– National Ground Water Association, Dublin, Ohio,17–35.

TOMLJENOVIĆ, B. & CSONTOS, L. (2001): Neogene–Quaternary structures in the border zone between Alps, Dinarides and Pannonian Basin (Hrvatsko zagorje and Karlovac Basins, Croatia).– Int. J. Earth Sci., 90/3, 560–578. doi: 10.1007/s005310000176

TOMLJENOVIĆ, B. (2002): Strukturne značajke Medvednice i Samoborskog gorja [*Structural features of Medvednica and Samobor hills* – in Croatian].– Unpubl. PhD Thesis, Faculty of Mining, Geology and Petroleum Engineering, University of Zagreb, Zagreb.

TOMLJENOVIĆ, B., CSONTOS, L., MÁRTON, E. & MÁRTON, P. (2008): Tectonic evolution of the northwestern Internal Dinarides as constrained by structures and rotation of Medvednica Mountains, North Croatia.– Geol. Soc. London Spec. Publ., 298/1, 145–167. doi: 10.1144/SP298.8

TORRESAN, F., PICCININI, L., CACACE, M., POLA, M., ZAMPIERI, D. & FABBRI, P. (2022): Numerical modeling as a tool for evaluating the renewability of geothermal resources: the case study of the Euganean Geothermal System (NE Italy).– Environ. Geochem. Health, 44/7, 2135–2162. doi: 10.1007/s10653-021-01028-4

TÓTH, J. (2009): Gravitational systems of groundwater flow: theory, evaluation, utilization.– Cambridge University Press, Cambridge. doi: 10.1017/CBO9780511576546

TURCOTTE, D.L. & SCHUBERT, G. (1982): Geodynamics: Applications of continuum mechanics to geological problems.– Wiley, New York, 464 p.

USTASZEWSKI, K., SCHMID, S. M., FÜGENSCHUH, B., TISCHLER, M., KISSLING, E. & SPAKMAN, W. (2008): A map-view restoration of the Alpine-Carpathian-Dinaridic system for the early Miocene.– Swiss J. Geosci., 101/Suppl 1, 273-294. doi: 10.1007/s00015-008-1288-7

USTASZEWSKI, K., KOUNOV, A., SCHMID, S. M., SCHALTEGGER, U., KRENN, E., FRANK, W. & FÜGENSCHUH, B. (2010): Evolution of the Adria-Europe plate boundary in the northern Dinarides: From continent-continent collision to back-arc extension.– Tectonics, 29/6. doi: 10.1029/2010TC002668

USTASZEWSKI, K., HERAK, M., TOMLJENOVIĆ, B., HERAK, D. & MATEJ, S. (2014): Neotectonics of the Dinarides-Pannonian Basin transition and possible earthquake sources in the Banja Luka epicentral area.– J. Geodyn., 82, 52–68. doi: 10.1016/j.jog.2014.04.006

VASS, I., TÓTH, T.M., SZANYI, J. & KOVÁCS, B. (2018): Hybrid numerical modelling of fluid and heat transport between the overpressured and gravitational flow systems of the Pannonian Basin.– Geothermics, 72, 268–276. doi: 10.1016/j.geothermics.2017.11.013

VELIĆ, I. & SOKAČ, B. (1982): Novi nalazl naslaga donjeg i srednjeg trijasa u zapadnom Kordunu (središnja Hrvatska) [*New discoveries of the Lower and Middle Triassic in the western part of Kordun area (central Croatia)* – in Croatian].– Geološki vjesnik, 35, 47–57.

VLAHOVIĆ, I., TIŠLJAR, J., VELIĆ, I. & MATIČEC, D. (2005): Evolution of the Adriatic Carbonate Platform: Palaeogeography, main events and depositional dynamics.– Palaeogeogr. Palaeoclimatol. Palaeoecol., 220/3–4, 333–360. doi: 10.1016/j.palaeo.2005.01.011

WORTHINGTON, S.R.H., FOLEY, A.E., & SOLEY, R.W.N. (2019): Transient characteristics of effective porosity and specific yield in bedrock aquifers.– J. Hydrol., 578, 124129. doi: 10.1016/j.jhydrol.2019.124129

XIONG, J., LIN, H., DING, H., PEI, H., RONG, C. & LIAO, W. (2020): Investigation on thermal property parameters characteristics of rocks and its influence factors.– Natural Gas Industry B, 7/3, 298–308. doi: 10.1016/j.ngib.2020.04.001

URL 1: https://www.avenza.com/avenza-maps/. Accessed on 29 April, 2024.

URL 2: https://www.esri.com/news/arcnews/spring12articles/introducing-arcgis-101.html. Accessed on 29 April, 2024.

3. DISCUSSION

The main goal of this research was to establish a reliable conceptual model of the Topusko hydrothermal system (THS). To achieve this, six objectives were established: (1) to establish a complete geochemical characterisation of the thermal water and determine the geothermal reservoir equilibrium temperature; (2) to reconstruct the structural setting of the discharge area using electrical resistivity tomography (ERT) to identify fault structures in the subsurface; (3) to determine the hydrogeological parameters of the geothermal aquifer in the discharge area from new hydrodynamic measurements; (4) to reconstruct the structural setting of the proposed recharge area and geothermal aquifer based on collected structural-geological data; (5) to perform geological modelling of THS based on newly acquired data; and (6) to perform numerical modelling of fluid flow and heat transport in THS based on the new data.

To address these objectives, four hypotheses were tested using a multidisciplinary approach involving hydrogeochemical, hydrogeological, structural-geological and geophysical methods. The synthesis of the results is presented and discussed below, along with the new findings observed during this research and perspectives for future research.

Hypothesis #1: Topusko geothermal aquifer is of hydrothermal origin.

The research by Pavić et al. (2024a,b) confirmed that the Topusko geothermal aquifer is of hydrothermal origin. Comprehensive geochemical characterisation of the thermal waters revealed Ca-HCO_3 hydrochemical facies, together with the stable isotope data from both precipitation and thermal water, indicating a system dominantly recharged by precipitation, with water interaction occurring primarily within a geothermal aquifer hosted in Mesozoic carbonates. Major ions analysis from three sampling locations in Topusko showed that the thermal water samples originate from the same aquifer, with carbonate dissolution being the primary process driving the solute content. Additionally, the data shows no significant changes over the two-year period, indicating a large and stable system (Pavić et al., 2024a). ^{14}C dating of DIC in thermal water suggested a mean residence time of around 9,500 years, indicating recharge during colder climatic conditions, a conclusion supported by stable water isotope analyses. All findings listed above support the hypothesis that the Topusko geothermal aquifer is of hydrothermal origin, further corroborated by structural-geological investigations and numerical modelling of groundwater flow and heat transport (Pavić et al., 2024b). The unique

combination of a thinned lithosphere, higher than average terrestrial heat flow, and the presence of regional faults and structures, such as the Topusko anticline, enable the gravity-driven groundwater flow and the formation of the hydrothermal system in the Topusko area.

Hypothesis #2: Recharge area of the Topusko geothermal aquifer is west of the Petrova gora nappe.

The structural setting reconstruction of the proposed recharge area involved extensive structural-geological field investigations (Pavić et al., 2024b). The newly collected structural and geological data, combined with the existing data, indicate that the recharge area of the THS lies south of the Topusko area, where Triassic carbonates extensively crop out as a part of the hangingwall cover within the Petrova gora nappe system. Regional fault systems and cogenetic folds favour the deep circulation of thermal water, facilitating its upwelling in the Topusko area in the highly fractured and permeable hinge zone of the Topusko anticline. This contradicts the hypothesis proposed by Šimunić (2008) that the recharge area lies west of the Petrova gora Mt. Extensive field investigations and constructed geological profiles of approximately 6 km investigation depth enabled detailed cross-validation of the proposed recharge area, which was further used for viable numerical simulation and modelling of groundwater flow and heat transport.

Hypothesis #3: Natural thermal springs in Topusko occur in a fault damage zone with high permeability.

Constructed regional geological profiles, reaching approximately 6 km in depth, along with the novel conceptual model of the THS proposed by Pavić et al. (2024b), suggest the presence of the Topusko anticline below the Topusko area, which facilitated the uplift of the aquifer closer to the surface. The tensile fractures occurring as a result of folding due to tectonic movement are denser and more developed near fold hinges than in the fold limbs (Li et al., 2018), which likely correspond to higher permeability zones in hydrogeological terms.

Furthermore, ERT geophysical surveys identified fault damage zones in the hinge zone of the Topusko anticline, i.e., the Topusko spring area, providing preferential pathways for groundwater upwelling to the surface from the confined geothermal aquifer (Pavić et al., 2023). These fault zones, characterised by high permeability, align with the geographical location of the thermal springs, suggesting the presence of fault and fracture patterns below the surface. The transmissivity values derived from step-drawdown tests, approximately 2×10^{-2} m^2/s, and

the hydraulic conductivity of about 2×10^{-4} m/s further confirm the high permeability, which is characteristic of carbonate rocks in fault damage zones. This supports the hypothesis that the natural thermal springs in Topusko occur in a fault damage zone with sufficient permeability for thermal water upwelling.

Hypothesis #4: Temperatures in the geothermal aquifer are higher than at the natural springs.

Hydrochemical data and chemical geothermometers were used to estimate the equilibrium temperature of the geothermal aquifer. The SiO_2-quartz geothermometer using historical data (Pavić et al., 2023) indicated an equilibrium temperature of approximately 78 °C, suggesting a circulation depth of about 2 km, considering the average geothermal gradient of 35 – 40 °C/km (Macenić, 2020). This is significantly higher than the measured discharge temperatures of an average of 53 °C at the Livadski izvor thermal spring and 65 °C at the nearby production well TEB-4. The SiO_2 concentrations measured during 2021 – 2023 suggest the equilibrium temperature of the geothermal aquifer of 90 °C (Pavić et al., 2024a). Numerical modelling of fluid flow and heat transport in THS corroborated these findings, simulating a local temperature anomaly in the Topusko subsurface and approaching the field observations (Pavić et al., 2024b). This modelling demonstrated the synergetic effect of regional geological structures on fluid flow and heat transport, affirming that temperatures in the geothermal aquifer are higher than at the natural springs.

Perspectives and Future Research

Throughout the work presented in this doctoral dissertation, new challenges and questions have emerged that suggest the need for further investigation. Here are several recommendations for future detailed hydrogeological research on the THS that would be beneficial to pursue.

To study and monitor geothermal resources used for district heating, health care, and tourism, it is necessary to continuously monitor *in situ*, hydrochemical, and isotope parameters such as groundwater levels (pressure), pH, temperature, EC, major anions and cations, $\delta^{18}O$ and $\delta^{2}H$ in water, and $\delta^{34}S$ and $\delta^{18}O$ in sulphate at a minimum quarterly resolution. The newly installed system for monitoring abstraction rates, pressure, and temperature at the Topusko central heating station will provide valuable data. This data can be further correlated with recommended monitoring practices to gain insights into the system's dynamics and its interaction with human intervention. It is advised that tritium levels in the TEB-4 well in

Topusko are monitored twice a year, particularly before and after the heating season, since study results show that thermal water mixes with water from shallower aquifers. Following that, cold springs in the surrounding area of Topusko should be sampled to address knowledge gaps in hydrogeological interactions from regional to local scale. These investigations will allow us to compare the composition of thermal water to that of cold springs.

The proposed novel conceptual model of the THS assumes a recharge area located south of Topusko, where Triassic carbonates crop out at the surface, in neighbouring Bosnia and Herzegovina (BiH). Future precipitation sampling should focus on this area, necessitating transboundary investigations with BiH. Additionally, the existence of thermal springs south of Topusko in BiH provides a basis for transboundary collaboration to compare existing systems. The simplest initial step would be to combine the results of hydrochemical analyses of thermal water samples. The proposed transboundary study area presents significant potential for future geological research, especially regarding confirmation of the evaporite presence or outcropping at the surface. This presence is indicated in Topusko thermal water samples through stable isotopes $\delta^{34}S$ and $\delta^{18}O$ of the sulphate anion (SO_4^{2-}). The results suggest evaporites are the primary source of sulphate anion, despite their limited surface occurrence in significant quantities. Korolija et al. (1980) mention the existence of Permian evaporites southwest of Topusko (Cetingrad town area), which warrants further detailed investigation and verification.

Future geophysical surveys should prioritise investigating fault damage zones in the Topusko spring area. These surveys should aim to cover a larger area and greater depths to gather more comprehensive data for improved interpretation of subsurface relationships.

Integrating collected structural data on strata orientation, fault, and fracture systems with both existing and newly acquired geological data is crucial for constructing composite geological profiles and further developing of a comprehensive 3D model of the THS. More detailed regional and local-scale geological reconstructions at the 3D level will significantly enhance the proposed conceptual model of THS, laying the groundwork for structural model improvements, and open detailed questions on numerical modeling of fluid flow and heat transport at the regional and local scale. Such a model will provide a robust foundation for sustainable management of this geothermal resource.

4. CONCLUSION

In the town of Topusko, thermal waters with temperatures of up to 65 °C have been utilised for district heating, medicinal, and recreational purposes since the 1980s. However, detailed research into the processes driving this hydrothermal system has never been conducted. In the study of hydrothermal systems, it is necessary to determine the origin of the fluid and the area of recharge, the aquifer spatial distribution, the direction of the fluid flow and the depth to which it descends, as well as the causes and the means of heating and upwelling to the surface.

The multidisciplinary research done as a part of this doctoral dissertation provided a comprehensive understanding of the Topusko hydrothermal system (THS) by integrating new hydrogeochemical, hydrogeological, geophysical, geothermal, and structural–geological data. Such a multidisciplinary approach is preferred because it helps eliminate ambiguities by cross-verifying findings from various applied methods. Each method complements the others, by filling in the gaps and providing a more accurate model of the system. Such investigations are an essential part of the initial exploration phase during the development of a geothermal project or in assessing the potential for future geothermal energy utilisation at a specific location.

All set research objectives were achieved and published in three original scientific papers that are part of this doctoral dissertation, including: (i) the complete geochemical characterisation of the thermal water and determination of the geothermal reservoir's equilibrium temperature, (ii) reconstruction of the structural settings of the discharge area using electrical resistivity tomography to identify the supposed fault structures in the subsurface, (iii) reconstruction of the structural setting of the proposed recharge area and geothermal aquifer based on new structural-geological data, and (iv) determination of hydrogeological parameters of the geothermal aquifer from new hydrodynamic measurements. Finally, based on the newly acquired data, (v) geological and (vi) numerical modelling of the THS fluid flow and heat transport were successfully conducted. The achieved research objectives helped refine the conceptual model of the THS by proposing a new one, offering more profound insights into its dynamics, clarifying key mechanisms, and supporting more sustainable geothermal resource utilisation and future research.

The research hypotheses, formulated following the purpose of the research and its objectives, were systematically evaluated and validated through the studies conducted within this doctoral dissertation. Hypothesis 1, which proposed that the Topusko geothermal aquifer is of hydrothermal origin, was confirmed in research papers two and three (Pavić et al., 2024a,

2024b). Hypothesis 3, suggesting that natural thermal springs in Topusko occur in a fault damage zone with high permeability that enabled the upwelling of thermal water, and Hypothesis 4, stating that temperatures in the geothermal aquifer are higher than at the natural springs, were both validated through findings presented in all three research papers (Pavić et al., 2023, 2024ab). However, Hypothesis 2, which posited that the recharge area of the Topusko geothermal aquifer is west of the Petrova gora nappe, was disapproved in the third research paper (Pavić et al., 2024b).

Here follow the key findings and conclusions from the three original scientific papers presented in this doctoral dissertation, along with the scientific contributions of this work and proposals for future research based on the new scientific questions that arose during the course of this research.

The ERT survey revealed fault damage zones in the Topusko spring area, which serve as preferential pathways for groundwater upwelling from the confined geothermal aquifer. The geographical location of the springs themselves further indicates the presence of underlying faults. The correlation between observed resistivity and lithology, alongside stratigraphic well logs, has enhanced our geological understanding and confirmed the presence of a fault system below the surface.

Step-drawdown tests on production wells TEB-1 and TEB-3 provided crucial hydrogeological parameters, estimating a transmissivity of approximately 2×10^{-2} m^2/s and a hydraulic conductivity of around 2×10^{-4} m/s, given the 106 m thickness of the carbonate aquifer in TEB-1. These values are consistent with the hydraulic parameters reported for fractured carbonates in the literature, validating our findings.

The systematic monitoring of the thermal waters revealed important hydrochemical characteristics, indicating that the Topusko thermal waters exhibit Ca-HCO_3 hydrochemical facies, which confirms the influence of geological formations dominated by carbonate rocks. The major ions data suggest that approximately 75 % of the weathering is due to carbonates and 25-30 % to silicates. High Ca^{2+}, Na^+, and Mg^{2+} concentrations can be attributed to mineral dissolution and cation exchange. Ion exchange and silicate weathering processes contribute to the increase of Na^+ from the recharge to the discharge zone. Historical data comparison indicates that the thermal water composition is stable, with observed differences in silica content likely due to varying measurement methodologies.

Stable water isotope data (δ^2H and $\delta^{18}O$) suggest that the recharge of thermal water is of meteoric origin, meaning it is sourced from precipitation. The lower mean values of stable isotopes (-1.51 ‰ in $\delta^{18}O$) compared to weighted mean precipitation values suggest that

recharge occurred under colder climatic conditions than present. The uniform $\delta^{18}O$ values, ranging from –11.3 ‰ to –10.73 ‰, imply deep circulation and extensive areal coverage and thickness of the aquifer, with longer residence times that homogenise seasonal precipitation variations.

Radiocarbon (^{14}C) dating of dissolved inorganic carbon (DIC) indicates that the thermal water has residence times ranging from 6,668 years BP to 10,687 years BP. Traditional models provide an average residence time of 8,473 years BP, and qualitative estimation using the Han-Plummer plot suggests 9,536 years BP. These ages align with the notion that the thermal water represents recharge from a colder climate period in the late Pleistocene or early Holocene.

Tritium activity in thermal water is generally below detection limits, except during periods of extensive abstraction for district heating when some tritium activity is detected. This suggests infiltration of modern precipitation from overlying younger layers, indicating that the hanging wall is not entirely impermeable. Regular and precise tritium activity measurement is recommended to assess the sustainability of abstraction rates.

Chemical geothermometers were employed to estimate the maximum equilibrium temperature reached by the thermal waters in the aquifer, with the quartz geothermometer indicating the most plausible equilibrium aquifer temperature of 90 °C. Data on stable sulphate anion isotopes ($\delta^{34}S$ and $\delta^{18}O$) suggest gypsum and/or anhydrite dissolution at depth, based on hydrochemical data only, due to the absence of deep boreholes or seismic reflection profiles.

Integrating structural-geological field investigations and numerical modelling has led to the development of a novel conceptual model of the THS. New insights into the THS dynamics have been provided by constructing new geological profiles and integrating them with hydrogeological and geochemical data. The recharge area of THS is located south of Topusko, where Triassic carbonates crop out. Regional and local scale fold and fault systems facilitate the deep circulation of thermal water and its upwelling in Topusko, forming a valuable geothermal resource. Numerical modelling corroborates the proposed conceptual model, simulating a local temperature anomaly in the Topusko subsurface that aligns with field observations. The occurrence of such localised thermal anomalies in the hinge zone of the Topusko anticline suggests enhanced fluid flow and heat transport, pointing to the impact of terrestrial heat flow and local geological structures on the system. The synergistic effect of the anticline hinge, identified through structural investigations, and the cogenetic fault/fracture systems, determined by surface geophysical research, results in an enhanced permeability field in the discharge area. This allows for the formation of abundant natural thermal springs.

This research makes significant scientific contributions by advancing the understanding of the THS and emphasising the importance of integrating field observations with numerical modelling to physically validate and refine conceptual models. An integrated multidisciplinary approach, which included the determination of hydrogeological, hydrogeochemical, and geothermal characteristics, enabled a more detailed reconstruction of the hydrogeological and thermal processes driving the development of geothermal resources. These findings are crucial for developing site-specific exploitation plans to ensure the long-term sustainable utilisation of the THS, highlighting the importance of continuous monitoring and management of this geothermal resource. By identifying the recharge area of the THS, this research will contribute to the future protection of the geothermal aquifer from adverse impacts, ensuring the preservation of its good quantitative and chemical status. Moreover, the multidisciplinary approach used in this study lays the groundwork for developing a methodology to study carbonate geothermal aquifers of hydrothermal origin, which supply water to the largest number of natural thermal springs in Croatia.

Future research should focus on detailed regional studies and continuous monitoring to ensure the long-term viability of the geothermal resources in Topusko. This includes ongoing *in situ* monitoring of physico-chemical, hydrochemical and isotopic parameters of thermal water samples and precipitation in the proposed recharge area. The newly implemented monitoring system at the Topusko central heating station will provide essential data on abstraction rates, pressure, and temperature dynamics, complementing recommended practices for understanding system dynamics and human interactions. Additionally, periodic tritium monitoring in the TEB-4 is needed to assess seasonal variations and potential interactions with other aquifers. Collaboration with researchers from neighbouring Bosnia and Herzegovina is crucial for investigating the cross-border recharge area and thermal springs, aiming to compare hydrochemical data and explore potential evaporite presence. Future geological research should prioritise verifying the existence of Permian evaporites southwest of Topusko and expanding electrical resistivity tomography (ERT) surveys to investigate fault damage zones comprehensively. Integrating structural and geological data into a comprehensive 3D model will enhance the conceptual understanding and management of the THS and hydrothermal systems in the Bosnia and Herzegovina border area. This integrated approach will support sustainable resource utilisation by facilitating forecasts based on a future numerical groundwater flow and heat transport model.

5. LITERATURE

Scientific literature:

Aliyu, S. & Garba, M. M. (2019) Review on Current Global Geothermal Energy Potentials and the Future Prospects. International Journal of Advances in Scientific Research and Engineering, *5*(4), 133–140, doi:10.31695/ijasre.2019.33153

Ármannsson, H. (2012) 7.04 - Geochemical Aspects of Geothermal Utilization. In Comprehensive Renewable Energy, 97–170, Elsevier, doi: 10.1016/B978-0-08-087872-0.00709-5

Anderson, M., Woessner, W. & Hunt, R. (2015) Applied Ground Water Modeling: Simulation of Flow and Advective Transport.–Elsevier, London, 533 p.

Ármannsson, H., & Fridriksson, T. (2009) Application of Geochemical Methods In Geothermal Exploration. https://www.researchgate.net/publication/228706025

Balderer, W., Synal, H. A., Deák, J., & Leuenberger, F. (2014) Origin of thermal waters in budapest based on chemical and isotope investigations including chlorine-36. In *Thermal and Mineral Waters: Origin, Properties and Applications* (pp. 49–60). Springer Berlin Heidelberg. doi: 10.1007/978-3-642-28824-1_5

Blake, S., Henry, T., Murray, J., Flood, R., Muller MR, Jones AG, Rath V. (2016) Compositional multivariate statistical analysis of thermal groundwater provenance: A hydrogeochemical case study from Ireland Applied Geochemistry, 75, 171-188, doi:10.1016/j.apgeochem.2016.05.008

Blasco, M., Auqué, L. F., & Gimeno, M. J. (2017) Application of Different Geothermometrical Techniques to a Low Enthalpy Thermal System. Procedia Earth and Planetary Science, 17, 65–68, doi: 10.1016/j.proeps.2016.12.034

Bowen, R. (1989) Geothermal Systems Models. In Geothermal Resources, 2nd ed.; Springer: Dordrecht, Netherlands, 66-75, doi: 10.1007/978-94-009-1103-1

Borović, S., & Marković, I. (2015) Utilization and tourism valorisation of geothermal waters in Croatia. In *Renewable and Sustainable Energy Reviews* (Vol. 44, pp. 52–63). Elsevier Ltd. doi: 10.1016/j.rser.2014.12.022

Bošnjak, R. et al. (1998) GEOEN - Program of geothermal energy utilization. Energy Institute "Hrvoje Požar", Zagreb.

Bredehoeft, J.D. & Papadopulos, I.S. (1965) Rates of vertical ground-water movement estimated from the earth's thermal profile. Water Resources Research, 1:325–328.

Borović, S., Marković, T., Larva, O., Brkić, Ž. & Mraz, V. (2016) Mineral and Thermal Waters in the Croatian Part of the Pannonian Basin.– In: PAPIĆ, P. (ed.): *Mineral and Thermal Waters of Southeastern Europe*. Springer, Cham, doi: 10.1007/978-3-319-25379-4_2

Caine, J.S., Evans, J.P. & Forster, C.B. (1996) Fault zone architecture and permeability structure. Geology, 24, 11,1025–1028.

European Commission (2019) Communication from the Commission - The European Green Deal. COM/2019/640. *Available online:* https://eur-lex.europa.eu/legal-content/EN/TXT/?uri=COM%3A2019%3A640%3AFIN (accessed on 19 August 2024)

Čepelak, R. (2007) Balneološko ispitivanje peloida okolice Topuskog. (16/1-07). Zagreb: Zavod za fizikalnu medicinu i rehabilitaciju medicinskog fakulteta Sveučilišta u Zagrebu.

Čepelak, R. & Mandić, V. (1989) Ispitivanje peloida okolice Topuskog (lokacije Crne rijeke i Vidnjevića) (6/2-89). Zagreb: Zavod za fizikalnu medicinu i rehabilitaciju medicinskog fakulteta Sveučilišta u Zagrebu.

Deming, D. (2002) Introduction to hydrogeology. McGraw-Hill, New York, pp. 468.

Dhia, Hamed ben. (1987) Geothermal energy in Tunisia: Potential of the southern province. Geothermics, 16(3), 299–318, doi: 10.1016/0375-6505(87)90008-3

Directive EU/2023/2413 of the European Parliament and of the Council of 18 October 2023 amending Directive (EU) 2018/2001, Regulation (EU) 2018/1999 and Directive 98/70/EC as regards the promotion of energy from renewable sources, and repealing Council Directive (EU) 2015/652, *OJ L, 2023/2413, Available online:* http://data.europa.eu/eli/dir/2023/2413/oj (accessed on 31 May 2024).

DHMZ (2021) Monthly values and extremes. Državni Hidrometeorološki Zavod [Croatian Meteorological and Hydrological Service – in Croatian]. Retrieved January 18, 2021, from https://meteo.hr/klima.php?section=klima_podaci&param=k2_1

DZS (2022) Državni Zavod za Statistiku – Popis ’21. [Croatian Bureau of Statistics – Census 2021] Available online: https://popis2021.hr (accessed on 22 November 2022). (In Croatian)

Dilsiz, C., Marques, J. M., & Carreira, P. M. M. (2004) The impact of hydrological changes on travertine deposits related to thermal springs in the Pamukkale area (SW Turkey). Environmental Geology, 45(6), 808–817, doi: 10.1007/s00254-003-0941-8

Dublyansky, Y. V. (1995) Speleogenetic history of the Hungarian hydrothermal karst. Environmental Geology, 25(1), 24–35, doi: 10.1007/BF01061827

Drogue, C. (1985) Geothermal gradients and groundwater circulation in fissured and karstic rocks: the role played by the structure of the permeable network. Journal of Geodynamics, 4(1–4), 219–231.

Economides, M. & Ungemach, P. (1987) Applied geothermics. Wiley, Chichester, UK, 238.

European University Institute, Belmans, R., Conti, I., Ferrari, A., Galdi, G., Hancher, L., et al., (2022) The EU Green Deal (2022 ed.) (L. Hancher, A. Nouicer, V. Reif, & L. Meeus, Eds.). European University Institute, doi: 10.2870/00714

Fabbri, P. (1997) Transmissivity in the Geothermal Euganean Basin: A Geostatistical Analysis. Groundwater, 35, 881–887, doi: 10.1111/j.1745-6584.1997.tb00156.x

Farr, G., & Bottrell, S. H. (2013) The hydrogeology and hydrochemistry of the thermal waters at Taffs Well, South Wales, UK. In *AND KARST SCIENCE* (Vol. 40, Issue 1).

Faulkner, D. R., Jackson, C. A. L., Lunn, R. J., Schlische, R. W., Shipton, Z. K., Wibberley, C. A. J., & Withjack, M. O. (2010) A review of recent developments concerning the structure, mechanics and fluid flow properties of fault zones. Journal of Structural Geology, 32(11), 1557–1575, doi: 10.1016/j.jsg.2010.06.009

Fetter, C. W. (2001) Applied Hydrogeology (4th edition). Prentice Hall, Upper Saddle River, New Jersey.

Flóvenz, Ó. G., Hersir, G. P., Sæmundsson, K., Ármannsson, H. & Fridriksson, T. (2012) Geothermal Energy Exploration Techniques. In: SAYIGH, A. (ed.): Comprehensive Renewable Energy, 51–95, doi: 10.1016/B978-0-08-087872-0.00705-8

Ford, D., & Williams, P. (2007) Karst Hydrogeology and Geomorphology. Wiley, doi: 10.1002/9781118684986

Forster C. & Smith L. (1988a) Groundwater flow systems in mountainous terrain 1: numerical modelling technique. Water Resources Research, 24, 999–1010.

Forster C, Smith L (1988b) Groundwater flow systems in mountainous terrain 2: controlling factors. Water Resources Research, 24, 1011–1023.

Goldscheider, N., Hötzl, H., Käss, W., & Ufrecht, W. (2003) Combined tracer tests in the karst aquifer of the artesian mineral springs of Stuttgart, Germany. Environmental Geology, *43*(8), 922–929, doi: 10.1007/s00254-002-0714-9

Goldscheider, N., Mádl-Szőnyi, J., Erőss, A., & Schill, E. (2010) Review: Thermal water resources in carbonate rock aquifers. Hydrogeology Journal, 18(6), 1303–1318, doi: 10.1007/s10040-010-0611-3

Grasby, S. E., Hutcheon, I., & Krouse, H. R. (2000) The influence of water–rock interaction on the chemistry of thermal springs in western Canada. Applied Geochemistry, 15, 4, 439–454, doi: 10.1016/S0883-2927(99)00066-9

Havril, T., Molson, J.W. & Mádl-Szőnyi, J. (2016) Evolution of fluid flow and heat distribution over geological time scales at the margin of unconfined and confined carbonate sequences - A numerical investigation based on the Buda Thermal Karst analogue. Marine and Petroleum Geology, 78, 738–749, doi: 10.1016/j.marpetgeo.2016.10.001

Heasler, H.P., Jaworowski, C. & Foley, D. (2009) Geothermal systems and monitoring hydrothermal features. In: YOUNG, R. & NORBY, L. (eds.): Geological Monitoring. Geological Society of America, Boulder, doi:/10.1130/2009.monitoring(05)

Horváth, F., Musitz, B., Balázs, A., Végh, A., Uhrin, A., Nádor, A., Koroknai, B., Pap, N., Tóth, T. & Wórum, G. (2015) Evolution of the Pannonian basin and its geothermal resources. Geothermics, 53, 328–352, doi: 10.1016/j.geothermics.2014.07.009

IAEA. (2013) Isotope Methods for Dating Old Groundwater, Non-serial Publications, International Atomic Energy Agency, Vienna. https://www.iaea.org/publications/8880/isotope-methods-for-dating-old-groundwater

Khodayar, M. & Björnsson, S. (2024) Conventional Geothermal Systems and Unconventional Geothermal Developments: An Overview. Open Journal of Geology, 14(2), 196–246, doi: 10.4236/ojg.2024.142012

Kaminskaite-Baranauskiene, I., Wang, H., Liu, Z., & Li, H. (2023) Geothermal carbonate reservoirs and their sustainability: what can natural hydrothermal systems tell us? Geothermics, 114, 102798, doi: 10.1016/j.geothermics.2023.102798

Kovačić M, Perica R. (1998) The degree of geothermal water utilization in the Republic of Croatia. Croatian Waters, 25, 355–61. (in Croatian)

Kosović, I., Matoš, B., Pavičić, I., Pola, M., Mileusnić, M., Pavić, M. & Borović, S. (2024) Geological modeling of a tectonically controlled hydrothermal system in the southwestern part of the Pannonian basin (Croatia). Frontiers in Earth Science, 12, doi: 10.3389/feart.2024.1401935

Keegan-Treloar, R., Irvine, D. J., Solórzano-Rivas, S. C., Werner, A. D., Banks, E. W., & Currell, M. J. (2022) Fault-controlled springs: A review. In *Earth-Science Reviews* (Vol. 230). Elsevier B.V, doi:10.1016/j.earscirev.2022.104058

Lei, Y., Zhao, Z., Zhang, B., Tang, X., Luo, Y., Wang, G., Gao, J., & Zhang, D. (2022) Genesis of Significance of Carbonated Thermal Water Springs in Xining Basin, China. Water (Switzerland), 14 (24), doi: 10.3390/w14244058

Lenkey, L., Dövényi, P., Horváth, F. & Cloetingh, S.A.P.L. (2002) Geothermics of the Pannonian basin and its bearing on the neotectonics. In: Cloetingh, S.A.P.L, Horváth, F., Bada, G., Lankreijer, A.C. (eds) EGU Stephan Mueller Special Publication Series, 3, 29-40, doi: 10.5194/smsps-3-29-2002

Li, M., Li, G.M., Yang, L., Dang, X.Y., Zhao, C.H., Hou, G.C. & Zhang, M.S. (2007) Numerical modeling of geothermal groundwater flow in karst aquifer system in eastern Weibei, Shaanxi Province, China. Sci China Series D: Earth Science, 50, 36–41.

Li, Y., Hou, G., Hari, K. R., Neng, Y., Lei, G., Tang, Y., Zhou, L., Sun, S., & Zheng, C. (2018) The model of fracture development in the faulted folds: The role of folding and faulting. *Marine and Petroleum Geology*, *89*, 243–251, doi: 10.1016/j.marpetgeo.2017.05.025

Montanari, D., Minissale, A., Doveri, M., Gola, G., Trumpy, E., Santilano, A. & Manzella, A. (2017) Geothermal resources within carbonate reservoirs in western Sicily (Italy): A review. Earth-Science Reviews, 169, 180–201, doi: 10.1016/j.earscirev.2017.04.016

Marini, L. (2004) Geochemical techniques for the exploration and exploitation of geothermal energy. 1–106.

Muffler, P. & Cataldi, R. (1978) Methods for regional assessment of geothermal resources. Geothermics, 7(2–4), 53–89, doi: 10.1016/0375-6505(78)90002-0

Macenić, M., Kurevija, T., & Medved, I. (2020) Novel geothermal gradient map of the Croatian part of the Pannonian basin system based on data interpretation from 154 deep exploration wells. Renewable and Sustainable Energy Reviews, 132, doi: 10.1016/J.RSER.2020.110069

Moeck, I. S. (2014) Catalog of geothermal play types based on geologic controls. In Renewable and Sustainable Energy Reviews, 37, 867–882, doi: 10.1016/j.rser.2014.05.032

Ojha, L., Karunatillake, S., Karimi, S. & Buffo, J. (2021) Amagmatic hydrothermal systems on Mars from radiogenic heat. Nature Communications, 12(1), doi: 10.1038/s41467-021-21762-8

Pavić, M., Kosović, I., Pola, M., Urumović, K., Briški, M., & Borović, S. (2023). Multidisciplinary Research of Thermal Springs Area in Topusko (Croatia). Sustainability, 15(6), 5498, doi: 10.3390/su15065498

Pavić, M., Briški, M., Pola, M., & Borović, S. (2024a). Hydrogeochemical and environmental isotope study of Topusko thermal waters, Croatia. Environmental Geochemistry and Health, 46(4), 133, doi: 10.1007/s10653-024-01904-9

Pavić, M., Pola, M., Matoš, B., Mišić, K., Kosović, I., Pavičić, I. Borović, S. (2024b) A conceptual and numerical model of fluid flow and heat transport in the Topusko hydrothermal system, Geologia Croatica, 77/3, doi: 10.4154/gc.2024.14

Pavelić, D., & Kovačić, M. (2018) Sedimentology and stratigraphy of the Neogene rift-type North Croatian Basin (Pannonian Basin System, Croatia): A review. In Marine and Petroleum Geology, 91, 455–469, Elsevier Ltd, doi: 10.1016/j.marpetgeo.2018.01.026

Pentecost, A., Jones, B., Renaut, R.W. (2003) What is a hot spring? Canadian Journal of Earth Sciences, 40, 1443–1446.

Pouraskarparast, Z., Aghaei, H., Colombera, L., Masoero, E., & Ghaedi, M. (2024) Fracture aperture: A review on fundamental concepts, estimation methods, applications, and research gaps. Marine and Petroleum Geology, 164, 106818, doi: 10.1016/j.marpetgeo.2024.106818

Roscini, A.V., Rapf, O., Kockat, J., Milne, C., Jeffries, B. & D'angiolella, R. (2020) On the way to a Climate-Neutral Europe Contributions From The Building Sector To A Strengthened 2030 Climate Target; Buildings Performance Institute Europe (BPIE), 2020. Available online: www.bpie.eu (accessed on 14 November 2022).

Sass I. (2007) Geothermie und Grundwasser [Geothermics and groundwater]. Grundwasser 12(2):93.

Simler, R. (2012). Software Diagrammes, V6.72, Laboratoire d'Hydrologie d'Avignon; Université d'Avignon et pays du Vaucluse: Avignon, France.

Schäffer, R., & Sass, I. (2014) The thermal springs of Jordan. *Environmental Earth Sciences*, *72*(1), 171–187, doi: 10.1007/s12665-013-2944-4

Schmid, S.M., Bernoulli, D., Fügenschuh, B., Matenco, L., Schefer, S., Schuster, R., Tischler, M. & Ustaszewski, K. (2008) The Alpine-Carpathian-Dinaridic orogenic system: Correlation and evolution of tectonic units. Swiss Journal of Geosciences, 101, 139–183, doi: 10.1007/s00015-008-1247-3

Schmid, S.M., Fügenschuh, B., Kissling, E. and Schuster, R. (2004) Tectonic map and overall architecture of the Alpine orogen. Eclogae geologicae Helvetiae, 97, 93-117, doi: 10.1007/s00015-004-1113-x

Stevanović, Z., Dulić, I. & Dunčić, M. (2015) Some experiences in tapping deep thermal waters of the Triassic karstic aquifer in the Pannonian Basin of Serbia. Central European Geology, 58(1–2), 50–61, doi: 10.1556/24.58.2015.1-2.3

Šimunić, A. (2008) Topusko. In: Šimunić, A., Hećimović, I. (eds.): Geotermalne i mineralne vode Republike Hrvatske [Mineral and Thermal Waters of the Republic of Croatia – in Croatian]. Croatian Geological Survey, Zagreb.

Thiébaud, E., Dzikowski, M., Gasquet, D., & Renac, C. (2010). Reconstruction of groundwater flows and chemical water evolution in an amagmatic hydrothermal system (La Léchère, French Alps). Journal of Hydrology, 381(3–4), 189–202, doi: 10.1016/j.jhydrol.2009.11.041

Ufrecht, W. (2006) Hydrogeologie des Stuttgarter Mineralwassersystems [Hydrogeology of the mineral water system of Stuttgart]. Schrift Amters Umweltschutz,(3):1–151.

Ufrecht, W. (2015) Die Stuttgarter Mineralquellen – Geologie und Hydrogeologie im Überblick. In Chlorierte Kohlenwasserstoffe im Grundwasser (pp. 5–17). Springer Fachmedien Wiesbaden, doi: 10.1007/978-3-658-09249-8_2

Torresan, F., Piccinini, L., Cacace, M., Pola, M., Zampieri, D., & Fabbri, P. (2022) Numerical modeling as a tool for evaluating the renewability of geothermal resources: the case study of the Euganean Geothermal System (NE Italy). Environmental Geochemistry and Health, 44(7), 2135–2162, doi: 10.1007/s10653-021-01028-4

Tóth, J. (2009) Gravitational systems of groundwater flow: theory, evaluation, utilization. Cambridge University Press, Cambridge, doi: 10.1017/CBO9780511576546

Tomljenović, B. & Csontos, L. (2001) Neogene–Quaternary structures in the border zone between Alps, Dinarides and Pannonian Basin (Hrvatsko zagorje and Karlovac Basins, Croatia). International Journal of Earth Sciences, 90(3), 560–578, doi: 10.1007/s005310000176

Volpi, G. (2018) Numerical modelling of fluids related thermal anomalies. *Tesi di dottorato, Università degli Studi di Milano-Bicocca.*, hdl:10281/199141 https://doi.pangaea.de/10281/199141

Widhen, F., Séranne, M., Ballas, G., Labaume, P., Le-Ber, E., Pezard, P., Girard, F., Lamotte, C., & Ladouche, B. (2023) Long-term evolution of a carbonate reservoir submitted to fresh, saline and thermal waters interactions- Jurassic carbonates in the coastal area of the Gulf of Lion margin (southern France). *BSGF - Earth Sciences Bulletin*, *194*. doi: 10.1051/bsgf/2023005

White, D.E. (1957) Thermal waters of volcanic origin. Bulletin of the Geological Society of America, 68:1637–1658.

Vass, I., Tóth, T.M., Szanyi, J. & Kovács, B. (2018) Hybrid numerical modelling of fluid and heat transport between the overpressured and gravitational flow systems of the Pannonian Basin. Geothermics, 72, 268–276, doi: 10.1016/j.geothermics.2017.11.013

Vlahović I., Tišljar, J., Velić, I. & Matičec, D. (2005) Evolution of the Adriatic Carbonate Platform: Palaeogeography, main events and depositional dynamics. Palaeogeography, Palaeoclimatology, Palaeoecology, 220, 333– 360, doi: 10.1016/j.palaeo.2005.01.011

Underschultz JR, Otto CJ, Bartlett R (2005) Formation fluids in faulted aquifers: examples from the foothills of Western Canada and the North West Shelf of Australia. In: Boult P, Kaldi J (eds) Evaluating fault and cap rock seals. AAPG Hedberg Series no. 2, AAPG, Tulsa, OK, pp 247–260.

Verbovšek, T. (2008) Estimation of transmissivity and hydraulic conductivity from specific capacity and specific capacity index in dolomite aquifers. Journal of Hydrologic Engineering, 13, 817–823, doi: 10.1061/(ASCE)1084-0699(2008)13:9(817)

Williams, C. F., Reed, M. J. & Anderson, A. F. (2011) Updating the classification of geothermal resources. In: *Proceedings of Thirty-Sixth Workshop on Geothermal Reservoir Engineering*. Stanford University, Stanford, California.

Worthington, S. R. H., Foley, A. E., & Soley, R. W. N. (2019) Transient characteristics of effective porosity and specific yield in bedrock aquifers. Journal of Hydrology, 578, 124129, doi: 10.1016/j.jhydrol.2019.124129

Zaninović, K., Gajić-Capka, M., Perčec Tadić, M., Vučetić, M., Milković, J., Bajić, A.,Cindrić, K., Cvitan, L., Katušin, Z. & Kaučić, D. (2008) Klimatski atlas Hrvatske/Climate atlas of Croatia 1961–1990, 1971–2000; Državni Hidrometeorološki Zavod: Zagreb, Croatia. (In Croatian and English)

Unpublished reports:

Bać, J. & Herak, M. (1962) Prijedlog određivanja užih i širih zaštitnih zona termomineralnih izvora u Hrvatskoj [Recommendation for determination of wider and narrow protection zones for thermo-mineral springs in Croatia – in Croatian]. Unpublished report, Institute for geological research, Zagreb, 147a.

Bahun, S. & Raljević, B. (1969) Mineralna, termalna i ljekovita vrela [Mineral and Thermal Springs – in Croatian]. Unpublished report, Institute for geological research, Zagreb.

Čubranić, A. (1984) Osmatranje termalnih voda u Topuskom [Thermal water monitoring in Topusko – in Croatian]. Zagreb: INAPROJEKT, OOUR Kompleksna geološka istraživanja.

Šegotić, B. & Šmit, I. (2007) Studija optimirane energetske učinkovitosti korištenja geotermalnih voda [Study of Optimized Energy Efficiency of Geothermal Water Use – in Croatian]. Unpublished report, Termoinženjering-projektiranje, Zagreb.

Pavleković, M. (1986) Istraživanje peloida područja Topuskog [Peloid research in the Topusko area – in Croatian]. Zagreb: INAProjekt Zagreb, OOUR Kompleksna geološka istraživanja.

6. BIOGRAPHY OF THE AUTHOR

Mirja Pavić was born on the 4 February 1991 in Zagreb, where she attended primary school, primary music school and high school. After graduating from the V. gymnasium in 2009, she enrolled for two years in the Integrated educational studies of Physics and Chemistry at the Department of Physics at the Faculty of Science, University of Zagreb. Upon discovering the research field of Geology at the Faculty of Science, she decided to shift her educational and career path, bringing her closer to her passions for hiking and orienteering running. Mirja obtained her Bachelor's degree in 2014 at the Geology Department of the Faculty of Science, defending the thesis entitled „Modalni sastav recentnih sedimenata jugoistočnog Jadranskog sliva“ (The modal composition of recent sediments in the southeastern Adriatic catchment – in Croatian).

In academic year 2014/2015, she enrolled in the Graduate Study of Geological Engineering at the Faculty of Mining, Geology and Petroleum Engineering, obtaining a Master's degree in 2016, defending the thesis entitled „Zone sanitarne zaštite planiranog vodocrpilišta Ježdovec“ (Sanitary protection areas for planned public water system Ježdovec– in Croatian). After graduation, she was employed as a Junior Associate in 2017 at the Ministry of Defense, Department of Geoinformation Systems and Meteorology, Zagreb. From the beginning of 2018 to the end of 2020, she has been employed by the Department of Hydrogeology and Engineering Geology of the Croatian Geological Survey as a Project Associate. At the end of 2020, 2020/2021 academic year, she entred the Doctoral studies of Applied Geosciences, Mining and Petroleum Engineering at the Faculty of Mining, Geology and Petroleum Engineering, under the supervision of Assoc. Prof. Željko Duić, PhD. Since the beginning of the academic year 2020/2021, she has been employed as an assistant at the Department of Hydrogeology and Engineering Geology of the Croatian Geological Survey under the supervision of Staša Borović, PhD. The PhD thesis topic arose from the research project HyTheC (Multidisciplinary Approach to Conceptual Modelling of Hydrothermal Systems in Croatia, UIP-2019-04-1218), financed by the Croatian Science Foundation. Mirja Pavić has attended additional training in Thermogeology and Geothermal from 2021 to 2023 at the Faculty of Natural Sciences and Engineering in Slovenia, Geological Survey of Slovenia, Delft University of Technology, and Cyprus University of Technology. She is a member of the Croatian Geological Association and the International Association of Hydrogeologists (IAH). Scientific and professional interests of Mirja Pavić focus on geotermics, karst and alluvial

hydrogeology, GIS and numerical modelling of groundwater flow and heat transport, and engineering geology and geomorphology.

Additionally, in her free time during graduate studies, employment, and enrollment in PhD studies, Mirja Pavić has won several titles as the National Champion of Croatia in orienteering running and won the awards for the best female sports team in Zagrebačka County. She represented the Faculty of Science at the University of Zagreb in the University Sports Games in swimming and has four times represented the Republic of Croatia in orienteering, running at the World Orienteering Championships in Sweden, Estonia, Latvia, and Norway. During her PhD, she also completed the course to become a Junior Alpinist. She continued to volunteer as an assistant and educator for the course in the following years.

List of published papers (June 2024):

Original scientific work

1. Pavić, M., Pola, M., Matoš, B., Mišić, K., Kosović, I., Pavičić, I. & Borović, S. (2024b) A conceptual and numerical model of fluid flow and heat transport in the Topusko hydrothermal system, Geologia Croatica, 77/3, doi: 10.4154/gc.2024.14

2. Pavić, M., Briški, M., Pola, M., & Borović, S. (2024a). Hydrogeochemical and environmental isotope study of Topusko thermal waters, Croatia. Environmental Geochemistry and Health, 46(4), 133, doi: 10.1007/s10653-024-01904-9

3. Pavić, M., Kosović, I., Pola, M., Urumović, K., Briški, M., & Borović, S. (2023) Multidisciplinary Research of Thermal Springs Area in Topusko (Croatia). Sustainability, 15(6), 5498, doi: 10.3390/su15065498

4. Kosović, I., Matoš, B., Pavičić, I., Pola, M., Mileusnić, M., Pavić, M. & Borović, S. (2024) Geological modeling of a tectonically controlled hydrothermal system in the southwestern part of the Pannonian basin (Croatia), Frontiers in earth science (Lausanne), 12, 1-24, doi: 10.3389/feart.2024.1401935

5. Kosović, I., Briški, M., Pavić, M., Padovan, B., Pavičić, I., Matoš, B., Pola, M. & Borović, S. (2023) Reconstruction of Fault Architecture in the Natural Thermal Spring Area of Daruvar Hydrothermal System Using Surface Geophysical Investigations (Croatia), Sustainability, 15,

12134, doi: 10.3390/su151612134

6. Frangen, T., Pavić, M., Gulam, V. & Kurečić, T. (2022) Use of a LiDAR-derived landslide inventory map in assessing Influencing factors for landslide susceptibility of geological units in the Petrinja area (Croatia), Geologia Croatica, 75(1), 35-49, doi: 10.4154/gc.2022.10

7. Bostjančić, I., Avanić, R., Frangen, T. & Pavić, M. (2022) Spatial distribution and geometrical characteristics of landslides with special reference to geological units in the area of Slavonski Brod, Croatia, Geologia Croatica, 75 (1), 3-16, doi: 10.4154/gc.2022.03

8. Pollak, D., Gulam, V., Novosel, T., Avanić, R., Tomljenović, B., Hećej, N., Terzić, J., Stipčević, J., Bačić, M., Kurečić, T. et al. (2021) The preliminary inventory of coseismic ground failures related to December 2020 – January 2021 Petrinja earthquake series, Geologia Croatica, 74 (2), 189-208, doi: 10.4154/gc.2021.08

9. Paar, D., Mance, D., Stroj, A. & Pavić, M. (2019) Northern Velebit (Croatia) karst hydrological system: results of a preliminary ^{2}H and ^{18}O stable isotope study, Geologia Croatica, 72, (3), 205-213, doi: 10.4154/gc.2019.15

Master thesis

Pavić, Mirja
Zone sanitarne zaštite planiranog vodocrpilišta Ježdovec (Sanitary protection areas for planned public water system Ježdovec – in Croatian) / Posavec, Kristijan (supervisor); Faculty of Mining, Geology and Petroleum Engineering, Univeristy of Zagreb, Croatia, 2016.